1. INTRODUCTION

1.1 Eutrophication of Rotorua Lakes

The eutrophication of New Zealand's Rotorua lakes is of considerable concern with a number already affected and many others showing signs of degradation. Eutrophication, the enrichment of surface waters by plant nutrients, specifically phosphorus and nitrogen, results in increased biological activity. This leads to an increased growth of macrophytes or the development of algae blooms. Algae blooms decrease the amenity, aesthetics, and recreational values of lakes, as they decrease water clarity, cause oxygen deficiency in deep water, and reduce biodiversity. High inputs of nutrients from agricultural activities, septic tanks and wastewater can all be significant factors of eutrophication (Foy and Withers, 1995).

Lake Rotorua is one of the most eutrophic of the Rotorua Lakes. Rotorua City is situated on the southern shore of the lake and is a key tourism centre in New Zealand. The poor water quality of the lake not only affects tourism but prolific blooms of cyanobacteria are also a public health concern. Public concern for the poor water quality of Lake Rotorua and other eutrophic lakes in the region has led to investigations into potential for restoration of the lakes (Parliamentary Commissioner for the Environment, 2006).

1.2 Restoration

The restoration of eutrophic lakes generally involves the reduction of phosphorus and nitrogen loads from external sources. However many eutrophic lakes, especially shallow lakes, do not show an improvement in water quality after substantial reduction in external nutrient loads. Internal loading of nutrients, especially phosphorus, from lake sediments has delayed the recovery of many eutrophic lakes (Jeppesen et al., 2005).

Phosphorus release from sediments results from enhanced biological activity in response to increasing organic matter input to lake sediments. Decomposition of this organic matter results in the deoxygenation of bottom waters under thermal stratification. When oxygen is depleted the chemistry of the sediments changes such that nutrients in the sediments are released into the water column (Bostrom et al., 1988, Sondergaard et al., 2003).

To reduce internal nutrient loading *in situ* remediation of the sediments may be required. Possible remediation of internal loading can be achieved by a variety of methods. Two that directly involve the sediments are:

- Sediment dredging - removing phosphorus rich sediment

- Sediment sealing – covering phosphorus rich sediment

Both these methods have the potential to change the sediments physically or chemically. Therefore an understanding of the chemical and physical processes occurring in sediments is needed before these remediation techniques are considered.

1.3 Early diagenesis

Early diagenesis, the oxidation of organic matter, dominates the chemical processes in sediments. Many studies have found diagenetic reactions within the sediments to enhance release of phosphorus and other trace elements into the overlying water column. As organic matter is the driving force of early diagenesis, these reactions are expected to be very important in lakes that receive high organic matter input (Berner, 1980).

In studying early diagenesis, the focus is on the chemical composition of pore water. Pore waters are extremely sensitive indicators of digenetic reactions occurring within the sediments and show marked changes in chemical composition, whereas changes in the chemical composition of sediments may be undetectable (Berner, 1980).

1.4 Study Site

Lake Rotorua is located in the Central Volcanic Plateau of the North Island, New Zealand, formed 140 000 years ago by the eruption of the Mamaku Ignimbrite, resulting in a lake that occupies the Rotorua Caldera (Lowe and Green, 1987). The lake is shallow, with a mean depth of 10.7 m, and polymictic, with periods of stratification over summer lasting from days to weeks. Lake Rotorua is the largest (area of 80 km^2) of the twelve lakes in the Rotorua district (Figure 1.1). One third of international visitors to New Zealand stay in Rotorua, with the lake popular for tourist activities and local recreation such as boating and fishing. However these activities are limited by the lakes poor water quality (EBOP, 2006).

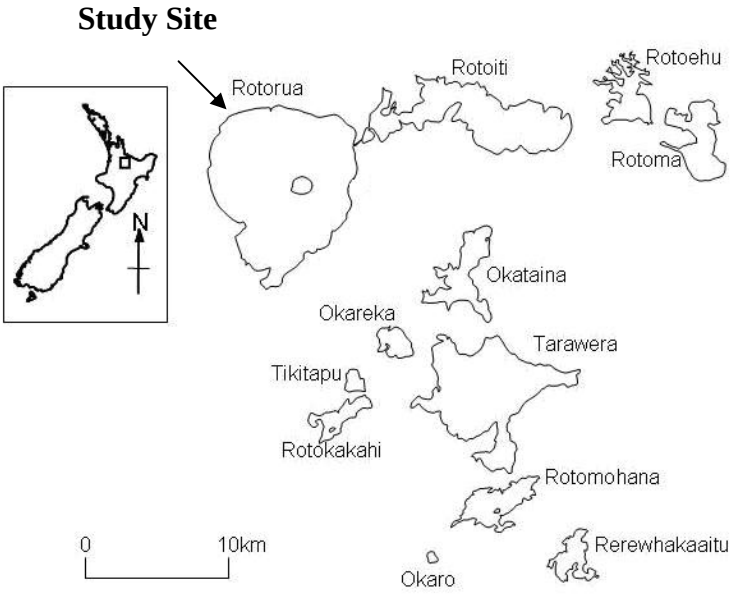

Figure 1-1 *Location of study site, Lake Rotorua and other Rotorua lakes.*

Lake Rotorua has become increasingly eutrophic in recent decades, with nuisance growth of macrophytes observed in the early 1960s (White, 1977). Prolific blooms of nuisance cyanobacteria are now common over summer. In the past Lake Rotorua received high external nutrient inputs when Rotorua City's waste water was discharged into the lake from 1973 until 1991 when it was diverted to the Whakarewarewa Forest for spray irrigation. Despite the diversion of waste water the lake has remained eutrophic, with water column concentrations of total phosphorus reported as 0.055 mg/L and total nitrogen as 0.814 mg/L (Burger,

2006). Nutrient inputs from land use activities such as agriculture are becoming an important source of nutrients, and nitrate concentrations in groundwater are increasing in response to these activities (Morgenstern and Gordon, 2006).

Lake Rotorua has a catchment area of 424 km^2 with 50% in agriculture (Rutherford, 1984). There are nine major inflows into Lake Rotorua and 17 minor inflows. The external nutrient loading though these inflows was found to be 50 t yr^{-1} for TP and 532 t yr^{-1} for TN. The Ohau Channel is the only outflow yeilding 19 tonnes TP and 236 tonnes TN from the lake per year (Beyá et al., 2005). Two geothermal fields drain into Lake Rotorua, Tikitere, and Rotorua, contributing nitrogen and phosphorus but also elevated concentrations of sulfate (White et al., 2004).

A number of previous studies have indicated that the sediments of Lake Rotorua are a significant source of nutrients to the overlying water column (Rutherford et al., 1996, White et al., 1978). Burger (2006) found nutrient release rates of soluble reactive phosphorus (SRP) and ammonium (NH_4) from the sediments of Lake Rotorua by benthic chambers to be more significant than external nutrient sources.

1.5 Aims and Objectives

The major aim of this thesis is to gain an understanding of the transfer of nutrients and trace elements from the pore waters of Lake Rotorua and the early diagenetic processes controlling the transfer. This information contributes to a larger project on Lake Rotorua's sediments, which is designed to examine potential for their remediation as part of the lake restoration strategy.

The specific objectives of this study are;

- Collection, analysis and interpretation of sediment pore water chemistry, paying particular attention to the nutrients phosphorus and ammonium.

- Calculation of nutrient release rates from pore water concentration profiles by Fick's first law of diffusion.

- Investigation of the composition and source of gas present in the sediments.

- Determination of ebullition rates of gas by measuring release rate from the sediments.

1.6 References

BERNER, R. A. (1980) *Early Diagenesis: A theoretical approach,* New Jersey, Princeton University Press.

BEYÁ, J., HAMILTON, D. & BURGER, D. (2005) Analysis of catchment hydrology and nutrient loads for lakes Rotorua and Rotoiti. Centre for Biodiversity and Ecology Research, The University of Waikato.

BOSTROM, B., ANDERSEN, J. M., FLEISCHER, S. & JANSSON, M. (1988) Exchange of phosphorus across the sediment-water interface. *Hydrobiologia,* 170**,** 229-244.

BURGER, D. (2006) Dynamics of internal nutrient loading in a eutrophic, polymictic lake (Lake Rotorua, New Zealand) Phd thesis. *Department of Biological Sciences.* Hamilton, University of Waikato.

EBOP (2006) Rotorua Lakes Recreation Strategy. *Environment Bay of Plenty, Rotorua District Council, and Te Arawa Maori Trust Board joint publication.* Environmental Publication 2006/01.

FOY, R. H. & WITHERS, P. J. A. (1995) The contribution of agricultural phosphorus to eutrophication. *The Fertiliser Society* London, The Fertiliser Society.

JEPPESEN, E., SONDERGAARD, M., JENSEN, J. P., HAVENS, K. E., ANNEVILLE, O., CARVALHO, L., COVENEY, M. F., DENEKE, R., DOKULIL, M. T., FOY, B., GERDEAUX, D., HAMPTON, S. E., HILT, S., KANGUR, K., KOHLER, J., LAMMENS, E., LAURIDSEN, T., MANCA, M., MIRACLE, M. & MOSS, B. (2005) Lake responses to reduced nutrient loading - an analysis of contemporary long-term data from 35 case studies. *Freshwater Biology,* 50**,** 1747-1771.

LOWE, D. & GREEN, J. D. (1987) Origins and development of the lakes. IN VINER, A. B. (Ed.) *Inland Waters of New Zealand.* Wellington, DSIR.

MORGENSTERN, U. & GORDON, D. (2006) Prediction of future nitrogen loading to Lake Rotorua, The Institute of Geological and Nuclear Sciences (GNS Science) science report 2006/10.

PARLIAMENTARY COMMISSIONER FOR THE ENVIRONMENT (2006) Restoring the Rotorua Lakes: The ultimate endurance challenge. Wellington, Parliamentary Commissioner for the Environment.

RUTHERFORD, J. C. (1984) Trends in Lake Rotorua water quality. *New Zealand Journal of Marine and Freshwater Research,* 18**,** 355-365.

RUTHERFORD, J. C., DUMNOV, S. M. & ROSS, A. H. (1996) Predictions of phosphorus in Lake Rotorua following load reductions. *New Zealand Journal of Marine and Freshwater Research* 30**,** 383-396.

SONDERGAARD, M., JENSEN, J. P. & JEPPESEN, E. (2003) Role of sediment and internal loading of phosphorus in shallow lakes. *Hydrobiologia,* 506-509**,** 135-145.

WHITE, E. (1977) Eutrophication of Lake Rotorua. *DSIR Information Series No. 123*

WHITE, E., DON, B. J., DOWNES, M. T., KEMP, L. J., MACKENZIE, A. L. & PAYNE, G. W. (1978) Sediments of Lake Rotorua as sources and sinks for plant nutrients. *New Zealand Journal of Marine and Freshwater Research,* 12**,** 121-130.

WHITE, P. A., CAMERON, S. G., KILGOUR, G., MROCZEK, E., BIGNALL, G., DAUGHNEY, C. & REEVES, R. R. (2004) Review of groundwater in the Lake Rotorua catchment. *Report to Environment Bay of Plenty (2004/130).* Taupo, Institute of Geological & Nuclear Sciences.

2. LITERATURE REVIEW

2.1 Introduction

The purpose of this chapter is to provide a review of the diagenetic processes that occur within lake sediments, with particular attention on processes contributing to eutrophication of a water body. This review will provide a framework which will aid in the interpretation of the results presented within this thesis.

2.2 Pore water

Pore water is the aqueous solution that fills the pore spaces of solid particles within sediments of a water body. The interface between the sediment and overlying water is an important reference point that separates the two phases: the sediment, i.e., the solid particles and pore water, and the overlying water column (Lerman, 1979). This region is commonly referred to as the sediment-water interface (Figure 2.1). The pore water is the link between the sediments and the overlying water, with the sediment-water interface associated with steep gradients in density, particle and solution composition, activities of chemical species, pH, redox potential and biological activity between the two phases (Santschi, 1990).

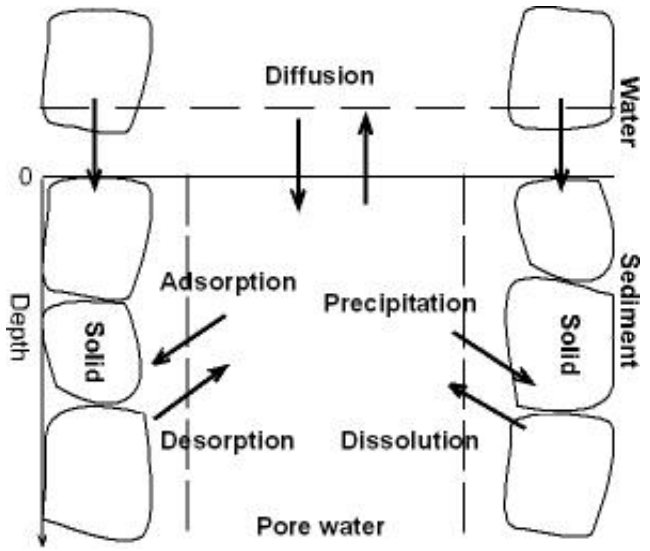

Figure 2-1 *Sediment-pore water interaction showing adsorption/desorption and precipitation/dissolution reactions (Lerman, 1979).*

2.3 Early diagenesis

Upon deposition, sediments undergo early diagenesis. Early diagenesis is the chemical, physical and biological changes that sediments undergo after they are deposited at the sediment-water interface (Berner, 1980).

Sediment can be a source or sink for chemical species. Authigenic processes within sediment remove chemical species permanently from the recycling within the system by formation of minerals. However before being permanently buried chemical species may be recycled many times across the sediment-water interface by chemical, physical, and biological reactions (Santschi, 1990). Inorganic and organic particles within sediment may react within pore water, changing concentrations of dissolved species. Chemical reactions between pore water and solid particles include precipitation/dissolution and adsorption/desorption reactions (Figure 2.1). Dissolution, desorption, and decomposition are sources of dissolved species. Precipitation and adsorption reactions are sinks for dissolved species. Molecular diffusion transports dissolved species in pore water in directions generated from gradients in concentration. In a sediment column at steady state, pore water and solid particles move downward from the sediment-water interface (Lerman, 1979). In the study of early diagenesis measurements of pore water concentration profiles are required as these reflect diagenetic processes occurring within the sediment.

2.4 Concentration profiles

There are three key processes that affect concentration profiles of substances in pore water

1. A substance is removed within pore water, i.e. by precipitation or adsorption.
2. A substance is released into pore water from the solid phase, i.e. by dissolution or desorption.
3. Dissolved substances are transported by diffusion within pore water and across the sediment-water interface (Schulz, 2006).

There have been many concentration profiles observed in pore water. Figure 2.2 outlines some common profiles that have been reported in multiple pore water studies.

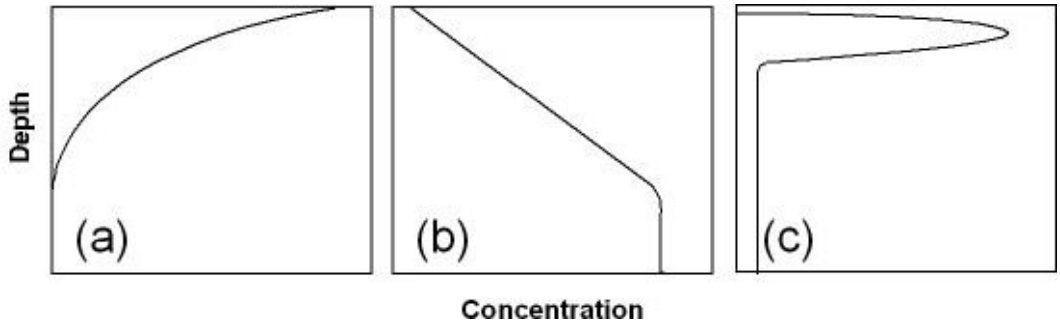

Figure 2-2 *Common concentration profiles measured in pore water showing, (a) profile of a substance being removed from the pore water to the sediment or diffusing from the lake to the pore waters (Schulz, 2006), (b) profile of a substance being released into pore water at depth (Schulz, 2006), (c) profile of a substance being released into pore water near the sediment surface then removed from pore water at depth (Berner, 1980).*

The concentration profile illustrated by Figure 2.2a indicates a substance being consumed in the upper layers of the sediment by diagenetic processes, or diffusing from the lake into the pore water. This profile is characteristic of dissolved oxygen. The concentration gradient is greatest at the surface and as it diffuses through the sediment it is being consumed or removed and the concentration approaches zero deeper within the profile.

The concentration profile in Figure 2.2b shows a substance being released into the pore water at a certain depth. Above the release depth is a constant concentration gradient where the substance is removed from the pore water in the upper sediment layers (Schulz, 2006). Ammonium concentrations often show this profile. The decomposition of organic matter at depths of 50-100 cm can release ammonium for decades after it was initially deposited at the sediment-water interface (Carignan and Lean, 1991).

The profile in Figure 2.2c shows a peak in concentration just below the sediment surface. This peak indicates that the substance is diffusing in both upward and downward directions along the concentration gradient. The substance is released

into the overlying water body, and then removed from the pore water by diagenetic reactions deeper in the sediment. The absence of a concentration gradient at depth indicates no further removal through the profile. Phosphate often displays this profile. Berner (1980) interpreted the profile as two separate processes:

1. Organic phosphorus is decomposed by bacteria in the upper layers of the sediment releasing dissolved phosphate into the pore water.
2. Phosphate is removed from pore water by the precipitation of authigenic minerals, such as vivianite, deep in the sediment.

Three basic rules can be applied when interpreting concentration profiles:

1. Diffusive fluxes of substances occur as concentration gradients; these gradients represent existence of diffusive fluxes.
2. In most cases reactions occurring in pore water result in changes in concentration gradients.
3. A concave shape in the concentration profile as shown in (Figure 2.2a) shows the depletion of a substance from pore water. A convex shape concentration profile as shown in Figures 2.2b and Fig. 2.2c shows the release of a substance into pore water (Schulz, 2006).

2.5 Organic Matter

Decomposition of organic matter is the driving force of early diagenesis, especially within eutrophic lakes where organic matter accumulation in sediments is high. The decomposition of organic matter is shown by the Redfield reaction:

$$(CH_2O)_{\alpha C}(NH_3)_{\alpha N}(H_3PO_4)_{\alpha P} + \tfrac{1}{2}\alpha_C SO_4^{2-} \rightarrow \alpha_C HCO_3^- + \alpha_N NH_3 + \alpha_P H_3PO_4 + \tfrac{1}{2}\alpha_C H_2S$$

Where CH_2O is the organic matter and α_C, α_N, and α_P are the stoichiometric coefficients of C, N, and P in the organic matter (Lerman, 1979). These are commonly reported as a ratio of 106:16:1 for α_C, α_N, and α_P, respectively, for oceanic plankton, however in freshwater this ratio has been found to be higher and more variable (Hecky et al., 1993), with Carignan and Lean (1991) reporting values of 157:11.5:1 in a mesotrophic lake in Canada.

The Redfield reaction shows production of bicarbonate, ammonia, phosphate and reduction of sulfate to sulfide during organic matter decomposition. In freshwater systems methane is commonly produced in the absence of sulfate (Lerman, 1979, Capone and Kiene, 1988).

Organic matter undergoes decomposition by oxidation. Initially organic matter is oxidised by reduction of dissolved oxygen. In lake sediments oxygen is usually only found in the top 1-2 cm of sediment due to the slow process of molecular diffusion and rapid consumption by microbes. In eutrophic lakes oxygen may be present only to a depth in the sediments of a few mm beneath the sediment-water interface due to rates of oxygen consumption exceeding resupply rates (Santschi, 1990). Once oxygen is consumed microorganisms reduce various other electron acceptors in order of decreasing reduction potential, as shown in Table 2.1.

Table 2-1 Sequence of redox reactions in natural environments involving organic carbon (Stumm and Morgan, 1981).

O_2 consumption	
¼ (CH_2O) + ¼O_2	= ¼CO_2 + ¼H_2O
Denitrification	
¼ (CH_2O) + 1/5 NO_3^- + 1/5 H^+	= ¼CO_2 + 1/10 N_2 + ½H_2O
Nitrate reduction	
¼ (CH_2O) + ⅛NO_3^- + ¼H^+	= ¼CO_2 + ⅛NH_4^+ + ⅛H_2O
Manganese reduction	
¼ (CH_2O) + ½$MnO_{2(s)}$ + H^+	= ¼CO_2 + ½Mn^{2+} + ⅛H_2O
Iron reduction	
¼ (CH_2O) + $FeOOH_{(s)}$ + 2H^+	= ¼CO_2 + 7/4 H_2O + Fe^{2+}
Sulfate reduction	
¼ (CH_2O) + ⅛SO_42^- + ⅛H^+	= ¼CO_2 + ⅛HS^- + ¼H_2O
Methane fermentation	
¼ (CH_2O)	= ⅛CO_2 + ⅛CH_4

These reactions result in sediments becoming increasingly anoxic with depth, as each reaction decreases the redox potential. The reduced species, NH_4^+, Mn^{2+}, Fe^{2+}, H_2S, and CH_4, are released into pore water and are able to diffuse along concentration gradients. If they come into contact with oxygen at the sediment-

water interface they are quickly oxidised. In eutrophic lakes, where oxygen is commonly absent due to respiration arising from decomposition of organic matter, oxidation is prevented and elements are able to migrate into the overlying water body, commonly describe by the migration of the redox boundary (Santschi, 1990).

These principal reactants of redox transformations and their effect on trace element recycling are discussed below.

2.6 Nitrogen

In natural waters inorganic nitrogen is found mostly in the forms NO_3^-, N_2 and NH_4^+, as these are the thermodynamically stable forms found in the characteristic Eh-pH conditions. In the absence of oxygen, nitrate has the ability to stabilise the redox potential of surface sediments by preventing the reduction of iron oxides at concentrations >1 mg N L^{-1} (Kleeberg and Kozerski, 1997). Nitrate and iron oxides can be reduced by the same microbes. These microbes prefer nitrate and will only reduce iron oxides when nitrate is depleted (Wetzel, 2001).

Within sediments inorganic nitrogen is found mostly as the reduced form ammonium. Ammonium is formed from the decomposition of organic matter, where organic nitrogen compounds are hydrolysed, and also from the reduction of nitrate (Forsberg, 1989). When ammonium comes into contact with dissolved oxygen, either at the sediment-water interface or the overlying water column, it quickly undergoes nitrification. Nitrate is then available for uptake by algae or it can be denitrified and released as N_2 (Wetzel, 2001).

Nitrogen compounds, as well as carbon compounds can be released from sediments for decades after the initial deposition of organic matter. The decomposition of nitrogen and carbon in freshwater systems has been described by three classes of organic compounds, commonly referred to as G_0, G_1, and G_2. G_0 decomposes as it descends through the water column, and has a half life of ~ 1 week, while G_1 and G_2 decompose within the sediments with much longer half lives of ~ 3 and 75 years, respectively. G_2 has been found to account for the

majority of the regeneration from decomposition of organic matter (Carignan and Lean, 1991).

2.7 Iron and Manganese

Iron and manganese have very similar chemistry in sediments and are therefore discussed together. Under oxic conditions iron and manganese are found as Fe^{3+} and Mn^{4+}, commonly as insoluble oxide/hydroxides. Theses oxide/hydroxides have very large surface areas in which many trace elements and oxyanions can be adsorbed. Under anoxic conditions and when there is nitrate depletion, these oxides undergo reduction to their soluble reduced forms, ferrous and manganous (Fe^{2+} and Mn^{2+}). These redox reactions greatly affect the biogeochemical cycling of many trace elements as they are desorbed and the oxide/hydroxides undergo dissolution to be released into the pore water (Santschi, 1990). This release of trace elements was first observed by Mortimer (1941, 1942), whose classical theory outlines the enhanced release of phosphorus and other elements into overlying lake water under anoxic conditions in bottom waters during thermal stratification.

Two main differences exist between iron and manganese chemistry. Manganese is reduced at a higher redox potential than iron and iron oxidises more rapidly than manganese (Balistrieri et al., 1992).

While Fe^{2+} and Mn^{2+} are extremely soluble relative to most inorganic ions, solid phases can form when the solubility product is exceeded. Many studies of eutrophic lakes have observed authigenic mineral formation of siderite ($FeCO_3$), iron sulfides (FeS, FeS_2), vivianite [$Fe_3(PO_4)_2 \cdot 8H_2O$], rhodochrosite ($MnCO_3$), manganese sulfides (MnS) and reddingite ($Mn_3(PO_4)_2 \cdot 3H_2O$) (Davison, 1993, Holdren and Armstrong, 1986).

2.8 Sulfur

Sulfur is present as sulfate (SO_4^{2-}) in its oxidised form and sulfide (S^{2-}) in its reduced form. The reduction of sulfur usually occurs deep within the sediment when all other electron acceptors have been depleted (Santschi, 1990). However, flocculent layers of organic matter observed above the sediment-water interface have been found to cause the zone of SO_4^{2-} reduction to migrate above the sediment-water interface (Sherman et al., 1994).

Sulfate is generally present in low concentrations in lakes. However, within eutrophic lakes organic matter availability is higher and therefore sulfate concentrations increase (Holmer and Storkholm, 2001). Lakes that are fed by geothermal waters can also have significantly higher sulfate concentrations.

Dissolved sulfide in the pore water is able to precipitate with trace metals forming metal sulfides. One of the most important in regards to eutrophication is the formation of iron sulfides such as pyrite. Iron sulfides prevent the readsorption of phosphorus to iron oxides, due to reduced iron availability, enhancing the release of phosphorus into overlying lake water (Holmer and Storkholm, 2001). High availability of sulfate ions stimulates the decomposition of organic matter due to its role as an electron acceptor. Sulfate concentrations of 2 mmol L^{-1} added to pore waters have been found to increase PO_4^{3-} and NH_4^+ concentrations in pore water (Smolders et al., 2006).

2.9 Methanogenesis

Methanogenesis frequently occurs in anoxic sediments undergoing early diagenesis. An end product of the decomposition of organic matter, methanogenesis can occur by two different pathways: reduction of carbon dioxide,

$$CO_2 + 4H_2 \rightarrow CH_4 + 2H_2O.$$

and acetate fermentation,

$$CH_3COO^- + H^+ \rightarrow CH_4 + CO_2.$$

Acetate fermentation is regarded as the most common pathway for methane formation within freshwater sediments, with it reported as accounting for 70% of methane production (Whiticar et al., 1986).

Values of $\delta^{13}C$ have been used to determine the dominant pathway of methanogenesis as methane is generally depleted in $\delta^{13}C$ and carbon dioxide enriched in $\delta^{13}C$. Methane produced from acetate fermentation is more enriched in $\delta^{13}C$ than CO_2, with stable isotope compositions ranging from -50 to -65‰ (Woltemate et al., 1984). Methane produced by CO_2 reduction can have isotope compositions of -60 to -110‰ (Whiticar et al., 1986, Lansdown et al., 1992). $\delta^{13}C$ of CO_2 in both processes enriches ^{13}C. By plotting values against each other, as in Figure 2.3 the dominant pathway can be established.

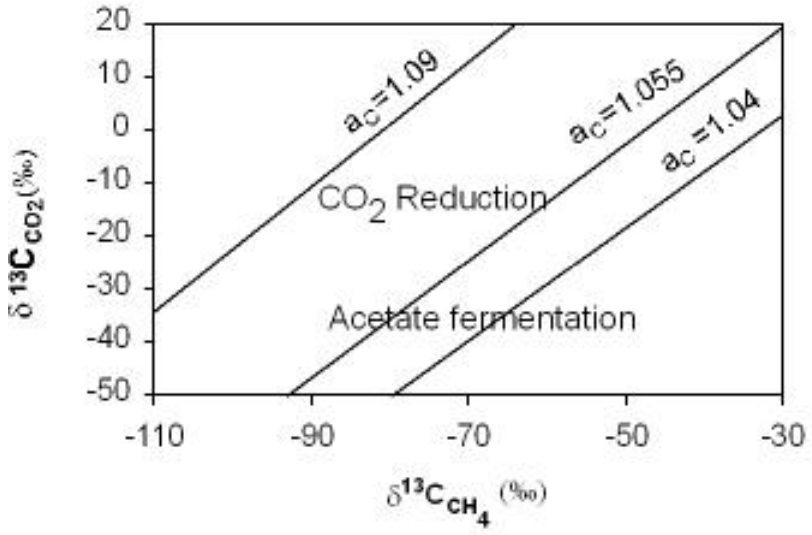

Figure 2-3 *Cross-plot of $\delta^{13}C$ values for CH_4 and CO_2 on how to resolve carbon dioxide reduction and actetate fermentation (Whiticar et al., 1986).*

The lines of constant α_C shown in Figure 2.3 indicate the boundaries of the two pathways as suggested by Whiticar (1986). Acetate fermentation falls between α_C values 1.04 and 1.055, and carbon dioxide reduction falls between 1.055 and 1.09. With α_C defined as the stable isotope fractionation between CO_2 and CH_4.

Either methanogenesis or sulfate reduction is commonly the dominant process in the decomposition of organic matter, and is dependant on concentrations of sulfate. In systems of high sulfate concentration sulfate reduction can suppress

methanogenesis and is the dominant process in organic matter decomposition. Sulfate reducing bacteria out-compete methanogens for acetate. In low sulfate environments methanogenesis is the dominant pathway for terminal carbon metabolism (Capone and Kiene, 1988). However in freshwater sediments both processes can occur. At sulfate concentrations of > 30 μM a zone of sulfate reduction can occur. Here sulfate reducing bacteria maintain acetate concentrations that are too low for methanogens to grow. When sulfate concentrations become so low, a methanogenic zone develops below the zone of sulfate reduction. Sulfate reducers are limited by low sulfate concentrations and are out-competed by methanogens for acetate (Lovley and Klug, 1986). Sherman et al. (1994) observed this shift in decomposition at 10 cm below the sediment-water interface in an oligotrophic lake in Wisconsin, USA.

2.9.1 Dissolved Inorganic Carbon.

Dissolved inorganic carbon (DIC) includes $CO_{2(aq)}$, HCO_3^-, and CO_3^{2-}. In sediments the oxidation of particulate organic carbon (POC) by O_2, NO_3^-, Mn_4^+, Fe_3^+, SO_4^-, and CH_4 releases dissolved inorganic carbon into pore water, with SO_4^- reduction generally the dominant process of anaerobic respiration. When SO_4^- is depleted, methanogenesis can become the dominant process of anaerobic respiration (Herczeg, 1988).

^{13}C stable isotope analysis of DIC has been used by many authors to distinguish if methanogenesis is the dominant process driving anaerobic respiration. DIC derived from the oxidation of O_2, NO_3^-, Mn_4^+, Fe_3^+, and SO_4^-, will have an isotopic value similar to that of its source POC. The $\delta^{13}C$ of C-3 plants is around -28‰, whereas DIC released from methanogenesis as a by-product can be significantly enriched in ^{13}C relative to the source POC, by 30 to 40 ‰. This is due to the methyl moiety in the acetate fraction of the C_{org} preferentially incorporating ^{12}C (Herczeg, 1988, LaZerte, 1981).

2.9.2 Ebullition

Bubbles of methane can form when the concentration of dissolved methane in pore water exceeds its solubility (Whiticar et al., 1986). Release of methane from the sediments can then occur, known as ebullition. Methane is an important greenhouse gas, and when released by ebullition it commonly enters the atmosphere as little undergoes oxidation to CO_2 within the sediment and water column (Martens and Klump, 1980).

The ebullition of gas has long being suspected of enhancing nutrient release from sediments as it causes turbulence within the sediments and resuspension of sediment particles and pore water (Bostrom et al., 1988). A laboratory microcosm study of undisturbed sediment cores by Liikanen et al. (2003) found significant relationships between ebullition rate of gas and increased nutrient release rates of PO_4 and NH_4. For every 30 mg CH_4-C m^{-2} d^{-1} released from lake sediments, Liikanen et al. (2003) found release of 4 mg PO_4-P m^{-2} d^{-1} and 50 mg NH_4-N m^{-2} d^{-1}.

2.10 Trace element recycling

Of all of the diagenetic reactions the biogeochemical cycling of iron and manganese has the largest impact on the biogeochemical cycling of many trace elements. One of the most important of the trace elements influenced by iron and manganese cycling is phosphorus.

2.10.1 Phosphorus

The role of phosphorus in lake sediments has been extensively studied due to its role as a limiting nutrient in lake productivity. Two main forms of phosphorus are found in sediments: dissolved phosphorus, consisting of phosphate, and organic phosphorus, and particulate phosphorus, which include organic compounds and inorganic sediment components which phosphorus binds with, e.g., iron and calcium. Phosphorus generally enters the sediment in particulate form and is returned to the water column in dissolved form (Marsden, 1989). Lake sediments

can either retain or release phosphorus depending largely on the trophic status of a lake. In nutrient-poor oligotrophic lakes phosphorus deposited to the sediment is mostly retained, however, as the trophic level increases, phosphorus in increasingly released from the sediment and transported to the overlying water column. This release can exceed the amount of phosphorus that is deposited and will therefore enhance primary productivity of the lake (Boström et al., 1982).

Sinks of phosphorus within sediments include adsorption onto iron and manganese oxides/hydroxides under aerobic conditions. In anoxic environments phosphorus commonly forms mineral phases with iron and calcium when the solubility product is exceeded. Phosphorus reacts with calcium to form apatite, and with iron to form vivianite (Lerman, 1979, Sarazin et al., 1995). Vivianite has been found to be major sink for phosphorus in lake sediments by controlling concentrations in pore water (Holdren and Armstrong, 1986). However Emerson and Widmer (1978) found less than 15% of the phosphate released by organic matter degradation over the summer months was removed by the sediments of a eutrophic lake. The low efficiency of the sediments for phosphorus retention is due to the low rate of crystal growth of vivianite (Emerson and Widmer, 1978).

2.10.1.1 Release Mechanisms

There are two important steps in the release of phosphorus. Phosphorus must first be released into solution from the solid sediment, and then dissolved phosphorus is transported to the overlying water column, as illustrated in Figure 2.4. Mobilisation of phosphorus from sediment includes physico-chemical processes; desorption, dissolution, and ligand exchange, and microbial processes; enzymatic hydrolysis and ligand exchange. Diffusion, wind-induced turbulence, bioturbation, and gas ebullition are transport mechanisms (Boström et al., 1982a).

Mechanisms of phosphorus release from sediment are largely dependent on lake morphology. In deep lakes that undergo anoxic thermal stratification, phosphorus release occurs mostly by reduction of iron and manganese oxides, and released phosphorus is then transported by molecular diffusion.

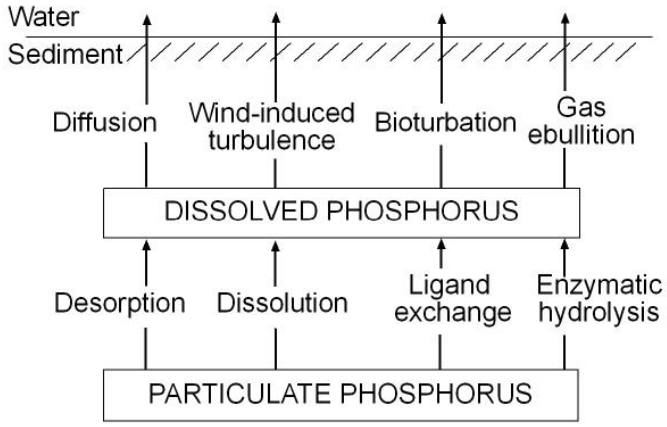

Figure 2-4 *Processes involved in phosphorus release from lake sediments (Boström et al., 1982).*

In polymictic lakes (shallow, and nonstratified), mechanisms of release can also include redox-related transitions, but can also include a range of other chemical, biological, and physical processes (Bostrom et al., 1988). A range of various processes that have been found to influence phosphorus release from sediments are listed below:

- In eutrophic lakes, sediments receive large amounts of organic matter. During remineralisation of organic matter, microbes in the sediment take up, store and release phosphorus (Sondergaard et al., 2003)**.**

- Warmer temperatures indirectly affect the release of phosphorus by stimulating microbial activity. This increases remineralisation of organic matter and hence decreases the depth of oxygen penetration into the sediment, which results in increased concentrations of phosphorus in pore water (Holdren and Armstrong, 1986, Marsden, 1989).

- Observations have been made of high rates of phosphorus release from aerobic sediments in association with elevated pH. Removal of CO_2 by photosynthesis, which may be enhanced for example by blooms of phytoplankton, can also result in large increases in pH. Desorption of

phosphorus from iron oxides increases as the pH rises above 8 due to increased competition of ligand exchange on the surface of iron oxides ($OH^{-1} \leftrightharpoons H_2PO_4^{-1}$) (Drake and Heaney, 1987).

- Under aerobic conditions the Fe:P ratio in pore water can affect the release of phosphorus. Phosphorus is immobilised by adsorption when Fe^{2+} is oxidised if the Fe:P ratio within the sediment is greater than 1.8 (Holdren and Armstrong, 1986, Marsden, 1989). This results in the diffusive flux of phosphorus that will be larger than that of iron, so more phosphorus can be transported across the sediment-water interface than can be adsorbed onto recently precipitated iron oxides (Löfgren and Böstrom, 1989).

- Bioturbation by benthic invertebrates and gas bubbles (ebullition) can enhance the release of phosphorus from sediments by disturbing concentration gradients. Bioturbation from benthic invertebrates can also prevent phosphorus release by distributing oxygenated lake water into the sediment (Sondergaard et al., 2003).

- Iron sulfide formation can cause dissolution of vivianite:

  $$Fe_3(PO_4)_2 \cdot 8H_2O + 3H_2S \rightarrow 3FeS + 2H_3PO_4 + 8H_2O$$

  This reaction lowers concentrations of Fe^{2+} in the pore water, resulting in higher phosphate concentrations in the pore water that enhance the diffusive flux into the overlying water column (Gächter and Müller, 2003).

2.10.2 Heavy metals

Low concentrations of the heavy metals arsenic, cadmium and lead can cause toxicity in organisms. These heavy metals can accumulate in the sediments and hence may be released into the pore water by diagenetic reactions where they are available from biological uptake. The recycling of heavy metals within sediments is controlled by two key processes:

1. Redox transformations – the adsorption/desorption of trace metals on iron and manganese oxide/hydroxides, and also formation of sulfides.

2. Biological uptake and release – the adsorption/desorption of trace metals onto organic matter and also uptake and release by assimilation.

Numerous studies have found organic matter to be an important carrier phase of trace metals, with elevated concentrations of these metals found in association with the remineralisation of dead algae (Sigg et al., 1987). Similarly, many studies have observed the recycling of heavy metals in sediments associated with the iron and manganese redox reactions that result in adsorption/desorption of the metals. The formation of metal sulphides in sediments has been reported to reduce concentrations of trace metals As, Pb, and Cd within pore water. Mucci et al. (2000) found that arsenic was incorporated into authigenic iron sulfides at levels up to 800-1000 ppm As. Dissolved arsenic, lead and cadmium move by molecular diffusion within the pore water where they can either diffuse up into the lake water and be removed by iron and manganese oxides or diffuse down into anoxic sediments were they can precipitate authigenic minerals (Belzile and Tessier, 1990, De Vitre et al., 1991, Song and Müller, 1995).

2.12 References

BALISTRIERI, L. S., MURRAY, J. W. & PAUL, B. (1992) The cycling of iron and manganese in the water column of Lake Sammamish, Washington. *Limnology and Oceanography,* 37**,** 510-528.

BELZILE, N. & TESSIER, A. (1990) Interactions between arsenic and iron oxyhydroxides in lacustrine sediments. *Geochimica et Cosmochimica Acta,* 54**,** 103-109.

BERNER, R. A. (1980) *Early Diagenesis: A theoretical approach,* New Jersey, Princeton University Press.

BOSTROM, B., ANDERSEN, J. M., FLEISCHER, S. & JANSSON, M. (1988) Exchange of phosphorus across the sediment-water interface. *Hydrobiologia,* 170**,** 229-244.

BOSTRÖM, B., JANSSON, M. & FORSBERG, C. (1982) Phosphorus release from lake sediments. *Archiv fuer Hydrobiologie,* 18**,** 5-59.

CAPONE, D. G. & KIENE, R. P. (1988) Comparison of microbial dynamics in marine and freshwater sediments: Contrasts in anaerobic carbon catabolism. *Limnology and Oceanography,* 33**,** 725-749.

CARIGNAN, R. & LEAN, D. R. S. (1991) Regeneration of dissolved substances in a seasonally anoxic lake: The relative importance of processes occurring in the water column and in the sediments. *Limnology and Oceanography,* 36**,** 683-707.

DAVISON, W. (1993) Iron and manganese in lakes. *Earth-Science Reviews,* 34**,** 119-163.

DE VITRE, R., BELZILE, N. & TESSIER, A. (1991) Speciation and adsorption of arsenic on diagenetic iron oxyhydroxides. *Limnology and Oceanography,* 36**,** 1480-1485.

DRAKE, J. C. & HEANEY, I. (1987) Occurrence of phosphorus and its potential remobilisation in the littoral sediments of a productive English lake. *Freshwater Biology,* 17**,** 513-523.

EMERSON, S. & WIDMER, G. (1978) Early diagenesis in anaerobic lake sediments-II. Thermodynamic and kinetic factors controlling the formation of iron phosphate. *Geochimica et Cosmochimica Acta,* 42**,** 1307-1316.

FORSBERG, C. (1989) Importance of sediments in understanding nutrient cycling in lakes. *Hydrobiologia,* 176/177**,** 263-277.

GÄCHTER, R. & MÜLLER, B. (2003) Why the phosphorus retention of lakes does not necessarily depend on the oxygen supply to their sediment surface. *Limnology and Oceanography,* 48**,** 929-933.

HECKY, R. F., CAMPBELL, P. & HENDZEL, L. L. (1993) The stoichiometry of carbon, nitrogen, and phosphorus in particulate matter of lakes and oceans. *Limnology and Oceanography.,* 38**,** 709-724.

HERCZEG, A. L. (1988) Early diagenesis of organic matter in lake sediments: A stable carbon isotope study of pore waters. . *Chemical Geology (Isotope Geoscience Section),* 72**,** 199-209.

HOLDREN, G. C. & ARMSTRONG, D. E. (1986) Interstitial ion concentrations as an indicator of phosphorus release and mineral formation in lake sediments. IN SLY, P. G. (Ed.) *Sediments and Water Interactions.* New York, Springer-Verlag.

HOLMER, M. & STORKHOLM, P. (2001) Sulfate reduction and sulfur cycling in lake sediments: a review. *Freshwater Biology,* 46**,** 431-451.

KLEEBERG, A. & KOZERSKI, H. (1997) Phosphorus release in Lake Grosser Müggelsee and its implications for lake restoration. *Hydrobiologia,* 342/343**,** 9-26.

LANSDOWN, J. M., QUAY, P. D. & KING, S. L. (1992) CH_4 production via CO_2 reduction in a temperate bog: A source of ^{13}C-depleted CH_4. *Geochimica et Cosmochimica Acta,* 56**,** 3493-3503.

LAZERTE, B. D. (1981) The relationship between total dissolved carbon and its stable isotope ratio in aquatic sediments. *Geochimica et Cosmochimica Acta,* 45**,** 647-656.

LERMAN, A. (1979) *Geochemical processes: Water and sediment environments,* Toronto, John Wiley & Sons.

LIIKANEN, A., HUTTUNEN, J. T., MURTONIEMI, T., TANSKANEN, H., VÄISÄNEN, T., SILVOLA, J., ALM, J. & PERTTI, J. (2003) Spatial and seasonal variation in greenhouse gas and nutrient dynamics and their interactions in the sediments of a boreal eutrophic lake. *Biogeochemistry,* 65**,** 83-103.

LÖFGREN, S. & BÖSTROM, B. (1989) Interstitial water concentrations of phosphorus, iron and manganese in a shallow eutrophic swedish lake - implications for phosphorus cycling. *Water Research,* 23**,** 1115-1125.

LOVLEY, D. R. & KLUG, M. J. (1986) Model for the distribution of sulfate reduction and methanogenesis in freshwater sediments. *Geochimica et Cosmochimica Acta,* 50**,** 11-18.

MARSDEN, M. W. (1989) Lake restoration by reducing external phosphorus loading: the influence of sediment phosphorus release. *Freshwater Biology,* 21**,** 139-162.

MARTENS, C. S. & KLUMP, J. V. (1980) Biogeochemical cycling in an organic rich coastal marine basin. Methane sediment-water exchange processes. *Geochimica et Cosmochimica Acta,* 44**,** 471-490.

MORTIMER, C. H. (1941) The exchange of dissolved substances between mud and water in lakes. *The Journal of Ecology,* 29**,** 280-329.

MORTIMER, C. H. (1942) The exchange of dissolved substances between mud and water in lakes. *The Journal of Ecology,* 30**,** 147-201.

SANTSCHI, P. (1990) Chemical processes at the sediment-water interface. *Marine Chemistry,* 30**,** 269-315.

SARAZIN, G., GAILLARD, J.-F., PHILIPPE, L. & RABOUILLE, C. (1995) Organic matter mineralisation in the pore water of a eutrophic lake (Aydat Lake, Puy de Dôme, France). *Hydrobiologia,* 315**,** 95-118.

SCHULZ, H. D. (2006) Quantification of early diagenesis: Dissolved constituents in marine pore water. IN SCHULZ, H. D. & ZABEL, M. (Eds.) *Marine Geochemistry.* 2nd ed. Berlin, Springer.

SHERMAN, L. A., BAKER, L. A., WEIR, E. P. & BREZONIK, P. L. (1994) Sediment pore-water dynamics of Little Rock Lake, Wisconsin: Geochemical processes and seasonal and spatial variability. *Limnology and Oceanography.,* 39**,** 1155-1171.

SIGG, L., STURM, M. & KISTLER, D. (1987) Vertical transport of heavy metals by settling particles in Lake Zurich. *Limnology and Oceanography,* 32**,** 112-130.

SMOLDERS, A. J. P., LAMERS, L. P. M., LUCASSEN, E. C., VAN DER VALDE, G. & ROELOFS, J. G. M. (2006) Internal eutrophication: How it works and what to do about it-a review *Chemistry and Ecology,* 22**,** 93-111.

SONDERGAARD, M., JENSEN, J. P. & JEPPESEN, E. (2003) Role of sediment and internal loading of phosphorus in shallow lakes. *Hydrobiologia,* 506-509**,** 135-145.

SONG, Y. & MÜLLER, G. (1995) Biogeochemical cycling of nutrients and trace metals in anoxic freshwater sediments of the Neckar River, Germany. *Marine and Freshwater Research,* 46**,** 237-243.

STUMM, W. & MORGAN, J. (1981) *Aquatic chemistry: An introduction emphasizing chemical equilibria in natural waters,* Toronto, John Wiley & Sons.

WETZEL, R. G. (2001) *Limnology: Lake and River Ecosystems,* San Diego, Academic Press.

WHITICAR, M. J., FABER, E. & SCHOELL, M. (1986) Biogenic methane formation in marine and freshwater environments: CO_2 reduction *vs.* acetate fermentation - Isotope evidence. *Geochimica et Cosmochimica Acta,* 50**,** 693-709.

WOLTEMATE, I., WHITICAR, M. J. & SCHOELL, M. (1984) Carbon and hydrogen isotopic composition of bacterial methane in shallow freshwater lake. *Limnology and Oceanography,* 29**,** 985-992.

3. METHODS

3.1 Introduction

The following chapter is divided into two sections; the collection and analysis of pore waters from the sediments of Lake Rotorua by sediment cores and peepers; and the collection and analysis of gas present in the sediment. Each section outlines the measures and procedures taken in the collection and analysis of samples used in this thesis.

3.2 Pore water

3.2.1 Sample locations

There are two types of sediments in Lake Rotorua. Coarse dense sediments cover the shallow margins (<10 m water depth) where wave action reworks the sediments preventing settling of finer material. In water depths generally greater than 10 m low density diatomaceous ooze dominates the sediments. Approximately 40 km^2 of Lake Rotorua's lake bed is covered in this light diatomaceous ooze. Sediment cores collected by gravity corer for pore water analysis were collected from 60 locations within this area on three occasions. Pore water from peepers was also collected from two locations, on two occasions. Figure 3.1 outlines sample locations and Appendix 1 contains full range of information for each sample collected.

3.2.2 Sediment core collection

Sediment cores were collected by a specially modified gravity corer. The gravity corer consists of a clear perspex core barrel that has a diameter of 65 mm and is 600 mm in length (Figure 3.2a). The corer was lowered to the lake bottom attached to a supporting line, until it touched the sediment bottom, then raised a metre above the sediment surface and dropped so that the core barrel was driven into the sediment by the weight of the corer. A valve seal snapped shut when tension was released and external weights were applied to trigger a supporting

line. A length of chain attached to the supporting line was used to aid the trigger to shut the seal (Figure 3.2b). This procedure allowed an undisturbed sediment sample to be removed from the lake bottom. The seal prevented lake water from flowing back into the core barrel as it was being winched to the surface of the lake. A piston was inserted into the bottom of the core barrel before being lifted above the lake water, in order to retain the sediment.

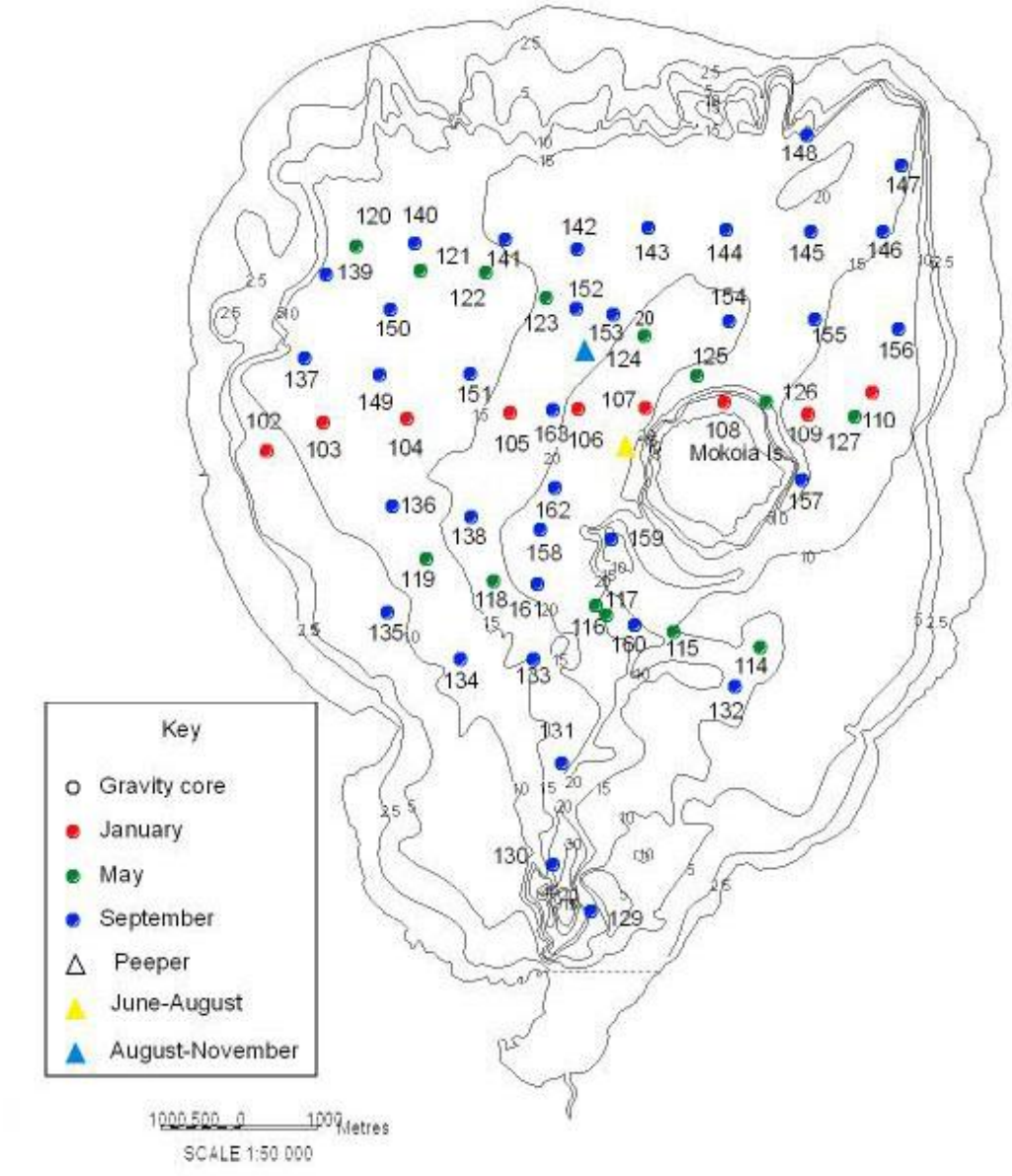

Figure 3-1 *Bathymetric map of Lake Rotorua with locations of sediment cores and peepers.*

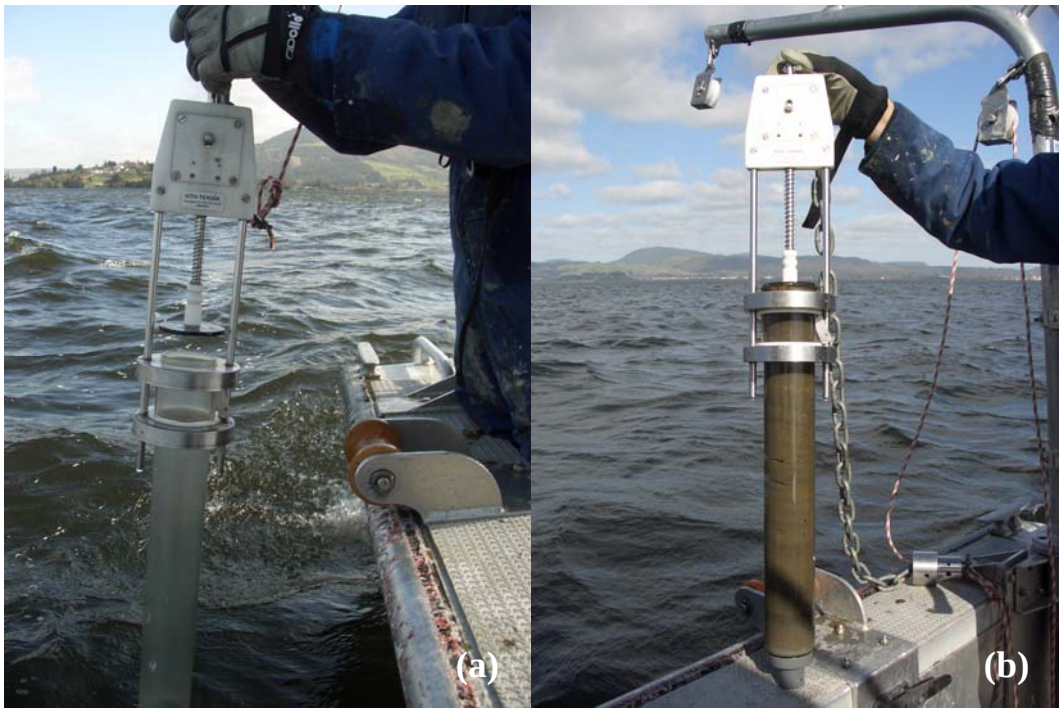

Figure 3-2 *Gravity corer showing (a) empty core barrel with open seal, (b) core barrel full with seal shut and piston inserted.*

Cores were extruded by attaching the piston to a core barrel driver on top of a threaded vertical pole, and locked into place. A sealed perspex box, with a horizontal piston was placed on top of the core barrel (Figure 3.3a). The core barrel driver was rotated around the threaded pole, pulling the core barrel down and forcing the piston up at a rate of 5 mm per rotation. Once the core had been extruded the desired distance of 2 cm, the extruded sediment core was forced laterally with the horizontal piston in the perspex box and driven down into a 50 mL centrifuge tube with a nylon plunger (Figure 3.3b). The piston was then retracted, a new centrifuge tube attached and the core driver advanced a further 2 cm interval, and the process repeated until the desired core length had been collected. This process was designed to limit access of oxygen into the sample.

Eh and pH measurements were taken immediately in the field for each 2 cm sediment interval, then sediment samples sealed and stored at 0°C until transported back to the laboratory.

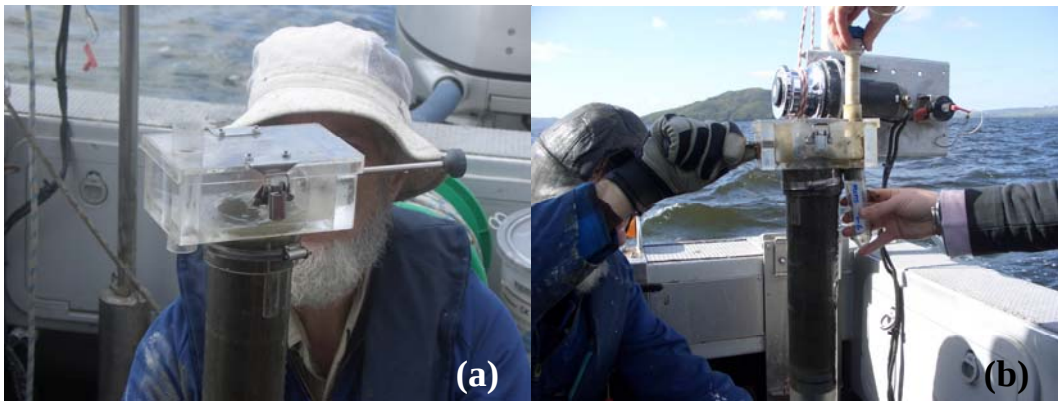

Figure 3-3 *Core extruded from core barrel into (a) sealed perspex box, then (b) collected into tube by plunger.*

3.2.3 Sample preparation

Pore waters were obtained by centrifugation of sediment samples at 4000 rpm for 20 minutes, within 24 hrs of sediment collection. Pore waters were filtered through 0.45 μm GF/C syringe filters, preserved with two drops of concentrated HCl, and frozen until chemical and nutrient analysis.

3.2.4 Peepers

Peepers, also known as pore water equilibrators, were first described by Hesslein (1976). The concept of a peeper is to allow solutes in lake and pore water to equilibrate with distilled water held in chambers over a period of time. After equilibration the concentrations within the chambers will equal those at the corresponding sediment depth.

The peepers were constructed of nylon, with a length of 60 cm and width of 10 cm. The peeper contained 25 chambers, each with a volume of 15 cm^3, 0.5 cm apart. Each chamber was filled with distilled water, with one side overlaid with a hydrophobic tight nylon material, and the other with plastic sheeting. The chambers were held in place with an outer frame of nylon, and screwed together (Figure 3.4a). This procedure was carried out in a water bath of distilled water to ensure air was absent from chambers. Peepers were transported from the lab to the field in a water bath.

Peepers were deployed in the lake on two occasions. The first occasion was in June when a single peeper was placed in the lake sediments. Before deployment the peeper was attached to a metal grid by clamps and then partially submerged vertically into sediments. The peeper was attached to a buoy and left for a period of 50 days to allow for equilibration with pore water and, for chambers above the sediments, with the overlying lake water. The second deployment consisted of three peepers attached to a single grid, each at different heights to capture the sediment-water interface (Figure 3.4b), and left for 95 days to allow for equilibration. Appendix 1 outlines locations for each deployment.

On resurfacing peepers, water was extracted from each chamber by syringe, and stored in 15 mL centrifuge tubes. Eh and pH measurements were taken immediately. Samples were sealed and stored at 0°C while transported back to the laboratory, where they were preserved with HCl and frozen until chemical and nutrient analysis.

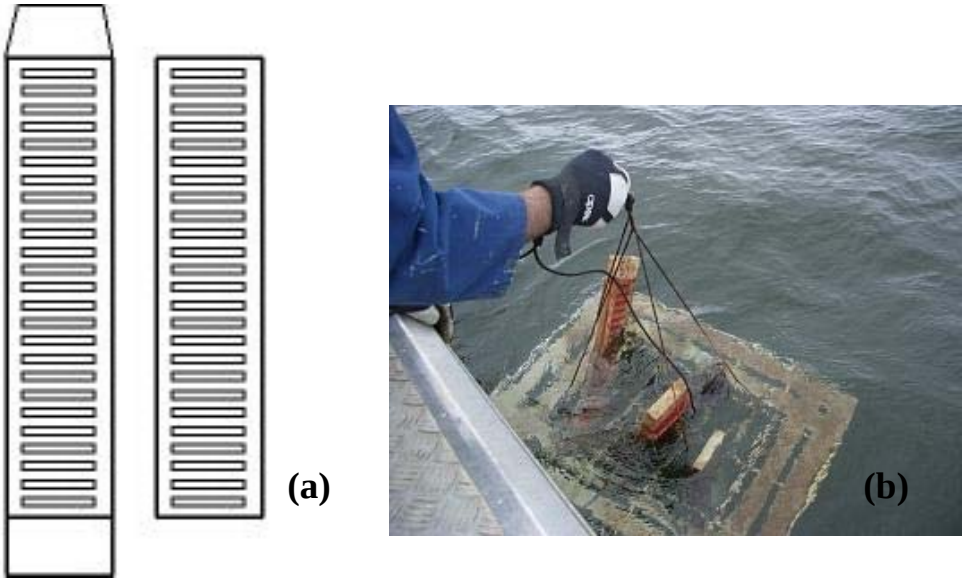

Figure 3-4 *(a) Diagram of peeper showing frame consisting of 25 chambers and outer frame. (b) Photo of resurfacing of the three peepers attached to metal grid.*

A laboratory experiment was performed to measure the equilibration time of diffusion of solutes between the inside and outside of chambers through the hydrophobic tight nylon material used. Peepers were filled with a solution

containing 0.6 mg/L of Rubidium and placed in a water bath containing 10 mg/L phosphorus. Two chambers were measured periodically over three months to measure how fast the peeper approached equilibrium. Figure 3.5a shows the concentrations of rubidium diffusing out of the peeper and Figure 3.5b shows phosphorus diffusing into the peeper over time. These show peepers did not reach equilibrium over the measured time frame. This contrasts with the comparison between the peepers and adjacent gravity core pore waters (Ru164), with comparable results after 95 days of contact.

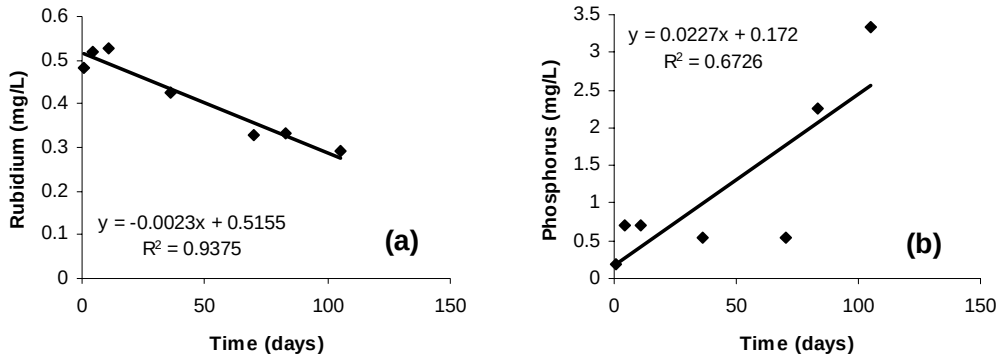

Figure 3-5 *(a) Rubidium diffusing out of peeper chambers and (b) phosphorus diffusing into peeper chambers over time.*

3.2.5 Pore water analysis

3.2.5.1 Inductively Coupled Plasma – Mass Spectrometer (ICP–MS)

Total dissolved phosphorus (TDP), and the trace metals iron (Fe), manganese (Mn), arsenic (As), cadmium (Cd), and lead (Pb) were analysed by ICP-MS on all pore water samples. Standards were prepared from Merck standards diluted to within a working range corresponding approximately to concentrations in samples. Standards were run every twenty samples, with a blank every ten samples. To measure for instrument drift and reproducibility of results, a quality assurance solution was prepared from stock solutions of the measured elements and run as a sample between every core. Deionised water of 17.9 MΩ resistance was used for blanks, preparation of standards and quality assurance solution.

3.2.5.2 Inductively Coupled Plasma–Optical Emission Spectroscopy (ICP-OES)

Total sulfur was analysed by ICP-OES. Hydrogen sulfide (H_2S) is generally only present in small quantities so sulfate is likely the dominant form of sulfur. Due to instrument failure not all pore water samples were analysed. For small available sample volumes, a ten-fold dilution with deionised water was used before samples were run on the ICP-OES.

Calibration standards were prepared from a 1000 ppm stock solution of sulfur. A quality assurance solution prepared from a stock solution of sulfur, as well as a blank was run between every core sample. This procedure was used to measure for instrument drift and reproducibility of results. Deionised water of 17.9 MΩ resistance was used for all preparation of blanks, standards and for quality assurance.

3.2.5.3 Flow Injection Analysis

Dissolved nutrients (ammonium, nitrate, nitrite and soluble reactive phosphorus (SRP)) were analysed colorimetrically by a Lachat QuikChem® Flow Injection Analyser following a 1:10 dilution. Ammonium was analysed by the QuikChem® Method 10-107-06-2-C (Prokopy, 1992). SRP was analysed by the QuikChem® Method 10-115-01-1-A (Diamond, 2000). Nitrate and nitrite were analysed by the QuikChem® Method 10-107-04-1-A (Wendt, 2000). Nitrate is reduced to nitrite by passing through a copperised cadmium column before analysis as NOx. Nitrite is determined identically but without the cadmium column. Nitrate concentration is then determined by subtraction of nitrite concentration from the combined nitrate/nitrate concentration (NOx).

Calibration standards ranging from 0–4 mg/L were prepared by dilution of a 1000 mg/L stock solution for PO_4, NH_4 and NO_3, and a 500 mg/L stock solution for NO_2. Deionised water (17.9 MΩ resistance) was used for all solution preparations. Results from the standards were used to construct a calibration

curve for each element, which was used as a reference to determine the concentration in the samples. Reagents were prepared as outlined in the above methods with deionised water (17.9 MΩ resistance).

To measure instrument drift and reproducibility of results, samples were run in duplicate and a calibration standard and blank were analysed between each core sample.

3.2.5.4 Diffusive fluxes

The diffusive flux of nutrients dissolved phosphorus and ammonium, across the sediment-water interface were calculated by Fick's first law of diffusion. Assuming steady state conditions, the flux (F) is equal to the concentration gradient with depth ($\Delta C/\Delta Z$), the diffusion coefficient (D) and porosity (ϕ);

$$F = \phi D (\Delta C/\Delta Z)$$

Porosity was assumed to be 0.8 for surface sediments, the concentration gradient calculated from the surface sample of each sediment core and the diffusion coefficient assumed to be $1x10^{-5}$ cm^2 s^{-1} (Stokes, 1951).

3.3 Gas

3.3.1 Field collection

Gas present in the sediments of Lake Rotorua was collected by a specially designed gas trap (Figure 3.6). Gas within the sediment was disturbed by a hose that pumped lake water to below the sediment surface at depths of 20 and 50 cm. Gas that evolved was captured by displacement of lake water in a funnel attached to a 100 mL bottle, attached to a metal grid. The gas was collected just beneath the lake surface by withdrawing by vacuum pump into gas sample bottles. Gas sample bottles were stored out of sunlight at room temperature until analysis.

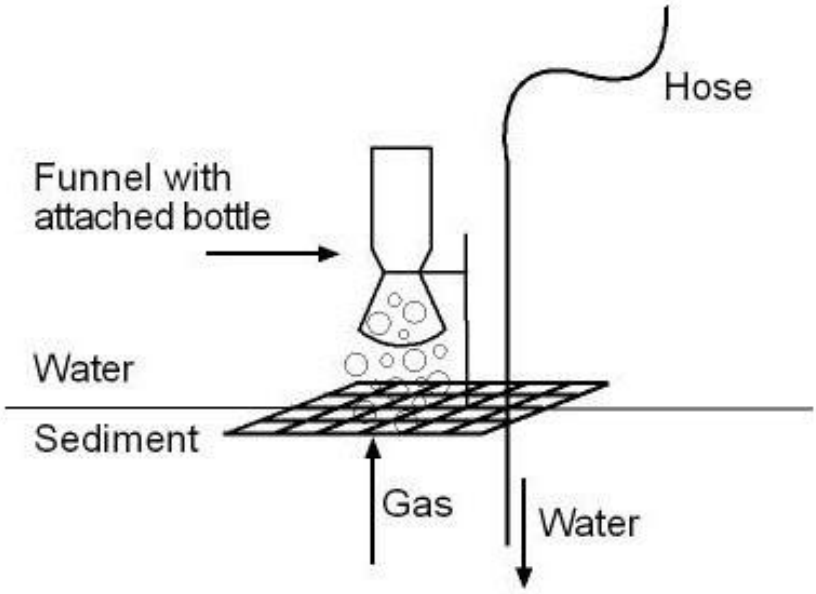

Figure 3-6 *Schematic of gas tap used in the collection of gas present in the sediments of Lake Rotorua.*

3.3.2 Gas Analysis

3.3.2.1 Gas Chromatography

Gas composition was analysed for CO_2 and CH_4, by a Perkin Elmer Autosystem XL Gas Chromatograph, with a 6 foot Hayesep Q (80/100) column attached to a Thermal Conductivity Detector (TCD). Helium was used as a carrier gas at flow rates of 20 mL/min. Oven temperature was 35°C. Instrument calibration was performed using standard mixture Matheson Tri-Gas sourced from Allech.

A volume of 1 µL gas was analysed in triplicate via injection into the gas chromatograph-TCD. Sample analysis time was three minutes with a sampling rate of 12.5 points/sec. Resulting chromatographs were analysed by TurboChrom 6.1.1.0.0:K20 software.

3.3.2.2 $\delta^{13}C$ Isotope Analysis

To measure the $\delta^{13}C$ of the gas evolved, the methane was combusted to carbon dioxide on the vacuum line by a copper oxide furnace as outlined by Kennel

(1998). The samples were then collected in a sample vial and methane and carbon dioxide $\delta^{13}C$ values measured by a Europa Scientific 20-20 isotope analyser. Samples are reacted with 100% H_3PO_4 acid and the CO_2 gas separated from H_2O by cryogenic distillation.

At natural abundance levels, the $^{13}C/^{12}C$ ratio is measured to a precision of ± 0.005‰, with respect to a house standard. The house standard is cross-referenced to the original standard Pee Dee Belemnite, from the Pee Dee Formation in South Carolina, U.S.A. The $^{13}C/^{12}C$ ratio is presented in the delta notation (δ) and expressed as parts per mille (‰) with respect to PDB.

3.3.2.3 Bicarbonate analysis

To determine if CO_2 was dissolving into solution, one sediment core (Ru128) was collected by gravity corer and pore water was extracted by methods outlined in section 3.2. Bicarbonate concentrations within unpreserved pore water sample were analysed by Gran titration as outlined by Gran (1952), using 0.1024M HCl on a TITRINO titrator, within 24 hours of collection. Acid was added to pore water to react with the bicarbonate and reduce the pH. The change of pH was recorded and Gran's function was plotted to read endpoints by:

$$(Vo + V).10^{-pH} \text{ against } V$$

Where Vo = volume of sample used

V = volume of acid added

The resulting plot gives a straight line which crosses the horizontal axis at V_2 (the end point). V_2 is the volume of acid added to neutralise the bicarbonate (Figure 3.7). Therefore:

$$HCO_3^- \text{ concentration} = \frac{V_2 M(HCl)}{Vo} \text{ moles/L}$$

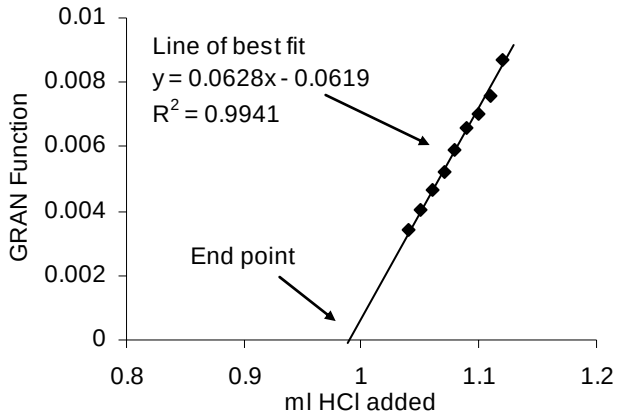

Figure 3-7 *Example of Gran Plot for calculation of HCO_3^- in core Ru128 at interval depth of 4-6 cm.*

3.3.2.4 $\delta^{13}C$ analysis of Dissolved Inorganic Carbon (DIC)

Preparation of samples for $\delta^{13}C$ analysis in DIC from pore water involved addition of 1 mL barium hydroxide solution to approximately 10 mLs of pore water obtained from sediment core Ru124. This procedure allowed for dissolved inorganic carbon to be extracted out of solution. The solution was left to sit for one day to allow precipitation, then centrifuged and the precipitate washed with distilled water two times. The precipitate was then left to dry in a dessiccator for five days. Samples were then analysed for $\delta^{13}C$ by a Europa Scientific 20-20 isotope analyser using the same procedure outline for gas (Section 3.3.2.2).

3.3.3 Gas ebullition

The rate of gas released from the sediments was measured by specially constructed traps (Figure 3.8). Five traps were placed along a transect across the lake on one occasion in August 2006 (Appendix 1 outlines locations, details and time intervals of each location). The traps consisted of a 1 m^2 frame with attached plastic sheeting held by a metal frame. An inverted funnel was held in the plastic sheeting with a glass burette to capture rising gas. The 1 m^2 frame with attached plastic sheeting and funnel was held by a pyramid-shaped metal frame with a base diameter of 1.6 m x 1.6 m, designed so that when lowered onto sediments, the gas

in the sediments disturbed by the legs would not be captured within the plastic sheeting. The gas traps were lowered beneath the lake water surface with the burette tap open to allow for air to be displaced. Tap was then closed and the trap lowered to the sediment surface by an attached rope and buoy. Traps were left for time intervals of approximately three hours. On resurfacing the traps, the plastic sheeting was not brought above the lake surface. The point on the burette between the gas and water interface was recorded. In the lab, water was added to this line and weighed to determine the volume of gas displaced water within the burette.

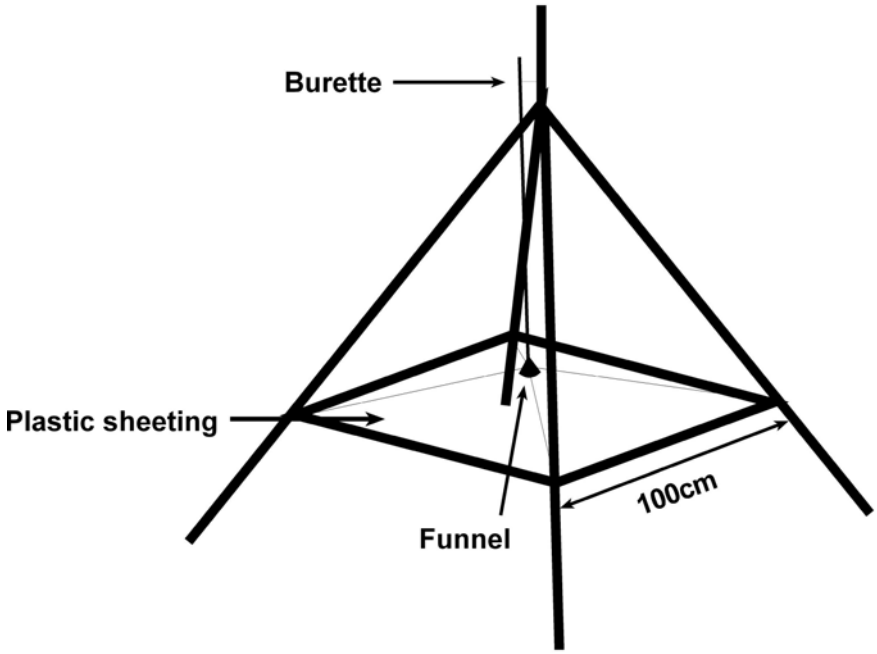

Figure 3-8 *Schematic of gas trap used to measure rate of gas ebullition.*

3.4 References

DIAMOND, D. (2000) QuikChem Method 10-115-01-1-A: Determination of orthophosphate in waters by flow injection analysis colorimetry. Lachat Instruments, Milwaukee, USA.

GRAN, G. (1952) Determination of the equivalence point in potentiometric titrations. Part II. *The Analyst,* 77**,** 661-671.

KENNEL, P. R. (1998) Tracing the Impact of Landfill Gases on Environmental Waters using Stable Isotopes. MSc Thesis. *Department of Chemistry.* Hamilton, University of Waikato.

PROKOPY, W. R. (1992) QuikChem Method 10-107-06-2-C: Ammonia in surface water, wastewater. Lachat Instruments, Milwaukee, USA.

STOKES, R.H. (1951) Integral diffusion coefficients of potassium chloride solutions for calibration of diaphragm cells. *Journal of the American Chemical Society*, 73, 3527.

WENDT, K. (2000) QuikChem Method 10-107-04-1-A: Determination of Nitrate/Nitrite in Surface and Wastewaters by Flow Injection Analysis., Lachat Instruments, Milwaukee, USA.

4. RESULTS: PORE WATER CHEMISTRY IN THE SEDIMENTS OF LAKE ROTORUA

4.1 Introduction

The objective of this thesis was to gain an understanding of the transfer of nutrients and trace elements from the pore waters of Lake Rotorua sediments. A large scale sampling program began in January 2006. Due to the large number of sediment cores required to be collected in order to achieve good spatial coverage, sampling was done over three occasions throughout the year. As Lake Rotorua is polymictic, a large seasonal difference was not expected to be found within pore water samples. However as the sampling program progressed, a seasonal influence became evident, and necessitated treating the results as three separate periods. Therefore this chapter is set out as follows:

- Pore water results obtained from sediment cores are presented as the three periods. Results have been reported by examining distributions of individual elements as a function of depth below the sediment-water interface and distance across the lake.

- Pore water results obtained by peepers. The purpose of sampling with peepers was to gain a greater understanding of concentration gradients between the lake water and pore water.

- Diffusive fluxes of nutrients from the sediment to the overlying lake water.

The most significant results obtained are discussed in the following chapter. Appendix 2 provides a complete list of concentrations for each element in each sample and concentration profiles of the individual sediment cores.

4.1.1 Observations

Sediments were dominated by dark olive diatomaceous ooze with black laminations, with a very low density of sediment in the upper part of the core. The very low density of the sediments meant that the lake water/sediment boundary may not have been accurately captured, possibly resulting in over-estimation of concentration gradients. A layer of flocculent material consisting of fine organic matter was often observed immediately above the sediment-water interface. Gas voids were often present within the sediment, causing disturbance of the sediment on retrieval (Figure 4.1).

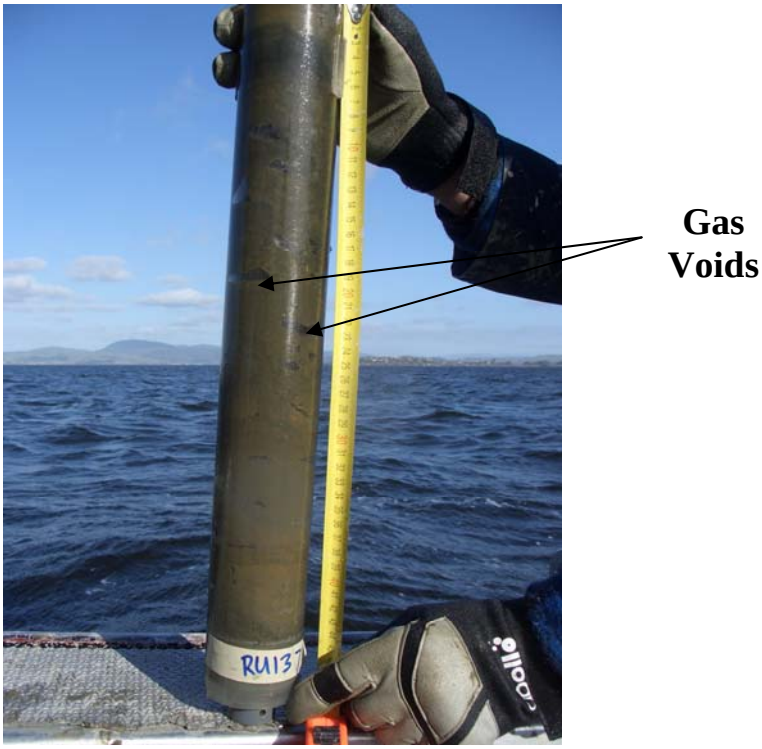

Figure 4-1 *Sediment core Ru137 from water depth 11 m showing gas voids.*

4.2 Summer

All elements, with the exception of dissolved lead and dissolved arsenic, show peaks in concentration at or near the sediment-water interface, with concentrations generally decreasing down the profile as concentration gradients decrease.

4.2.1 Iron

Ferrous iron is mostly concentrated in the upper 5 cm of the sediment profile (Figure 4.2). Peaks in concentration occur near the sediment-water interface, and range from 1.6-6.7 mg/L. Concentrations decrease rapidly with depth over most of the profile showing ferrous iron is being removed from solution, however in the centre of the lake ferrous iron concentrations increase between 10 and 20 cm depth showing release into pore water from the sediment column as evident in Ru106.

Figure 4.3 shows the concentration gradients of cores Ru106 (a) and Ru110 (b). There are peaks in concentration in the upper layers indicating diffusion of ferrous iron both upwards to the sediment-water interface and downwards to where ferrous iron is being removed by the sediment. Release of ferrous iron is evident in the deeper sediment layers of Ru106 (a) where concentrations increase with depth. There is a strong gradient indicating diffusion upwards where ferrous iron is removed from pore water to be released again into the overlying lake waters.

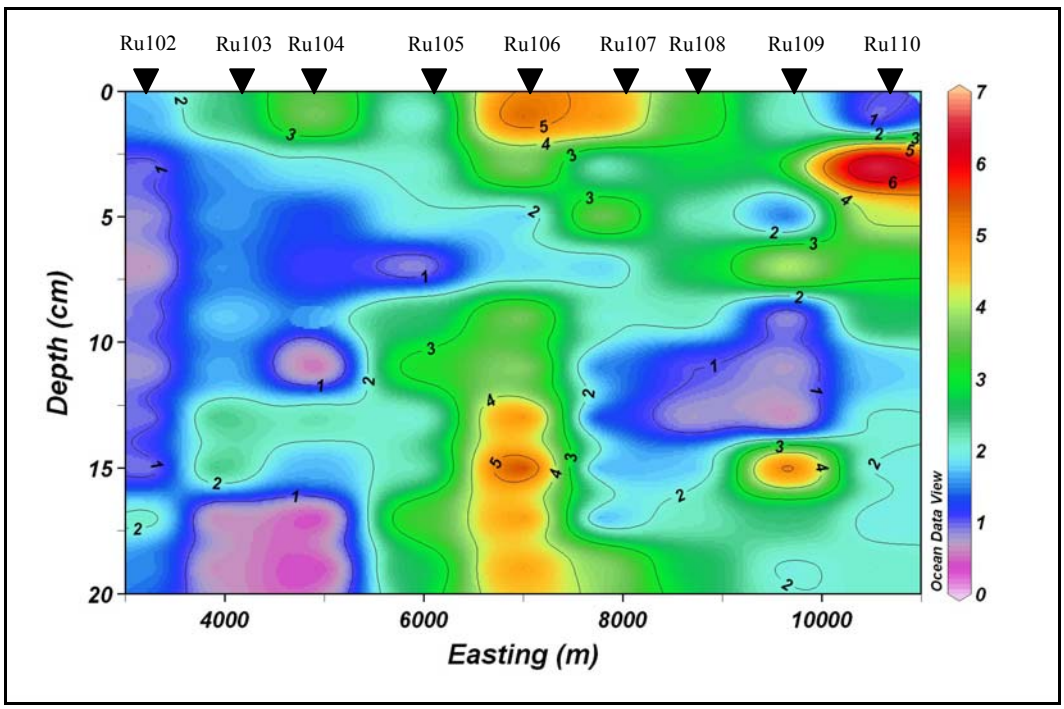

Figure 4-2 *Depth distribution of Fe^{2+} in pore water of January 2006 cross-section. Concentration isopleths are in mg/L.*

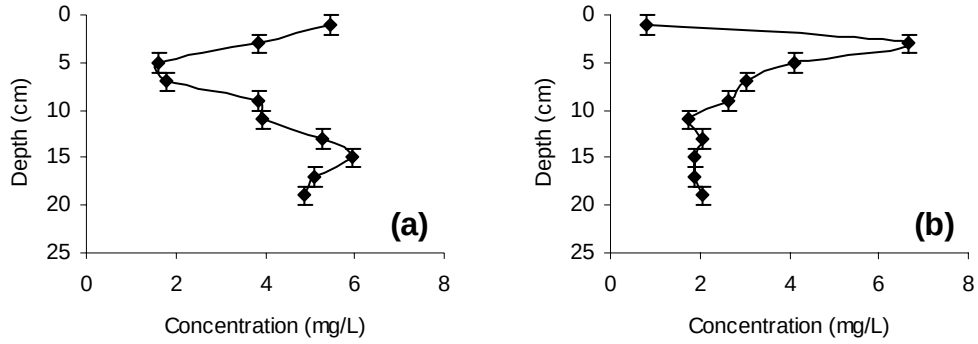

Figure 4-3 *January 2006 Fe^{2+} pore water concentration profiles of (a) Ru106, and (b) Ru110.*

4.2.2 Manganese

Manganous concentrations generally peak in the upper 5 cm of the sediment profile (Figure 4.4). Peaks in concentration in the upper pore water profile range from 1.6-8.9 mg/L, and decrease rapidly with depth. Some release of manganous deep in the sediment profile is indicated in Ru106 by an increase in concentration below 10 cm.

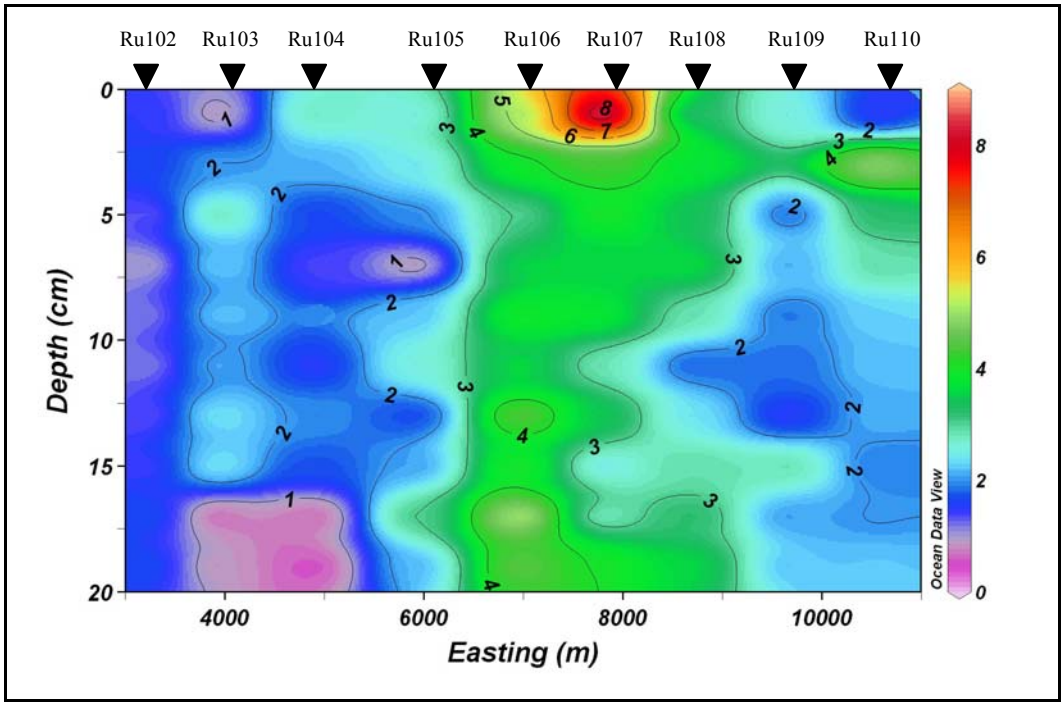

Figure 4-4 *Depth distribution of Mn^{2+} in pore water of January 2006 cross section. Concentrations of isopleths are in mg/L.*

Strong gradients in concentration are evident in Figure 4.5 (a) and (b) in the upper 5 cm of the sediment, where manganous is likely to be diffusing up toward the sediment-water interface and downward where it is being removed from pore water into the sediment. Core Ru106 shows increases in concentration of manganous deep in the profile (in Figure 4.5a), indicating that manganous is being released into pore water and removed as it diffuses up along the concentration gradient.

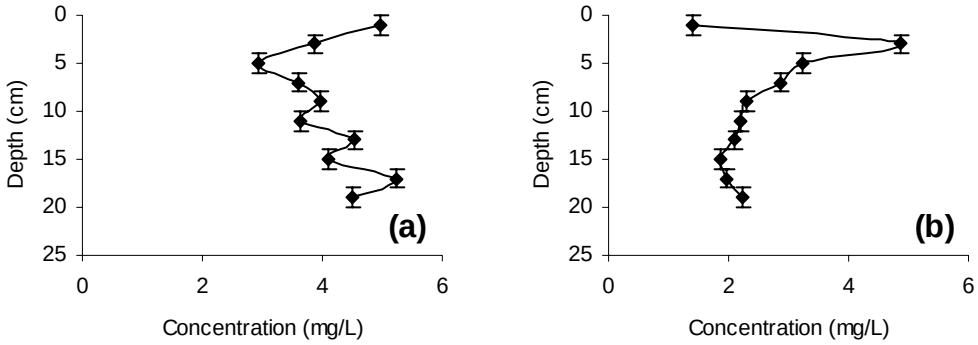

Figure 4-5 *January 2006 dissolved manganese pore water concentration profiles of (a) Ru106 and (b) Ru110.*

4.2.3 Sulfur

Total sulfur in pore water generally peaks in the upper 5 cm of the sediment core as shown by cores in Figure 4.6, Ru103 (a), Ru107 (c), Ru108 (d) and Ru110 (f). Peaks in concentration range from 5 to 25 mg/L, then rapidly decrease with depth. There is generally a rapid reduction in total sulphur between 10 and 15 cm depth. Strong concentration gradients generally occur at the sediment surface, possibly from diffusion into the sediment from the overlying lake water.

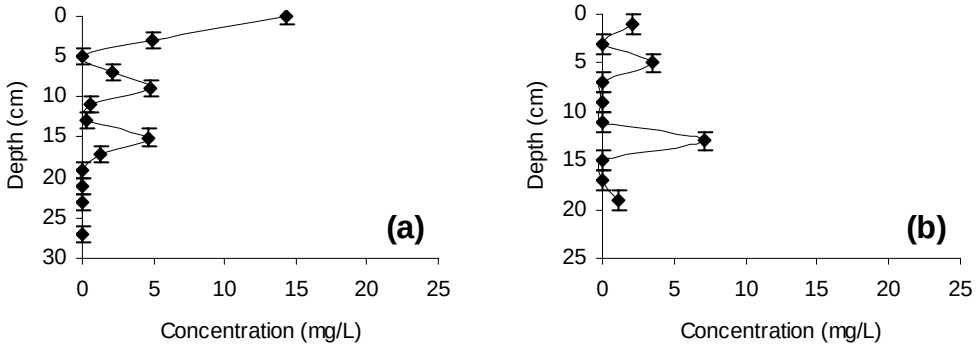

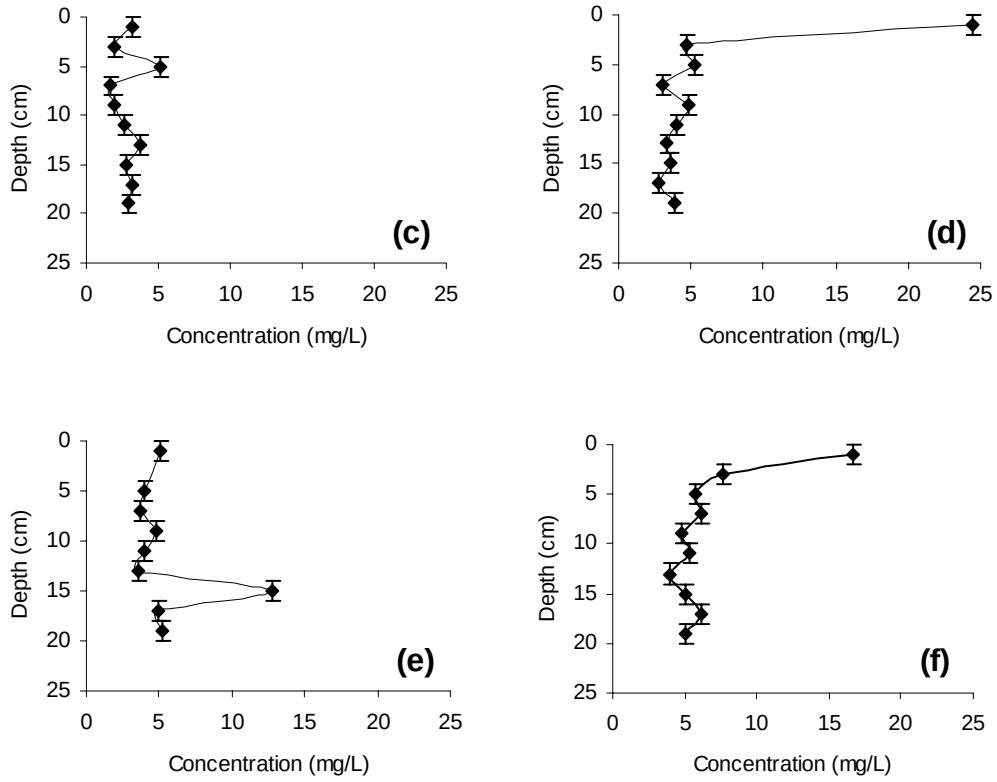

Figure 4-6 *Total sulfate pore water concentration profiles of (a) Ru103, (b) Ru106, (c) Ru107, (d) Ru108, (e) Ru109, and (f) Ru110 from January 2006.*

4.2.4 Phosphorus

Dissolved phosphorus concentrations peak at or near the sediment water interface, with concentrations ranging from 4.2 to 20.5 mg/L in the upper 5 cm of the pore water profile (Figure 4.7). Concentrations decrease rapidly below 5 cm where they tend towards a steady state value of ~ 2 mg/L.

Concentration profiles for selected cores show very strong gradients (Figure 4.8), implying that phosphorus is diffusing across the sediment-water interface into the overlying lake water and downward into the sediment where phosphorus is being removed from solution into the sediment.

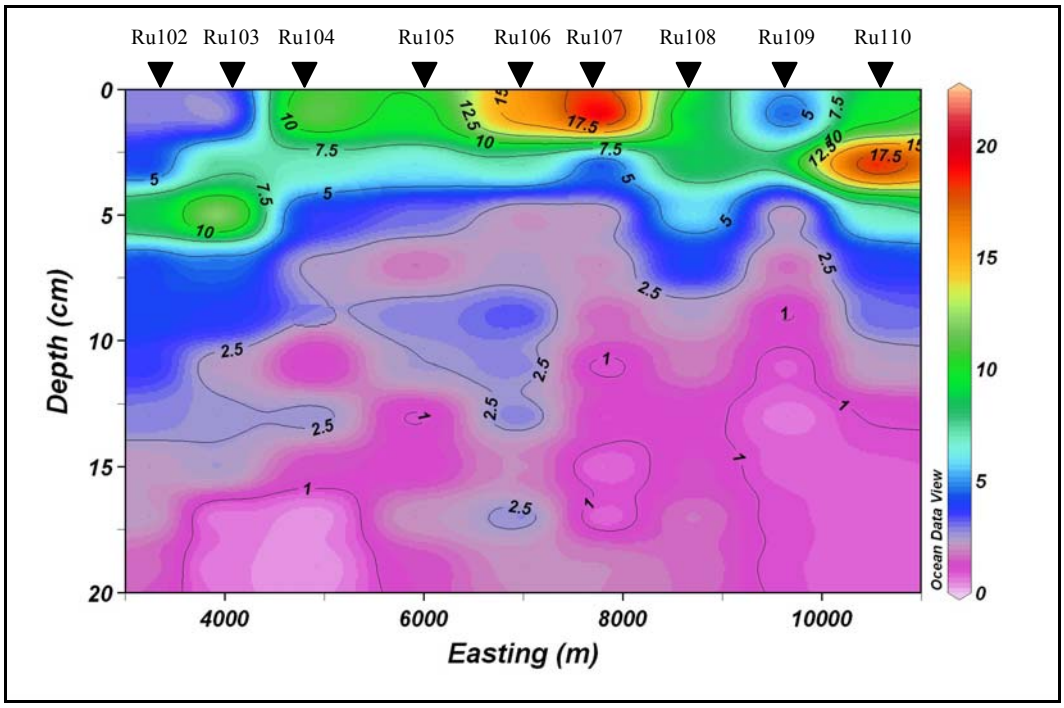

Figure 4-7 *Depth distribution of dissolved phosphorus in pore water of January 2006 cross section. Concentrations of isopleths are in mg/L.*

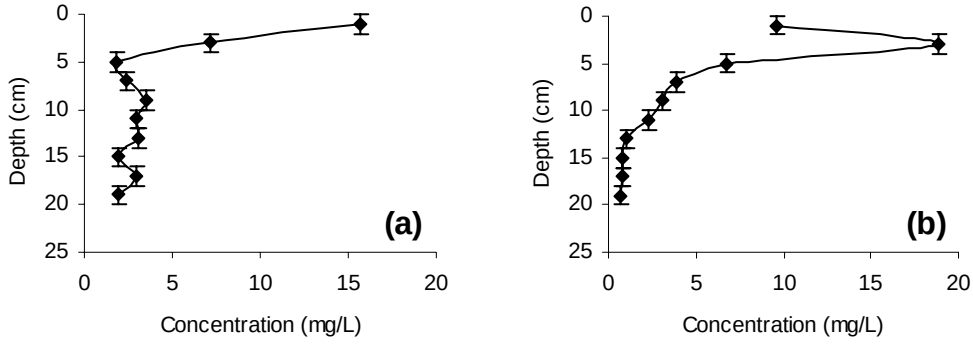

Figure 4-8 *January 2006 dissolved phosphorus pore water concentration profiles of (a) Ru106 and (b) Ru110.*

4.2.5 Ammonium

Concentrations of ammonium are very high in the pore water with peaks > 27.5 mg/L in the upper 5 cm of the sediment profile, and > 22.5 mg/L deep in the sediment profile (Figure 4.9).

Ammonium displays two different concentration profiles within the pore water. Figure 4.10(a) shows core Ru106 with ammonium increasing in concentration

down the profile. There is a slight concentration gradient indicating weak upward diffusion. Figure 4.10(b) shows core Ru110 with a near surface peak indicating high rates of organic matter decomposition, with the concentration gradient likely to produce diffusion across the sediment-water interface and also downwards into the sediment.

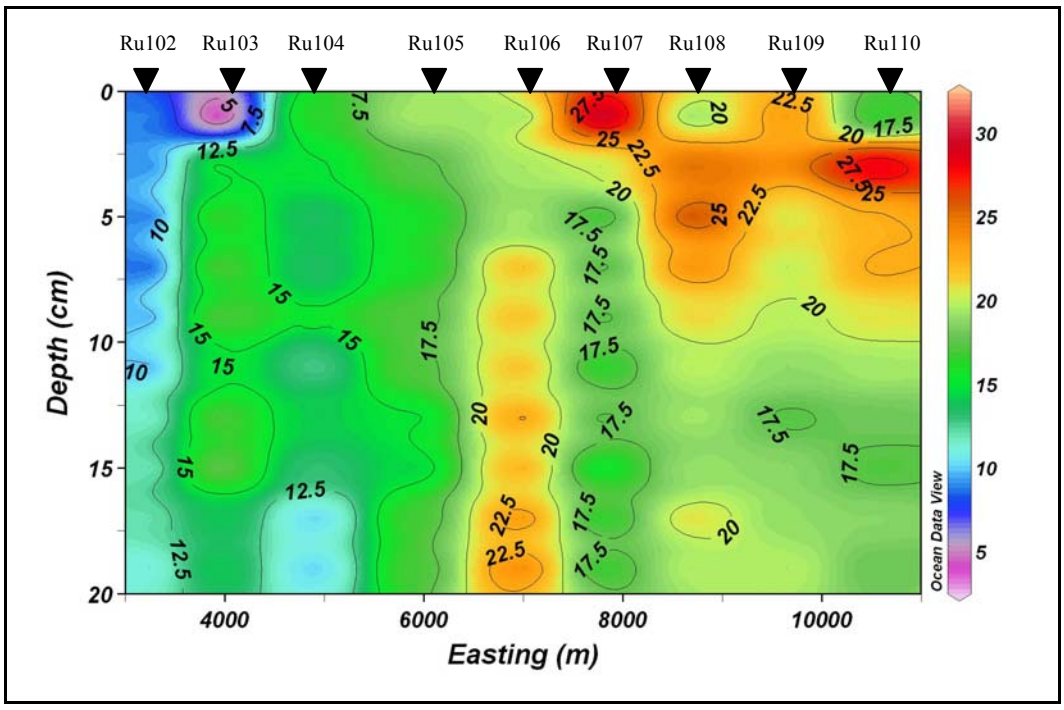

Figure 4-9 *Depth distribution of ammonium in pore water of January 2006 cross section. Concentrations of isopleths are in mg/L.*

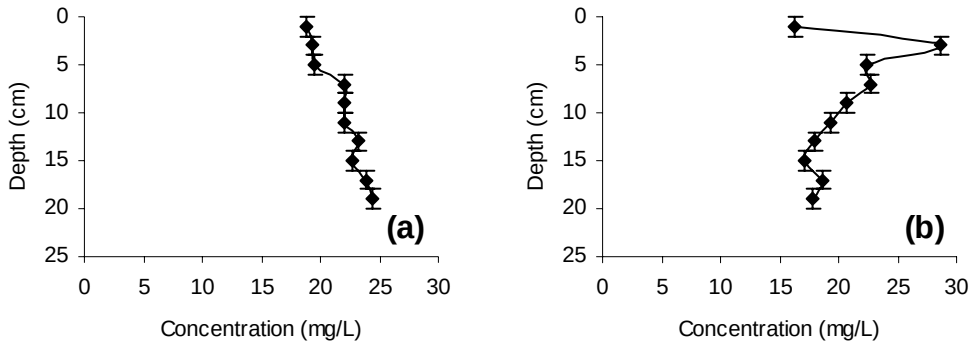

Figure 4-10 *January 2006 ammonium pore water concentration profiles of (a) Ru106 and (b) Ru110.*

4.2.6 Nitrate

Concentration profiles of nitrate are difficult to interpret (Figure 4.11). They may be from oxidation of very high ammonium in the profile. However the randomness suggests that oxidation occurred post-coring, between collection of cores and analysis on the FIA.

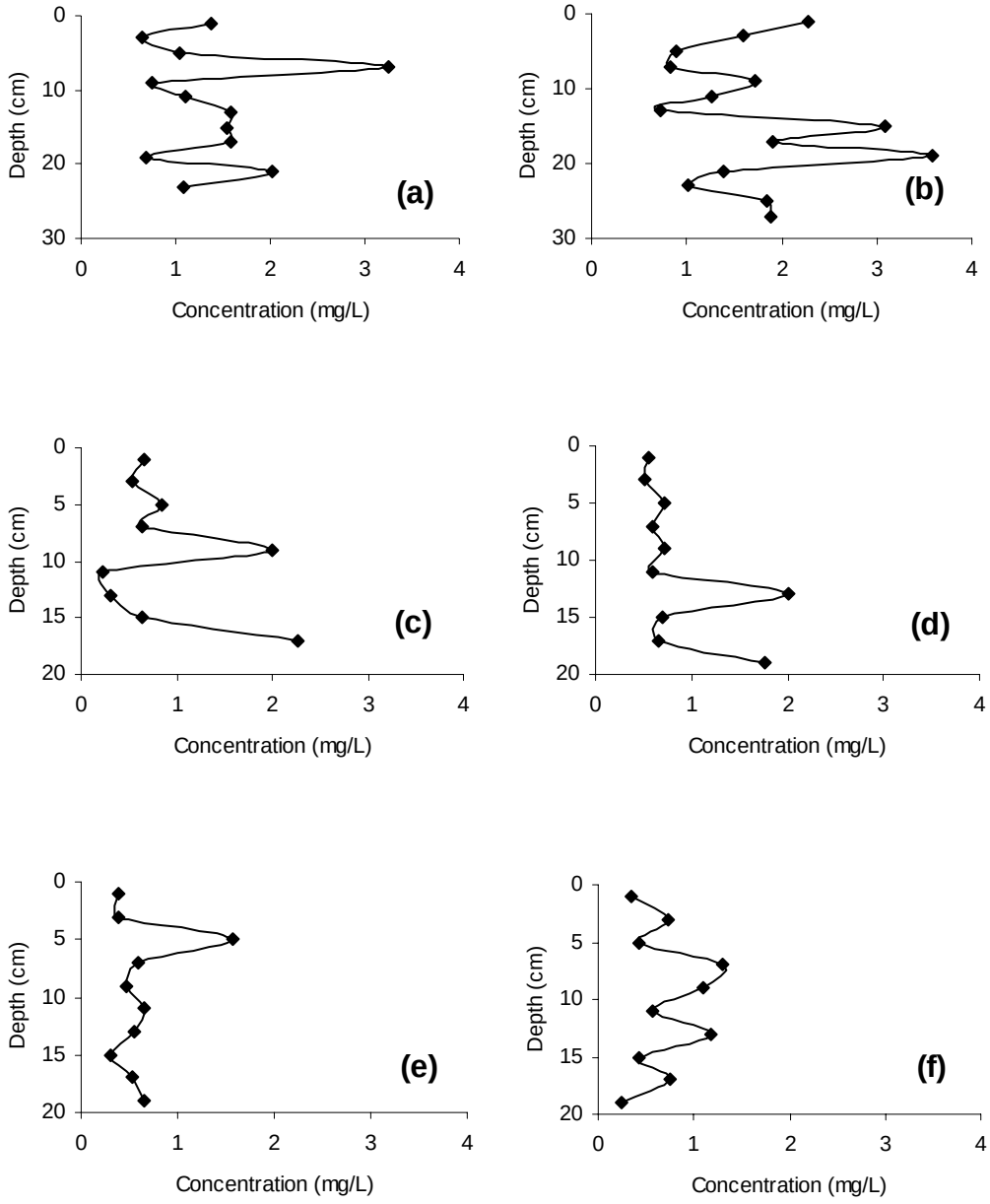

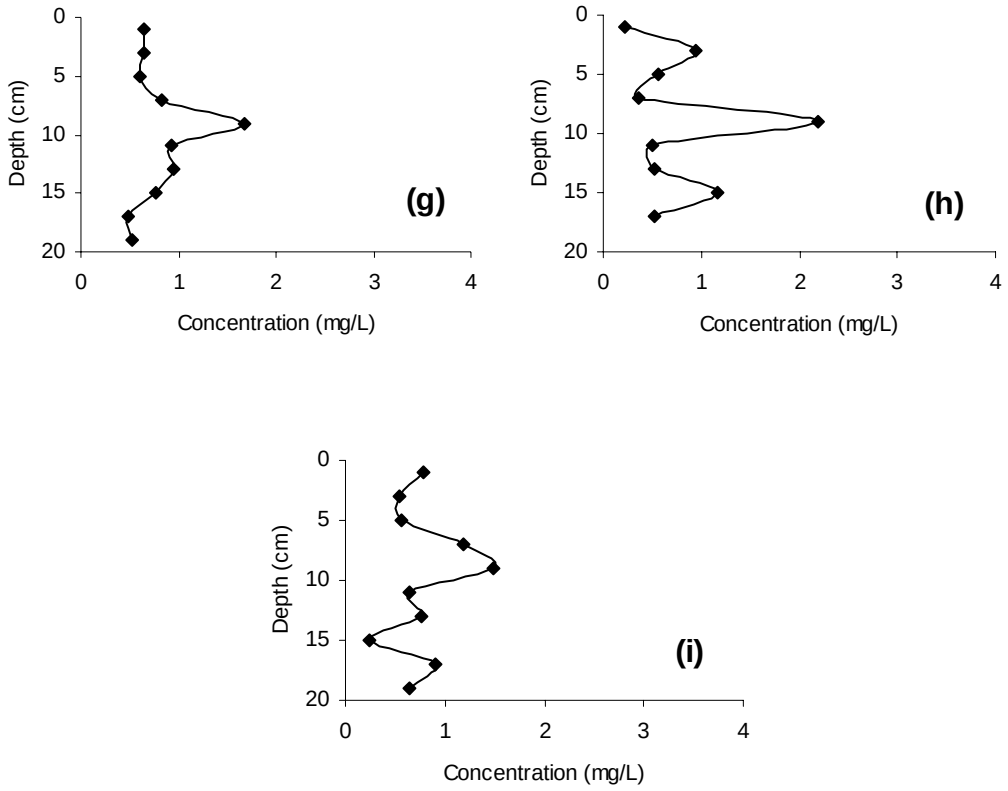

Figure 4-11 *January 2006 nitrate pore water concentration profiles of (a) Ru102, (b) Ru103, (c) Ru104, (d) Ru105, (e) Ru106, (f) Ru107, (g) Ru108, (h) Ru109, and (i) Ru110.*

4.2.7 Arsenic

Figure 4.12 shows that despite very low arsenic concentrations there is a general increase in concentration with depth. A small peak in concentration (> 0.5 mg/L) occurs in core Ru103, 3 cm below the sediment surface.

The concentration profiles in core Ru103 (Figure 4.13a) show a strong concentration gradient at 3 cm where arsenic is likely to diffuse upward towards the sediment-water interface and downwards were it is removed by the sediment. Core Ru106 (Figure 4.13b) shows dissolved arsenic concentrations increasing with depth in the pore water where it is likely to diffuse along the concentration gradient and be removed from solution into the sediment.

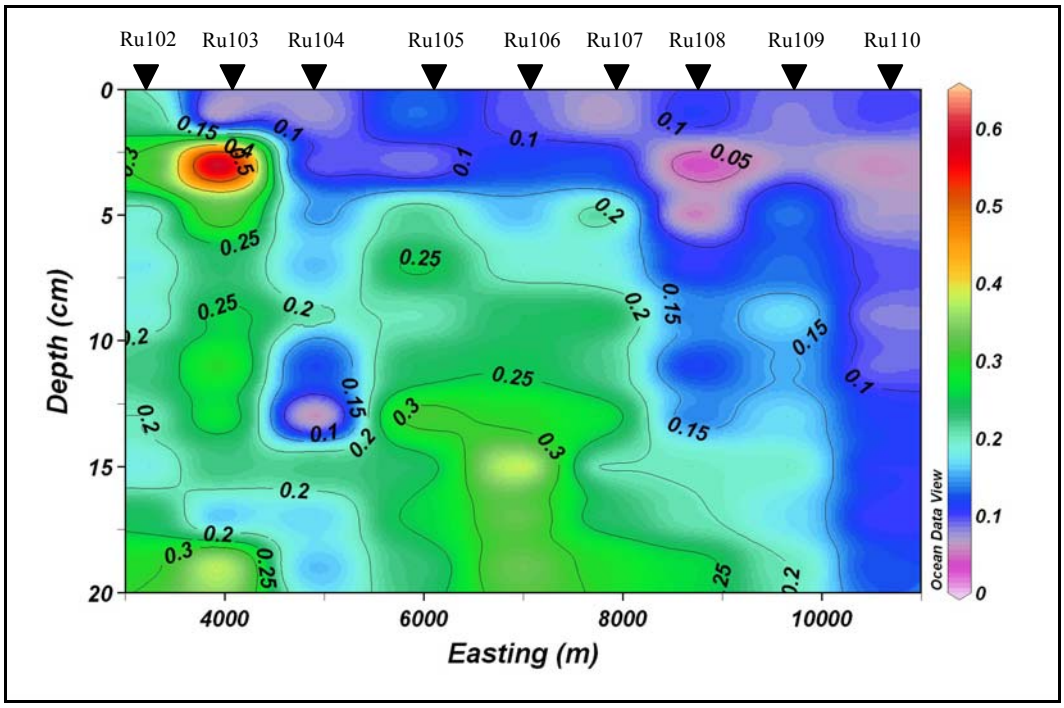

Figure 4-12 *Depth distribution of dissolved arsenic in pore water of January 2006 cross section. Concentrations of isopleths are in mg/L.*

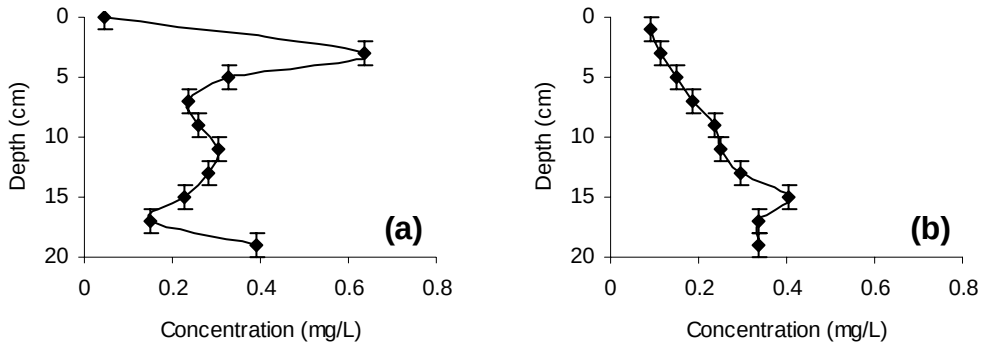

Figure 4-13 *Dissolved arsenic pore water concentration profiles of cores (a) Ru103 and (b) Ru106 from January 2006.*

4.2.8 Cadmium

Dissolved cadmium concentrations are generally very low at < 0.025 mg/L, with peaks in concentration at varying depths, in different cores (Figure 4.14). Cores Ru104 to Ru107 show concentration peaks at 7 cm depth with a maximum of > 0.2 mg/L in core Ru106. Concentrations of cadmium in core Ru109 peak deep in the sediment profile at > 0.25 mg/L.

Concentration profiles in Figure 4.15 show mid-core peaks in concentration. In the case of core Ru106 (Fig. 4.15a) there are peaks in concentration that are likely to result in cadmium diffusing up along its concentration gradients and downwards deeper in the sediment. Core Ru109 (Fig. 4.15b) shows an isolated high in cadmium concentration at the bottom of the core. Such scattered distribution patterns are difficult to interpret.

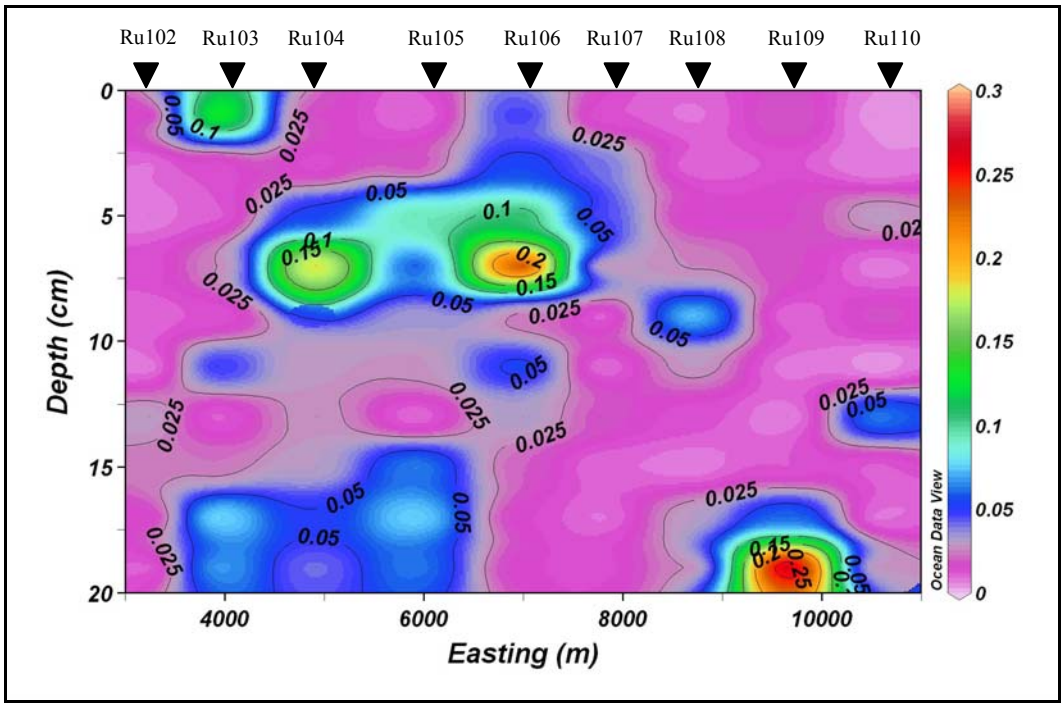

Figure 4-14 *Depth distribution of dissolved cadmium in pore water of January 2006 cross section. Concentrations of isopleths are in mg/L.*

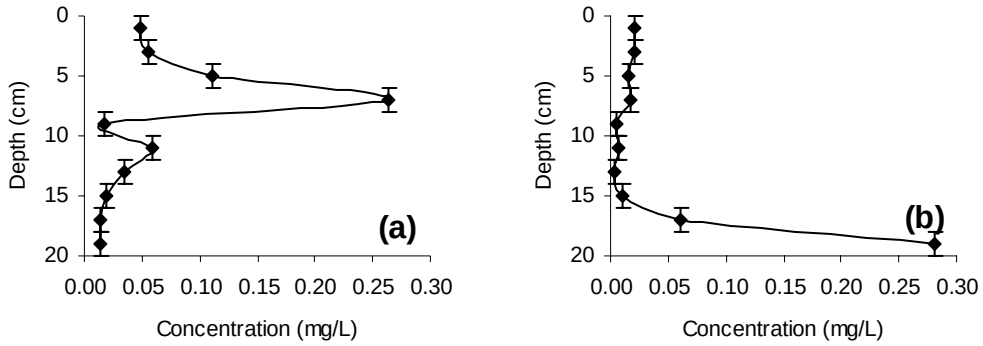

Figure 4-15 *Dissolved cadmium pore water concentration profiles of (a) Ru106 and (b) Ru109 from January 2006.*

4.2.9 Lead

Lead concentrations are very low, mostly > 0.01 mg/L, throughout the pore water profile, with a few peaks without a significant pattern of distribution (Figure 4.16). Core Ru109 exhibits the greatest concentration with > 0.3 mg/L at 9 cm below the sediment surface and another slight peak at 17 cm depth, possibly due to an analytical error. Core Ru106 shows a slight peak at 1 cm depth, and core Ru103 at 3 and 15 cm depth. It can be surmised on the basis of the concentration gradients that there is very little movement of lead within the sediment.

The concentration profile of Ru106 in Figure 4.17(a) shows little gradient throughout the profile, only a slight increase at the sediment surface. Core Ru109 (Fig. 4.17b) shows strong gradients where lead is likely to be released into the pore water as a result of removal through diffusion upwards and from sediment removal downwards.

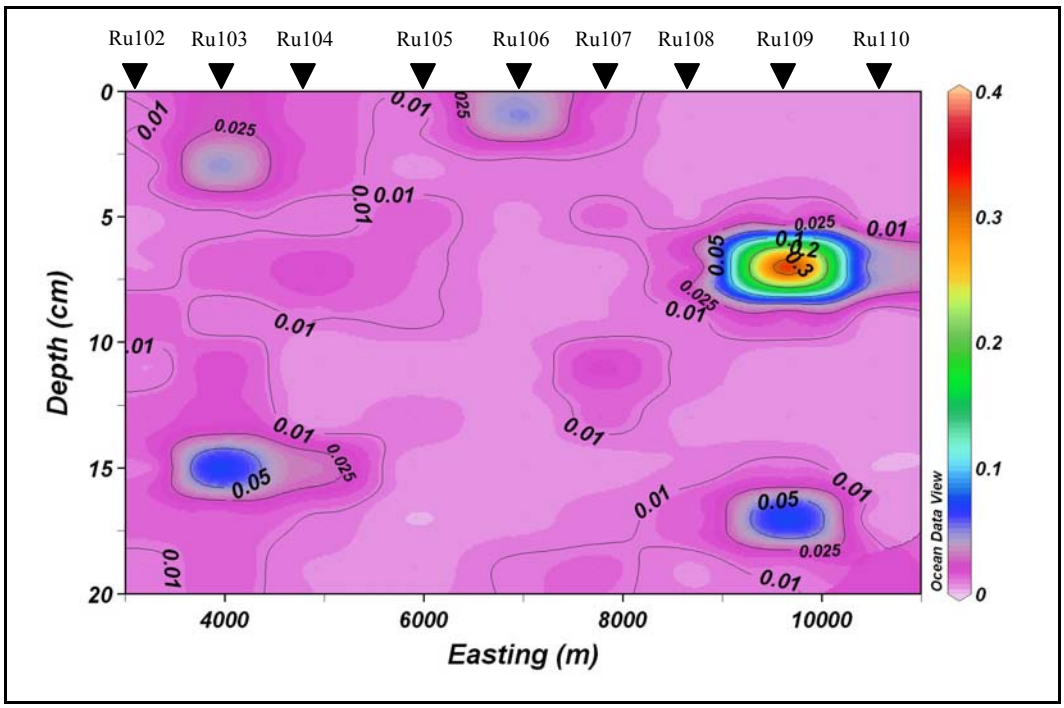

Figure 4-16 *Depth distribution of dissolved lead in pore water of January 2006 cross section. Concentrations of isopleths are in mg/L.*

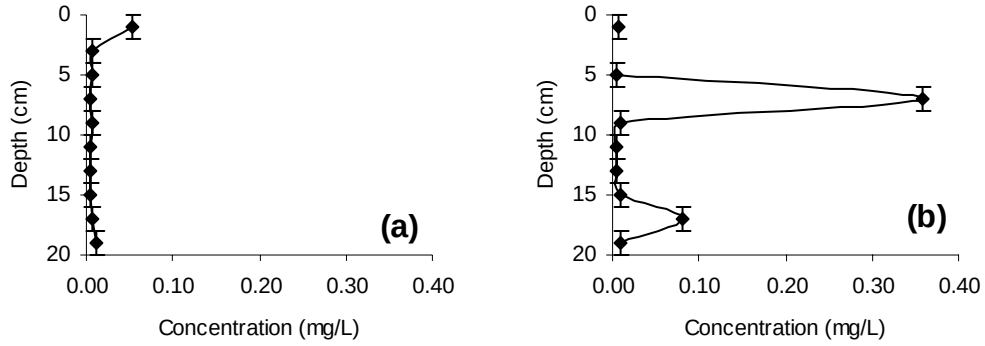

Figure 4-17 *Dissolved lead pore water concentration profiles of (a) Ru106 and (b) Ru109 from January 2006 cross section.*

4.3 Autumn

Two cross sections of sediment cores were taken in May. With the exception of sulfur and dissolved phosphorus concentrations in cross section 1, all other elements showed an increase in concentration down the pore water profile.

4.3.1 Eh-pH

Figure 4.18 shows the typical pH and Eh profiles in pore waters of May. pH remains relatively constant with depth at ~ 6 (Fig. 4.18a), with values from all samples in May ranging between 5.61 and 6.57. Eh shows a large drop in the upper 3 cm of the profile from just below 0 to where it is relatively constant at around -0.1 V with depth (Fig. 4.18b). All samples from May show the same trend with Eh, ranging from 0.161 V in the upper profile to -0.127 V in the lower profile.

Eh-pH diagrams of iron constructed for the conditions of Lake Rotorua's sediments from the two cross sections of May (Figure 4.19) show pore water lies on the boundary between Fe_2O_3 and FeS_2. Samples near the sediment surface usually fall within the Fe_2O_3 boundary and samples in the lower profile fall within the FeS_2 boundary.

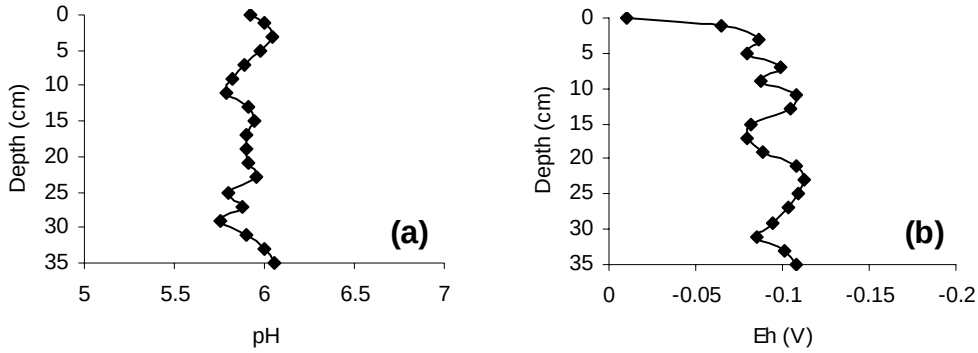

Figure 4-18 *Core Ru119 profile of (a) pH and (b) Eh profile in May 2006.*

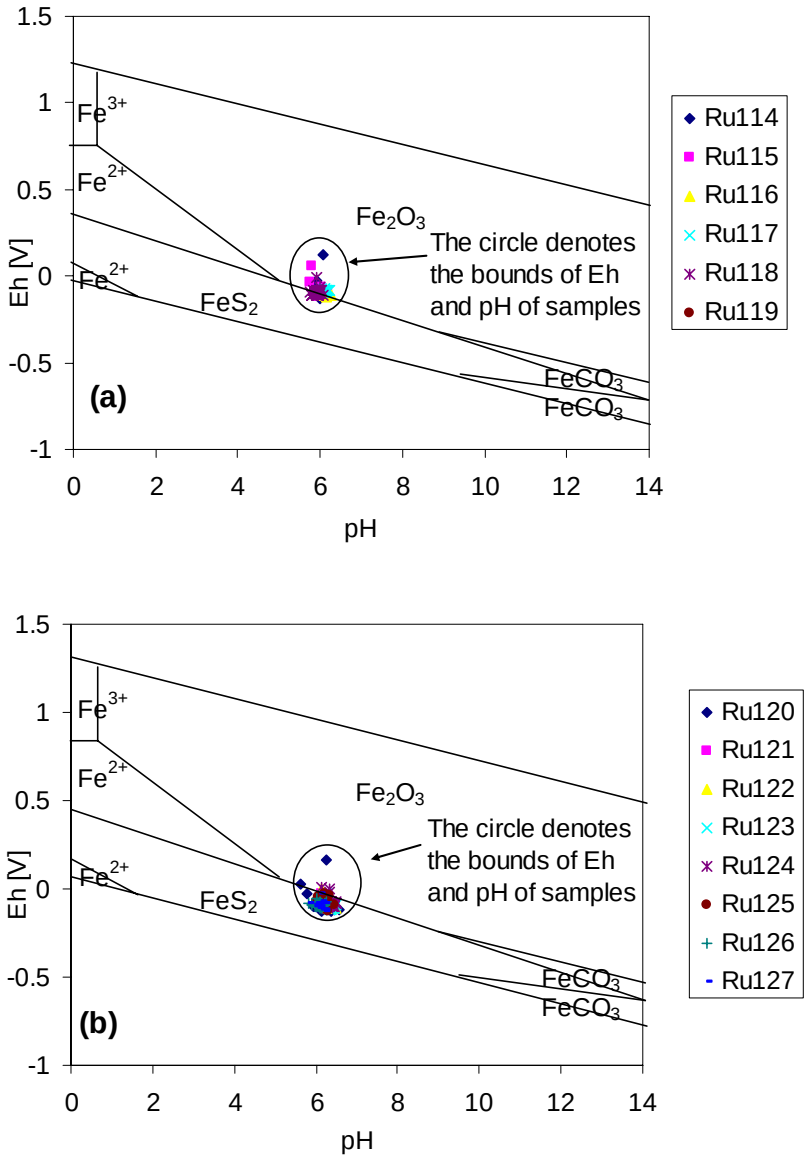

Figure 4-19 *Iron Eh-pH diagrams constructed for the conditions of Lake Rotorua sediments of (a) Cross section 1 and (b) Cross section 2 from May 2006.*

4.3.2 Iron

Ferrous iron profiles in May display mostly increasing concentrations with depth (Figure 4.20). Peaks in concentration occur at depth in the sediment profile, with cross section 1 (Fig. 4.20a) showing peaks of > 12.5 mg/L, and cross section 2 (Fig. 4.20b) peaking at > 20 mg/L below 40 cm depth.

Concentration profiles of ferrous iron in cores Ru118 (Fig. 4.21a) and Ru126 (Fig. 4.21b) show the irregular increase in ferrous iron concentrations with depth in the profile. A rapid reduction in the concentration gradient near the surface indicates an overall trend of upward diffusion where ferrous iron is removed from the pore water as it nears the sediment-water interface. Peak concentrations in the upper 5 cm in the January cross section are not present in May samples, but concentrations at depth are much greater.

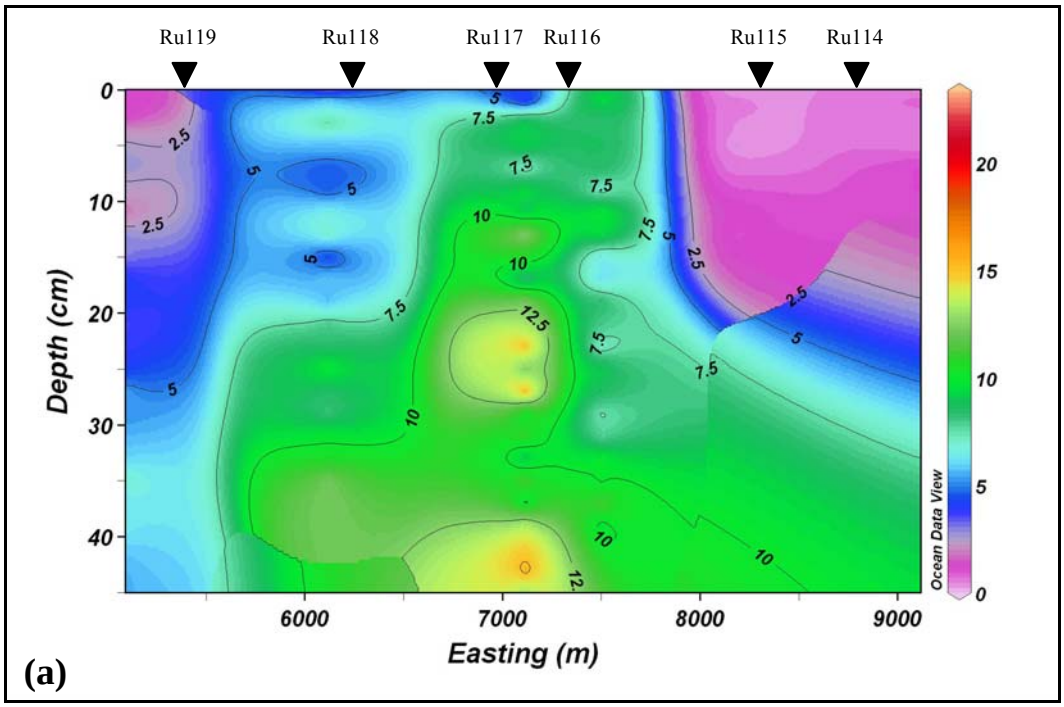

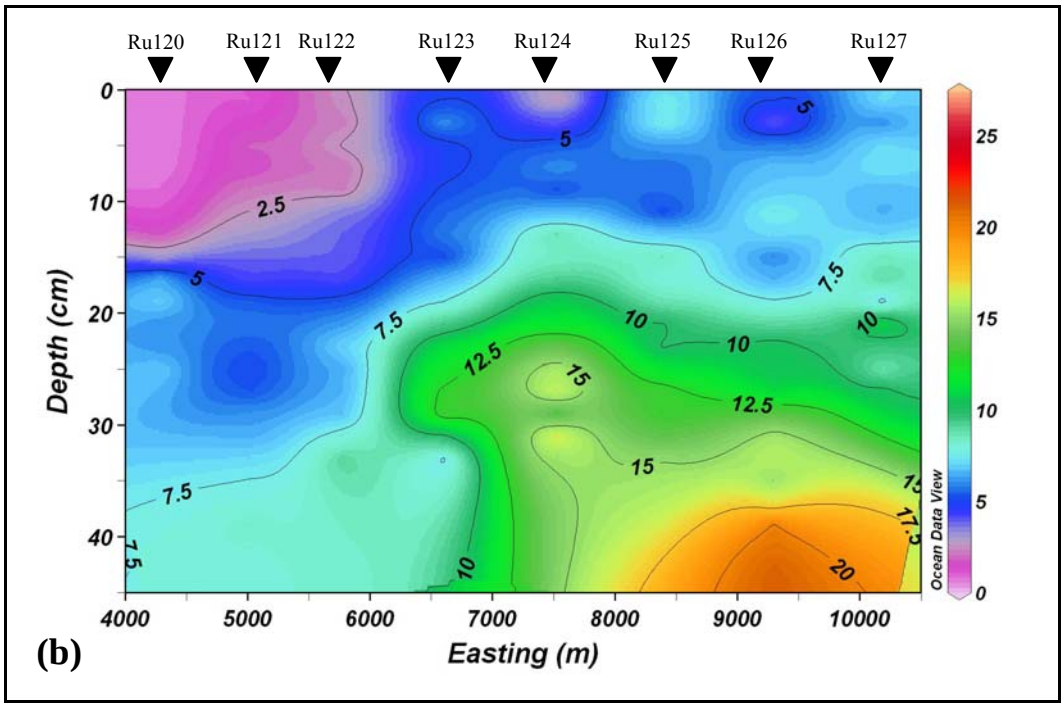

Figure 4-20 *Depth distribution of Fe^{2+} in pore water of (a) May 2006 cross section 1 and (b) May 2006 cross section 2. Concentrations of isopleths are in mg/L.*

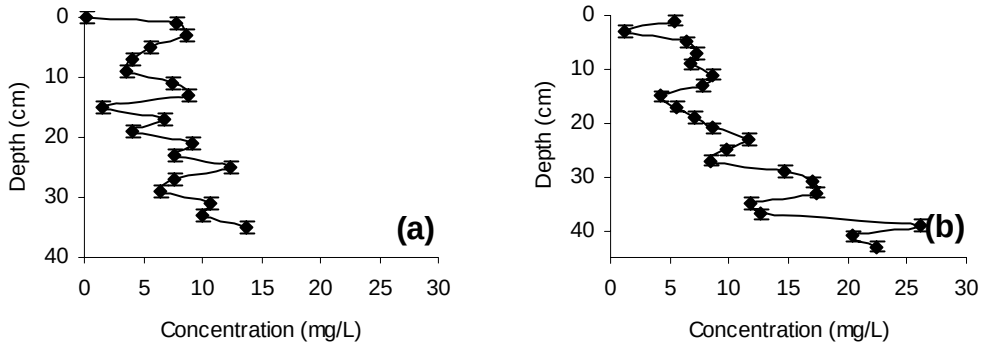

Figure 4-21 *Dissolved iron concentration profiles of cores (a) Ru118 and (b) Ru126.*

4.3.3 Manganese

Manganous concentrations within the pore water show a general trend of increase with depth (Figure 4.22), as observed with iron. Both cross sections display concentration maxima of manganous of > 3.5 mg/L at depth, with the highest concentrations in the same cores as iron. As with ferrous iron, the peak

concentrations in the upper 5 cm observed in the January cross section are not present in the May samples, but with concentrations at depth much greater.

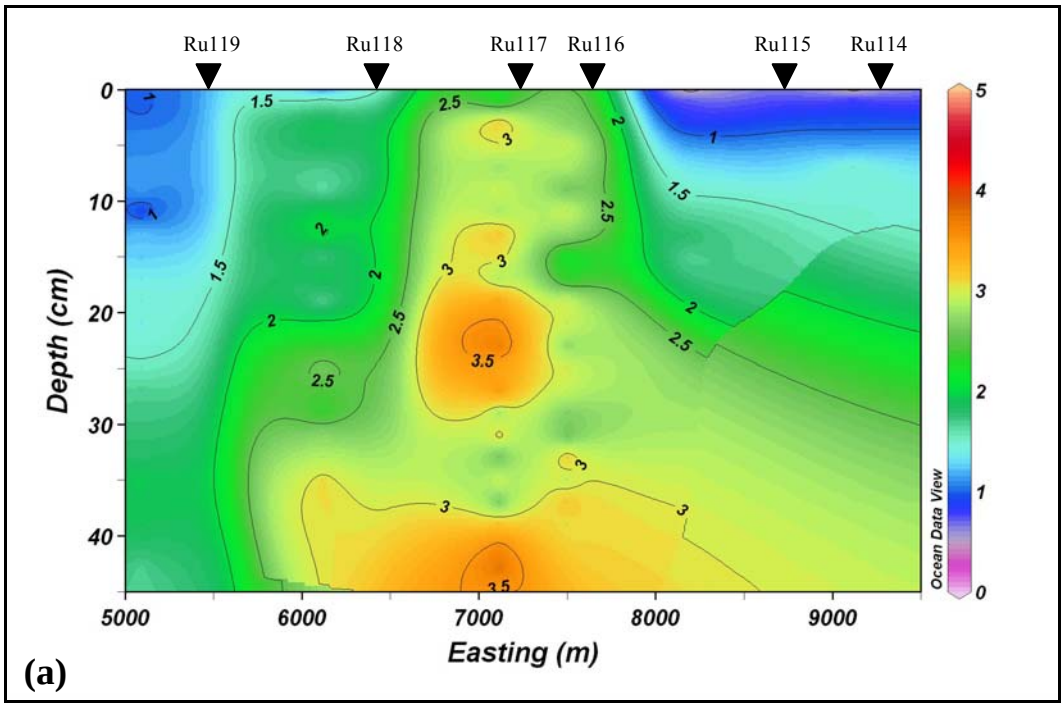

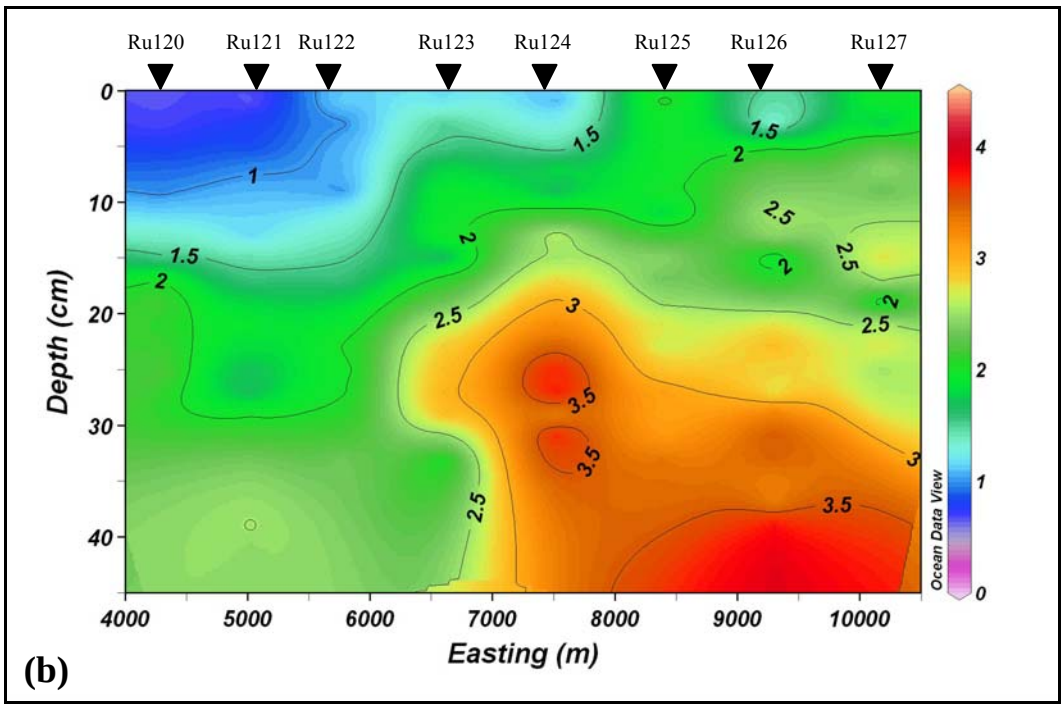

Figure 4-22 *Depth distribution of Mn^{2+} in pore water of (a) May cross section 1 2006 and (b) May cross section 2 in 2006. Concentrations of isopleths are in mg/L.*

Concentration profiles of manganous (Figure 4.23) in (a) Ru118 and (b) Ru126 show irregular increases of manganous with depth. Strong concentration gradients indicate upward diffusion where manganous is rapidly removed from solution as it approaches the sediment-water interface.

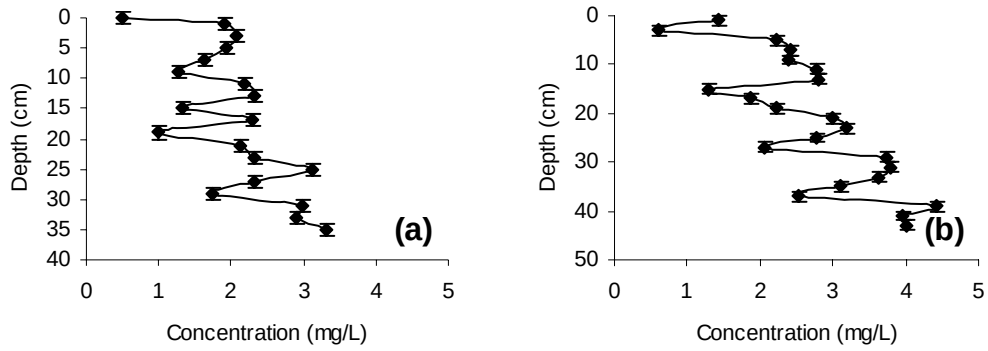

Figure 4-23 *Mn^{2+} pore water concentration profiles of (a) core Ru118 from May cross section 1 and (b) core Ru126 from May cross section 2.*

4.3.4 Sulfur

High rates of total sulfur removal from pore water are indicated by the upper 5 cm of the sediment profile of both cross sections, where concentration peaks range from ~10 to > 25 mg/L (Fig. 4.24). Sulfur concentrations decrease rapidly with depth where concentrations approach the limits of detection ~ 2.5-5 mg/L.

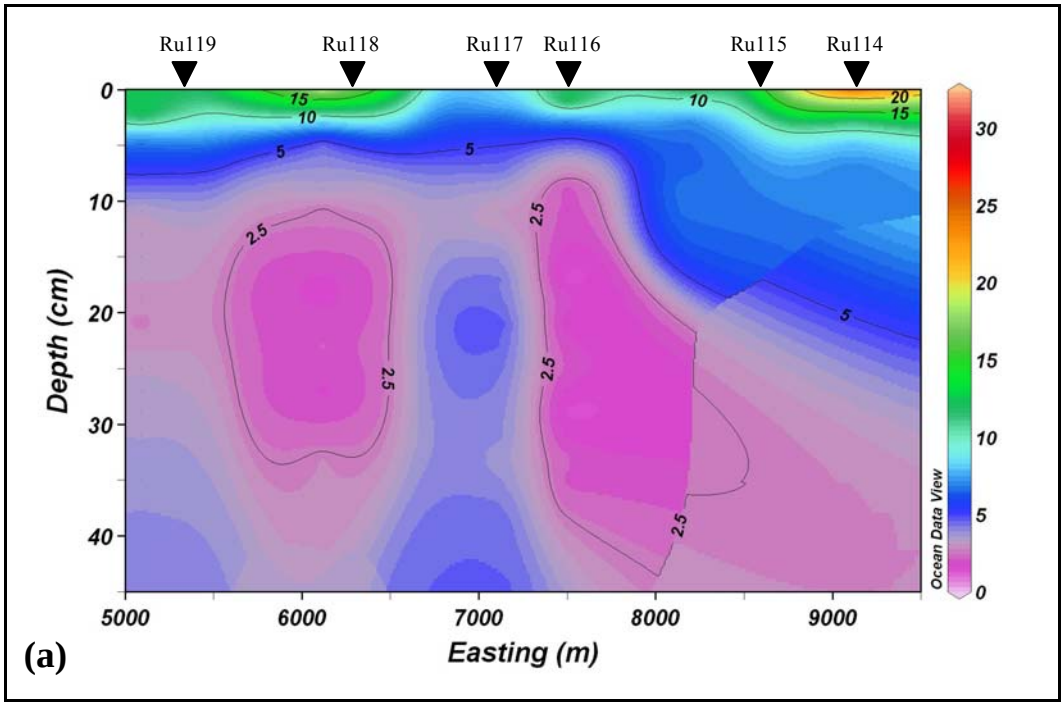

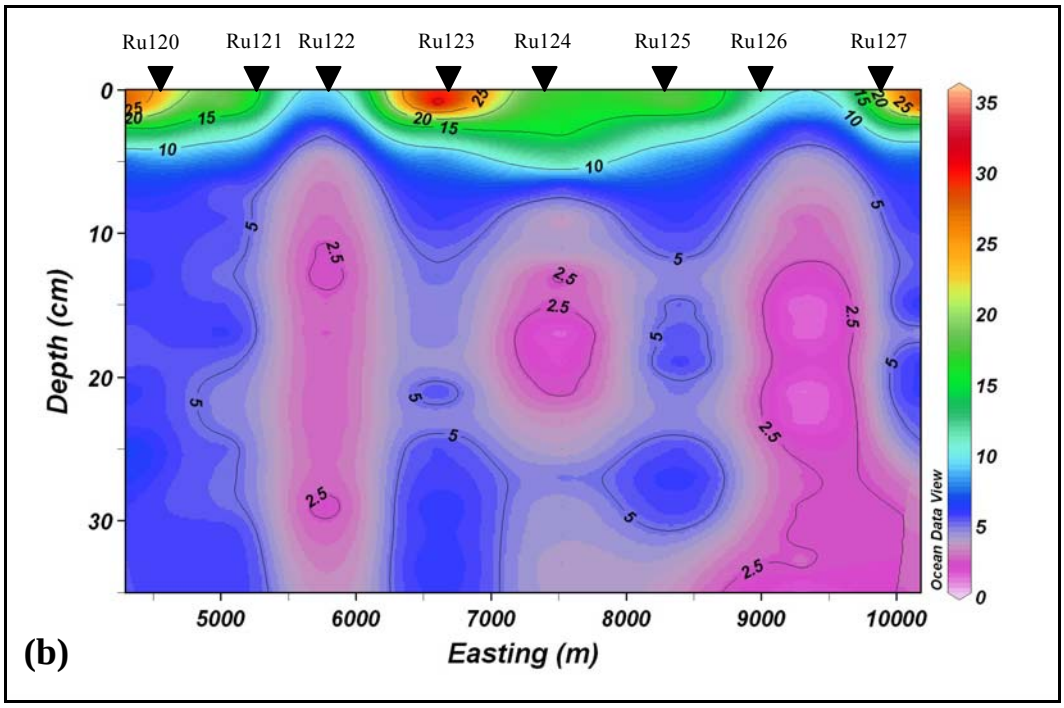

Figure 4-24 *Total sulfur distribution in pore water of (a) May cross section 1 and (b) May cross section 2 from 2006. Concentrations of isopleths are in mg/L.*

The concentration profiles of sulfur suggest possible diffusion from the overlying lake water (Figure 4.25) with sharp concentration gradients in which sulfur is likely to diffuse downward into the sediment and to be removed rapidly from pore water within the upper 5 cm, and into the solid phase of the sediment. Concentrations reach an approximately steady state below 5 cm, indicating no further removal from solution.

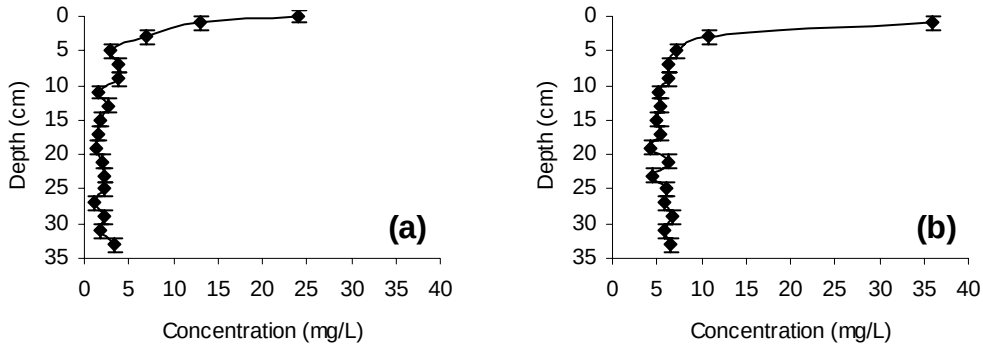

Figure 4-25 *Total sulfur pore water concentration profiles of (a) Ru118 from May cross section 1 and (b) Ru123 from May cross section 2.*

4.3.5 Phosphorus

Concentrations of phosphorus in the two cross sections of Figure 4.26 display quite different trends. Cross section 1 (Fig. 4.26a) displays a similar pattern to that in January, with peaks in concentration > 7 mg/L at or near the sediment-water interface, with a rapid decrease in concentration towards a steady value of ~ 2 mg/L. Cross section 2 (Fig. 4.26b) shows a general increase in concentration with depth, with concentrations > 3.5 mg/L at ~ 40 cm depth. Cores Ru123 and Ru127 show small concentration peaks at the sediment surface.

Concentration profiles in Figure 4.27 illustrate the different gradients in phosphorus. Core Ru118 from cross section 1 (Fig. 4.27a) indicates that diffusion is likely to occur from the strong concentration gradients both up towards the sediment-water interface and down into the sediment where phosphorus is removed from solution. Concentrations reach a relatively constant value of 2 mg/L at depth. Core Ru124 from cross section 2 (Fig. 4.27b) shows an irregular increase in concentration down the sediment profile, where phosphorus is likely to diffuse up along the concentration gradient with rapid removal from pore water from near the sediment-water interface.

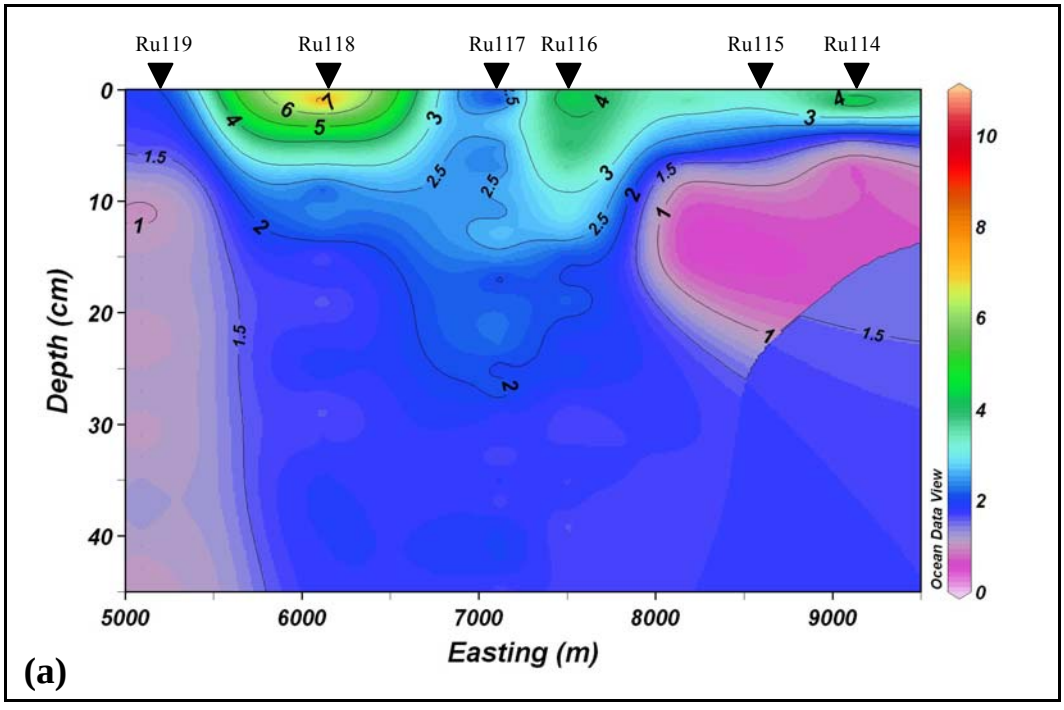

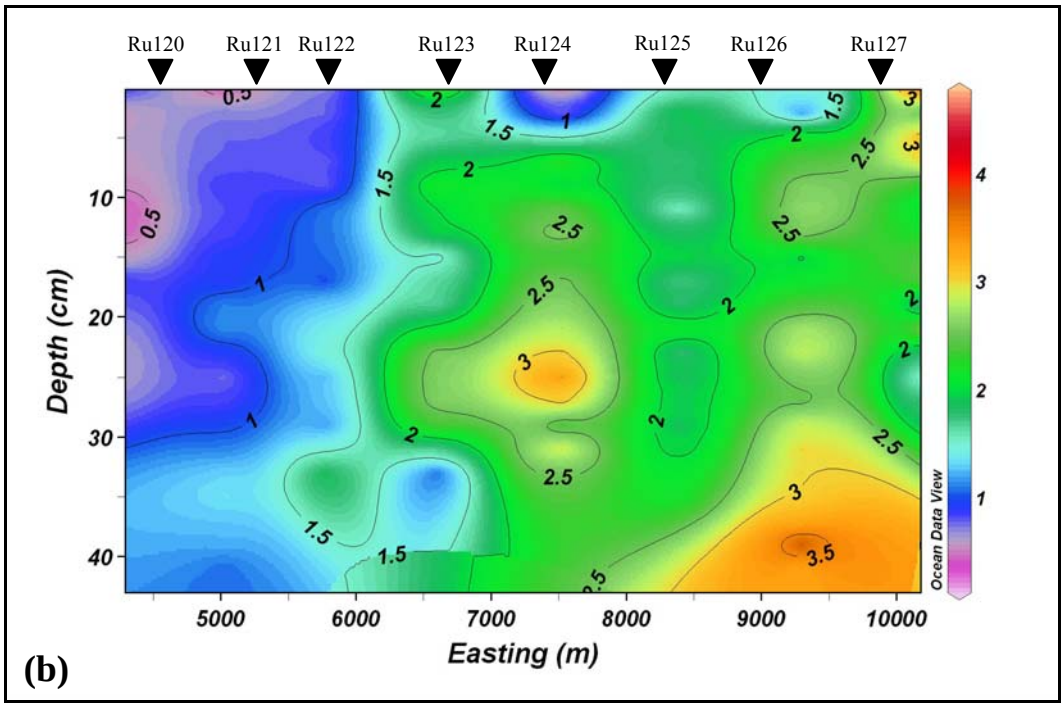

Figure 4-26 *Depth distribution of dissolved phosphorus in pore water of (a) May 2006 cross section 1 and (b) May 2006 cross section 2. Concentrations of isopleths are in mg/L.*

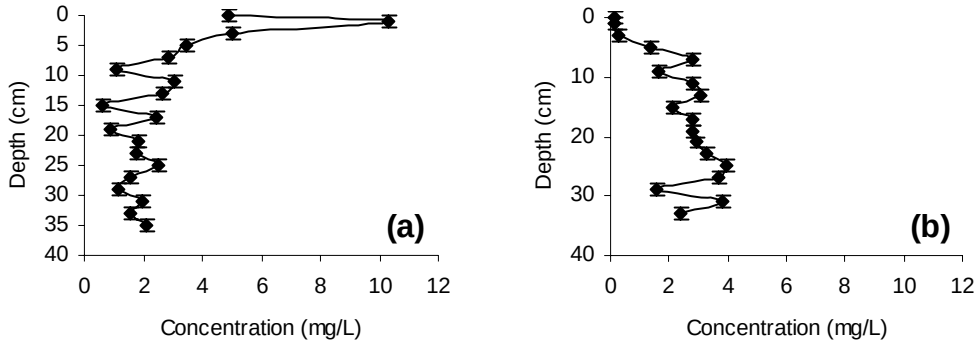

Figure 4-27 *May 2006 dissolved phosphorus pore water concentration profiles of (a) Ru118 from cross section 1 and (b) Ru124 from cross section 2.*

4.3.6 Ammonium

Ammonium concentrations show an increase down the pore water profile (Figure 4.28). Cross section 1 (Fig. 4.28a) has very high concentrations, > 30 mg/L in Ru116 and Ru117, below 5 cm depth. Cross section 2 (Fig. 4.28b) includes cores with concentration peaks > 27.5 mg/L below 35 cm depth in Ru126 and Ru127.

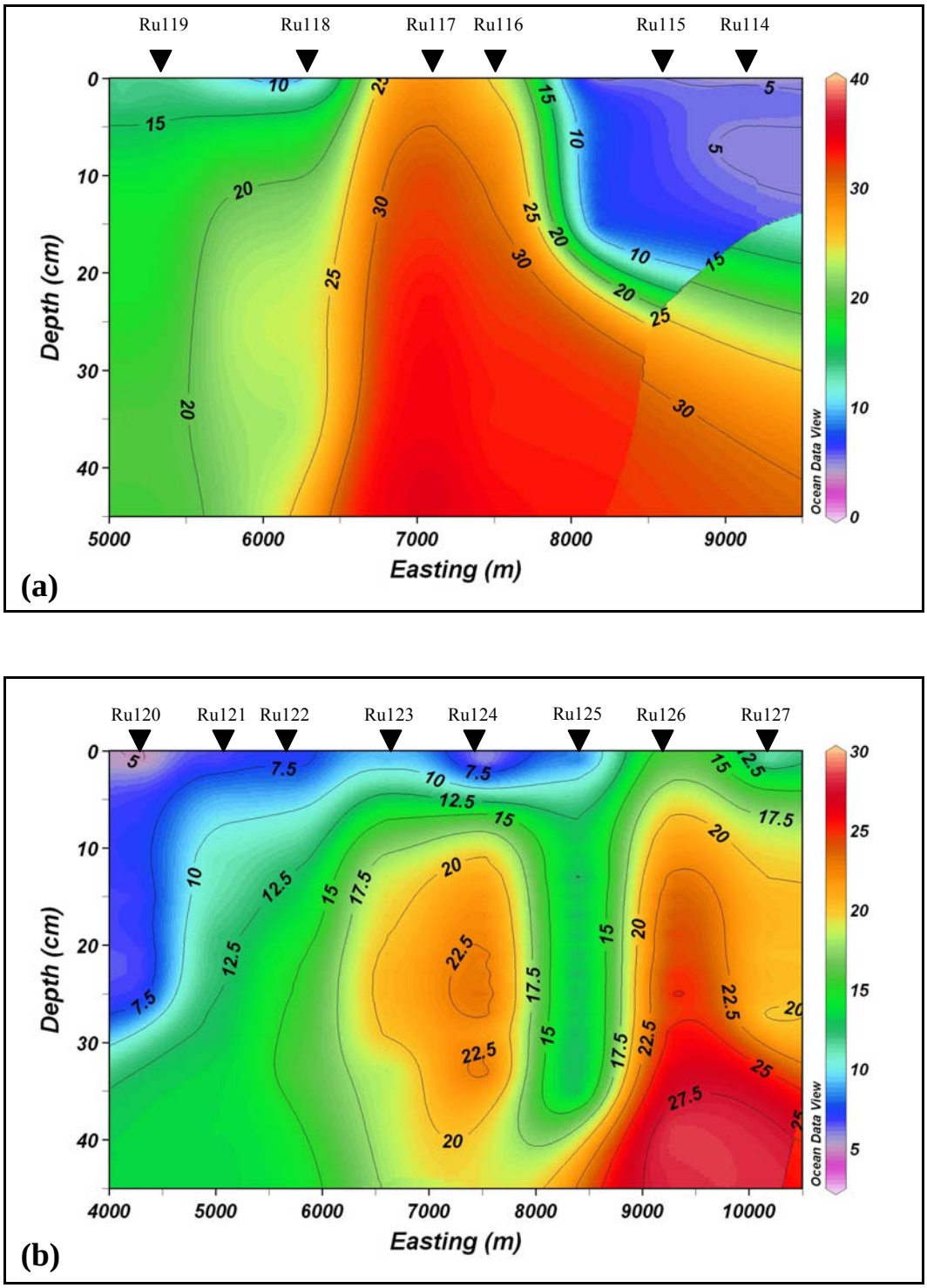

Figure 4-28 *Depth distribution of ammonium in pore water of May 2006 for (a) cross section 1 and (b) cross section 2. Concentrations of isopleths are in mg/L.*

Individual concentration profiles shows ammonium in Ru118 (Fig. 4.29a) and Ru123 (Fig. 4.29b) is likely to diffuse upwards along weak concentration gradients, then to be removed rapidly from the upper 10 cm of the pore water profile.

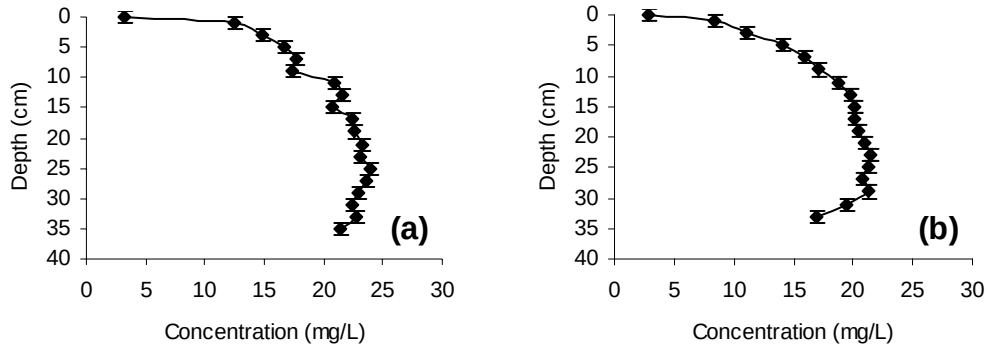

Figure 4-29 *May 2006 ammonium pore water concentration profiles of (a) core Ru118 from cross section 1 and (b) core Ru123 from cross section 2.*

4.3.7 Nitrate

As with January, concentration profiles of nitrate are difficult to interpret (Figure 4.30). They may be from oxidation of very high ammonium in the profile. However the randomness suggests that oxidation occurred post-coring, between collection of cores and analysis on the FIA.

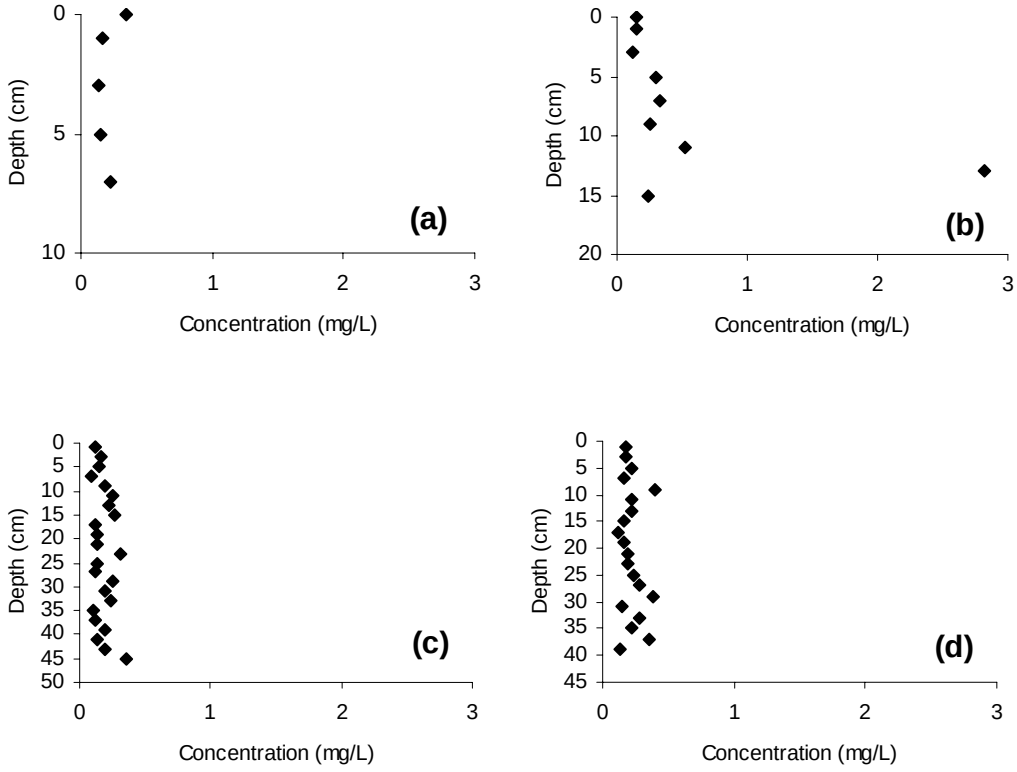

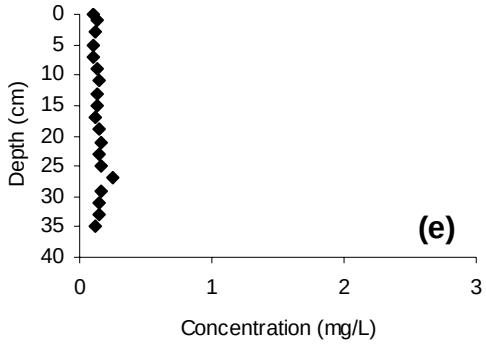
Depth (cm)
0
5
10
15
20
25
30
35
40
0
1
2
3
Concentration (mg/L)
(e)

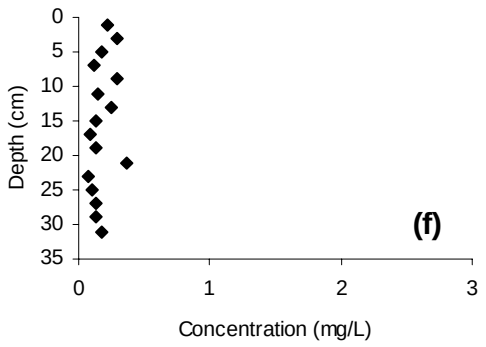
Depth (cm)
0
5
10
15
20
25
30
35
0
1
2
3
Concentration (mg/L)
(f)

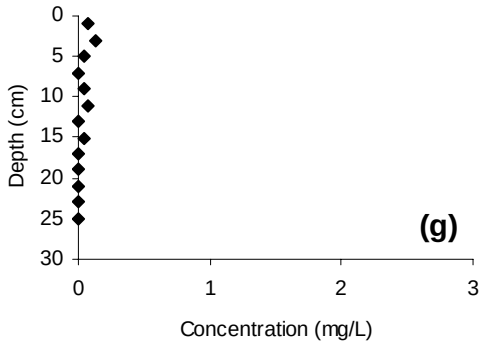
Depth (cm)
0
5
10
15
20
25
30
0
1
2
3
Concentration (mg/L)
(g)

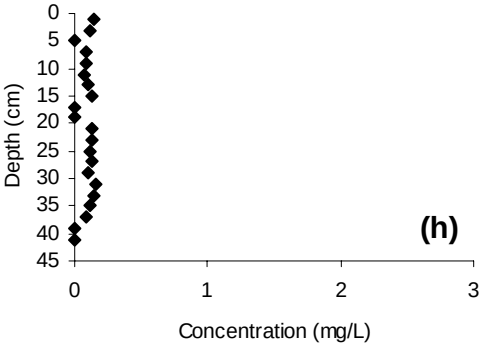
Depth (cm)
0
5
10
15
20
25
30
35
40
45
0
1
2
3
Concentration (mg/L)
(h)

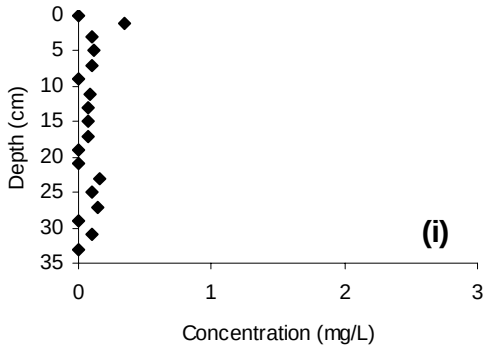
Depth (cm)
0
5
10
15
20
25
30
35
0
1
2
3
Concentration (mg/L)
(i)

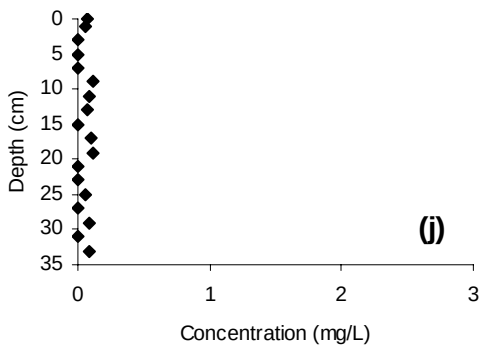
Depth (cm)
0
5
10
15
20
25
30
35
0
1
2
3
Concentration (mg/L)
(j)

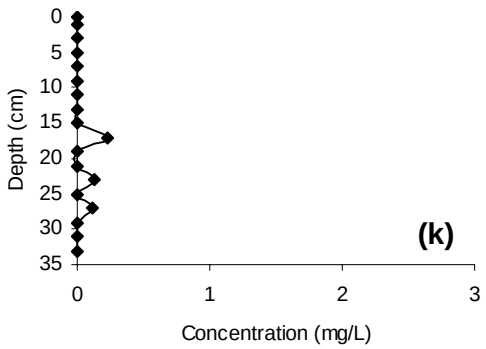
Depth (cm)
0
5
10
15
20
25
30
35
0
1
2
3
Concentration (mg/L)
(k)

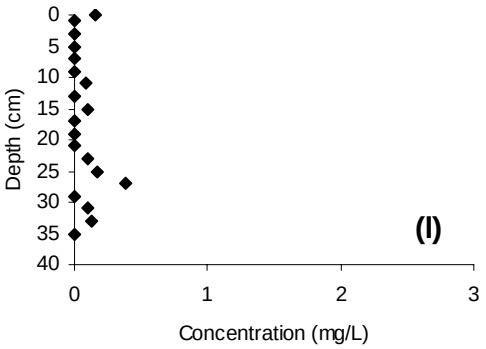
Depth (cm)
0
5
10
15
20
25
30
35
40
0
1
2
3
Concentration (mg/L)
(l)

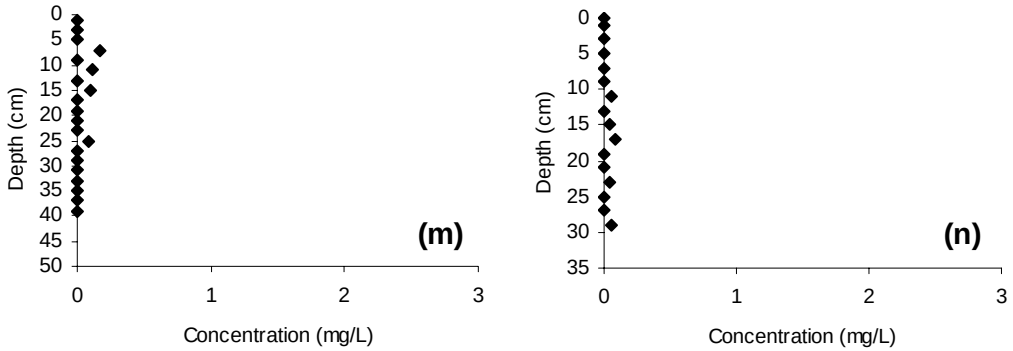

Figure 4-30 *Nitrate pore water concentration profiles of cores (a) Ru114, (b) Ru115, (c) Ru116, (d) Ru117, (e) Ru118, (f), Ru119, (g) Ru120, (h) Ru121, (i) Ru122, (j) Ru123, (k) Ru124, (l) Ru125, (m) Ru126, and (n) Ru127 from May 2006.*

4.3.8 Arsenic

Concentrations of dissolved arsenic are very low and increase down the pore water profile (Figure 4.31). Cross section 1 (Fig. 4.31a) shows concentrations generally below 0.4 mg/L, with a concentration peak > 1.25 mg/L at 15 cm depth in core Ru115. Cross section 2 (Fig. 4.31b) generally has concentrations below 0.4 mg/L but with a small peak in concentration of 0.6 mg/L in core Ru120.

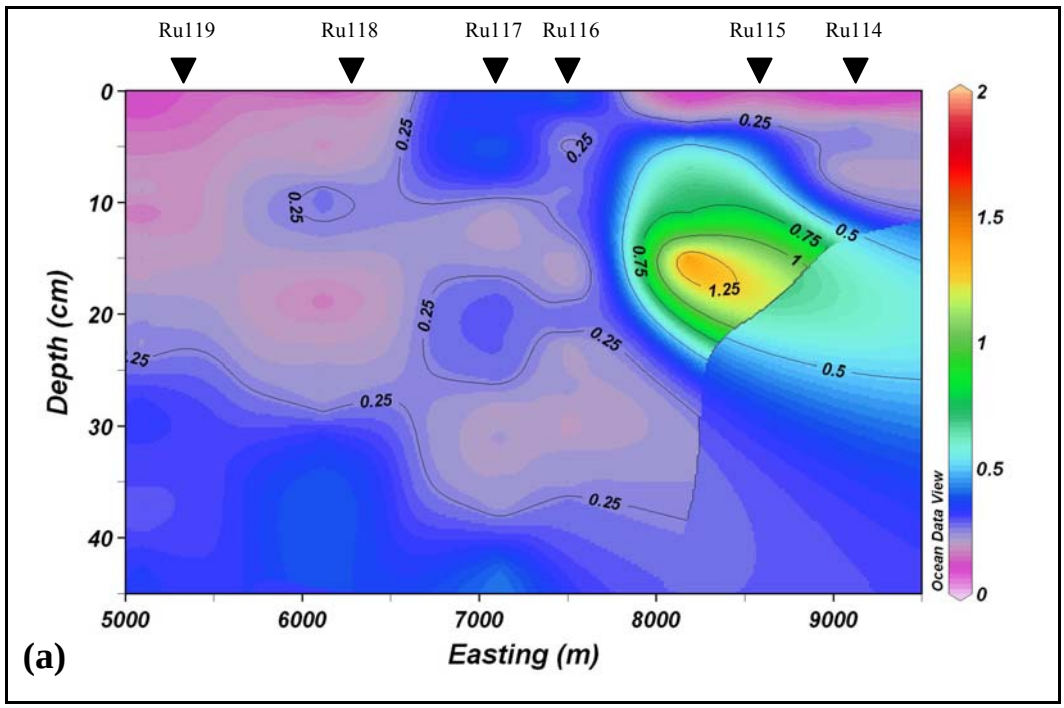

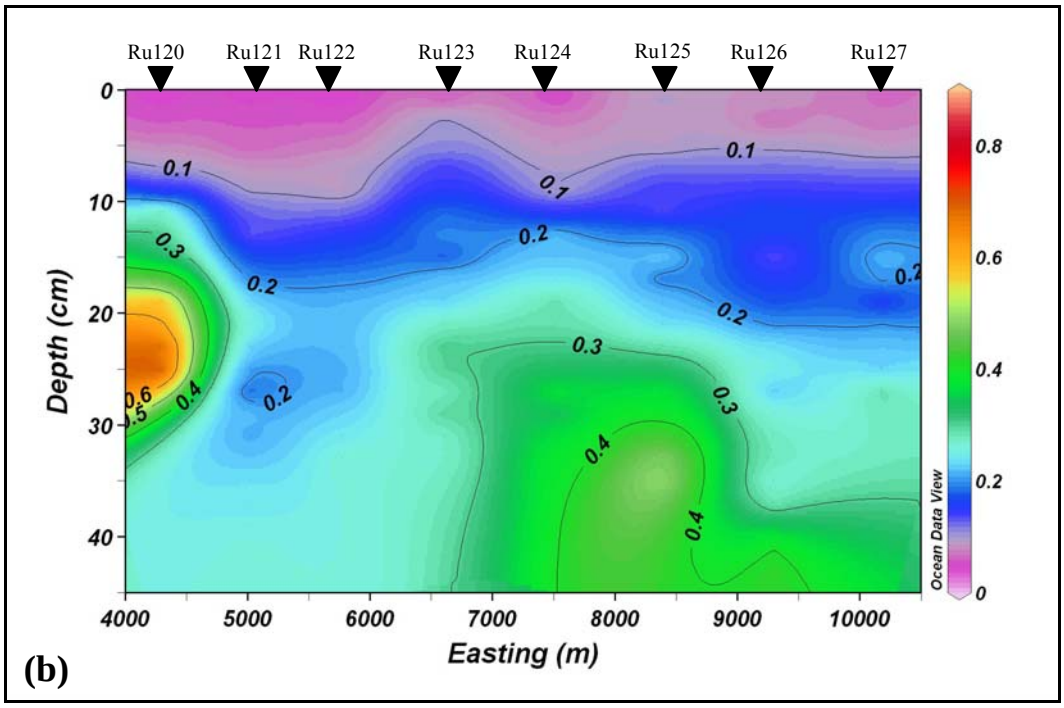

Figure 4-31 *May 2006 depth distribution of dissolved arsenic in pore water of (a) cross section 1 and (b) cross section 2. Concentrations of isopleths are in mg/L.*

Concentration profiles of core Ru119 (Fig. 4.32a) and core Ru123 (Fig. 4.32b) show irregular increases in concentration with depth where dissolved arsenic appears to diffuse upward along concentration gradients and may be removed from pore water as it approaches the sediment-water interface.

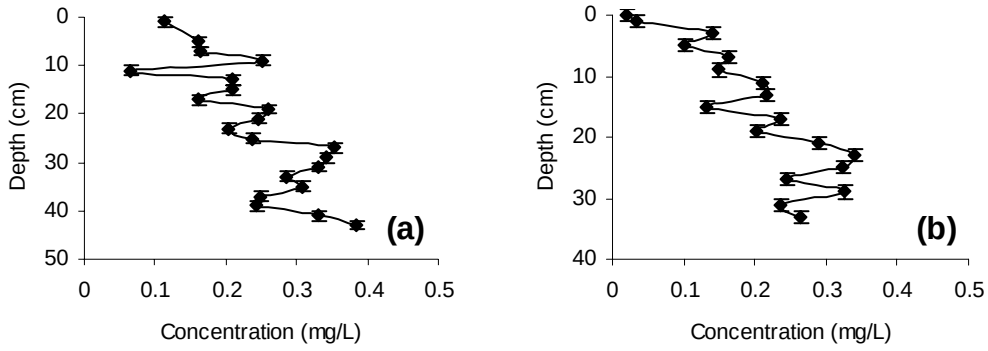

Figure 4-32 *May 2006 dissolved arsenic pore water concentration profiles of (a) Ru119 from cross section 1 and (b) Ru123 from cross section 2.*

4.3.9 Cadmium

Dissolved cadmium concentrations are very low but increase down the pore water profiles shown in Figure 4.33. Core Ru116 in cross section 1 (Fig. 4.33a) shows a small peak in concentration, > 0.015 mg/L, at the sediment-water interface. Concentrations are generally < 0.005 mg/L in both cross sections, with small peaks of up to 0.0075 mg/L deeper in the profile.

Pore water concentration profiles in Figure 4.34 show irregular increases in concentration with depth. Dissolved cadmium is likely to diffuse up along concentration gradients, where it is removed from pore water to the solid sediment.

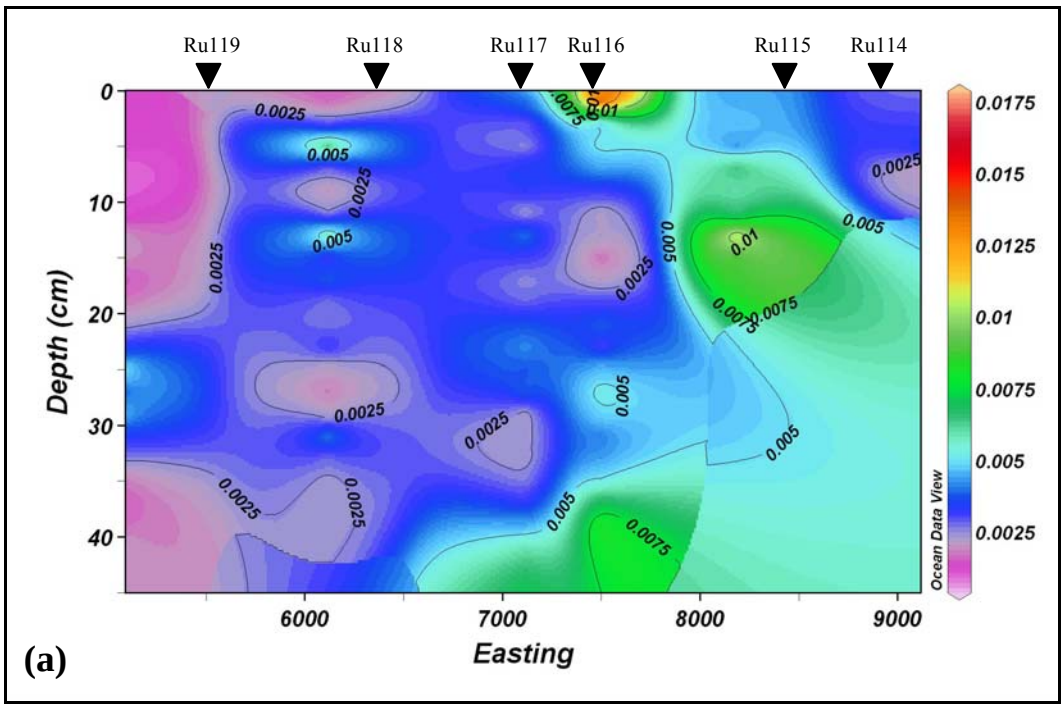

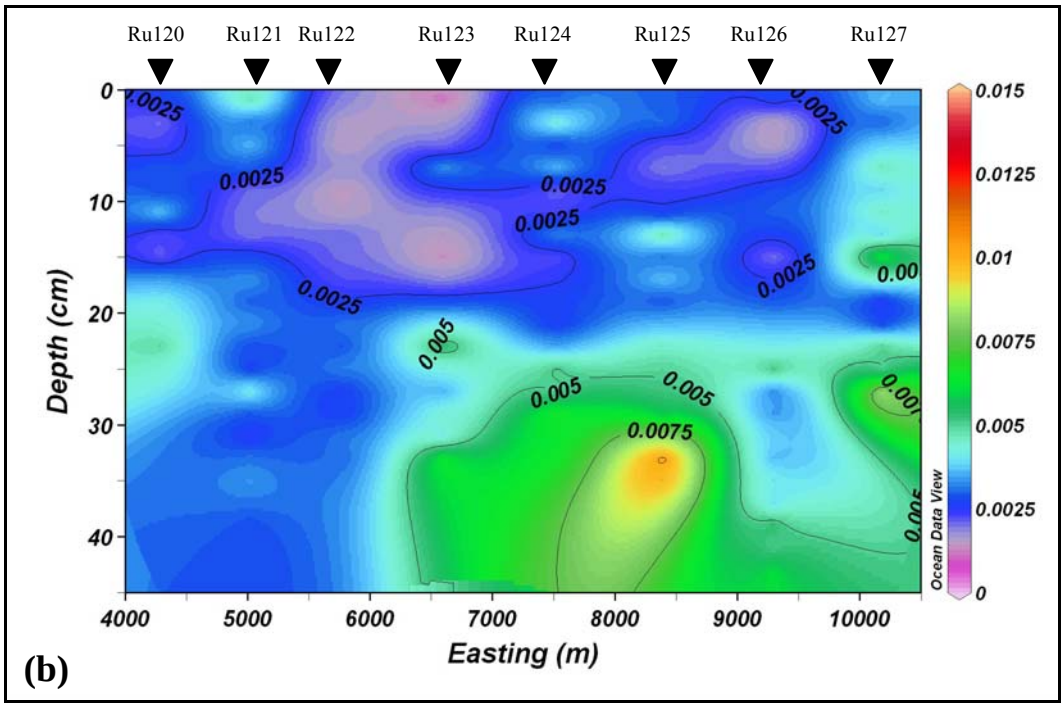

Figure 4-33 *May 2006 depth distribution of dissolved cadmium in pore water of (a) cross section 1 and (b) cross section 2. Concentrations of isopleths are in mg/L.*

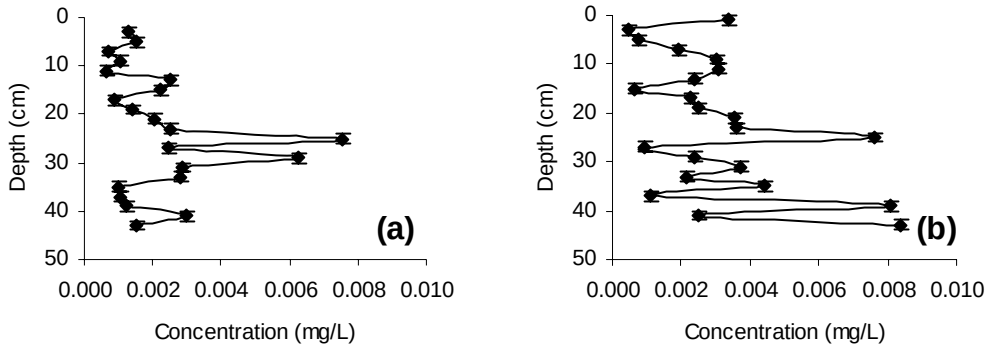

Figure 4-34 *May 2006 dissolved cadmium pore water concentration profiles of (a) Ru119 from cross section 1 and (b) Ru126 from cross section 2.*

4.3.10 Lead

Pore water profiles of dissolved lead show a general increase in concentration with depth (Figure 4.35). Concentrations are generally very low in both profiles, at < 0.005 mg/L. Core Ru119 in cross section 1 (Fig. 4.35a) shows a peak in concentration of > 0.006 mg/L at 23 cm depth. Core Ru125 (Fig. 4.35b) shows a peak in concentration of > 0.01 mg/L at 19 cm depth.

Pore water concentration profiles for cores Ru118 (Fig. 4.36a) and Ru126 (Fig. 4.36b) show that dissolved lead is likely to diffuse upwards along concentration gradients where it is likely to be removed from the pore water by the sediment as it moves toward the sediment-water interface.

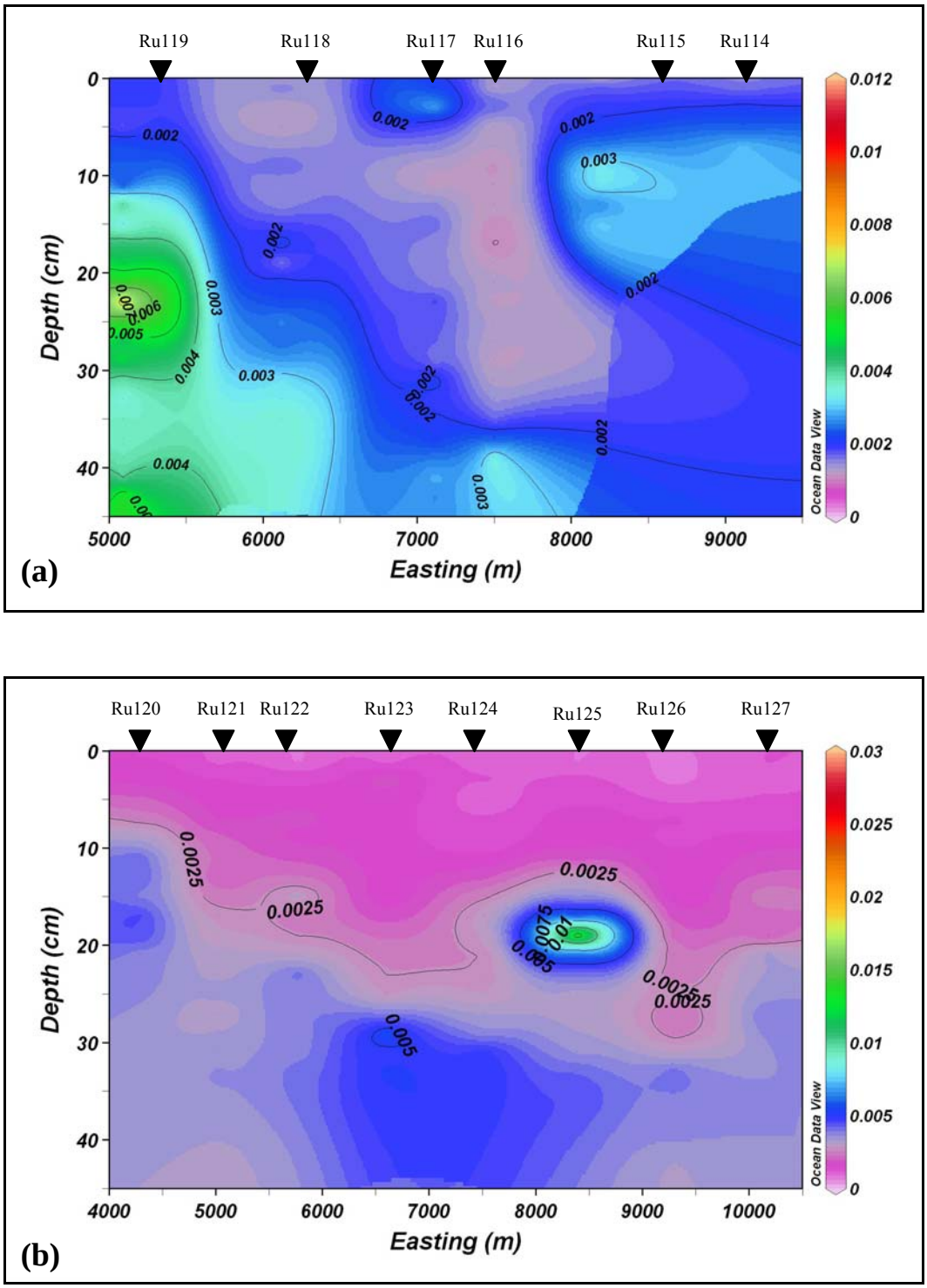

Figure 4-35 *May 2006 depth distribution of lead in pore water of (a) cross section 1 and (b) cross section 2. Concentrations of isopleths are in mg/L.*

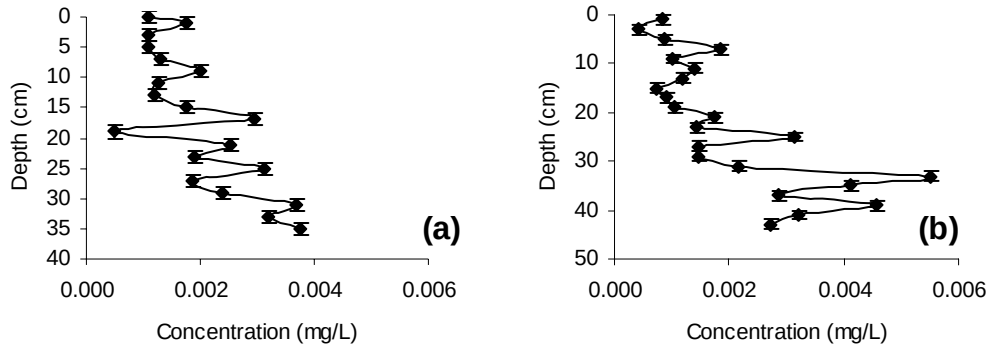

Figure 4-36 *Dissolved lead in pore water concentration profiles from May 2006 of (a) Ru118 from cross section 1 and (b) Ru126 from cross section 2.*

4.4 Spring

Three cross sections of cores were taken in September. A general increase in concentration with depth was observed in all elements, similar to those observed in May. Concentration gradients were generally weaker than those of May.

4.4.1 Eh-pH

Figure 4.37 shows typical pH and Eh profiles observed in pore waters in September. pH remains relatively constant with depth at ~ 6.1 (Fig. 4.37a), with values from all samples in September ranging between 5.78 and 6.8. Eh shows a large drop in the upper 3 cm of the profile from just below 0 V to where it attains a relatively constant value of around -0.1 V with depth (Fig. 4.37b). All samples from September show the same trend, with Eh values ranging from 0.056 V in the upper profile to -0.166 V in the lower profile.

Eh-pH diagrams of iron constructed for the conditions corresponding to Lake Rotorua in Figure 4.38 show pore water collected in September lies on the boundary between Fe_2O_3 and FeS_2. Samples near the sediment surface usually fall within the Fe_2O_3 boundary and samples in the lower profile fall within the FeS_2 boundary.

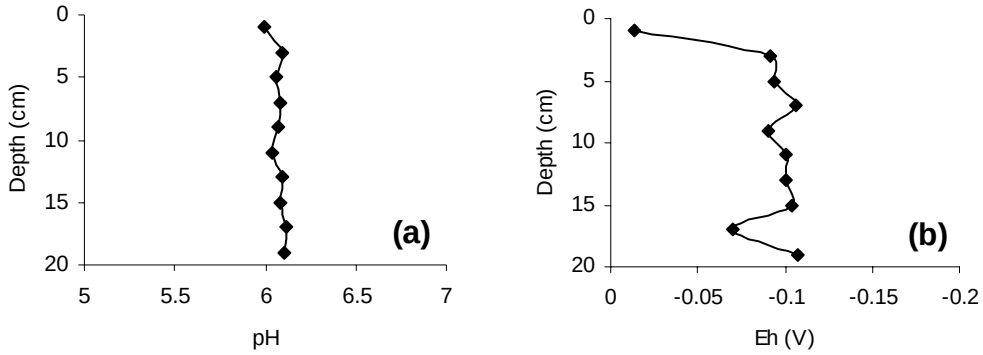

Figure 4-37 *Core Ru145 gradient of (a) pH and (b) Eh from September 2006.*

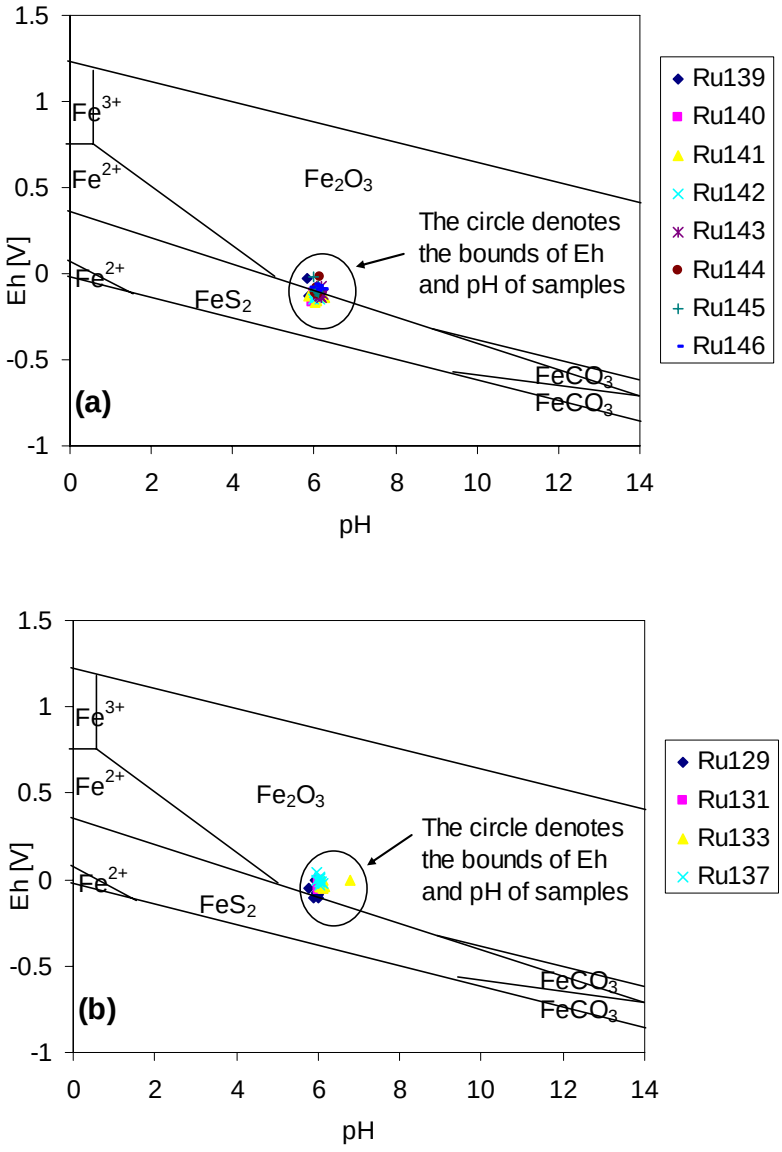

Figure 4-38 *Iron Eh-pH diagrams of (a) cross section 1 and (b) cores Ru129, Ru131, Ru133, and Ru137 from September 2006.*

4.4.2 Iron

Ferrous iron generally increases in concentration with depth (Figure 4.39), as observed in May, with cross sections 1 (Fig. 4.39a) and 2 (Fig. 4.39b) showing peaks in concentration > 10 mg/L. Cross section 3 (Fig. 4.39c) shows high concentrations in cores Ru129 and Ru130 (> 15 mg/L), and cores Ru161 and Ru162 (>12.5 mg/L). A few concentration peaks occur at the sediment surface of cross sections 1 and 3. Concentrations were generally less than those observed in May.

Concentration profiles of cores Ru145 (Fig. 4.40a) and Ru162 (Fig. 4.40b) indicate likelihood of upward diffusion along concentration gradients. Core Ru145 indicates removal of ferrous iron as it moves towards the sediment-water interface. Core Ru162 indicates little loss of ferrous iron to the sediment as gradients are likely to be mostly across the sediment-water interface. Concentration gradients in September were generally weaker than those in May.

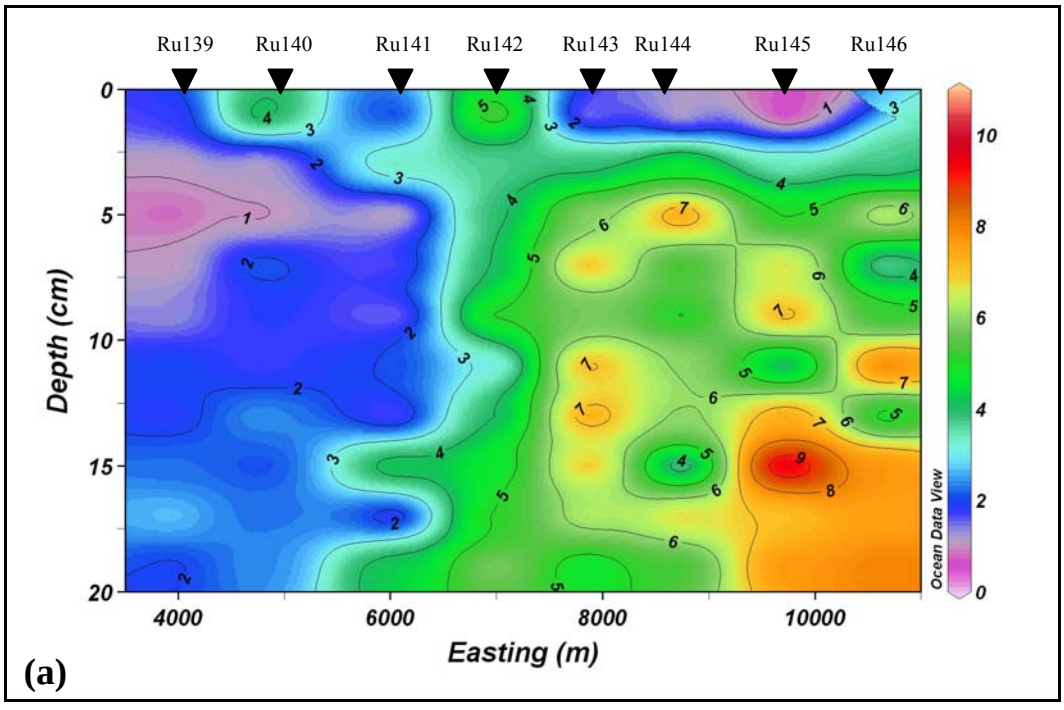

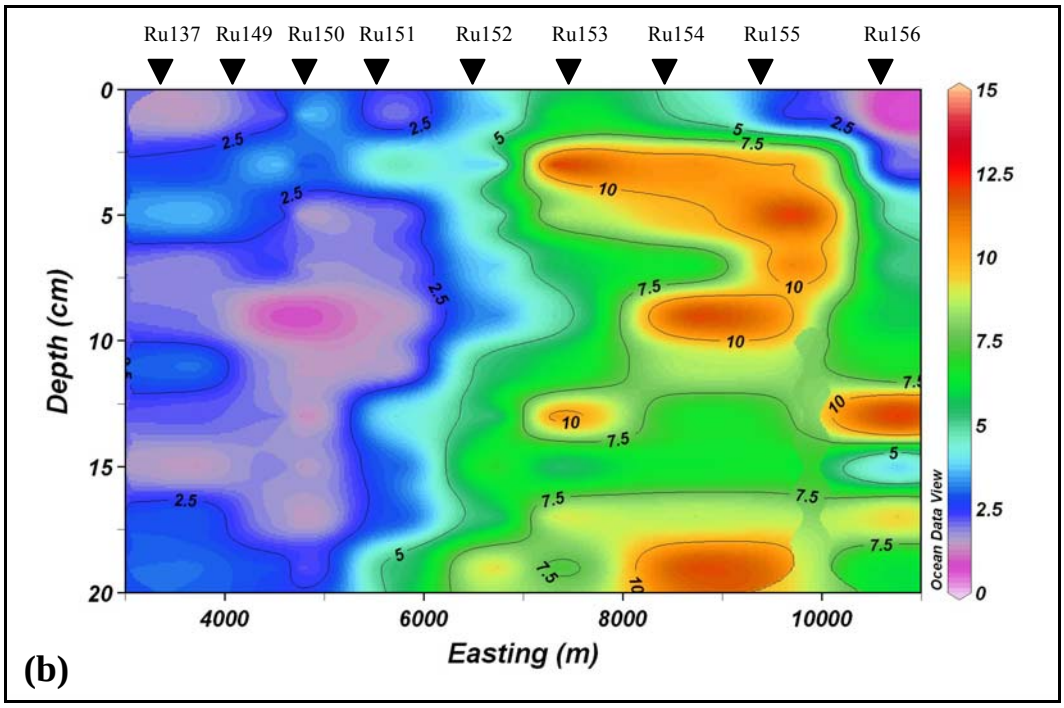

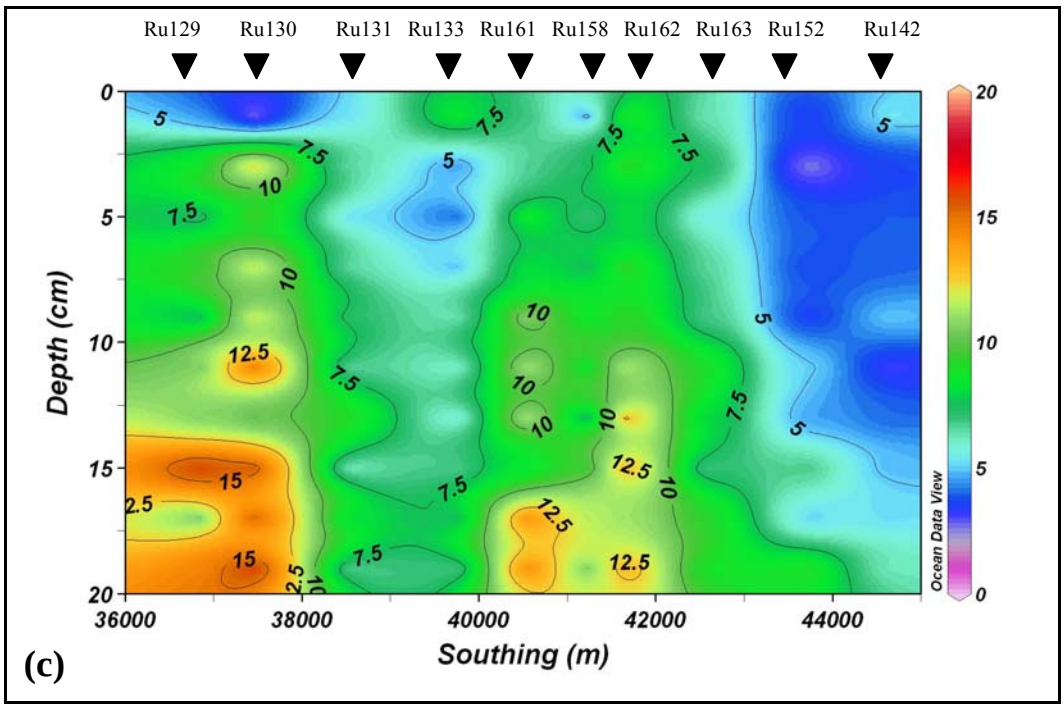

Figure 4-39 *September 2006 depth distribution of Fe^{2+} in pore water of (a) cross section 1, (b) cross section 2 and (c) cross section 3. Concentrations of isopleths are in mg/L.*

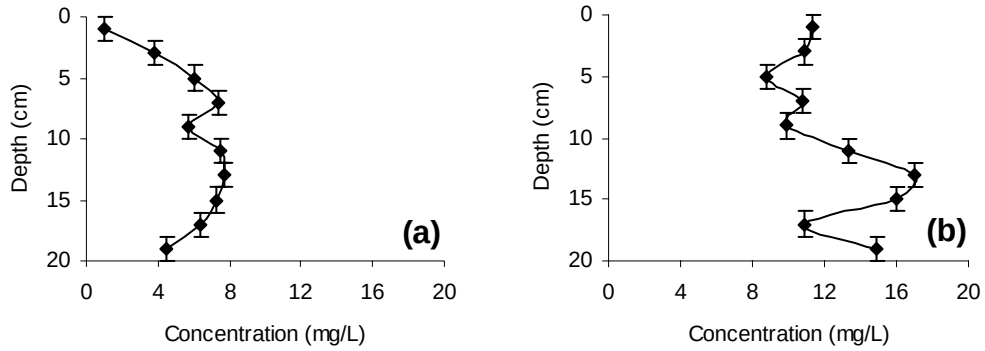

Figure 4-40 *September 2006 Fe^{2+} pore water concentration profiles of (a) core Ru143 from cross section 1 and (b) core Ru162 from cross section 3.*

4.4.3 Manganese

Manganese showed the same pattern as iron, with a general increase in concentration with depth (Figure 4.41), and concentration peaks that in some cases exceeded 5 mg/L. Concentrations in September transects were similar to those in May.

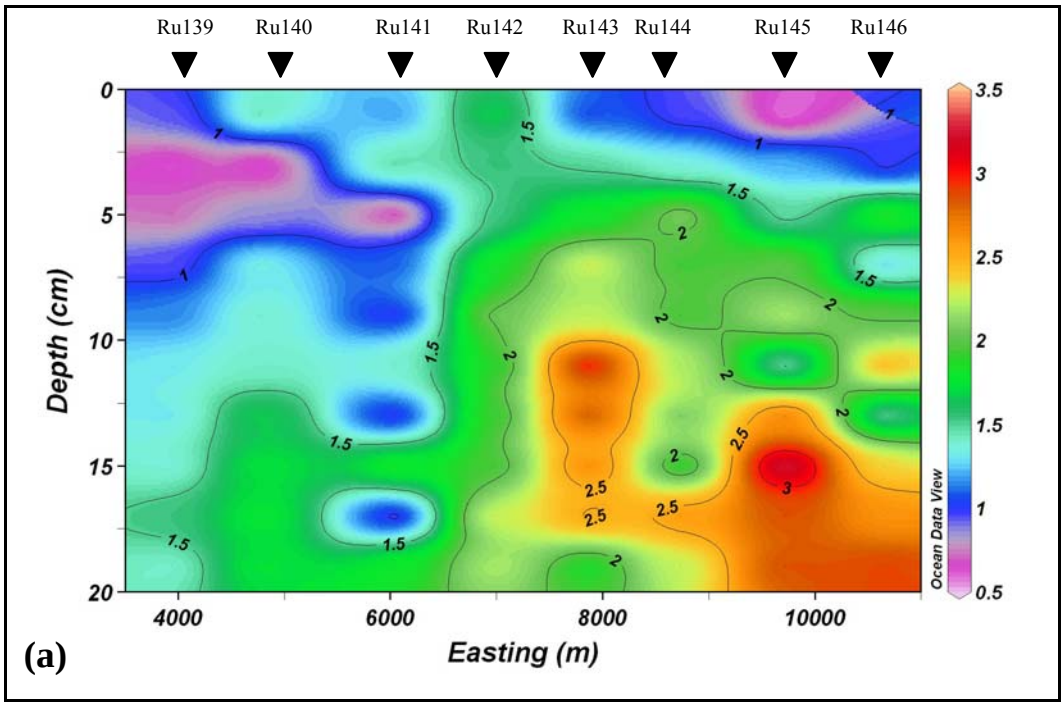

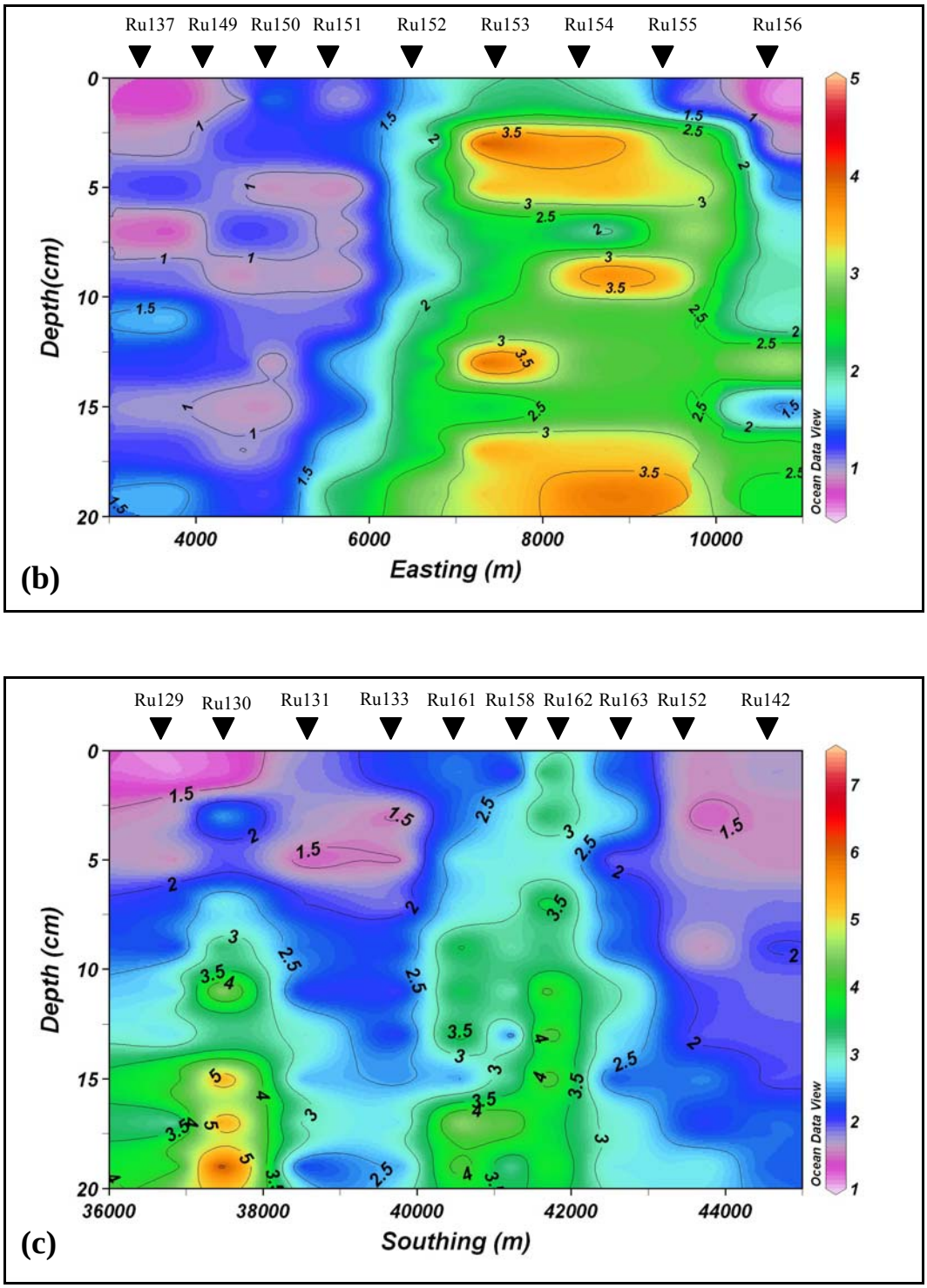

Figure 4-41 *September 2006 depth distribution of Mn^{2+} in pore water of (a) cross section 1, (b) cross section 2 and (c) cross section 3. Concentrations of isopleths are in mg/L.*

Concentration gradients in cores Ru145 (Figure 4.42a) and Ru162 (Figure 4.42b) indicate likelihood of upward diffusion. Core Ru145 suggest that there is removal of manganous from pore water as it moves towards the sediment-water interface.

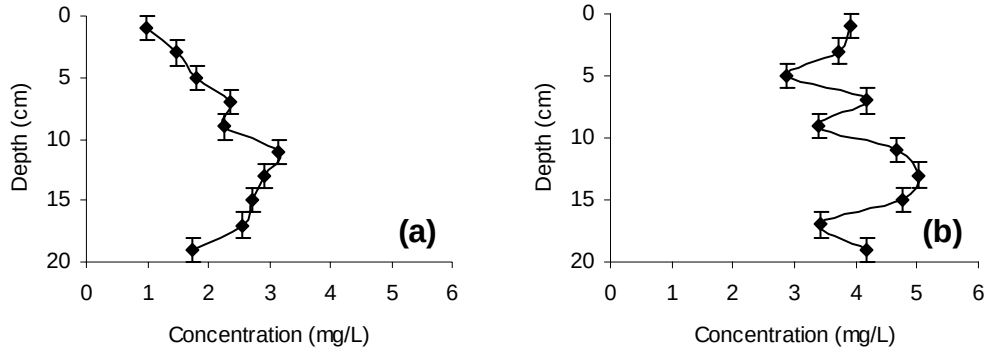

Figure 4-42 *September 2006 Mn^{2+} pore water concentration profiles of (a) core Ru143 from cross section 1 and (b) core Ru162 from cross section 2.*

4.4.4 Sulfur

Significant sulfate reduction is occurring in the upper 5 cm of the pore water profile as concentrations of sulfur decreased rapidly in this region and then reached near limit of detection levels 1 and 5 mg/L. The concentration profile in the pore waters of core Ru141 (Fig. 4.43e) shows very little sulfur at the top of the core. It would appear that the sediment-water interface was missed in the coring process. Sulfate reduction is also likely to occur below 10 cm depth in cores Ru129 (Figure 4.43a), Ru131 (Figure 4.43c), Ru140 (Figure 4.43d), Ru142 (Figure 4.43f), and Ru146 (Figure 4.43j). As all of core Ru144 (h) returned concentrations below the detection limit of the ICP-OES it is likely that the sediment water interface was missed.

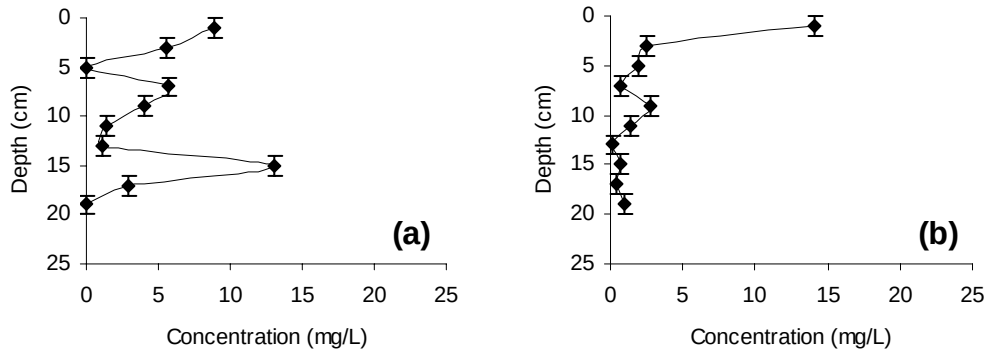

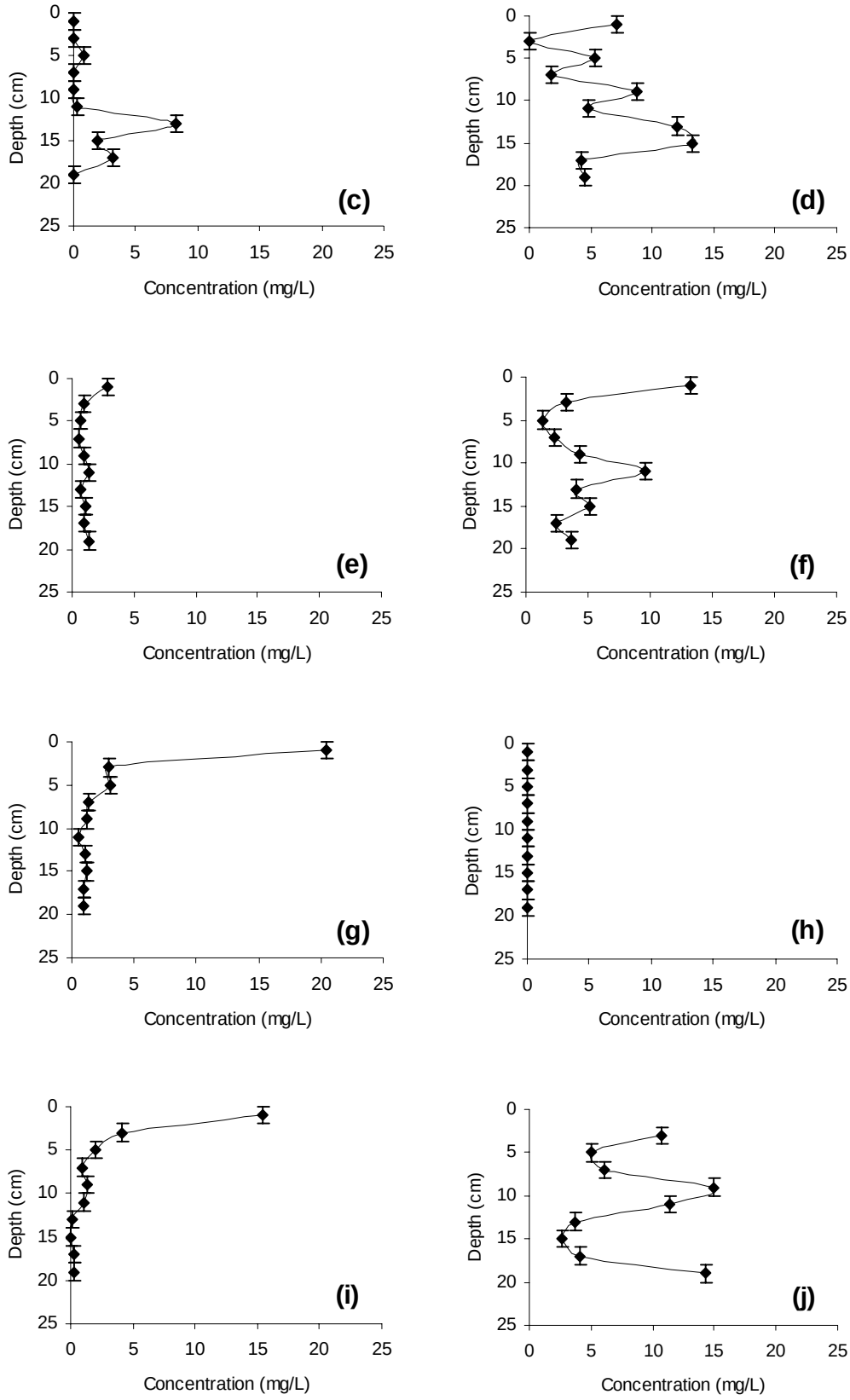

Figure 4-43 *Total Sulfur pore water concentration profiles of (a) Ru129, (b) Ru130, (c) Ru131, and from cross section 1 (d) Ru140, (e) Ru141, (f) Ru142, (g) Ru143, (h) Ru144, (i) Ru145 and (j) Ru146 from September 2006.*

4.4.5 Phosphorus

Dissolved phosphorus generally shows an irregular increase in concentration with depth through all cross sections (Figure 4.44). Patches of high concentration generally occur near the same depth as peaks in ferrous and manganous. Concentration peaks of 3-4 mg/L occurred in all cross sections.

Concentration profiles of dissolved phosphorus indicate that there is likely to be upward diffusion along concentration gradients where phosphorus is removed from pore water into the sediment (Figure 4.45a) and diffusion across the sediment-water interface (Figure 4.45b). Concentration gradients into the sediment occurred in both profiles suggesting that phosphorus is likely to be removed from solution at depth.

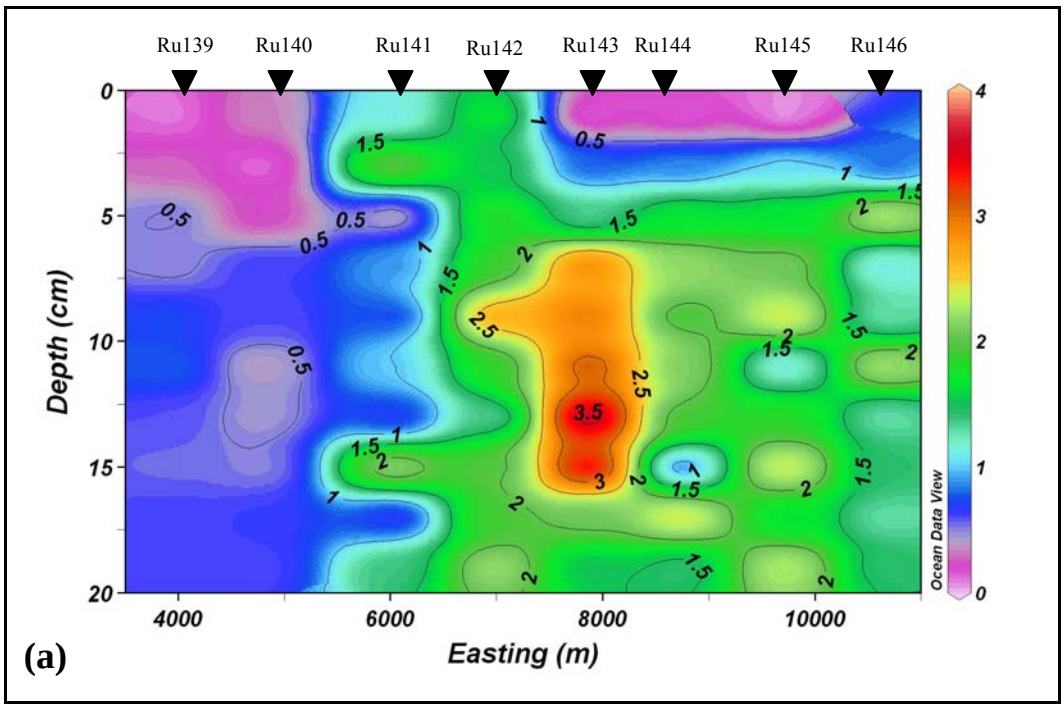

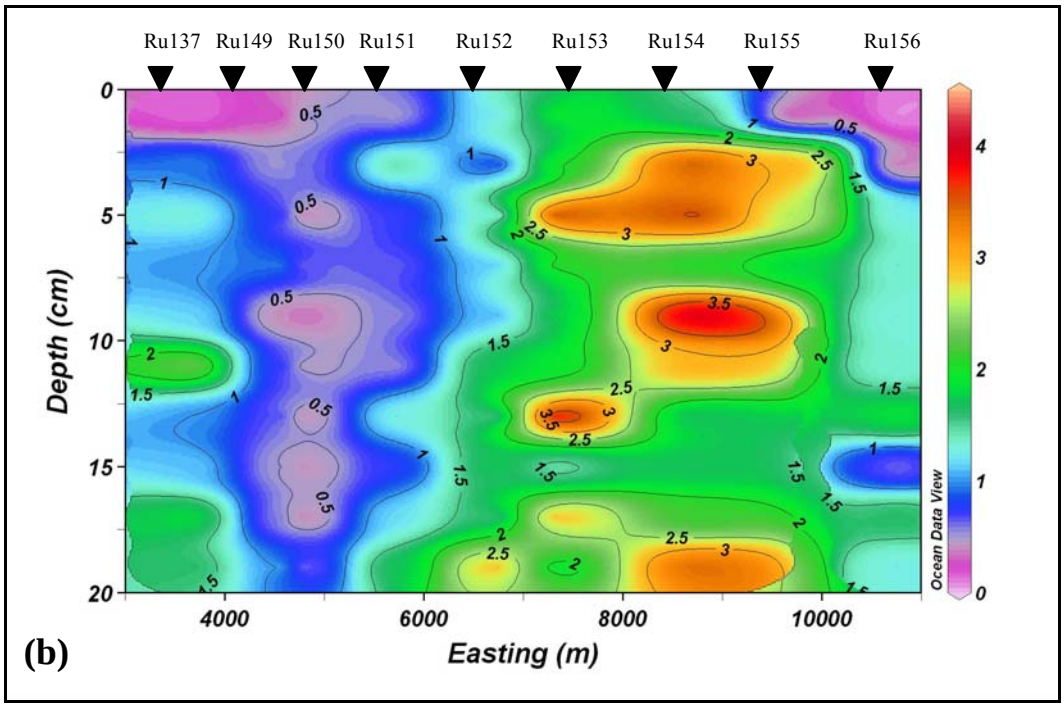

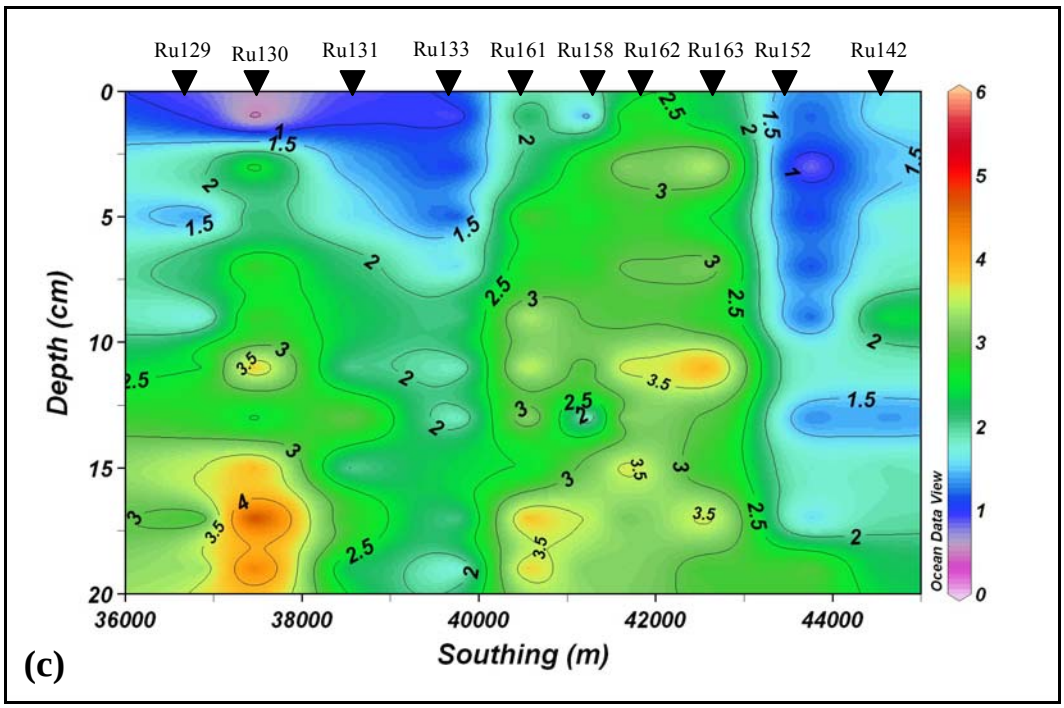

Figure 4-44 *September 2006 depth distribution of dissolved phosphorus in pore water of (a) cross section 1, (b) cross section 2 and (c) cross section 3. Concentrations of isopleths are in mg/L.*

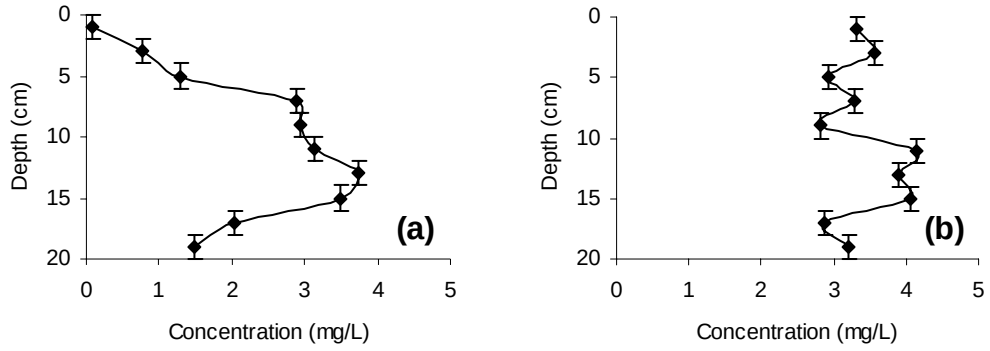

Figure 4-45 *September dissolved phosphorus pore water concentration profiles of (a) Ru143 from cross section 1 and (b) Ru162 from cross section 2.*

4.4.5 Ammonium

Ammonium concentrations in cross section 1 from September show an increase in concentration down the sediment profile (Figure 4.46), with peaks of > 22.5 mg/L in the lower 15 cm of the profile in Ru144-146. Concentration profiles of ammonium in Figure 4.47 indicate the likelihood of upward diffusion along concentration gradients with ammonium removed from pore water as it moves toward the sediment-water interface.

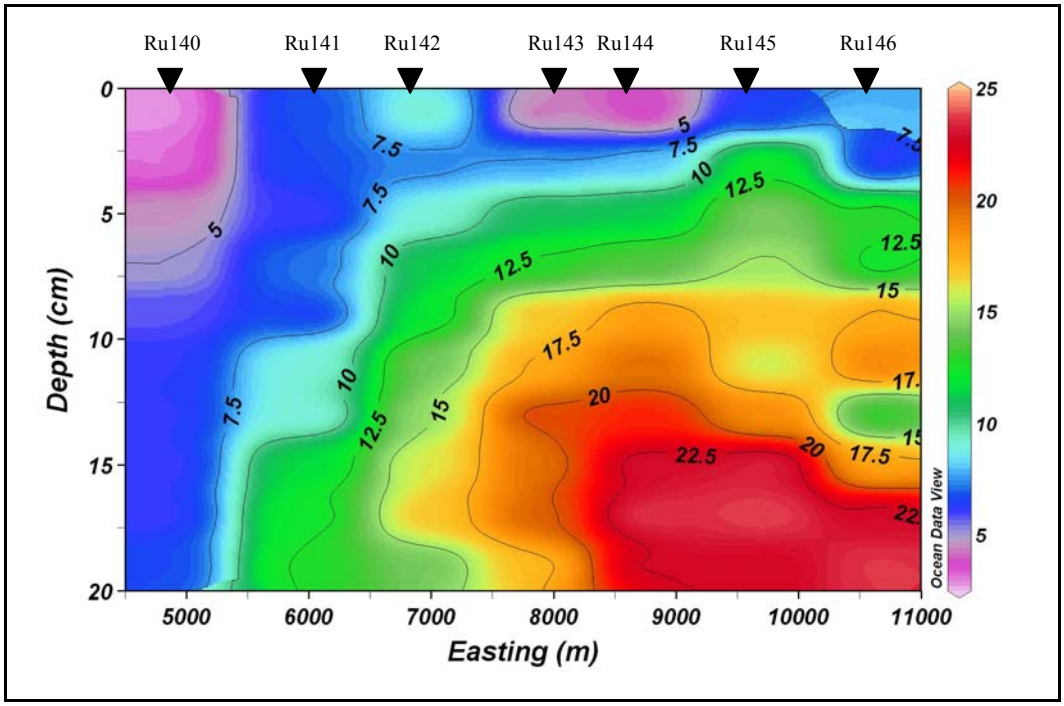

Figure 4-46 *September 2006 depth distribution of ammonium in pore water of cross section 1. Concentrations of isopleths are in mg/L.*

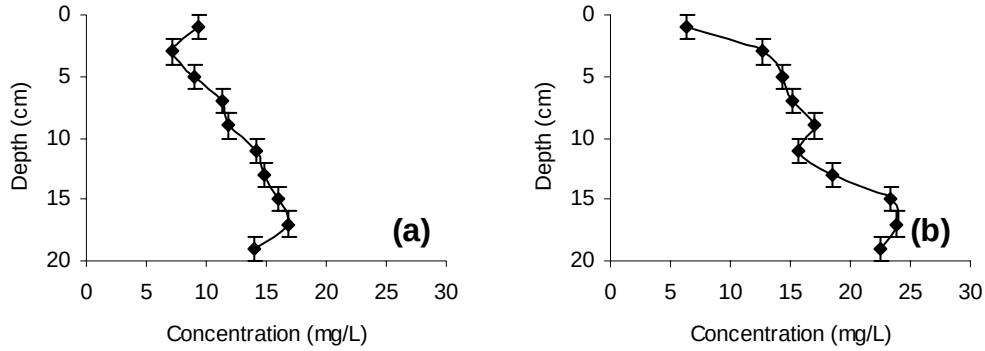

Figure 4-47 *Ammonium pore water concentration profiles of (a) Ru142 and (b) Ru145 from September 2006 cross section 1.*

Figure 4.48 illustrates the concentration profiles in cores Ru129 and Ru130. Core Ru129 (Figure 4.48a) has concentrations approaching 50 mg/L and core Ru130 approaching 70 mg/L at depth. The strong concentration gradients indicate that there is likely to be very strong removal from pore water at the sediment surface.

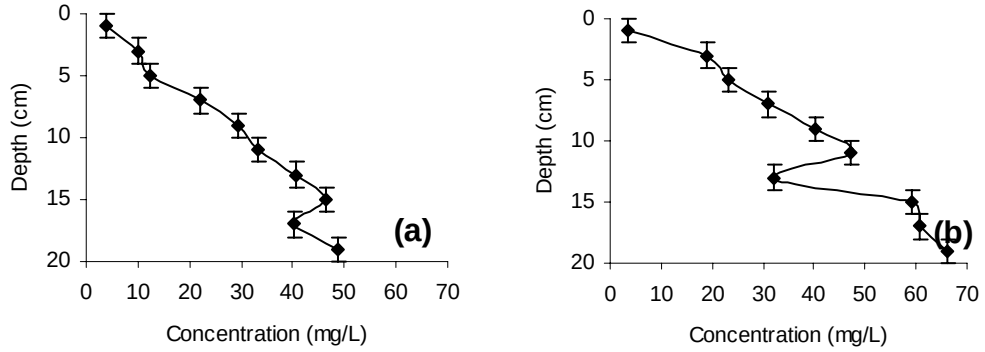

Figure 4-48 *Ammonium pore water concentration profiles of (a) core Ru129 and (b) core Ru130 from September 2006.*

4.4.7 Nitrate

As with January and May, concentration profiles of nitrate are difficult to interpret (Figure 4.49). They may be from oxidation of very high ammonium in the profile. However the randomness suggests that oxidation occurred post-coring, between collection of cores and analysis on the FIA.

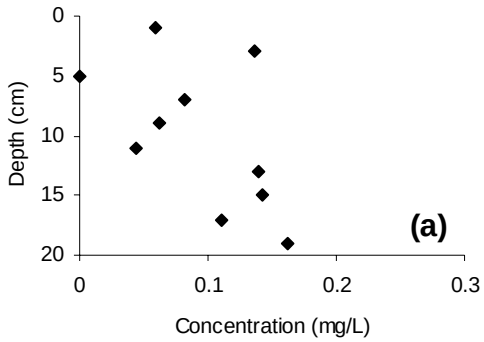
Depth (cm)
0
5
10
15
20
0
0.1
0.2
0.3
Concentration (mg/L)
(a)

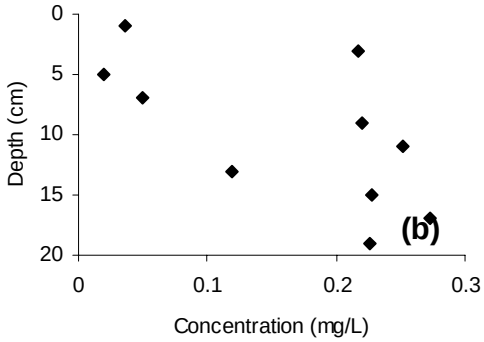
Depth (cm)
0
5
10
15
20
0
0.1
0.2
0.3
Concentration (mg/L)
(b)

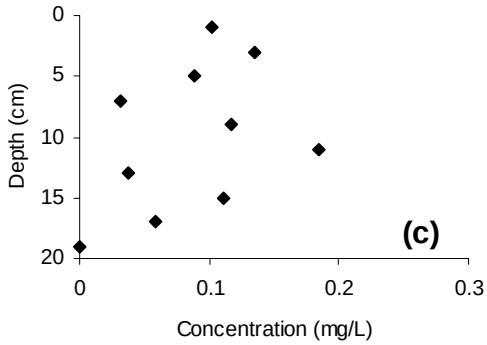
Depth (cm)
0
5
10
15
20
0
0.1
0.2
0.3
Concentration (mg/L)
(c)

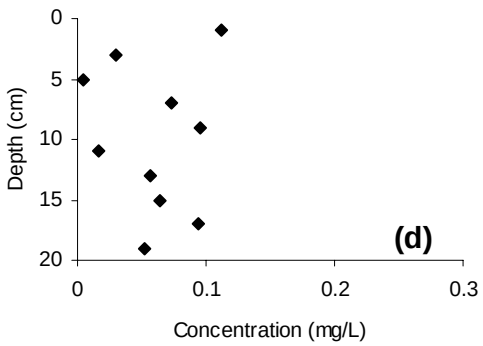
Depth (cm)
0
5
10
15
20
0
0.1
0.2
0.3
Concentration (mg/L)
(d)

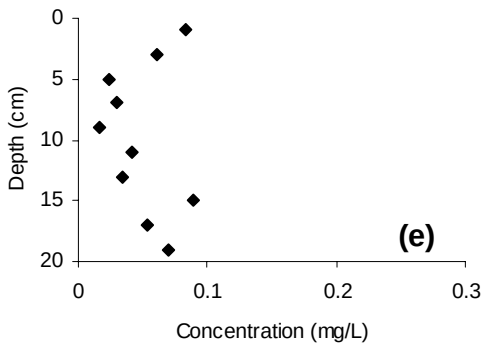
Depth (cm)
0
5
10
15
20
0
0.1
0.2
0.3
Concentration (mg/L)
(e)

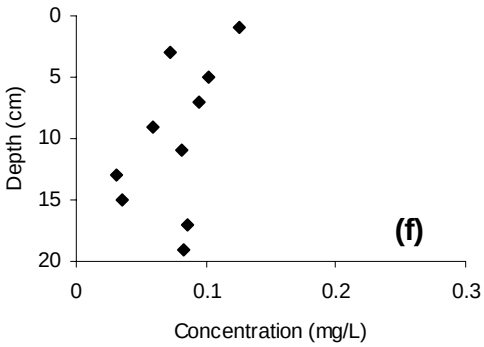
Depth (cm)
0
5
10
15
20
0
0.1
0.2
0.3
Concentration (mg/L)
(f)

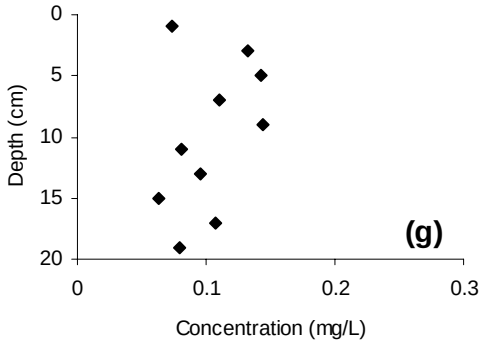
Depth (cm)
0
5
10
15
20
0
0.1
0.2
0.3
Concentration (mg/L)
(g)

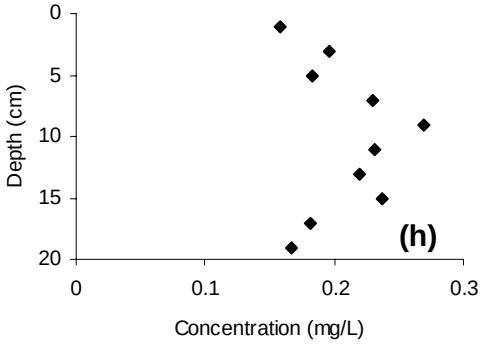
Depth (cm)
0
5
10
15
20
0
0.1
0.2
0.3
Concentration (mg/L)
(h)

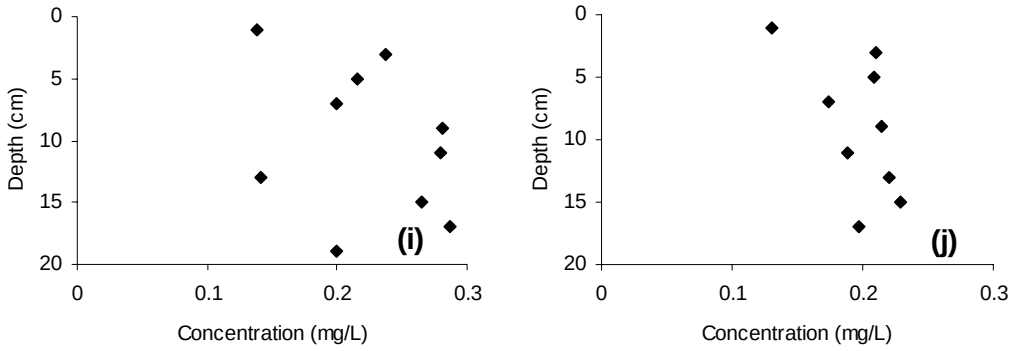

Figure 4-49 *Nitrate pore water concentration profiles of (a) Ru129, (b) Ru130, (c) Ru131, (d) Ru140, (e) Ru141, (f) Ru142, (g) Ru143, (h) Ru144, (i) Ru145, and (j) Ru146 from September 2006.*

4.4.8 Arsenic

Dissolved arsenic shows a general trend of increasing concentrations with depth (Figure 4.50). A concentration peak of 0.4 mg/L occurs in cross section 1 (Figure 4.50a) in core Ru145 at 15 cm depth. Cross sections 2 (Figure 4.50b) and 3 (Figure 4.50c) display patches of high concentration > 0.25 mg/L in the profile. Concentrations are generally very low, however, mostly < 0.15 mg/L, compared with those in May.

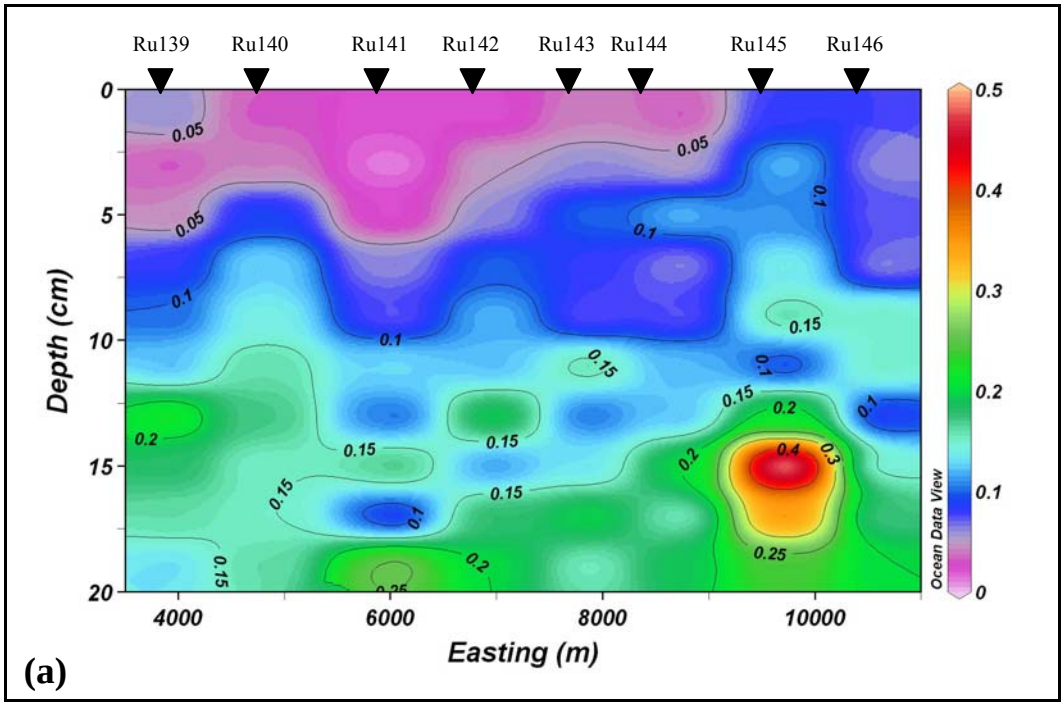

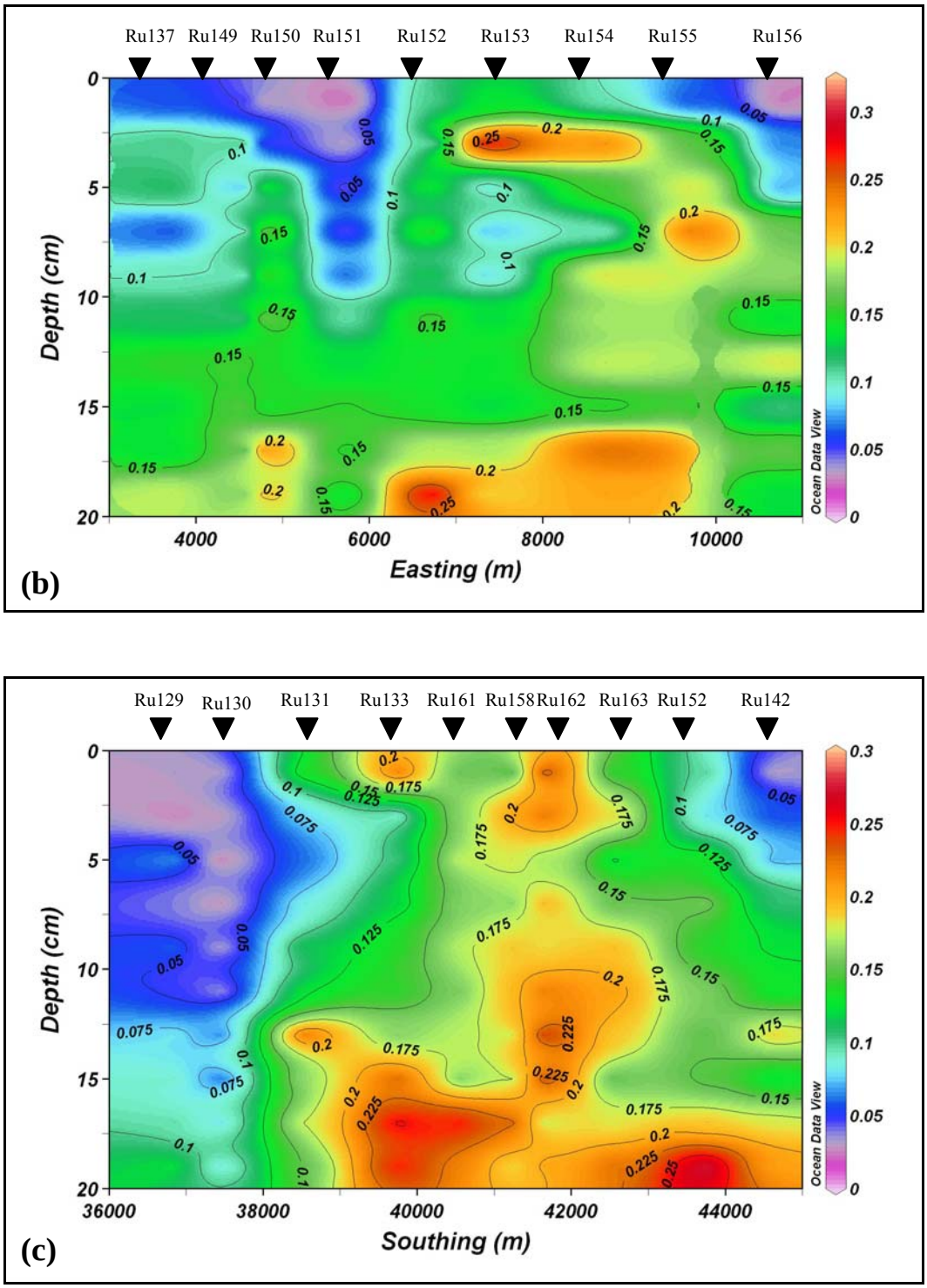

Figure 4-50 *September 2006 depth distribution of dissolved arsenic in pore water of (a) cross section 1, (b) cross section 2 and (c) cross section 3. Concentrations of isopleths are in mg/L.*

Pore water concentration profiles of dissolved arsenic shown in Figure 4.51 indicate that dissolved arsenic diffuses up along relatively weak concentration gradients to where arsenic is removed from pore water into the sediment.

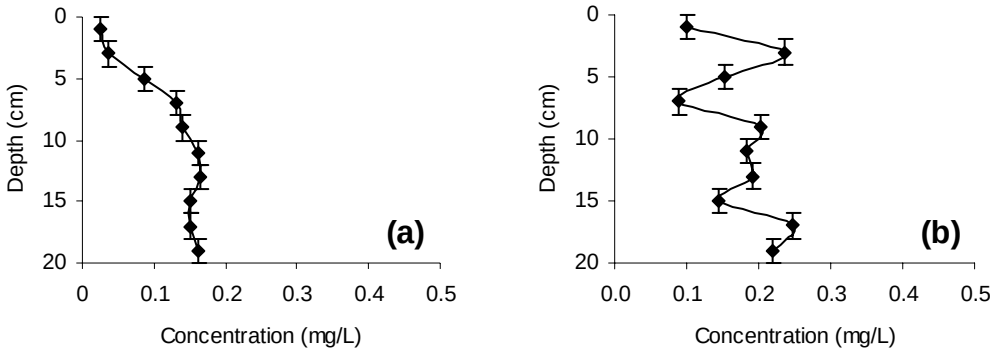

Figure 4-51 *September 2006 dissolved arsenic pore water concentration profiles of (a) core Ru140 from cross section 1 and (b) core Ru153 from cross section 2.*

4.4.9 Cadmium

Concentrations of dissolved cadmium were generally very low, < 0.005 mg/L (Figure 4.52). Cross section 1 (Fig. 4.52a) shows a general increase in concentration with depth, with peaks of 0.025 mg/L. Cross section 2 (Fig. 4.52b) indicates that there may be very little movement of dissolved cadmium throughout the profile, with the exception of Ru137 to Ru150, which shows an irregular increase in concentration with depth. Cross section 3 (Fig. 4.52c) shows little movement of dissolved cadmium throughout most of the profile, with the exception of cores Ru131 and Ru133, which show peaks of concentration of up to 0.05 mg/L.

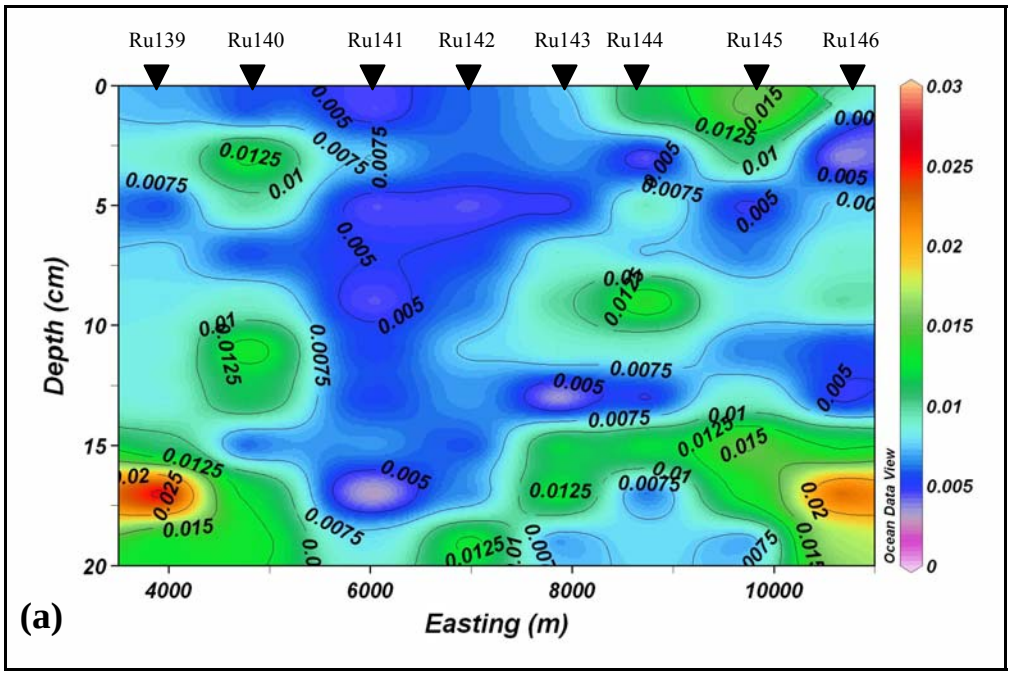

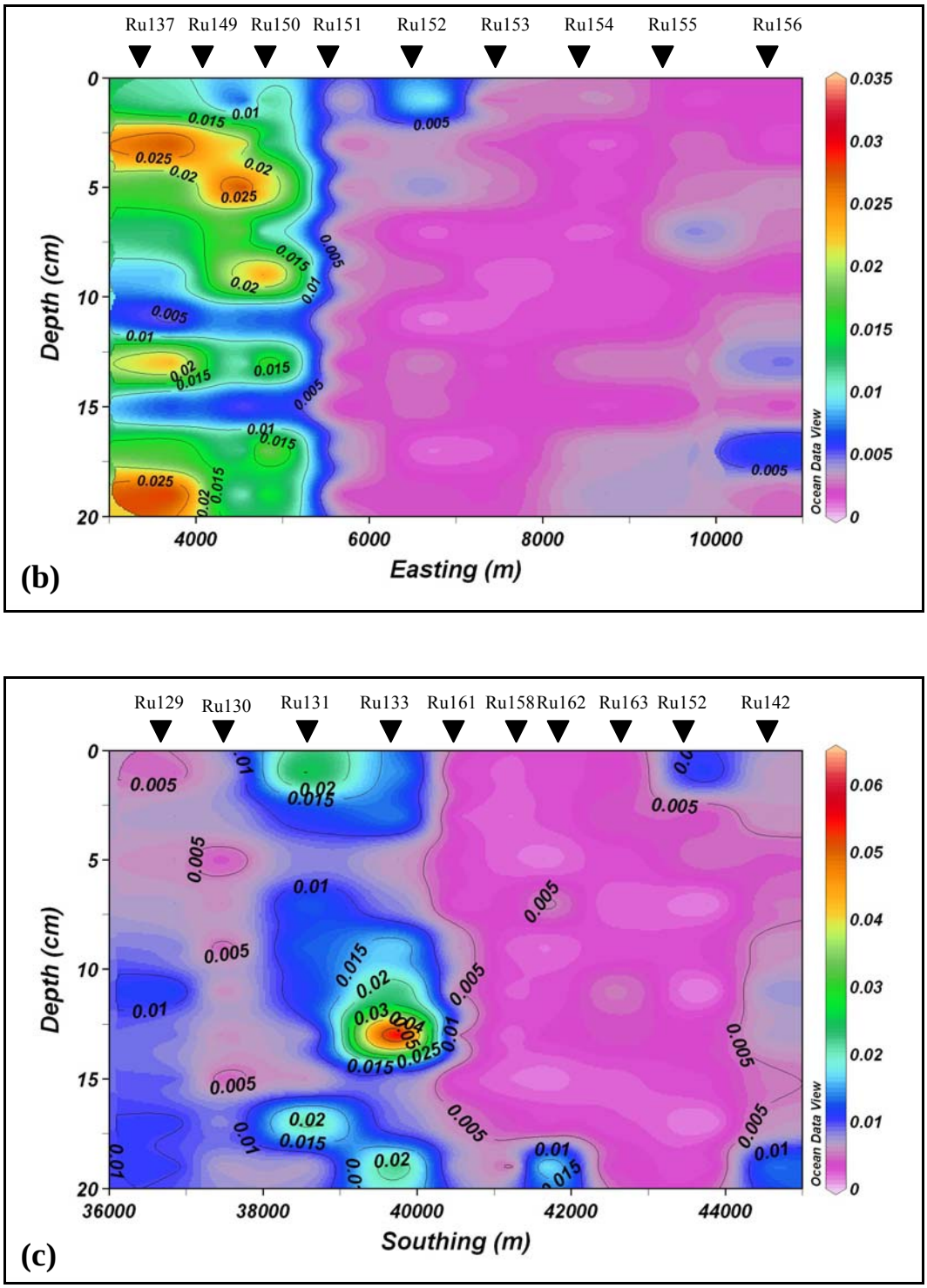

Figure 4-52 *September 2006 depth distribution of dissolved cadmium in pore water of (a) cross section 1, (b) cross section 2 and (c) cross section 3. Concentrations of isopleths are in mg/L.*

Concentration profiles of dissolved cadmium shown in Figure 4.53 have weak concentration gradients with dissolved cadmium possibly diffusing toward the sediment-water interface and removal from pore water into the sediment.

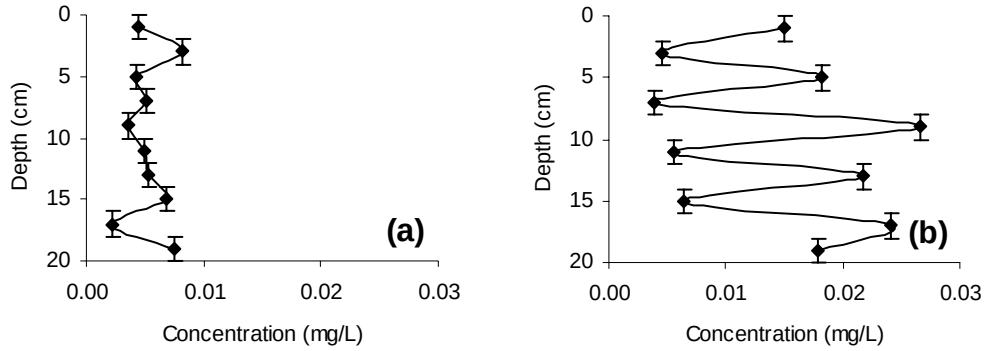

Figure 4-53 *September 2006 dissolved cadmium pore water concentration profiles of (a) core Ru141 and (b) core Ru150.*

4.4.10 Lead

Dissolved lead concentrations were low and close to the limits of detection but still demonstrated an irregular increase in concentration with depth (Figure 4.54). Cross section 1 (Figure 4.54a) had very low concentrations ranging from ~ 0.002 mg/L to 0.008 mg/L, with concentrations generally maximal at depth. Cross section 2 (Figure 4.54b) showed a general increase with depth, with concentrations generally < 0.01 mg/L. A peak in concentration of > 0.025 mg/L in core Ru152 occurred at the sediment surface. Cross section 3 (Figure 4.5c) followed the same concentration pattern as cross section 2.

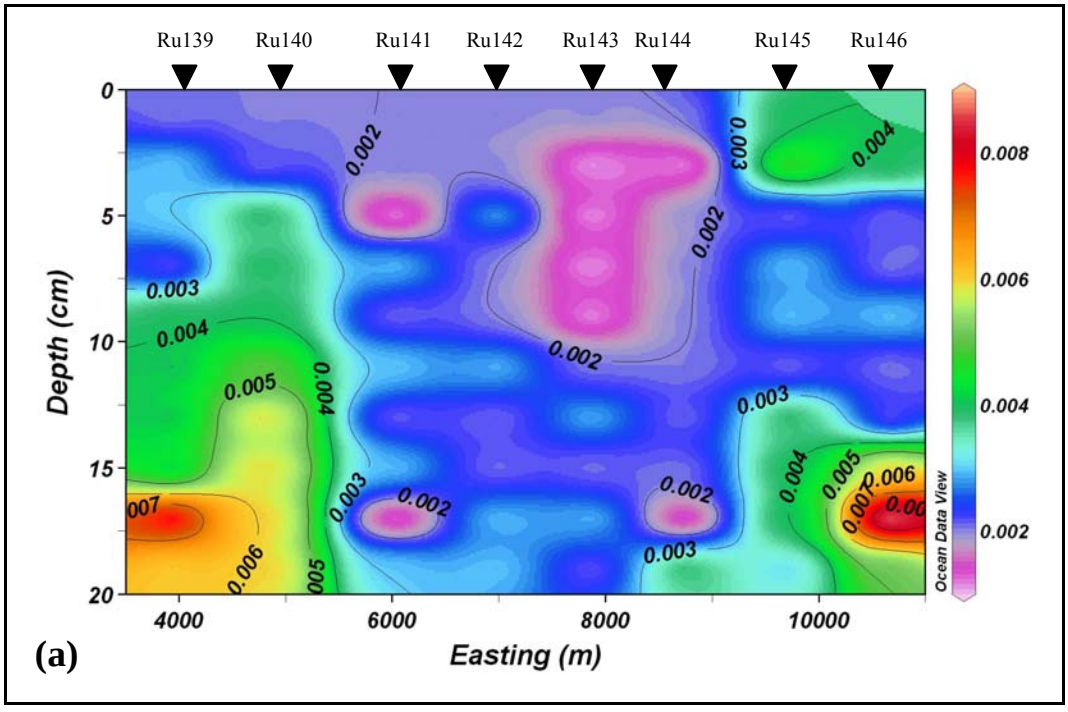

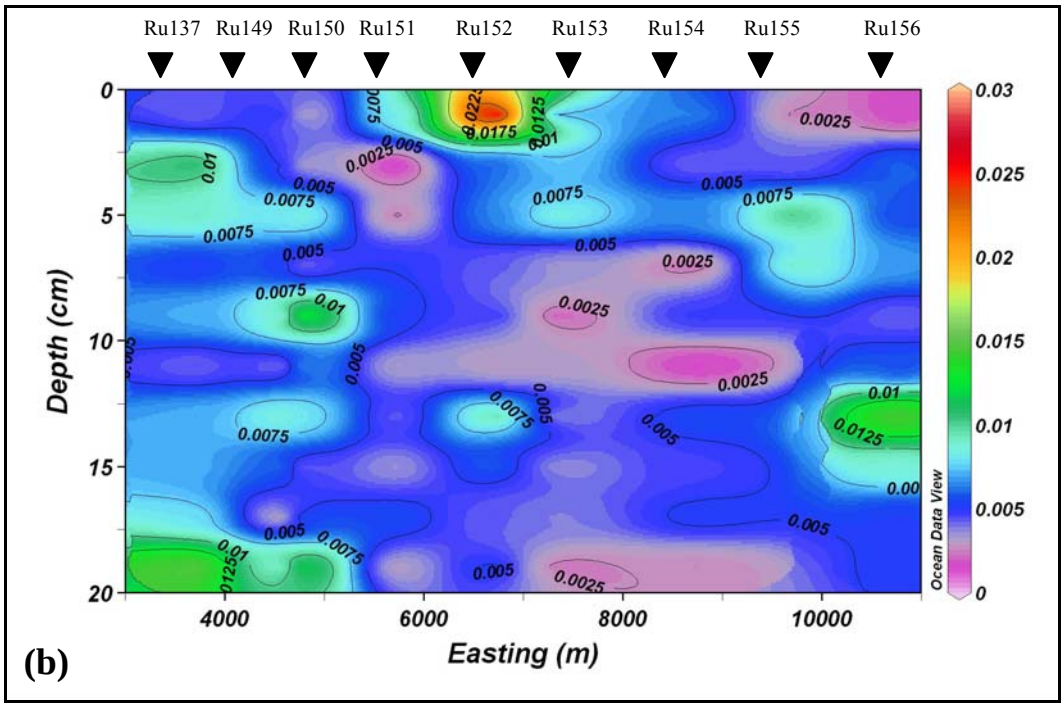

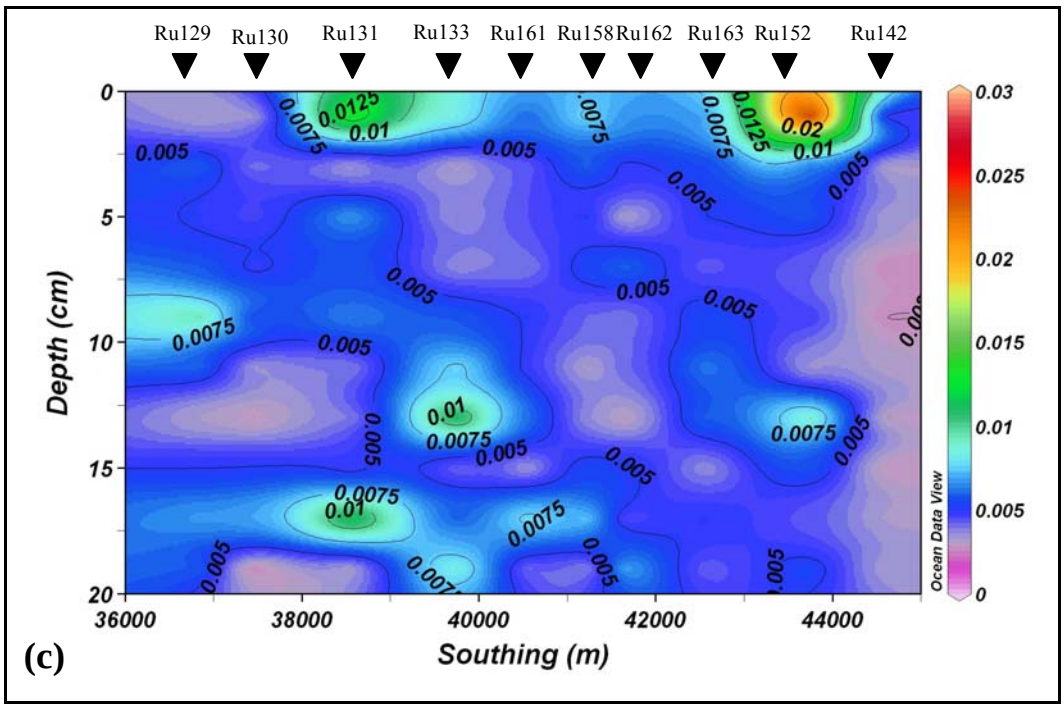

Figure 4-54 *September 2006 depth distribution of dissolved lead in pore water of (a) cross section 1, (b) cross section 2 and (c) cross section 3. Concentrations of isopleths are in mg/L.*

Pore water concentration profiles of dissolved lead (Figure 4.55) indicate that there may be upward diffusion along concentration gradients, where lead is removed from the pore water into the sediment.

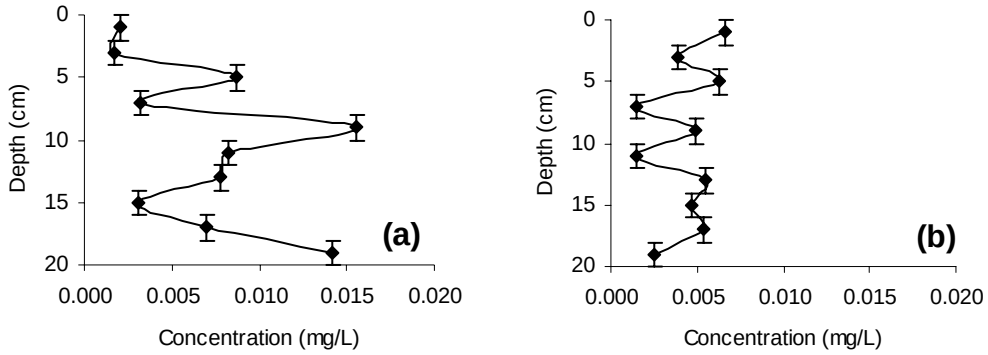

Figure 4-55 *September 2006 dissolved lead pore water concentration profiles of (a) core Ru150 from cross section 2 and (b) core Ru162 from cross section 3.*

4.5 Summary

Sediments of Lake Rotorua are mostly anoxic, as observed in the Eh and pH plots of Figures 4.18 and 4.37. Seasonal differences were observed in concentration profiles of the various elements that were sampled. In January 2006 concentration profiles generally showed a near surface peak, then a rapid decrease where concentrations reached a nearly constant value with depth. Concentration profiles in May showed an increase in concentration with depth, with the exception of sulfur and dissolved phosphorus in cross section 1, which showed near surface peaks then a rapid decrease before attaining a relatively constant value with depth. Concentration profiles in September showed an increase with depth but gradients were generally weaker than those observed in May. Sulfur showed a near surface peak in concentration with a rapid decrease with depth.

4.6 Peeper pore water profiles

Concentration profiles obtained from peepers were used to obtain greater resolution of concentration gradients in elements across the sediment-water interface.

4.6.1 June - August

The sediment-water interface was easily identified by staining of the peeper from benthic algae in the water column, and is indicated by 0 cm depth on the y axis of the figures below. Laboratory experiments measuring equilibration time showed peepers had not equilibrated after 50 day deployment. It should be noted that concentrations in peeper P1 presented below may underestimate actual concentrations and they may therefore provide only a general pattern of the concentration profile.

Figure 4.56 and 4.57 shows profiles obtained from the peeper deployed from 14th June to 03rd August 2006. Figure 4.56 shows profiles of pH (a) and Eh (b). A decrease in pH was observed above the sediment-water interface. Below the sediment-water interface pH maintained a relatively steady state at about pH 7. The profile of Eh remains relatively constant at -0.01 V. This steady state profile is likely due to the Eh electrode malfunctioning.

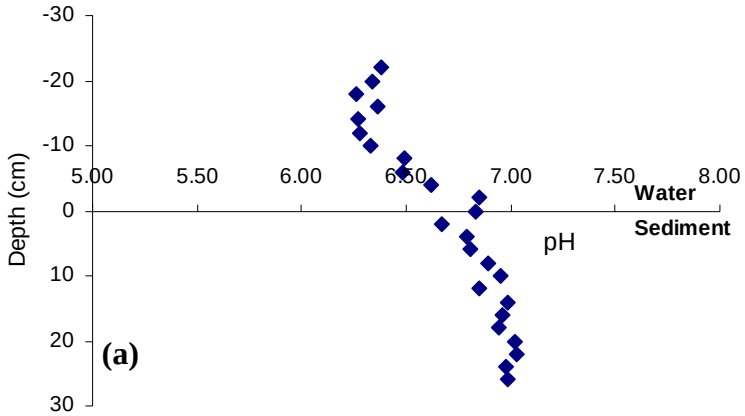

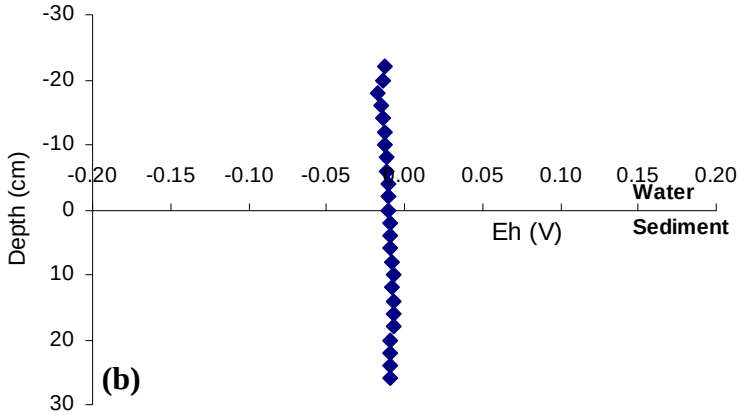

Figure 4-56 *Pore water profiles of (a) pH and (b) Eh from peeper P1 in place from 14th June to 03rd August 2006.*

Figure 4.57 shows concentration profiles obtained from the peeper. The profiles of ferrous iron show increasing concentrations with depth, with indications of upward diffusion along the concentration gradient (Fig. 4.57a). Ferrous iron decreased rapidly in the upper 5 cm of the sediment where it was likely to be removed from pore water by the sediment. Concentrations in the water column were very low, but with a slight peak between 18 and 20 cm above the sediment-water interface.

Manganous increased in concentration with depth (Fig. 4.57b). There was a rapid decrease in concentration in the upper 5 cm of the sediment where it was removed by the sediment indicating diffusion along the concentration gradient. Water column concentrations were very low just above the sediment-water interface then showed a peak of up to 0.5 mg/L between 8 and 22 cm above the sediment-water interface.

Dissolved phosphorus increased in concentration with depth in the pore water (Fig. 4.57c). Upward diffusion along the concentration gradient is likely to be responsible for rapidly decreasing concentrations from the upper sediment to below detection limits higher in the profile, and in the water column to 10 cm above the sediment-water interface, where there was a slight peak in concentration between 12 and 18 cm.

Ammonium pore water concentrations (Fig. 4.57d) increased with depth in the sediment. Concentrations decreased rapidly, most likely as ammonium diffused toward the sediment-water interface, where concentrations approached the detection limit (~0.01 mg N/L) in the overlying water column.

Dissolved arsenic concentrations (Fig. 4.57e) showed a concentration gradient that suggests diffusion into the sediments from the overlying lake water as the concentrations in the pore waters increase slowly with depth in a similar fashion to the results obtained from gravity coring.

Dissolved cadmium concentrations were higher in the lake water that in pore water from peepers, which suggests that cadmium may be rapidly removed from the pore water into the sediment (Fig. 4.57f).

Dissolved lead concentration gradients (Fig. 4.57g) indicate that there may be diffusion into the sediment from the above lake water and that there may be gradual removal from pore water into the sediment.

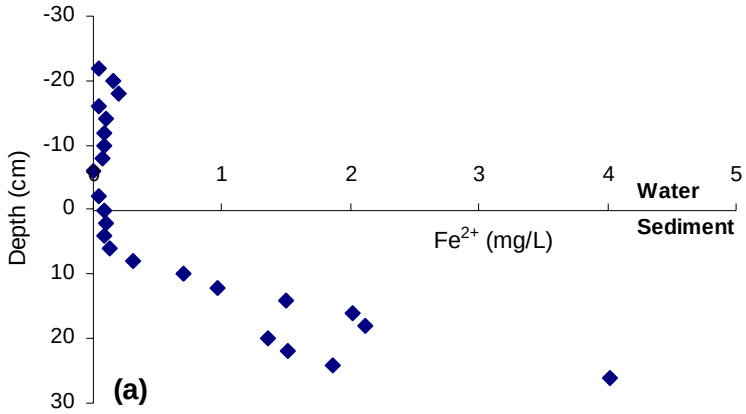

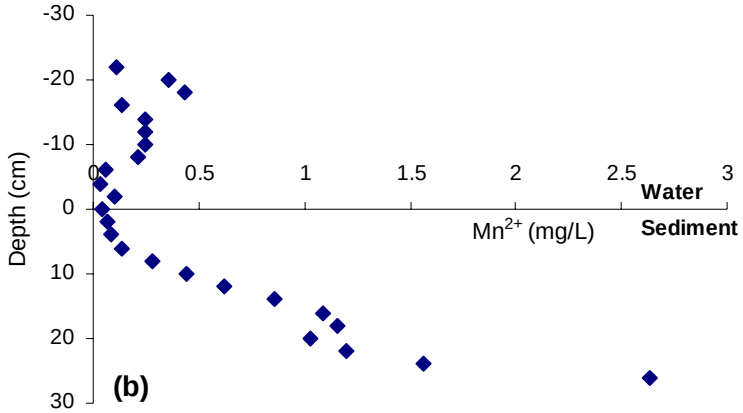
-30
-20
-10
0
10
20
30
Depth (cm)
0
0.5
1
1.5
2
2.5
3
Water
Sediment
Mn2+ (mg/L)
(b)

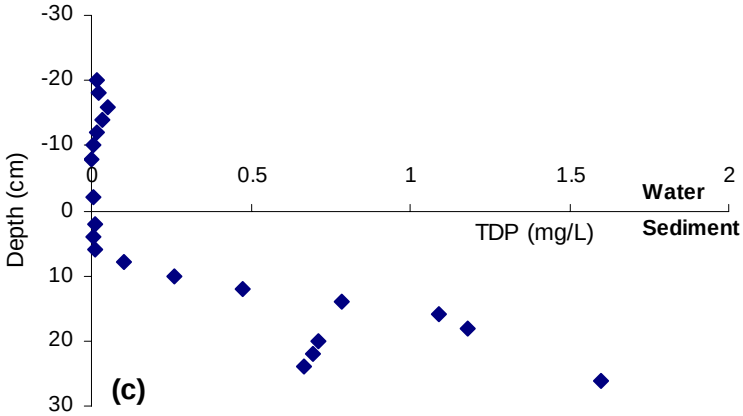
-30
-20
-10
0
10
20
30
Depth (cm)
0
0.5
1
1.5
2
Water
Sediment
TDP (mg/L)
(c)

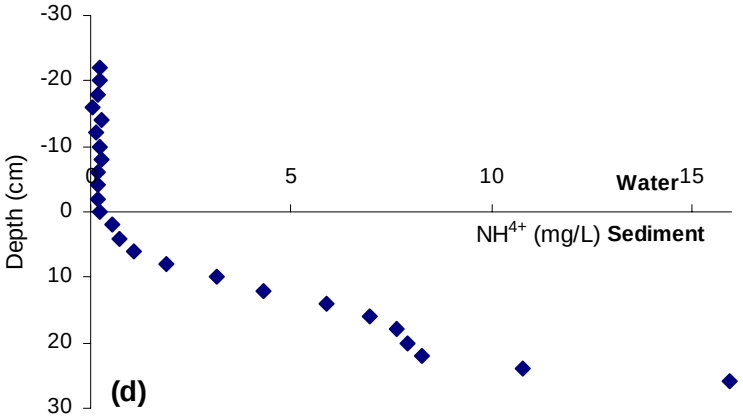
-30
-20
-10
0
10
20
30
Depth (cm)
0
5
10
15
Water
NH4+ (mg/L) Sediment
(d)

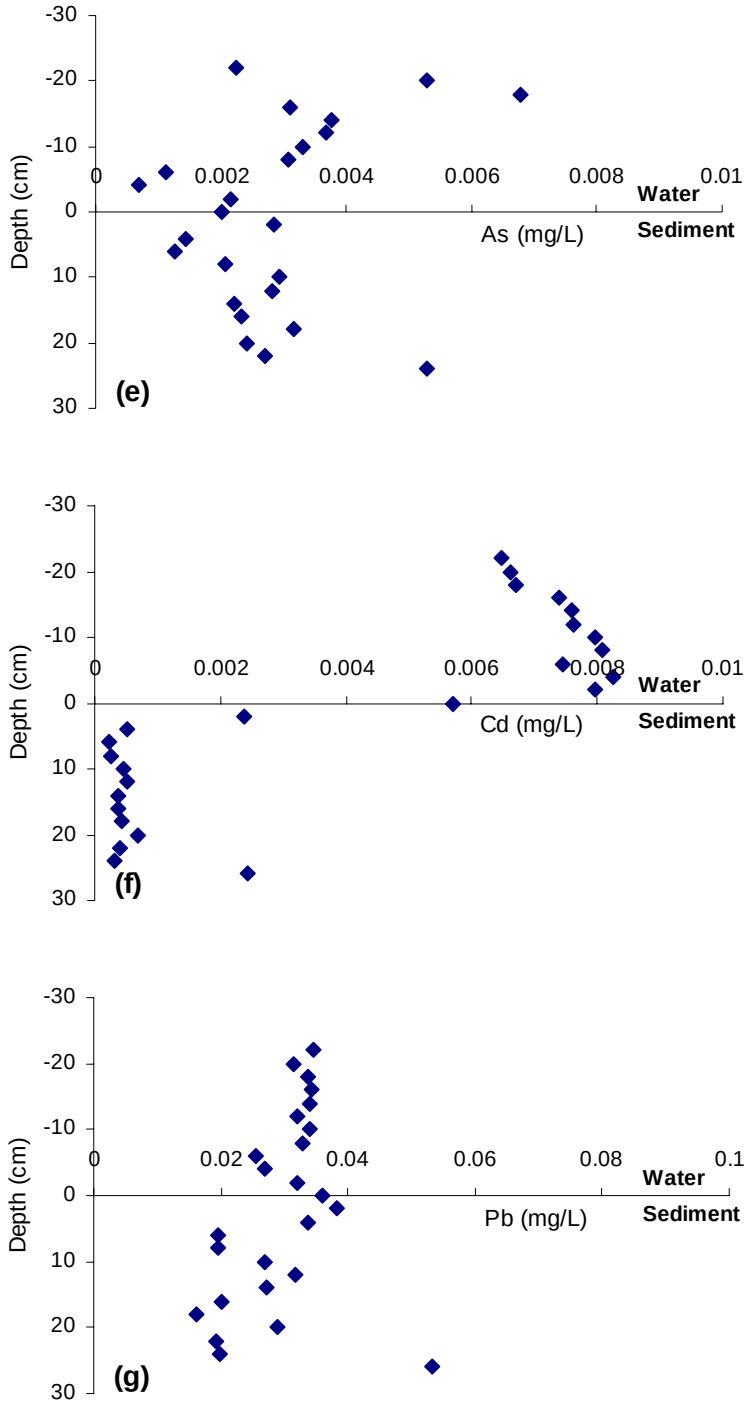

Figure 4-57 *Pore water concentration profiles of dissolved ion concentrations: (a) iron, (b) manganese, (c) phosphorus, (d) ammonium, (e) arsenic, (f) cadmium, and (g) lead from peeper (P1) deployed 14th June to 03rd August 2006.*

4.6.2 August – November

Like the peeper deployed from June-August, the sediment-water interface was identified by staining by benthic algae on the peepers in the lake water column. This area is indicated by 0 cm depth in the figures below. Laboratory experiments measuring equilibration time showed peepers had not equilibrated after 95 day deployment. However a core (Ru164) was collected adjacent to location of peepers when collected in November. Analysis of core Ru164 showed concentrations very close to those presented below in peepers P2, P3 and P4 (Figure 4.59), indicating peepers were very close to equilibrium. Concentrations of ions in core Ru164 are presented in Appendix 2.

Figure 4.58 shows the Eh and pH values measured in the peepers P2, P3 and P4 deployed from 03rd August to 06th November 2006. Above the sediment-water interface, pH (Figure 4.58a) shows an increase to above 7 and then below the sediment-water interface pH rapidly drops to 6.5. Eh values (Figure 4.58b) are positive above the sediment-water interface then rapidly drop below zero beneath the sediment-water interface.

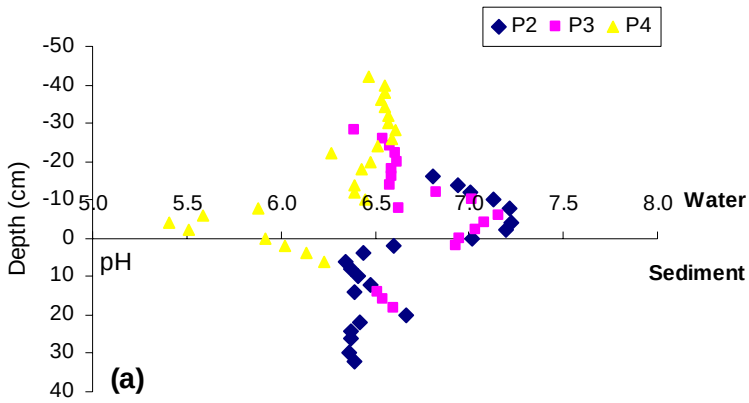

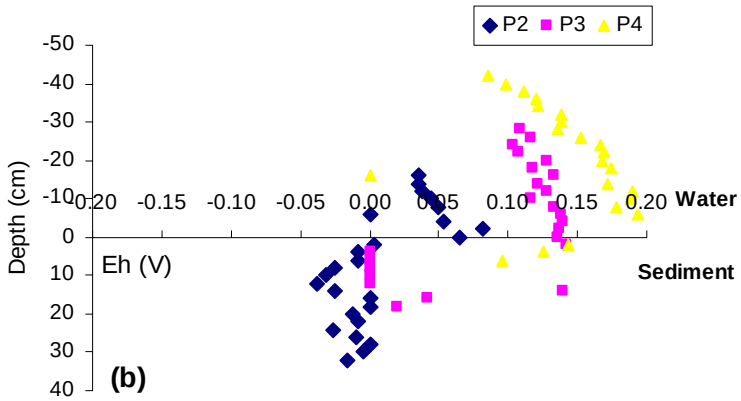

Figure 4-58 *Pore water profiles of (a) pH and (b) Eh from peepers P2, P3 and P4 deployed from 03rd August to 06th November 2006.*

Figure 4.59 shows the concentration profiles of ions obtained from the three peepers deployed from 3rd August to 6th November. Ferrous iron increased in concentration down the profile (Fig. 4.59a), where it is likely to diffuse along a concentration gradient across the sediment-water interface, with concentrations of ~ 2 mg/L in the immediately overlying lake water and dropping below detection limits over the next 5 cm. Ferrous iron was likely to be oxidised to ferric and removed from the water column by precipitation.

Manganous concentrations in the pore water (Fig. 4.59b) increased with depth in the sediment, with diffusion probably occurring along the concentration gradient across the sediment-water interface, where concentrations were ~ 1 mg/L immediately above the sediment-water interface and dropping to the limits of detection by 15 cm above the interface. Concentrations decreased rapidly about 20 cm above the sediment-water interface where manganous was likely oxidized to manganic, precipitated and removed from the water column.

Total sulfur analysis was performed only on P4 (Figure 4.59c). Sulfur appears to be diffusing into the sediment from the overlying water column. Sulfate reduction is already evident above the sediment-water interface were concentrations decrease before they cross the interface. Sulfur is rapidly removed once in the sediment with concentrations approaching detection limit of ~1 mg/L at 6 cm depth below the sediment-water interface.

The concentration profile of dissolved phosphorus (Figure 4.59d) follows that of manganous, and suggests that there is upward diffusion along a concentration gradient across the sediment-water interface. Dissolved phosphorus may be gradually removed by transport through the water column, especially from about 15 cm above the sediment-water interface, but it is also likely to be removed by iron and manganese oxide/hydroxide precipitation in the active zone immediately overlying the sediment water interface. Plotting P vs Fe (Fig. 4.60a) and P vs Mn (Fig. 4.60b) in the peeper waters above the interface shows no correlation between iron and phosphorus except in P4, but a definite correlation between manganese and phosphorus. This suggests co-precipitation of these two species between 0 and 15 cm above the interface.

Dissolved arsenic concentrations of P2 and P3 (Fig. 4.59e) increased with depth in the sediment, indicating that there may be diffusion upwards along the concentration gradient. There were indications of some release of arsenic into the overlying lake water as concentrations decreased with height in the water column. Concentrations of dissolved arsenic in peeper P4 appeared to indicate diffusion into the sediment from the overlying lake water.

Concentrations of dissolved cadmium (Fig. 4.59f) and lead (Fig. 4.59g) showed that there was likely to be downward diffusion from the water column into the sediment where concentrations decreased rapidly in the pore water but with considerable variations in concentration between 10 and 20 cm depth.

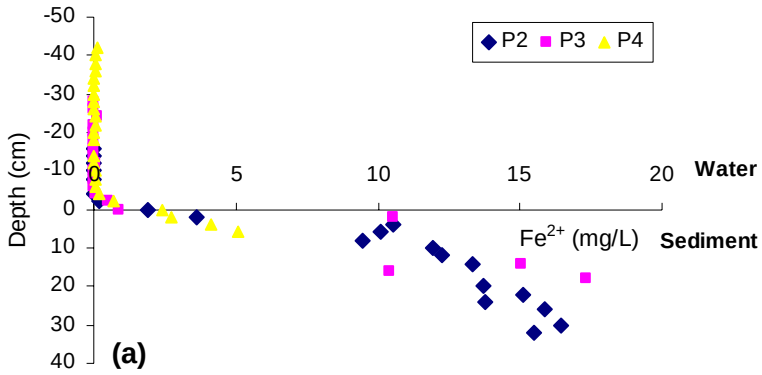

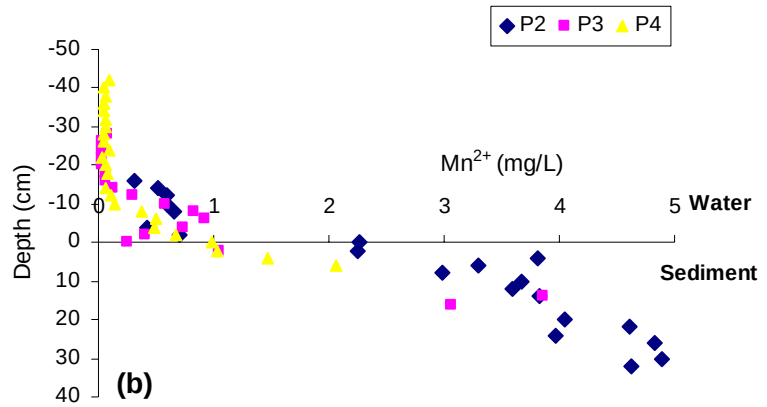
P2 P3 P4
-50
-40
-30
-20
-10
0
10
20
30
40
Depth (cm)
Mn2+ (mg/L)
0
1
2
3
4
5
Water
Sediment
(b)

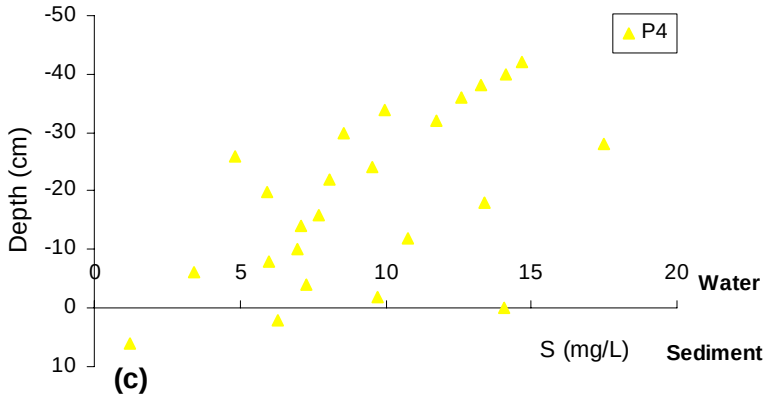
P4
-50
-40
-30
-20
-10
0
10
Depth (cm)
0
5
10
15
20
Water
S (mg/L)
Sediment
(c)

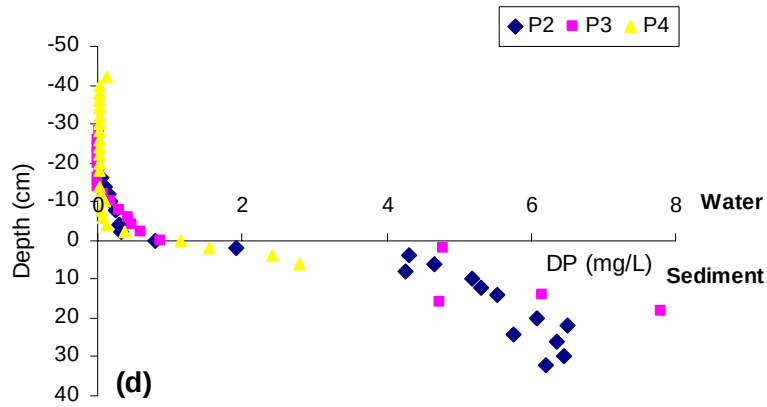
P2 P3 P4
-50
-40
-30
-20
-10
0
10
20
30
40
Depth (cm)
0
2
4
6
8
Water
DP (mg/L)
Sediment
(d)

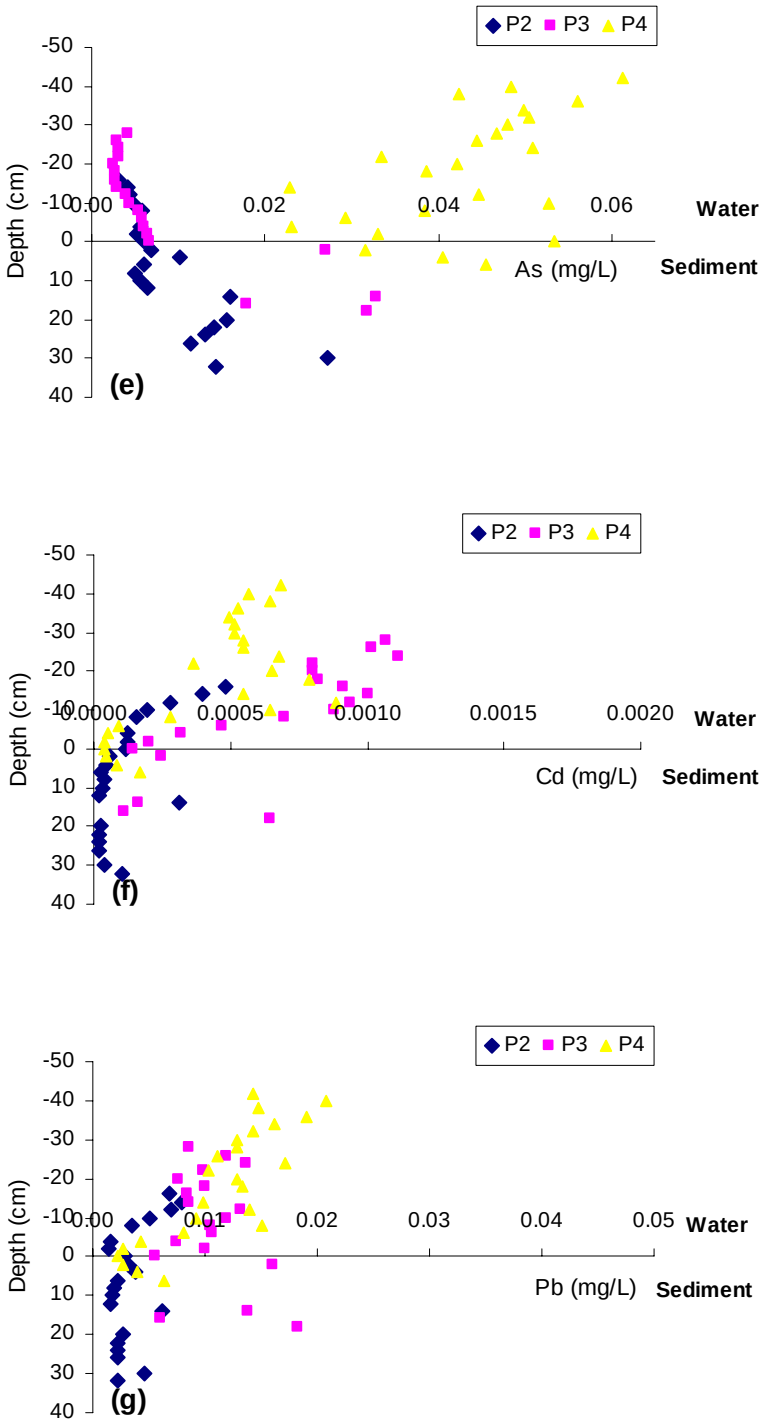

Figure 4-59 *Pore water concentration profiles of dissolved ions: (a) iron, (b) manganese, (c) total sulfur (d)phosphorus, (e) arsenic, (f) cadmium and (g) lead from peepers P2, P3, and P4 deployed 03rd August to 06th November 2006.*

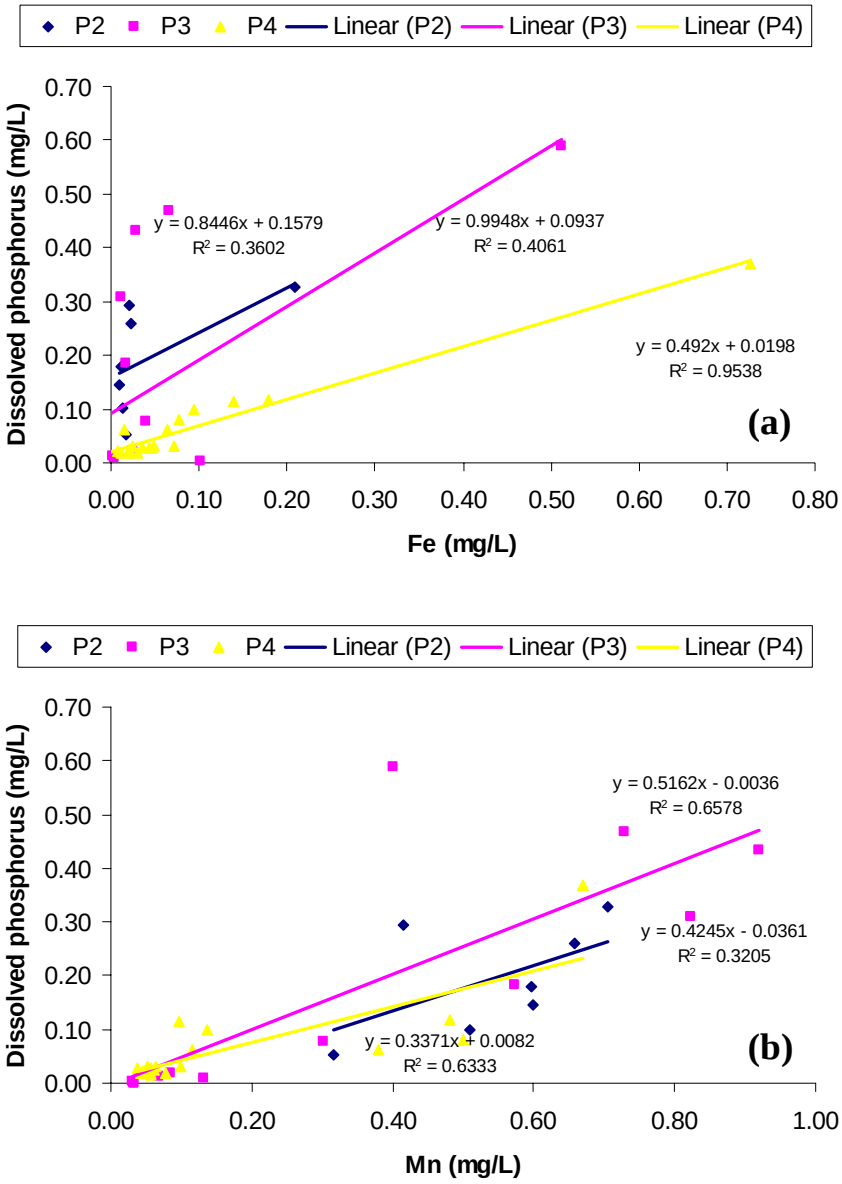

Figure 4-60 *Plots of dissolved phosphorus vs (a) ferrous and (b) manganous from above the sediment-water interface in peepers P1, P2 and P3 deployed August to November 2006.*

4.7 Soluble reactive phosphorus vs dissolved organic phosphorus

Figure 4.61 shows concentrations of total dissolved phosphorus (TDP) analysed by ICP-MS plotted against soluble reactive phosphorus (SRP) analysed by FIA from pore water collected by gravity core. An increase in the percentage of SRP in TDP occurs between the January, May and September 2006 data from gravity cores. In January 78% of the TDP is SRP, in May 77% was SRP, but in

September SRP in 89% of the TDP. The remaining percentage is assumed to be due to dissolved organic phosphorus.

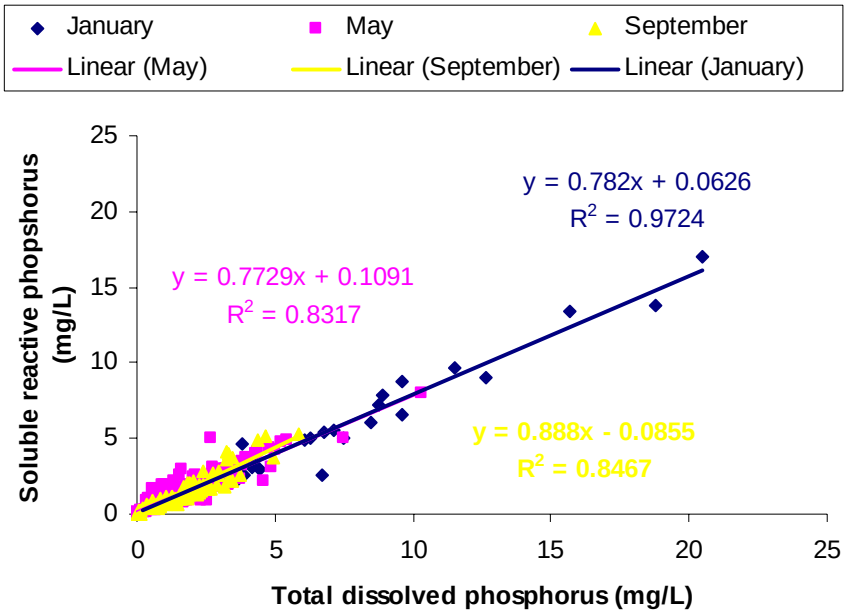

Figure 4-61 *Concentrations of total dissolved phosphorus vs soluble reactive phosphorus from January, May, and September sediment core pore water 2006.*

4.8 Nutrient release rates

Mean nutrient release rates calculated by Fick's first law of diffusion from pore water obtained from sediment cores are shown in Table 4.1, with minimum and maximum values shown. Appendix 3 contains individual release rates from each core that was collected.

There were large seasonal differences in nutrient release rates. Over summer dissolved phosphorus was released at an average rate of 62 mg m^{-2} d^{-1}, with a wide range from 15.6 to 140.8 mg m^{-2} d^{-1}. Ammonium was released at an average rate of 121 mg m^{-2} d^{-1}, with a range of 19.6 to 201.1 mg m^{-2} d^{-1}.

Nutrient release rates in May showed a large reduction with dissolved phosphorus released on average at a rate of 20.5 mg m^{-2} d^{-1}, with a range of 0.8 to 70.8 mg m^{-2}

d^{-1}. Ammonium was released at an average rate of 74.4 mg m^{-2} d^{-1}, with a range of 19.6 to 201.1 mg m^{-2} d^{-1}.

In September nutrient release rates were lowest, with dissolved phosphorus released at an average rate of 5.8 mg m^{-2} d^{-1}, with a range of 0.2 to 31.2 mg m^{-2} d^{-1}. Ammonium was released at an average rate of 41 mg m^{-2} d^{-1}, with release rates ranging from 19 to 92 mg m^{-2} d^{-1}.

Table 4-1 Mean nutrient release rates of dissolved phosphorus and ammonium from each sampling period, calculated by Fick's first law of diffusion. The year average is a mean of the mean value for the January, May and September values.

Month		**TDP**	**NH_4^+**
		mg m^{-2} d^{-1}	
January			
	Mean	62.0	121.1
	Min	15.6	41.2
	Max	140.8	212.3
May			
	Mean	20.5	74.4
	Min	0.8	19.6
	Max	70.8	201.1
September			
	Mean	5.8	41.0
	Min	0.2	19.3
	Max	31.2	92.1
Year Average		29.43	78.83

The equivalent release rate of dissolved phosphorus and ammonium in tonnes per day over the whole lake is presented in Table 4.2. On average 1.1 tonnes of dissolved phosphorus and 3.1 tonnes of ammonium are released to the lake every day, equating to 430 tonnes of dissolved phosphorus and 1152 tonnes of ammonium released to the lake water from the 40 km^2 zone of diatomaceous sediments each year.

Table 4-2 Tonnes of dissolved phosphorus and ammonium released per day over the whole lake over the three sampling periods. The year average is a mean of the mean value for January, May and September values.

Month	**P (tonnes/day)**	**NH_4 (tonnes/day)**
January	2.4	4.8
May	0.8	3
September	0.2	1.6
Year average	1.1	3.1

5. DISCUSSION – PORE WATER CHEMISTRY IN THE SEDIMENTS OF LAKE ROTORUA

5.1 Introduction

The diagenetic processes controlling the concentrations of elements and nutrients within the pore water of Lake Rotorua are discussed in the following chapter. Special attention is paid to iron diagenesis, and nutrient regeneration and release, particularly phosphorus diagenesis.

5.2 Diagenetic processes

Over January high rates of nutrient regeneration were indicated by peaks in concentrations of dissolved phosphorus and ammonium near the sediment surface. The low Eh values indicate that anaerobic decomposition of organic matter by the successive reduction of manganese and iron oxide/hydroxides followed by reduction of sulfate is likely to occur, however these concentration profiles exhibited maxima near the surface. Aerobic decomposition, if occurring at all in the sediments, appeared to be confined to a very thin layer at the sediment surface, most likely within the nepheloid layer.

The rapid decrease in concentrations of dissolved phosphorus, ferrous, manganous and sulfur with depth can be explained by the precipitation of authigenic minerals, for example the formation of iron and manganese sulfides. The lower concentrations of ferrous and manganous than dissolved phosphorus in the near surface peaks are possibly from the formation of sulfides that remove ferrous and manganous from the pore water. Once sulfur is depleted in the pore water, sulfides are no longer available as sinks for iron and manganese.

The increase in ferrous and manganous concentrations down the profile observed in May and September was likely from the precipitation of oxides/hydroxides at the sediment surface. Sulfate reduction occurring near the sediment surface is likely to be associated with formation of iron and manganese sulfides. Sulfide formation possibly acts as a sink for ferrous and manganous in the upper layers of

the sediment below the region of oxide/hydroxide precipitation. Once sulfur is depleted and no longer available as a sink, concentrations of ferrous and manganous increase at depth in the pore water.

Dissolved phosphorus concentrations were extremely high in the pore waters of Lake Rotorua compared with other eutrophic lakes, with some concentrations exceeding 17 mg/L. Sondergaard (1990) reported phosphate concentrations of up to 7 mg/L in the pore water of a hypertrophic lake in Denmark and Graneli (1999) reported concentrations of SRP of up to 2.2 mg/L within the pore water in a shallow, eutrophic lake in Sweden.

Concentration peaks of dissolved phosphorus observed in January and in cross section 1 of May suggest high rates of organic matter mineralization and burial of iron and manganese oxides/hydroxides by ongoing organic matter deposition to the sediments. Under this regime the sediments rapidly become anoxic and iron and manganese oxides undergo dissolution, releasing phosphorus into the pore water as well as phosphorus regenerated from organic matter mineralisation. Sulfide formation controlling ferrous and manganous concentrations in the pore waters results in a build up of phosphorus with less iron and manganese oxides available for adsorption, and strong concentration gradients that drive high rates of diffusion across the sediment-water interface and deeper into the sediment where it is possible that phosphorus is removed to form authigenic minerals. The rapid decrease of phosphorus at these depths could possibly be from precipitation of vivianite, ($Fe_3(PO_4)_2 \cdot 8H_2O$), although this mineral is yet to be observed in Lake Rotorua sediments.

Dissolved phosphorus concentrations in cross section 2 of May and September increased down the profile, with low concentrations of dissolved phosphorus at the surface most likely due to adsorption onto iron and manganese oxide/hydroxides. The increase of phosphorus with depth could be caused by reduction of the buried oxide/hydroxides followed by formation of iron sulfides. Concentration profiles indicate a downward flux into the sediment at depth. Authigenic phosphorus minerals such as vivianite may form well below the depth

of iron sulfide formation and remove phosphorus from pore waters at considerable depth.

Ammonium concentrations at depth were very high (> 30 mg/L), with indications of ongoing mineralization of organic matter through the sediment profile. Carignan and Lean (1991) reported ammonium release in sediments at depths of 50-100 cm in a mesotrophic lake resulting from the decomposition of G_2 organic compounds (Carignan and Lean, 1991). The concentration peaks of > 27 mg/L observed in Lake Rotorua in January at the sediment surface was likely to be caused by pulses of algal debris deposited to the surface, stimulating rapid diagenesis of the additional labile organic matter. Hansen and Blackburn (1992) observed large increases in NH_4 fluxes after the deposition of phytoplankton to sediments. After the observed increase in NH_4 release the fluxes returned to background rates, with the organic material derived from the phytoplankton estimated to have a half life of 2-3 weeks.

Over the colder months of May and September the top of the profiles showed rapid decreases in concentration, probably in association with ammonium diffusion towards the sediment surface. The rapid drop in concentration of ammonium at the top of the sediment column over the colder months is possibly from thermal convection bringing oxygenated cold water to the bottom of the lake. Replacement of anoxic nepheloid water with oxygenated bottom waters will encourage denitrification at the interface and could also accelerate the drawdown of ammonium in the adjacent pore waters.

The very high ammonium concentrations, approaching up to 70 mg/L (Figure 4.48) in the Motutara basin near Sulphur Point, are possibly a local influence associated with Rotorua City's previous sewage was discharged through the Puarenga stream, but perhaps also from being a site of geothermal discharge.

As sulfate reduction was generally taking place in the upper 5 cm, methanogenesis occurring deeper in the sediments (refer to Chapter 6) most likely becomes the dominant process in organic matter mineralization and may therefore control the availability of ammonium in pore waters. This depth within the

sediments indicates that ammonium is being regenerated from organic compounds many years after it was first deposited, suggesting internal loading of ammonium may take many years to decrease.

The geochemical behaviour of arsenic is known to follow the behaviour of iron. However, concentrations of arsenic in January showed a general increase down the profile. The low concentrations in the upper sediment may be associated with sulfides that act as an important sink for arsenic (Mucci et al., 2000). As sulfate becomes rapidly depleted with depth, sulfides are no longer available as a sink for arsenic and concentrations increase deeper within the profile. Over May and September dissolved arsenic follows this same pattern, following the same trend as iron in these months, suggesting concentrations are being controlled by sulfide formation.

Dissolved cadmium and lead concentrations are very low in sediments of Lake Rotorua. Concentration gradients imply little movement within or out of the sediment. Cadmium and lead form very stable sulfides, galena (PbS) and greenockite (CdS) (Wang and Chapman, 1999), which are likely to exert controls on concentrations in the pore water.

5.3 Nepheloid layer

Profiles from peepers deployed immediately above the sediment-water interface, indicated that an active flocculent layer of organic matter was present 10 to 20 cm above the sediment, which was affecting the cycling of elements, especially iron, manganese, phosphorus, sulphur, cadmium and lead.

Layers of flocculent material above lake sediments have been observed in a number of lakes, where dissolved oxygen in the water column has been found to be rapidly depleted as it diffuses through the flocculent layer in which oxidation of organic matter is taking place. As dissolved oxygen is depleted other reduction reactions take place including sulfate to sulfide (Sherman et al., 1994, Sweerts et al., 1986).

Sulfate concentrations have been reported as 30.5 mg/L in the lake water of Rotorua, sourced mostly from the geothermal inflows that enter the lake (Timperley and Vigor-Brown, 1986). Sulfur in the peepers (assumed to be mostly sulfate) was already below this concentration and dropped progressively towards the sediment-water interface by which stage concentrations had dropped to around levels of detection. Sulfur analyses were obtained for only one peeper (P4) (Figure 4.59c). In this case sulfate reduction was evidently occurring as much as 40 cm above the sediment-water interface. For this to occur dissolved oxygen must have already been reduced to zero. As a consequence of maintaining an anoxic zone above the sediment-water interface other redox sensitive species also showed evidence of reactions within the nepheloid layer.

Cadmium (Figures 4.57f and 4.59f) showed a rise, peak and fall in concentration within the nepheloid layer. This indicates first the release of cadmium from its supporting particulates (probably particulate organic matter) by remineralisation, then a decrease as cadmium reacts with sulfide ions and precipitates from solution. Arsenic (Figs. 4.57e and 4.59e) and lead (Figs. 4.57g and 4.59g) showed similar effects and are also likely being re-precipitated with metal sulfides.

Manganese (Figure 4.59b) and iron (Figure 4.59a) appear to be migrating into the nepheloid layer from the sediment. The more readily oxidizable ferrous ion is removed within 5 cm of the sediment interface while manganous migrates further into the nepheloid layer, but is largely removed by 15 cm. At most of the sites where peepers were deployed there was a strong correlation between manganese and phosphorus suggesting that re-precipitation of manganese oxides removed phosphorus from the water column (Figure 4.60b). One peeper (P4) showed a close correlation between iron and phosphorus (Figure 4.60a).

5.4 Pore water saturations

To investigate if authigenic mineral formation, specifically the formation of iron and sulfide minerals, had the potential to influence the cycling of phosphorus and other elements in the pore waters of Lake Rotorua, a range of solubility equilibrium equations were evaluated.

Equilibria calculations were performed on a range of minerals; carbonates: $CaCO_3$ (calcite), $FeCO_3$ (siderite) and $MnCO_3$ (rhodochrosite), sulfides: FeS (amorphous), FeS (mackinawite), Fe_3S_4 (greigite), FeS (pyrrhotite), and FeS_2 (pyrite), and $Fe_3(PO_4)_2 \cdot 8H_2O$ (vivianite) in a similar manner to Emerson (1976). Due to the lithology of the lake catchment, which contains very little calcium, apatite is not likely to form and was therefore not considered. The equilibrium calculations performed were based on thermodynamic data presented in Table 5.1. pH and Eh data were not measured in January, however, a pH of 6.5 has been applied to data as this value is similar to unpublished data collected in March (Taylor, pers comm).

Calcite and rhodochrosite were found to be undersaturated in all pore water samples and are not presented here. However ion activity products (IAPs) calculated for the range of iron minerals show saturation. Iron is able to form many minerals in association with other elements in lake sediments. Three have been considered here: sulfides (FeS (amorphous), FeS (mackinawite), FeS (pyrrhotite), and FeS_2 (pyrite)), siderite ($FeCO_3$) and vivianite ($Fe_3(PO_4)_2 \cdot 8H_2O$). For the full range of IAPs refer to Appendix 4.

Table 5-1 Equilibrium constants used in thermodynamic equilibrium calculations given by Emerson (1976) and $\Delta G°$ data for pyrite.

Equation	pK	Temperature (°C)
(1) $HCO_3^- \leftrightharpoons CO_3^{2-} + H^+$	10.38	20
(2) $CaCO_3 \leftrightharpoons CO_3^{2-} + Ca^{2+}$	8.44	20
(3) $FeCO_3 \leftrightharpoons CO_3^{2-} + Fe^{2+}$	10.7	25
(4) $MnCO_3 \leftrightharpoons CO_3^{2-} + Mn^{2+}$	10	25
(5) $HS^- \leftrightharpoons S^{2-} + H^+$	13.9	25
(6) $FeS(amorp) \leftrightharpoons Fe^{2+} + S^{2-}$	16.9	25
(7) $FeS(mack) \leftrightharpoons Fe^{2+} + S^{2-}$	17.5	25
(8) $Fe_3S_4(greg) \leftrightharpoons 3Fe^{2+} + 3S^{2-} + S^0$	18.2	25
(9) $FeS(pyrr) \leftrightharpoons Fe^{2+} + S^{2-}$	19	25
(10) $FeS_2(pyrite) \leftrightharpoons Fe^{2+} + 2S^{2-}$	29.2	25
(11) $Fe_3(PO_4)_2 \cdot 8H_2O \leftrightharpoons 3Fe^{2+} + 2PO_4^{3-} + 8H_2O$	36	25

5.4.1 Sulfides

The monosulfides amorphous FeS, greigite, and mackinawite (Fe_1 + xS, where x ~0.5) form first from the reaction of iron with sulfide, however these compounds are unstable thermodynamically compared with pyrrhotite and pyrite (Emerson, 1976). The ion activity products for the monosulfides are presented in Figure 5.1 for amorphous, mackinawite and pyrrhotite, and Figure 5.2 for pyrite, calculated with equations 5-10 of Table 5.1. Greigite data was not presented as ion activity products were extremely undersaturated.

Pore waters are supersaturated with respect to the monosulfides mackinawite, and pyrrhotite and saturated in respect to amorphous FeS, with pore water approaching equilibrium with amorphous FeS in the lower part of the sediment profile (Figure 5.1). Figure 5.2 shows pore waters in Lake Rotorua are super-saturated in respect to pyrite near the sediment surface, indicating the likelihood of transformation of the unstable monosulfides to pyrite, as summarised by the following equation: $FeS + S^0 \rightarrow FeS_2$ (Berner, 1980). Data from May (Fig 5.2b) and September (Fig. 5.2d) shows pyrite approaching equilibrium with depth, with Ru130 and Ru145 undersaturated with respect to pyrite at 12 cm below the sediment surface.

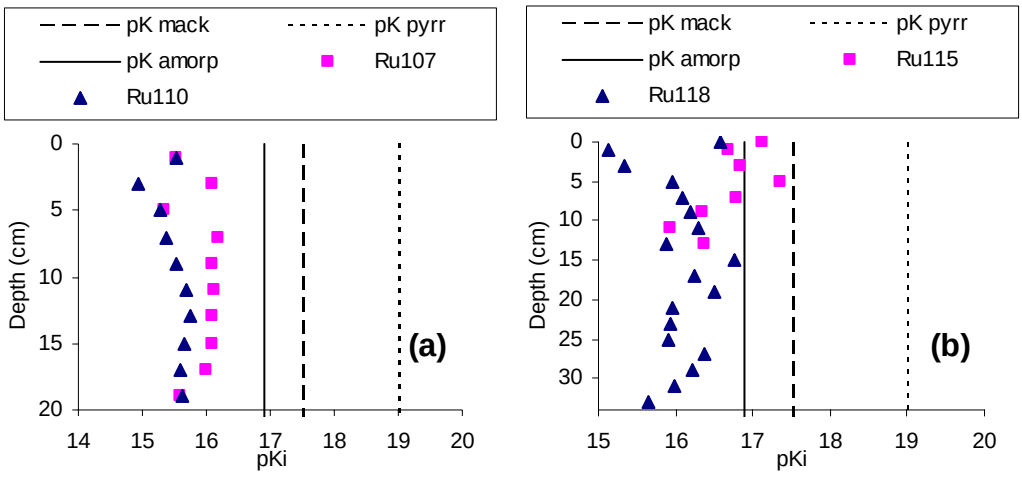

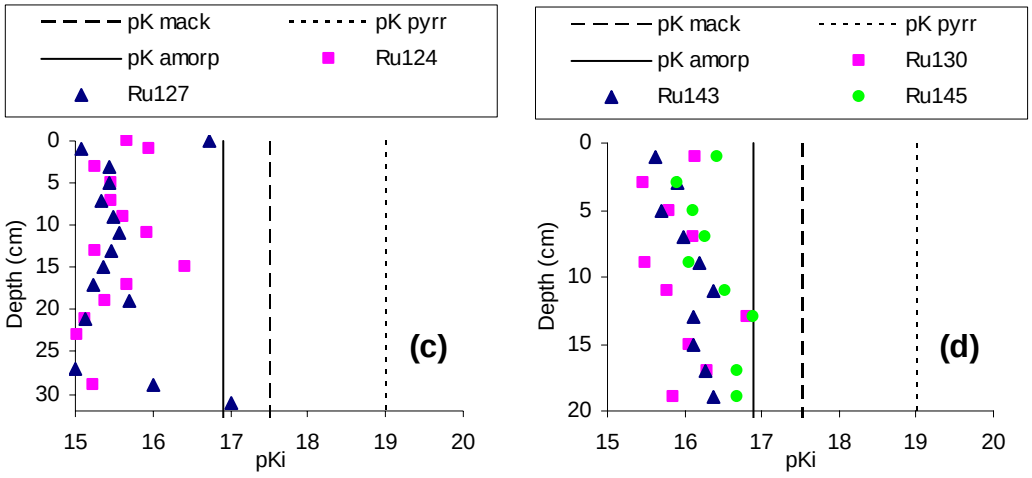

Figure 5-1 *The negative log of the ion activity product for monosulfides (FeS): amorphous, mackinawite, and pyrrhotite based on typical pore water data from (a) January cross section, (b) May cross section 1, (c) May cross section 2 and (d) September.*

The iron Eh-pH diagrams constructed for the conditions corresponding to Lake Rotorua sediments presented in Chapter Four (Figures 4.19 and 4.38) show a transition of pore water between the boundary of Fe_2O_3 and FeS_2 (pyrite). This data, along with framboidal pyrites observed in the sediments of Lake Rotorua by Mangan (In prep), provide strong evidence that pyrite forms in the sediments of Lake Rotorua and that it provides a sink for Fe^{2+} in the pore waters. This is most likely occurring in a pyrite-rich layer below the zone of organic matter decomposition in association with reduction of sulfate (Berner, 1980), and possibly explains black laminations commonly observed in sediment cores from Lake Rotorua. Pyrite is not often observed in freshwater environments due to generally low sulfate concentrations (Berner, 1980). The high concentrations of sulfate present in Lake Rotorua in association mostly with acid sulfate geothermal springs, as well as organic matter inputs, provide the necessary substrates to support the formation of pyrite.

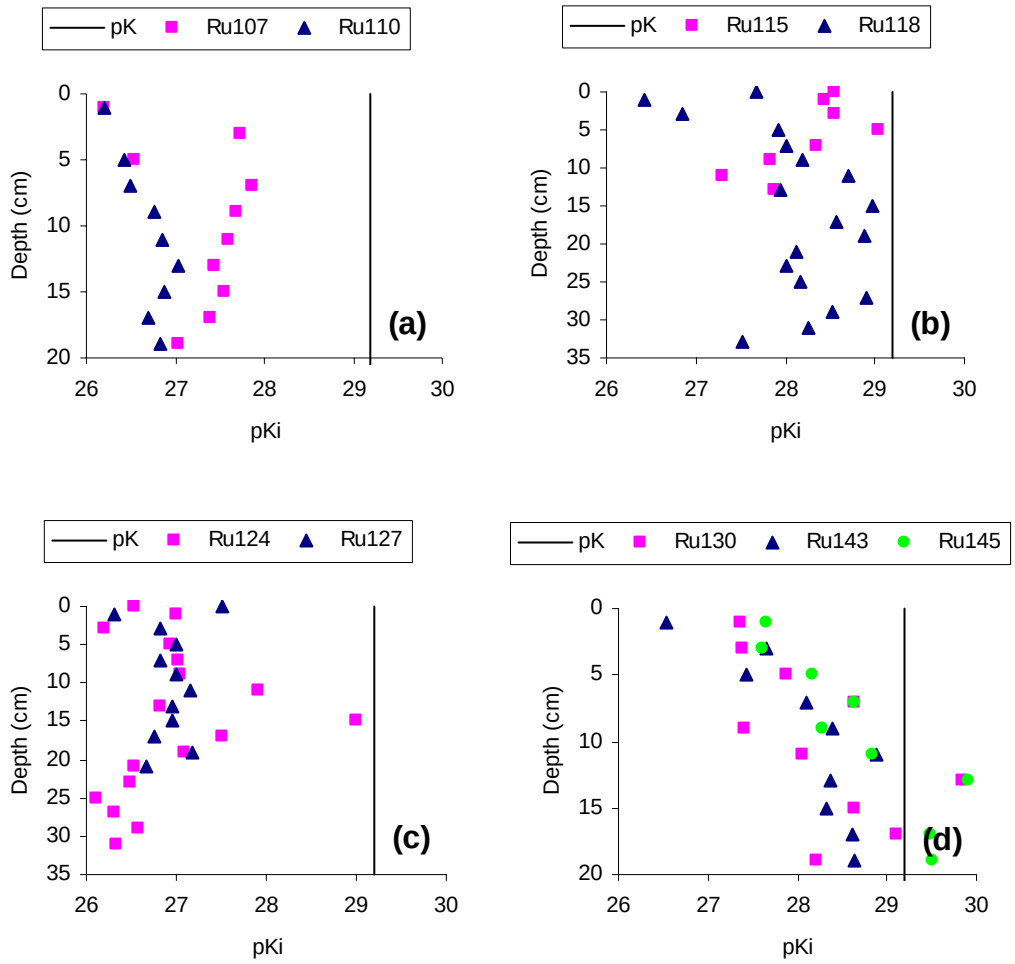

Figure 5-2 *The negative log of the ion activity product for pyrite (FeS_2) based on typical pore water data from (a) January cross section, (b) May cross section 1, (c) May cross section 2 and (d) September.*

5.4.2 Siderite

As bicarbonate concentrations were determined on one core only (Ru128), the concentration range for this core of 240-260 mg/L has been used in conjunction with the pH and iron results from the other cores to determine the ion activity products by equations 1 and 3 of Table 5.1. These calculations appear to show that all pore waters were saturated with respect to siderite at depth, but undersaturated near the sediment surface (Figure 5.3). Mangan (In prep) observed an unidentified iron mineral in the sediments of Lake Rotorua, and concluded it could be either goethite or siderite. These results indicate that siderite could possibly influence ferrous concentrations below the zone of pyrite formation.

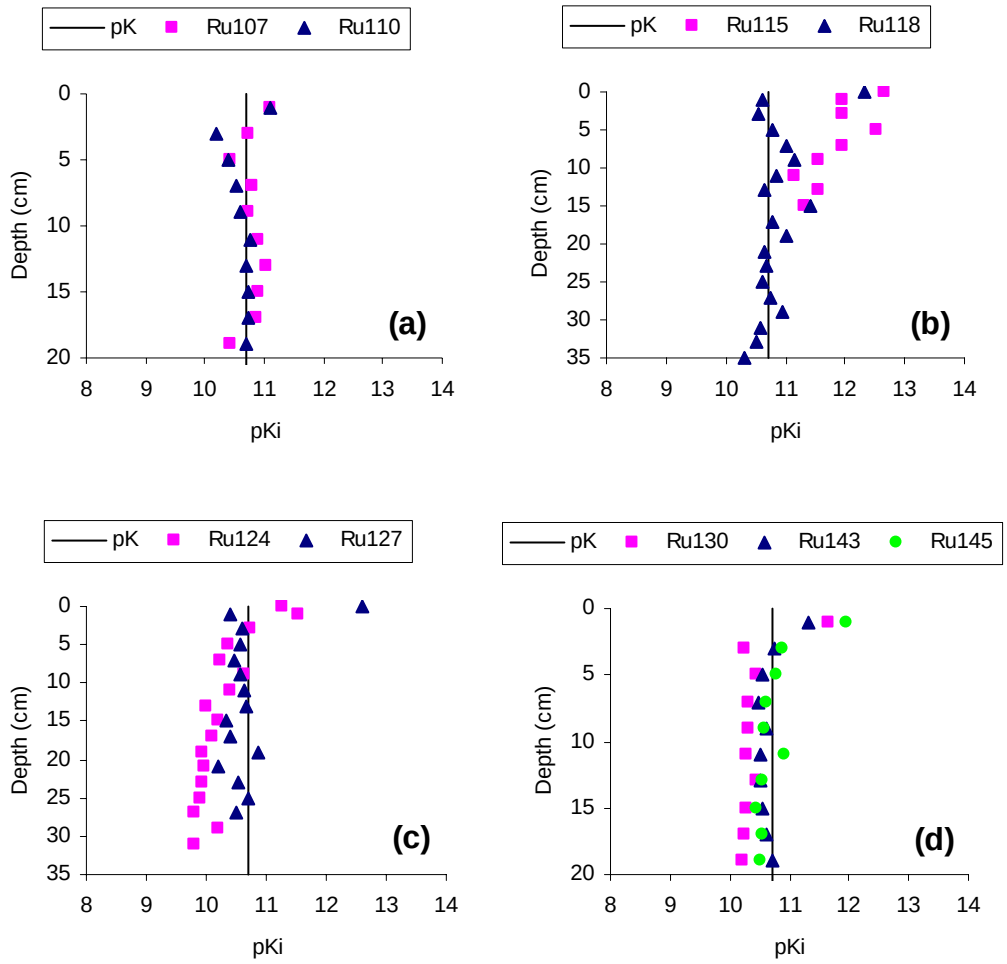

Figure 5-3 *The negative log of the ion activity product for siderite ($FeCO_3$) based on typical pore water data from (a) January cross section, (b) May cross section 1, (c) May cross section 2 and (d) September.*

5.4.3 Vivianite

The pore water saturation of vivianite appears to change seasonally. Data from January and May cross section 1 are undersaturated with respect to vivianite at depth (Figure 5.4a and b). Pore waters near the top of the profile are supersaturated, corresponding to the peak concentration of dissolved phosphorus in these cores. However it is unlikely that vivianite will form in the zone of sulfide formation (Gächter and Müller, 2003). The lower part of the profile nears equilibrium with respect to vivianite. The ion activity products of May cross section 2 (Fig. 5.4c) and September (Fig. 5.4d) are undersaturated with respect to vivianite in the upper 5cm of the profile, and supersaturated below 5 cm.

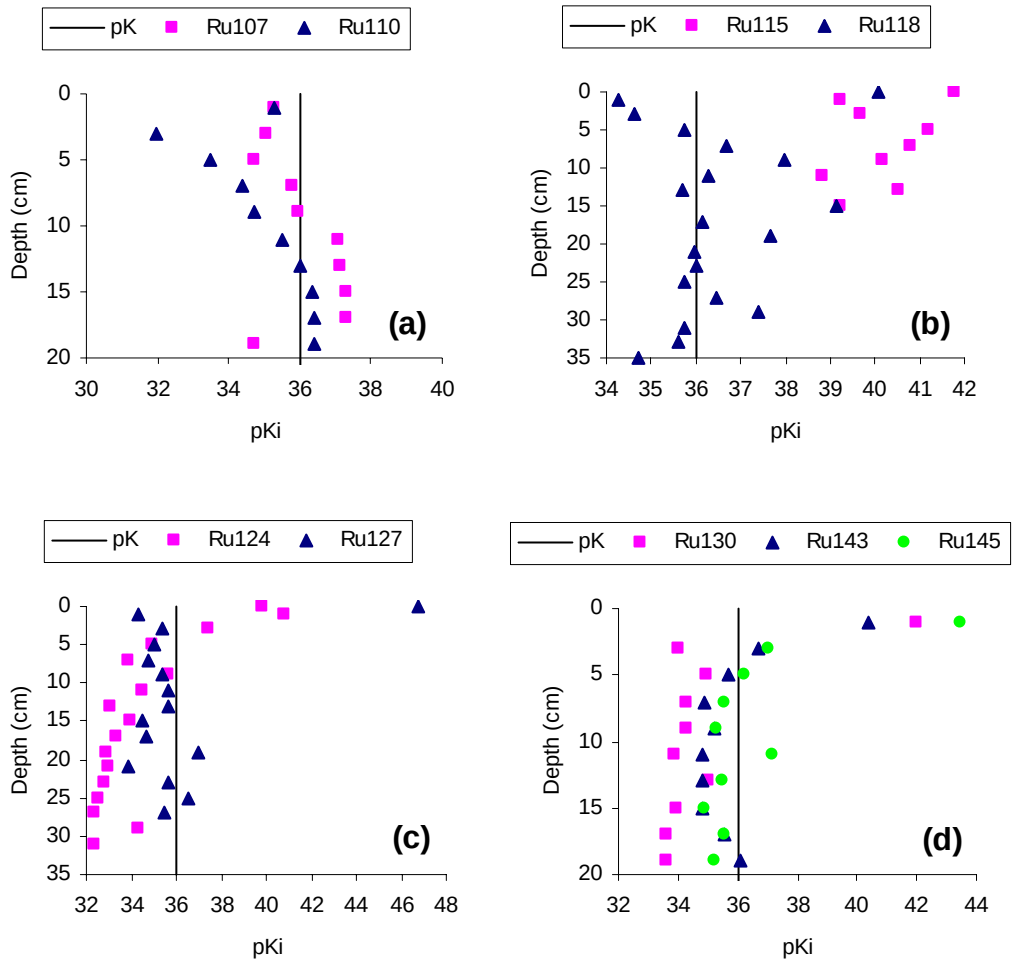

Figure 5-4 *The negative log of the ion activity product for vivianite based on typical pore water data from (a) January cross section, (b) May cross section 1, (c) May cross section 2 and (d) September cross section 1.*

Vivianite precipitation in the sediments of Lake Rotorua may be a transition stage, with phosphorus concentrations going in and out of saturation. Iron sulfide formation has been found to cause the dissolution of vivianite (Gächter and Müller, 2003), however, it has been found that both minerals are present within lake sediments (Taylor et al., 2003). Therefore vivianite could possibly be precipitating deep in the sediments of Lake Rotorua, well below the zone of sulfate reduction and pyrite formation.

5.5 Iron diagenesis

From pore water equilibria calculations there appear to be three zones of different authigenic iron minerals forming possibly controlling the phosphorus retention in the sediments of Lake Rotorua, as illustrated in Figure 5.5.

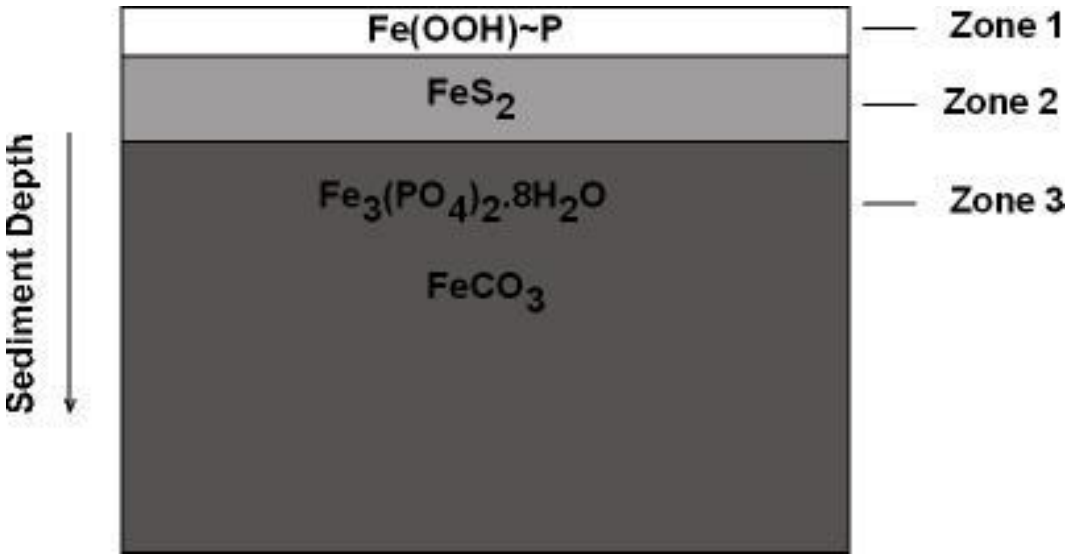

Figure 5-5 *Schematic of possible iron mineral phases controlling phosphorus retention in Lake Rotorua sediments.*

Zone 1 is a very thin layer of iron oxide minerals at the sediment surface or likely within the nepheloid layer, probably less than a few millimetres thick, where oxygen diffuses through the sediment before being rapidly consumed with depth.

Zone 2 is a slightly thicker layer of about 5 cm or less where sulfate reduction occurs to form pyrite, and appears to extend into the nepheloid layer. This layer acts as a sink for ferrous and phosphate ions from the pore water.

Zone 3 is where there is a build up of ferrous iron in the pore waters after sulfate is no longer available for the formation of iron sulfides. This process is likely to result in the precipitation of vivianite and/or siderite, possibly providing a sink for phosphorus.

While pore water equilibria do not necessarily prove the formation of authigenic minerals, they can show processes that may control concentrations of dissolved species within pore water. The only way to confirm if authigenic mineral formation is occurring is to physically identify minerals within the sediments of Lake Rotorua.

5.6 Phosphorus diagenesis

The diagenesis of phosphorus is given special consideration in this thesis, due to the role of phosphorus in maintaining high tropic status of Lake Rotorua even if external loading were to be strongly reduced.

In Lake Rotorua phosphorus concentrations in the pore water seem to be largely associated with high rates of organic matter mineralisation over summer months, releasing large quantities of dissolved phosphorus into the pore waters. This is evidenced by the higher percentage of dissolved organic phosphorus in the total dissolved phosphorus analysis compared with that of September (Figure 4.61). Dissolution of iron and manganese oxides/hydroxides from anaerobic decomposition will also release adsorbed phosphorus into the pore waters.

During the course of this study it became apparent there is a strong seasonal cycle in the behaviour of dissolved phosphorus within the pore water. While it is well known that phosphorus release from the sediments is enhanced during stratification and the associated reduction of oxygen concentrations in the hypolimnion, as well as by warmer temperatures that stimulate microbial activity, little has been observed of the phosphorus movement through the pore water profile over an annual basis. A possible explanation of the observations in this thesis is given below.

In mid summer (January) the classic profile of phosphorus was observed, with a sharp concentration peak near the sediment surface, which generates strong concentration gradients and results in transport of phosphorus away from this zone by molecular diffusion. Dissolved phosphorus is released into the overlying water column by strong upward diffusion. A strong downward flux also drives

concentrations of dissolved phosphorus deeper into the sediment, but at slower rates. The peak decreases in concentration and widens as the downward concentration gradients generated over summer drive the phosphorus deeper in the pore water profile where dissolved phosphorus is removed from the pore water by possible mineral precipitation. Sedimentation also results in the apparent deepening of the phosphorus peak. The upward concentration gradient results in phosphorus being lost to the overlying water column and adsorption onto iron and manganese oxides/hydroxides. This process is illustrated in Figure 5.6 which shows the gradual decrease in the concentration peak over time, with an ongoing loss of dissolved phosphorus from the pore water. Possibly dissolved phosphorus comes close to reaching a steady state concentration with depth in the pore water with a small decrease at the surface where it is removed from the pore water by adsorption onto iron and manganese oxides/hydroxides. This steady state concentration value is observed in the lower concentration profile in January. While organic matter deposition is ongoing to the sediments, when an algal bloom is deposited to the sediments in association with stratification events causing anoxic bottom waters, this stimulates another "pulse" of phosphorus release into the pore water and the cycle starts again. In order to test this hypothesis pore water samples would need to be taken on a monthly basis as well as dissolved oxygen monitored.

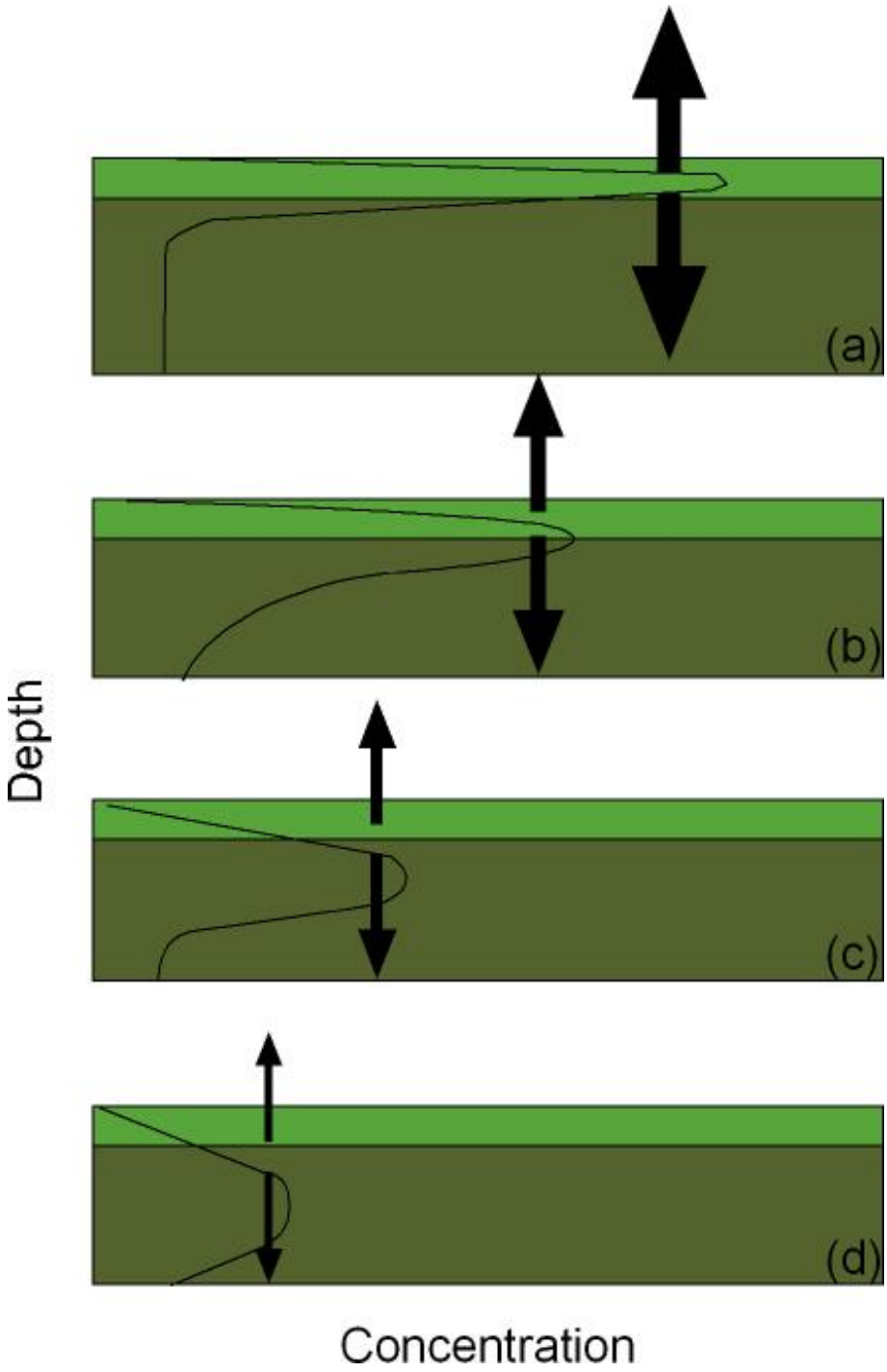

Figure 5-6 *Idealised diagram of phosphorus migration through the pore water profile showing (a) strong concentration gradient generated by a bloom in association with stratification and bottom water anoxia, (b) concentration gradient weakens with peak moving deeper down the profile, (c) concentration gradient weakens further with peak widening and moving further down the profile, and (d) concentration gradient weakens even further and peak widens as phosphorus is lost to sediments and overlying water column. The light green indicates freshly deposited organic matter to the sediments.*

5.7 Nutrient release rates

Nutrient release rates of dissolved phosphorus and ammonium display a strong seasonal trend, with mean rates as high as 62 mg P m^{-2} d^{-1} and 121.1 mg NH_4 m^{-2} d^{-1} observed over January (Table 4.1). The nutrient release rates calculated in this thesis fall within the range of nutrient release rates estimated by *in situ* benthic chamber incubations in Lake Rotorua (Burger, 2006).

The dissolved phosphorus release rate measured in January of 62 mg P m^{-2} d^{-1} is slightly higher than the rates measured by Burger (2006) who estimated ranges of 13–31 mg m^{-2} d^{-1} SRP over January 2004, however, it is lower than his maximum release rate of 86 mg m^{-2} d^{-1} measured in February 2003. Phosphorus release rates estimated in September 2006 of 6 mg m^{-2} d^{-1} (Table 4.1) closely match Burger's release rates of SRP in August 2003 of 2.1–5.6 mg m^{-2} d^{-1}. The average dissolved phosphorus release rate over 2006 calculated in this study was 30 mg m^{-2} d^{-1} (Table 4.1) which is within the range estimated by Burger (2006) of 8-44 mg m^{-2} d^{-1}.

Burger (2006) estimated release rates of NH_4 over January 2004 ranging between 75–172 mg m^{-2} d^{-1}, with the release rate of 121 mg m^{-2} d^{-1} calculated in this thesis falling within this range. Release rates of NH_4 estimated from this thesis in September of 41 mg m^{-2} d^{-1} (Table 4.1) also fall within the range of measurements made by Burger (2006) in August 2003 of 33–53 mg m^{-2} d^{-1}. The average ammonium release rate over 2006 calculated in this thesis was 79 mg m^{-2} d^{-1} (Table 4.1) falling within the range of 62 – 136 mg m^{-2} d^{-1} estimated by Burger (2006).

Table 4.2 gives the amount of dissolved phosphorus and ammonium released in tonnes per day over the whole lake, calculated from the diffusion equations. 430 tonnes of dissolved phosphorus and 1152 tonnes of ammonium are estimated to be released to the lake each year. Benthic chamber measurements made by Burger (2006) estimated release rates of 300 tonnes of soluble reactive phosphorus and 1400 tonnes of ammonium per year. The observed difference between the phosphorus release rates could possibly be from the overestimation of the

diffusive flux in the pore waters calculated in this thesis as some phosphorus may be adsorbed onto iron and manganese oxide/hydroxides present in the overlying nepheloid layer. The slightly higher release rate of ammonium observed by Burger (2006) is possibly from his high release rates of 270 mg m^{-2} d^{-1} measured in February 2003 possibly caused by high organic matter sedimentation rates in association with a stratification event.

With an external input of total P and total N of 50 t yr^{-1} and 532 t yr^{-1}, respectively, and only 19 t yr^{-1} and 236 t yr^{-1} of TP and TN, respectively, lost from the lake (Beyá et al., 2005), the internal loading of nutrients from the sediments determined in this study is the dominant flux of nutrients to Lake Rotorua with nutrients being recycled in the sediments of Lake Rotorua repeatedly before being removed from the recycling loopby mineral precipitation, denitrification, or through the Ohau Channel.

5.8 Remediation

There has been a long held desire by residents of the Rotorua District to reduce the trophic status of Lake Rotorua. Much of this effort has been directed at reducing nutrient inflows into the lake, especially from sewage and septic tank drainage. Recent studies have shown that the most significant contributor of nutrients, phosphorus and nitrogen, to the lake water column is via recycling from the sediment to the water column (Burger, 2006). There are several potential engineering solutions to reduce this input.

5.8.1 Sediment removal

Phosphorus is concentrated towards the top of the sediment column and the centre of the lake (Pearson, In Prep). Removal of this enriched material would reduce recycling of nutrients from the bottom of the lake. If dredging were to take place two significant impacts need to be considered:

1. How much nutrient loading would pore waters disturbed by the dredging contribute to the total load of nutrients to the lake?

2. How much phosphorus and nitrogen would be expected to diffuse from the newly exposed surface to the water column?

By estimating the average concentration profiles of dissolved phosphorus and ammonium in pore water collected by sediment cores over the three months in 2006, the amount of dissolved phosphorus and ammonium that would be released into the lake's water column if the top 10 cm of the 40 km^2 area of diatomaceous ooze was removed was estimated and present in Table 5.2. This is assuming that no pore water was captured in the dredging process.

Table 5-2 The quantity of phosphorus and ammonium in the upper 10 cm of the pore water of Lake Rotorua that would be released into the lake's water column by dredging if no pore water was captured.

	January (tonnes)	**May (tonnes)**	**September (tonnes)**
Phosphorus	13	7	5
Ammonium	80	45	43

Table 5.3 presents the quantity of dissolved phosphorus and ammonium that could diffuse into the lake if the top 10 cm was removed by dredging as the pore water returns to steady state. These quantities are about one quarter of the annual input of phosphorus and one eighth of the annual input of nitrogen to the lake.

Table 5-3 The quantity of dissolved phosphorus and ammonium that is capable of diffusing into the lake within 1 year of dredging the top 10 cm of the lake sediments.

	January (tonnes)	**May (tonnes)**	**September (tonnes)**
Phosphorus	3	5	4
Ammonium	80	40	39

As pore water concentrations for phosphorus decrease with depth, dredging the upper 10 cm could be a long term benefit to the lake as it would reduce the recycling of phosphorus. Increasing depth of sediment removal would have a

small benefit on the phosphorus budget but may not have any benefit for ammonium.

An associated risk with dredging is exposing the dredged sediment which is rich in pyrite to the atmosphere. Pyrite undergoes oxidation when exposed to oxygen by the following equation:

$$FeS_2 + 3½O_2 + H_2O \rightarrow Fe^{2+} + 2SO_4^{2-} + 2H^+$$

$$Fe^{2+} + 1/4\ O_2 + 2½\ H_2O \rightarrow Fe(OH)_3 + 2H^+$$

This oxidation process has the potential to create acid drainage waters as a result of the high rates of hydrogen ion formed in the product. Acidic drainage waters would also be likely to result in dissolution of heavy metals, potentially making the disposal area a contaminated site.

5.8.2 Sediment capping

The use of flocculants and materials such as sands and clays can be used to prevent the dissolution of phosphorus from the sediments. A physical barrier, i.e. sealing the sediments to prevent nutrient release, is likely to be disturbed by the ebullition of gas (refer Chapter Six). Iron and aluminium salts can be added to lakes to aid the precipitation of phosphorus. The use of iron salts needs to take into consideration the redox conditions of the lake sediments. The sediments of Lake Rotorua are extremely anoxic therefore the use of iron salts would not be recommended. Improving redox conditions in the sediments could reduce pyrite formation improving phosphorus binding with iron. The addition of aluminium salts to the soft water of Lake Rotorua could result in a loss of the buffering capacity which could decrease the pH to ecologically unacceptable levels. This potential impact can be decreased by the addition of lime (Klapper, 2003). While the use of flocculants has the potential to decrease phosphorus recycling to the lake water column, these treatments are unlikely to prevent ammonium release from the sediments.

5.9 Conclusion

Anaerobic degradation of organic matter is occurring at or near the sediment surface in the sediments of Lake Rotorua, with dissolution of iron and manganese oxide/hydroxides releasing ferrous and manganous and sulfate reduction releasing sulfide. Organic matter degradation releases high concentrations of dissolved phosphorus and ammonium into the pore waters, peaks at the sediment surface over summer. Over the colder months sulfate reduction continues to occur near the sediment surface. Ferrous, manganous, and nutrients increase in concentration with depth in the pore water.

Profiles above the sediment-water interface indicate the presence of a nepheloid layer where elements are actively being recycled. Sulfate reduction appears to be occurring above the sediment-water interface indicating dissolved oxygen must have already been reduced to near anoxic concentrations. Phosphorus is possibly being removed by iron and manganese oxide/hydroxide precipitation. Metal sulfide formation may be removing heavy metals cadmium, lead and arsenic from solution.

Pore water saturation calculations shows pyrite and the monosulfides, are supersaturated at the sediment surface, where pyrite and possibly other metal sulfides are acting as a sink for iron and other metals in a zone just below the sediment surface. Below this zone, sulfur is largely depleted and concentrations of iron and other metals increase in the pore water. Pore water is saturated with respect to siderite and vivianite at depth. These minerals are possibly acting as a sink for iron and phosphorus below the zone of pyrite formation.

Nutrient release rates calculated indicate 430 tonnes of dissolved phosphorus and 1150 tonnes of ammonium were released to Lake Rotorua's water column in 2006 suggesting nutrient release from the sediments is the dominant flux of nutrients to the water column of Lake Rotorua.

Remediation techniques that could reduce the internal load of nutrients released from the lake sediments include sediment removal by dredging and capping the

sediments. Dredging the top 10 to 20 cm of the sediments would reduce phosphorus in the pore waters but would not substantially reduce ammonium. The use of flocculants has the potential to decrease phosphorus recycling to the lake water column, however these treatments are unlikely to prevent ammonium release from the sediments. A sealing layer has the potential to prevent both phosphorus and ammonium release from the sediments but would be difficult to implement due to gas ebullition. Improving redox conditions in the sediments could reduce pyrite formation improving phosphorus binding with iron.

5.10 References

BERNER, R. A. (1980) *Early Diagenesis: A theoretical approach,* New Jersey, Princeton University Press.

BEYÁ, J., HAMILTON, D. & BURGER, D. (2005) Analysis of catchment hydrology and nutrient loads for lakes Rotorua and Rotoiti. Centre for Biodiversity and Ecology Research, The University of Waikato.

BURGER, D. (2006) Dynamics of internal nutrient loading in a eutrophic, polymictic lake (Lake Rotorua, New Zealand). *Department of Biological Sciences.* Hamilton, University of Waikato.

CARIGNAN, R. & LEAN, D. R. S. (1991) Regeneration of dissolved substances in a seasonally anoxic lake: The relative importance of processes occurring in the water column and in the sediments. *Limnology and Oceanography,* 36**,** 683-707.

EMERSON, S. (1976) Early diagenesis in anaerobic lake sediments: Chemical equilibria in interstitial waters. *Geochimica et Cosmochimica Acta,* 40**,** 925-934.

GÄCHTER, R. & MÜLLER, B. (2003) Why the phosphorus retention of lakes does not necessarily depend on the oxygen supply to their sediment surface. *Limnology and Oceanography,* 48**,** 929-933.

GRANELI, W. (1999) Internal phosphorus loading in Lake Ringsjon. *Hydrobiologia,* 404**,** 19-26.

HANSEN, L. S. & BLACKBURN, T. H. (1992) Effect of algal bloom deposition on sediment respiration and fluxes. *Marine Biology,* 112**,** 147-152.

KLAPPER, H. (2003) Technologies for lake restoration. *Journal of Limnology,* 62**,** 73-90.

MANGAN, C. (In prep) The sequestration of phosphate by iron phases in sediments from Lake Rotorua, New Zealand. MSc thesis. *Department of Chemistry.* Hamilton, University of Waikato.

MUCCI, A., RICHARD, L., LUCOTTE, M. & GUIGNARD, C. (2000) The differential behaviour of arsenic and phosphorus in the water column and sediments of the Saguenay Fjord Estuary, Canada. *Aquatic Geochemistry,* 6**,** 293-324.

PEARSON, L. (In Prep) The nature, composition and distribution of sediment, Lake Rotorua, New Zealand. MSc Thesis. *Department of Chemistry.* Hamilton, University of Waikato.

SHERMAN, L. A., BAKER, L. A., WEIR, E. P. & BREZONIK, P. L. (1994) Sediment pore-water dynamics of Little Rock Lake, Wisconsin: Geochemical processes and seasonal and spatial variability. *Limnology and Oceanography.,* 39**,** 1155-1171.

SONDERGAARD, M. (1990) Pore water dynamics in the sediment of a shallow and hypertrophic lake. *Hydrobiologia,* 192**,** 247-258.

SWEERTS, J. P., RUDD, J. W. M. & KELLY, C. A. (1986) Metabolic activities in flocculent surface sediments and underlying sandy littoral sediments. *Limnology and Oceanography,* 31**,** 330-338.

TAYLOR, K. G., BOYD, N. A. & BOULT, S. (2003) Sediments, porewaters and diagenesis in an urban water body, Salford, UK: impacts of remediation. *Hydrological processes,* 17**,** 2049-2061.

TIMPERLEY, M. H. & VIGOR-BROWN, R. J. (1986) Water chemistry of lakes in the Taupo Volcanic Zone, New Zealand. *New Zealand Journal of Marine and Freshwater Research,* 20**,** 173-183.

WANG, F. & CHAPMAN, P. M. (1999) Biological implications of sulfide in sediment -a review focusing on sediment toxicity. *Environmental Toxicology and Chemistry,* 18.

6. GAS PRODUCTION IN THE SEDIMENTS OF LAKE ROTORUA

6.1 Introduction

Gas bubbles were frequently observed rising to the surface of the lake in calm conditions and especially after sediment disturbance in Lake Rotorua. Gas in the sediments of Lake Rotorua was first considered in the early 1990s as evidenced by lack of seismic reflection by Davy (1992) who concluded that the gas was probably of geothermal origin. This chapter presents evidence of methane production in the sediments of Lake Rotorua and discusses the implications of methane generation.

6.2 Results

6.2.1 Gas Composition

Gas release was stimulated by pumping lake water through a hose to 20 and 50 cm depth below the sediment surface and was captured by a funnel and bottle as described in Section 3.3.1. The composition of the gas generated within the sediments of Lake Rotorua was found to be 97.7% methane and 2.3% carbon dioxide. Gas had the same composition at the two depths measured.

6.2.2 $\delta^{13}C$ Composition

The presence of methane indicates methanogenesis is occurring in the sediments. Measurements of $\delta^{13}C$ in the gas evolved from the sediments were made to determine the methanogenic pathway. Stable isotope analysis of $\delta^{13}C$ in CH_4 gave values ranging from -53.1 to -64.3‰. The $\delta^{13}C$ values in CO_2 range from +2.42 to +10.59‰. Stable carbon isotope fractionation between CO_2 and CH_4 was calculated by:

$$\alpha_C = \frac{(\delta^{13}C_{CO_2} + 1000)}{(\delta^{13}C_{CH_4} + 1000)}$$

with α_C values of 1.067 and 1.071 at 20 cm and 50 cm depth, respectively.

6.2.3 Dissolved Inorganic Carbon

The low percentage of CO_2 in the gas phase reflects the high solubility of CO_2. This gas is readily dissolving into solution enriching HCO_3^- concentrations in the pore water to 240-260 mg/L (Figure 6.1a).

A strong gradient is observed in $\delta^{13}C$ values of DIC in the pore water between 0 and 9 cm from -5‰ to +18‰ (Figure 6.1b). Below 7 cm $\delta^{13}C$ values maintain a relatively constant value of ~18‰ with depth.

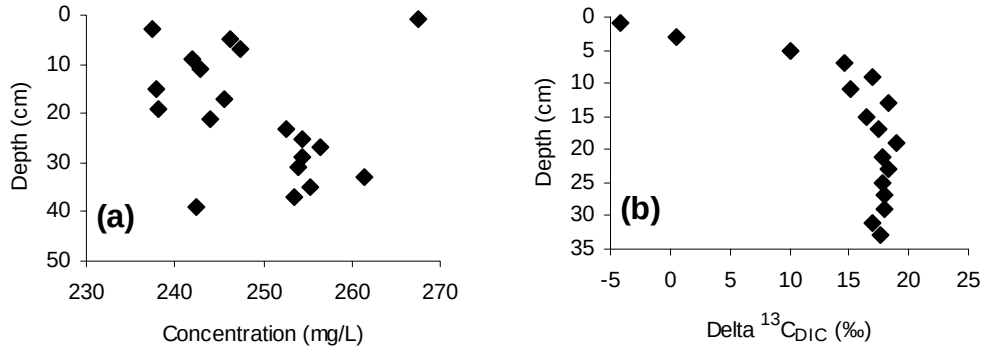

Figure 6-1 *Pore water profiles of (a) HCO_3 from RU128 and (b) $\delta^{13}C$ from Ru124.*

6.2.4 Gas Ebullition

The ebullition rate of gas released from Lake Rotorua was measured in August 2006 (Table 6.1). The rate of ebullition generally increased with water depth, with the exception of site 4. The average ebullition rate was 126 ml m^{-2} d^{-1}. Assuming that the 40 km^2 area of diatomaceous ooze in the sediments of Lake Rotorua is the sole source for ebullition of gas, the average gas ebullition rate over the whole lake is 1.38 x 10^6 m^3 yr^{-1}.

Table 6-1 Ebullition rate of gas from Lake Rotorua sediments.

Site	Water Depth (m)	Ebullition rate (ml m^{-2} d^{-1})
1	14.4	35
2	16.3	117
3	20.6	285
4	23.9	66
Average		126

6.3 Discussion

6.3.1 Gas Composition

The percentage CH_4 is high compared with many other studies. Huttunen et al. (2001) found CH_4 composition within gas bubbles produced in sediments to be on average 69.2% in a eutrophic lake. Martens and Klump (1980) found CH_4 composition of 86% derived from sediment production in a coastal marine basin. Chanton et al. (1989) found that methane composition in gas bubbles reflects vegetation status of the sediments. They found methane composition in bubbles to range from 50-80% with the higher figures associated with release from unvegetative sediments. Vegetated sediments cause oxidation of CH_4 due to an oxic rhizosphere, resulting in lower CH_4 composition. The sediments of Lake Rotorua are only partially vegetated in the shallow margins and totally unvegetated in the gas-rich zone of the centre of the lake, therefore the high CH_4 composition is most likely a result of the absence of vegetation in the deeper diatomaceous sediment. The CH_4/CO_2 ratio may also be affected by CO_2 produced from acetate fermentation dissolving into the pore waters as reflected by the HCO_3^- concentrations (Figure 6.1a).

6.3.2 Methanogenic pathway

Stable isotope analysis of CH_4 indicates that the gas is of biogenic origin, produced by acetate fermentation. Enrichment of $\delta^{13}C$ in CO_2 indicates possible CO_2 reduction. However the boundaries between acetate fermentation and CO_2 reduction are not well enough established to make an unequivocal assignment

based on $\delta^{13}C$ values alone (Hackley et al., 1996). The fractionation between CO_2 and CH_4 is typical of acetate fermentation of polysaccharides with an original $\delta^{13}C$ of ~ 25‰.

At temperatures of about 15°C the fractionation of ^{13}C from CO_2 to HCO_3^- is about 8‰, thus these pore waters are in isotopic equilibrium with carbon dioxide with a $\delta^{13}C$ of ~11‰ (Vogel et al., 1970). This enrichment is reflected in the pore water composition, where DIC $\delta^{13}C$ values are ~ +18‰ (Figure 6.1b). The strong gradient observed in DIC $\delta^{13}C$ values reflects the increasing proportion of anaerobic fermentation derived CO_2 with depth. The strong gradient also indicates a possible shift in degradation processes from sulfate reduction to methanogenesis. This transition fits with sulfate reduction observed in the pore water of Ru124 which occurs in the upper 5 cm of the sediment (refer to Chapter 4, Figure 4.24b). As sulfate is depleted in the pore water methanogens are no longer out-competed by sulfate reducers.

DIC produced from methanogenesis can be 30-40‰ more enriched in $\delta^{13}C$ than the source POC (Herczeg, 1988). The $\delta^{13}C$ values of Lake Rotorua sediments have been observed to range between -20 to -23‰ (McCabe, 2005), showing an enrichment of 40‰ of DIC within the pore water.

6.3.3 Gas Ebullition

The rate of gas ebullition observed in Lake Rotorua is not unusually high compared with ebullition rates observed in other eutrophic lakes. Huttunen et al. (2001) observed an average ebullition rate of 106 ml m^{-2} d^{-1} in a midboreal eutrophic lake. A eutrophic lake in Finland also had an average ebullition rate of 106 ml m^{-2} d^{-1} over summer, with a maximum of 345 ml m^{-2} d^{-1} (Saarijärvi and Lappalainen, 2001).

The ebullition of gas from lake sediments has been found to be highly variable. Large pulses of CH_4 ebullition have been associated with rapidly falling barometric pressure (Casper et al., 2000). The ebullition rate of 285 ml m^{-2} d^{-1}

observed at site 3 could be associated with a large pulse of CH_4 release, as large release of bubbles to the surface of the lake are commonly observed. The wide range of ebullition rates (35-285 ml m^{-2} d^{-1}) observed highlights the spatial variability of gas ebullition in the sediments.

6.4 Environmental implications

Two environmental implications can result from the ebullition of gas. First, gas consisting of CH_4 and CO_2 can contribute to greenhouse gas emissions. Second, nutrient release from the pore water can be enhanced by ebullition, and therefore the presence of gas has the potential to affect remediation of the lake sediments.

6.4.1 Global warming

Methane and carbon dioxide are both important greenhouse gases. Freshwater lakes are an important contributor to atmospheric concentrations of CH_4 and CO_2 (Cicerone and Oremland, 1988). Globally, freshwaters have the potential to release 72 x 10^{12} g CH_4 and 156 x 10^{12} g CO_2 annually to the atmosphere (Casper et al., 2000). The gas present in Lake Rotorua is mostly CH_4 which is a much more potent greenhouse gas than CO_2. The measurements made in this thesis indicate that Lake Rotorua discharges 9 x 10^8 g of CH_4 a year. Further investigation is required to provide a more accurate estimate of the ebullition of CH_4 and CO_2 taking into consideration spatial and temporal variability and temporal variations in gas release.

6.4.2 Nutrient release

The ebullition of gas has been found to enhance the release of nutrients from pore water to the overlying water column (Liikanen et al., 2003). Assuming volumes of pore water displaced is similar to volume of gas released from the sediments of Lake Rotorua, then at an ebullition rate of 1-3 x 10^6 m^3 yr^{-1}, 4-12.5 tonnes of dissolved phosphorus and 11-34 tonnes ammonium are released per year (Table 6.2). This amount is small compared to release rates estimated by molecular diffusion (Refer to Chapter 5), and small compared with the rate measured by

Likkanen et al. (2003). The release rate of nutrients from displacement by ebullition is an area of research that needs further investigation as the present results are preliminary.

Table 6-2 Tonnes of dissolved phosphorus and ammonium released from Lake Rotorua based on displacement volumes of gas.

Month	P (tonnes/year)	NH_4 (tonnes/yr)
January	9 -28	17-52
May	2 - 7	11-32
September	0.8 -2.5	6-18
Average	4-12.5	11-34

6.4.3 Lake remediation

The ebullition of gas within the sediments of Lake Rotorua could also impact on any in situ remediation procedures to aid the recovery of Lake Rotorua. If the lake was to be capped with a sealing layer, then ebullition of gas could disrupt the capped layer, opening up pathways that allow more readily for exchange between pore water nutrients and the water column. Dredging would remove this potential but the process of dredging is likely to stimulate the ebullition of most of the trapped gas and result in a rapid efflux of much of the nutrient rich pore water into the lake.

6.5 Conclusion

Methanogenesis is occurring in the sediments of Lake Rotorua producing large volumes of gas consisting of 97.7% methane and the remainder carbon dioxide. $\delta^{13}C$ values of the gas show that the CO_2 is enriched and the CH_4 depleted in $\delta^{13}C$, indicating biogenic origin produced by acetate fermentation. $\delta^{13}C$ values of DIC are extremely enriched at ~18‰ with a strong gradient seen between 0 and 9 cm reflecting the increasing proportion of anaerobic fermentation derived CO_2 with depth and a possible change in organic matter degradation processes from sulfate reduction to methanogenesis.

The observed average ebullition rate of 126 ml m^{-2} d^{-1} from the sediments of Lake Rotorua is expected to displace pore water enhancing nutrient release, and contribute greenhouse gases in the atmosphere. In situ remediation measures such as dredging and capping of the sediments could also be compromised by gas ebullition. Ebullition of gas would likely disrupt the capped layer exposing pore water to the water column. Dredging has the potential to stimulate ebullition resulting in a rapid efflux of nutrient rich pore water into the water column.

6.5 References

CASPER, P., MABERLY, S. C., HALL, G. H. & FINLAY, B. J. (2000) Fluxes of methane and carbon dioxide from a small productive lake to the atmosphere. *Biogeochemistry,* 49**,** 1-19.

CHANTON, J. P., MARTENS, C. S. & KELLEY, C. A. (1989) Gas transport from methane saturated, tidal freshwater and wetland sediments. *Limnology and Oceanography,* 34**,** 807-819.

CICERONE, R. J. & OREMLAND, R. S. (1988) Biogeochemical aspects of atmospheric methane. *Global Biogeochemical Cycles* 2**,** 299-327.

HACKLEY, K. C., LUI, C. L. & COLEMAN, D. D. (1996) Environmental isotope characteristics of landfill leachates and gases. *Ground Water,* 34**,** 827-836.

HERCZEG, A. L. (1988) Early diagenesis of organic matter in lake sediments: A stable carbon isotope study of pore waters. *Chemical Geology (Isotope Geoscience Section),* 72**,** 199-209.

HORNIBROOK, E. R. C., LONGSTAFFE, F. J. & FYFE, W. S. (2000) Evolution of stable carbon isotope compositions for methane and carbon dioxide in freshwater wetlands and other anaerobic environments. *Geochimica et Cosmochimica Acta,* 64**,** 1013-1027.

HUTTUNEN, J. T., MATTI LAPPALAINEN, K., SAARIJÄRVI, E., VÄISÄNEN, T. & MARTIKAINEN, P. J. (2001) A novel sediment gas sampler and a subsurface gas collector used for measurement of the ebullition of methane and carbon dioxide from a eutrophied lake. *The Science of the Total Environment,* 266**,** 153-158.

LIIKANEN, A., HUTTUNEN, J. T., MURTONIEMI, T., TANSKANEN, H., VÄISÄNEN, T., SILVOLA, J., ALM, J. & PERTTI, J. (2003) Spatial and seasonal variation in greenhouse gas and nutrient dynamics and their interactions in the sediments of a boreal eutrophic lake. *Biogeochemistry,* 65**,** 83-103.

MARTENS, C. S. & KLUMP, J. V. (1980) Biogeochemical cycling in an organic rich coastal marine basin. Methane sediment-water exchange processes. *Geochimica et Cosmochimica Acta,* 44**,** 471-490.

MCCABE, A. (2005) An investigation into carbon and nitrogen in Lakes Rotorua and Rotoiti: A stable isotope approach. MSc Thesis. *Department of Biological Sciences.* Hamilton, University of Waikato.

SAARIJÄRVI, E. & LAPPALAINEN, K. M. (2001) Floatation-like gas ebullition as a mechanism for sediment resuspension. *Verh. Internationale Verein Limnologie,* 27**,** 4093-4096.

VOGEL, J. C., GROOTES, P. M. & MOOK, W. G. (1970) Isotopic fractionation between gaseous and dissolved carbon dioxide. *Zeitschrift für Physik A Hadrons and Nuclei,* 230**,** 225-238.

7. CONCLUSION

Anaerobic degradation of organic matter occurs in the sediments of Lake Rotorua, and is associated with rapid loss of any free oxygen from within a mobile nepheloid layer at the sediment surface, followed immediately below this by reduction of manganese and iron oxides/hydroxides to ferrous and manganous, respectively, then reduction of sulfates to sulfides and finally production of methane. Negative Eh values are associated with these transitions which occur at scales of millimetres within the surface sediments or within the nepheloid layer. Organic matter degradation releases high concentrations of dissolved phosphorus and ammonium into the pore waters. Seasonal changes were evident, with these nutrients and reduced metal cations displaying near-surface concentration peaks over summer. Over the colder months sulfate reduction continues to occur near the sediment surface, with concentrations of ferrous, manganous, and nutrients increasing with depth in the pore water.

Sampling with peepers at fine scales immediately above the sediment-water interface indicated the presence of a nepheloid layer where elements are actively being recycled. Sulfate reduction appears to occur in the layer above the sediment-water interface, indicating that dissolved oxygen has already been reduced. Phosphorus is possibly being removed by iron and manganese oxide/hydroxide precipitation 5 to 15 cm above the sediment-water interface. Metal sulfide formation may be removing heavy metals (cadmium, lead and arsenic) from solution immediately at and below the sediment-water interface.

Pore water saturation calculations indicate potential for authigenic mineral formation. Pyrite and monosulfides are supersaturated just below the sediment surface, and may act as a sink for iron and other metals in the zone of sulfate reduction. Below this zone, sulfur is largely depleted and concentrations of iron and other metals increase in the pore water. Deeper pore waters are saturated with respect to siderite and vivianite. These minerals are possibly acting as a sink for iron and phosphorus below the zone of pyrite formation.

Below the zone of sulfate reduction, methanogenesis occurs and is the dominant process in organic matter degradation, producing relatively high concentrations of ammonium ions deep in the sediment. Methanogenesis results in ebullition of large volumes of gas comprised of 97% methane and the remainder carbon dioxide. An average gas release rate of 126 ml m^{-2} d^{-1} from the sediments was recorded. Enrichment of $\delta^{13}C$ in carbon dioxide and depletion of $\delta^{13}C$ in methane indicates that methane and carbon dioxide are produced by acetate fermentation, with carbon dioxide dissolving into solution enriching the pore waters with bicarbonate.

Nutrient release rates calculated from Fick's law of diffusion using surface pore water concentrations indicate that 430 tonnes of dissolved phosphorus and 1150 tonnes of ammonium were released to the water column in 2006. These figures are strongly dominant over catchment loads of total phosphorus of 50 tonnes yr^{-1} and total nitrogen of 532 tonnes yr^{-1}.

Possible remediation techniques that could reduce the internal load of nutrients released from the lake sediments include sediment removal by dredging or capping the sediments with an adsorbent or sealing layer. The ebullition of gas within the sediments of Lake Rotorua has the potential to impact on any *in situ* remediation procedures designed to assist with recovery of Lake Rotorua. Capping the sediments could be compromised by ebullition of gas that would disrupt the capped layer, opening up pathways that allow more readily for exchange between pore water nutrients and the water column. Dredging would remove this potential but the process of dredging is likely to stimulate the ebullition of most of the trapped gas and result in a rapid efflux of much of the nutrient rich pore water into the lake. Ignoring the risk of ebullition by dredging the top 10 to 20 cm of the sediments may partially reduce phosphorus in the pore waters but would not substantially reduce ammonium and fluxes would remain similar to current levels. Improving redox conditions in the sediments could reduce pyrite formation improving phosphorus binding with iron.

Appendices

Appendix 1

Location and details of samples

Gravity Cores

Core ID	Month	Site Location	Grid S Grid E	Water Depth (m)	Core Length (m)
Ru102	January	38 08152 S 176 22764 E	6341744.46 2793252.09	7	0.5
Ru103	January	38 07578 S 176 23499 E	6342357.67 2793919.50	11.5	0.32
Ru104	January	38 0751 S 176 2464 E	6342396.76 2794922.57	12.5	0.40
Ru105	January	38 07462 S 176 25782 E	6342413.51 2795925.72	15.5	0.55
Ru106	January	38 07325 S 176 72010 E	6342526.07 2797007.89	21.4	0.50
Ru107	January	38 07256 S 176 27891 E	6342574.26 2797783.10	22.7	0.50
Ru108	January	38 0719 S 176 2893 E	6342613.95 2798696.73	14.5	0.50
Ru109	January	38 07202 S 176 30025 E	6342565.21 2799656.26	13.8	0.55
Ru110	January	38 07123 S 176 31042 E	6342619.82 2800551.15	12.4	0.50
Ru111	March	38 07318 S 176 27041 E	6342532.84 2797035.36	21.7	0.45
Ru112	March	38 06692 S 176 29616 E	6343144.07 2799318.56	16.4	0.43
Ru114	May	38 09706 S 176 29528 E	6339804.23 2799118.00	11.9	0.1
Ru115	May	38 09507 S 176 28455 E	6340059.59 2798185.70	9.7	0.18
Ru116	May	38 09324 S 176 29528 E	6340302.04 2797118.11	21	0.6
Ru117	May	38 09324 S 176 29528 E	6340302.04 2797118.11	21	0.4
Ru118	May	38 09162 S 176 26004 E	6339804.23 2799118.00	17.6	0.36
Ru119	May	38 08863 S 176 24895 E	6340888.05 2795091.48	12.3	0.46
Ru120	May	38 05705 S 176 23838 E	6344424.18 2794292.12	10.2	0.3
Ru121	May	38 05886 S	6344196.52	11.9	0.36

		176 24683 E	2795025.82		
Ru122	May	38 06079 S 176 25546 E	6343954.90 2795774.78	13.4	0.36
Ru123	May	38 06245 S 176 26501 E	6343740.20 2796605.46	15.9	0.34
Ru124	May	38 06603 S 176 27568 E	6343308.88 2797526.50	20.4	0.36
Ru125	May	38 06850 S 176 28568 E	6343002.71 2798393.23	21.4	0.37
Ru126	May	38 07070 S 176 29611 E	6342725.01 2799298.70	16	0.48
Ru127	May	38 07277 S 176 30628 E	6342462.47 2800181.85	13.5	0.3
Ru128	June	38 07318 S 176 27041 E	6342532.84 2797035.36	21	0.40
Ru129	September	38 07268 S 176 16308 E	6336867 2797252	11.4	0.28
Ru130	September	38 07086 S 176 15598 E	6337455 2796517	21.4	0.42
Ru131	September	38 06330 S 176 16075 E	6338546 2796745	17.9	0.46
Ru132	September	38 06006 S 176 16502 E	6339472 2798770	13	0.24
Ru133	September	38 05540 S 176 15533 E	6339761 2796444	18.5	0.45
Ru134	September	38 05541 S 176 15183 E	6339787 2795591	13	0.25
Ru135	September	38 05388 S 176 14423 E	6340290 2794731	9.4	0.36
Ru136	September	38 04579 S 176 14387 E	6341553 2794690	12	0.36
Ru137	September	38 04012 S 176 18024 E	6343118 2793714	11.2	0.44
Ru138	September	38 05024 S 176 15188 E	6341380 2795662	16.1	0.10
Ru139	September	38 03337 S 176 14041 E	6344179 2793941	9.8	0.33
Ru140	September	38 03234 S 176 14375 E	6344467 2794766	11.5	0.40
Ru141	September	38 03213 S 176 15301 E	6344485 2796049	14.1	0.45
Ru142	September	38 03152 S 176 16444 E	6344638 2796989	16.1	0..36
Ru143	September	38 03162 S	6344575	17.4	0.35

		176 16444 E	2797866		
Ru144	September	38 03174 S 176 17202 E	6344507 2798736	18	0.42
Ru145	September	38 03161 S 176 18007 E	6344502 2799723	17.9	0.35
Ru146	September	38 03119 S 176 18389 E	6344606 2800661	15.9	0.43
Ru147	September	38 02479 S 176 17584 E	6345338 2800875	16.7	0.44
Ru148	September	38 02363 S 176 17584 E	6345738 2799714	10.6	0.11
Ru149	September	38 04146 S 176 14319 E	6342893 2794573	11.7	0.42
Ru150	September	38 03459 S 176 14391E	6343771 2794781	11.6	0.40
Ru151	September	38 04110 S 176 15193 E	6342964 2795731	14.4	0.47
Ru152	September	38 03439 S 176 15598 E	6343761 2796749	16.2	0.48
Ru153	September	38 03460 S 176 16237 E	6343676 2797329	20.1	0.27
Ru154	September	38 03474 S 176 17217 E	6343582 2798738	20.4	0.48
Ru155	September	38 03460 S 176 18013 E	6343588 2799705	16.6	0.07
Ru156	September	38 03476 S 176 18450 E	6343500 2800768	12.4	0.35
Ru157	September	38 04431 S 176 18023 E	6341829 2799664	14.2	0.47
Ru158	September	38 05063 S 176 15487 E	6341233 2796384	20.8	0.48
Ru159	September	38 05078 S 176 16304 E	6341150 2797399	16.6	0.24
Ru160	September	38 05373 S 176 15566 E	6340233 2797554	15.2	0.46
Ru161	September	38 05281 S 176 15521 E	6340560 2796443	21	0.47
Ru162	September	38 04526 S 176 15566 E	6341647 2796592	21.6	0.48
Ru163	September	38 02566 S 176 15541 E	6342552 2796663	19.4	0.48
Ru164	November		6343172 2798038	23.7	0.20

Peepers

Sample ID	Date of deployment	Equilibration time (days)	Location	Water depth (m)
P1	14/06/06-03/08/2006	50	N 6343091 E 2797097	20.6
P2	03/08/06-06/11/2006	95	N 6343172 E 6343172	23.7
P3	03/08/06-06/11/2006	95	N 6343172 E 6343172	23.7
P4	03/08/06-06/11/2006	95	N 6343172 E 6343172	23.7

Gas

Depth (cm)	Location	Water depth (m)
20	S38.07288 E176.27079	22
50	S38.07288 E176.27079	22

Ebullition rate

Gas release site	Location	Water depth (m)	Time deployed (minutes)
Site 1	E2795740, N6343218	14.4	201
Site 2	E2796320, N6343264	16.3	195
Site 3	E2797102, N6343144	20.6	187
Site 4	E2797724, N6343151	23.9	181
Site 5	E2798407, N6343125	20.0	166

Appendix 2 Raw Concentrations

Sediment core pore water

Sample ID (cm)	Fe^{2+}	Mn^{2+}	S	P	SRP	NH_4^+	NO_3^-	As	Cd	Pb
Ru102										
1	1.62	1.50		2.72	1.88	9.01	1.38	0.219	0.009	0.009
3	0.88	1.57		3.71	2.47	8.86	0.66	0.296	0.007	0.006
5	0.76	1.23		8.79	7.26	8.50	1.05	0.173	0.006	0.006
7	0.57	0.91		3.83	3.21	8.12	3.26	0.172	0.012	0.007
9	0.85	1.11		4.14	3.13	9.34	0.74	0.177	0.008	0.014
11	0.72	1.10		3.70	2.29	9.55	1.10	0.218	0.004	0.006
13	0.84	1.25		2.82	2.05	11.17	1.58	0.195	0.031	0.012
15	0.80	1.39		2.06	1.52	11.55	1.55	0.174	0.023	0.007
17	2.21	1.69		2.27	1.61	11.90	1.59	0.245	0.010	0.012
19	1.54	1.69		1.59	0.93	10.82	0.70	0.292	0.007	0.009
21	2.32	1.88		1.97	1.51	12.83	2.03	0.205	0.008	0.017
23	1.79	1.70		2.75	2.21	12.69	1.08	0.220	0.004	0.012
Ru103										
0	2.43	0.84	14.39	2.27	1.25	3.58	2.28	0.044	0.141	0.025
3	1.60	2.04	4.92	7.51	4.98	15.68	1.59	0.637	0.010	0.051
5	1.66	2.82	0.00	12.68	9.08	16.90	0.88	0.327	0.009	0.008
7	1.60	2.30	2.06	4.47	2.98	17.35	0.82	0.236	0.024	0.014
9	1.82	2.24	4.74	3.86	2.58	17.38	1.73	0.261	0.010	0.007
11	1.70	2.11	0.58	2.10	1.52	15.31	1.26	0.305	0.051	0.018
13	2.46	2.45	0.28	2.59	2.08	17.30	0.73	0.280	0.008	0.016
15	2.51	2.49	4.69	2.56	1.48	17.88	3.08	0.228	0.021	0.079
17	0.47	0.58	1.20	0.37	0.44	14.03	1.90	0.149	0.083	0.011

	Fe^{2+}	Mn^{2+}	S	P	SRP	NH_4^+	NO_3^-	As	Cd	Pb
19	0.56	0.80	0.00	0.39	0.35	14.25	3.59	0.389	0.070	0.013
21	1.05	1.22	0.00	0.39	0.34	16.19	1.39	0.194	0.023	0.006
23	3.51	3.57	0.00	0.70	0.65	19.42	1.01	0.274	0.020	0.005
27	1.38	1.20	0.00	0.70	0.51	15.04	1.84	0.203	0.119	0.017
29	4.06	2.68	0.00	1.20	1.09	19.11	1.88	0.222	0.044	0.011
Ru104										
1	3.71	2.72		11.54	9.73	16.40	0.66	0.071	0.015	0.012
3	1.88	2.12		6.80	5.46	14.86	0.53	0.080	0.011	0.013
5	1.20	1.59		3.49	3.00	13.44	0.84	0.140	0.052	0.007
7	1.08	1.35		2.27	1.96	13.35	0.65	0.153	0.190	0.017
11	0.39	1.48		0.95	0.87	12.56	2.00	0.111	0.028	0.004
13	2.23	1.97		2.76	2.53	14.13	0.22	0.040	0.027	0.004
15	1.65	1.68		1.26	1.25	12.99	0.30	0.227	0.029	0.031
17	0.30	0.58		0.22	0.19	10.05	0.65	0.162	0.050	0.009
19	0.32	0.50		0.23	0.23	10.08	2.27	0.152	0.039	0.007
Ru105										
1	1.92	2.52		9.61	8.77	19.38	0.56	0.135	0.007	0.008
3	1.99	2.41		6.05	4.91	17.27	0.50	0.078	0.015	0.006
5	2.02	1.94		2.94	2.41	15.74	0.72	0.222	0.095	0.013
7	0.75	0.79		1.54	1.73	15.72	0.59	0.262	0.053	0.011
9	2.49	2.20		2.81	2.72	17.00	0.73	0.198	0.032	0.011
11	3.20	2.55		2.53	2.21	17.13	0.60	0.239	0.026	0.004
13	1.92	1.57		0.82	0.72	14.69	2.02	0.321	0.006	0.010
15	2.06	2.00		0.99	0.62	14.23	0.70	0.232	0.066	0.005
17	3.39	3.05		2.11	1.49	16.81	0.65	0.256	0.079	0.003
19	2.60	2.12		1.25	1.11	16.89	1.77	0.225	0.063	0.006
Ru106										
1	5.45	4.98	2.2	15.69	13.41	18.73	0.38	0.091	0.049	0.054
3	3.86	3.88	0.0	7.14	5.60	19.35	0.39	0.115	0.056	0.007

	Fe^{2+}	Mn^{2+}	S	P	SRP	NH_4^+	NO_3^-	As	Cd	Pb
5	1.60	2.94	3.5	1.84	1.55	19.49	1.57	0.152	0.110	0.006
7	1.79	3.60	0.0	2.38	2.24	22.10	0.60	0.185	0.263	0.005
9	3.83	3.97	0.0	3.47	3.14	22.09	0.46	0.238	0.018	0.006
11	3.92	3.62	0.0	2.96	2.88	22.05	0.65	0.249	0.059	0.004
13	5.29	4.54	7.1	3.07	2.90	23.29	0.56	0.297	0.034	0.004
15	5.95	4.11	0.0	1.97	1.81	22.78	0.31	0.404	0.019	0.004
17	5.08	5.22	0.0	2.92	2.38	23.86	0.52	0.338	0.013	0.006
19	4.86	4.50	1.2	1.93	1.81	24.42	0.64	0.338	0.013	0.011
Ru107										
1	4.99	8.86	3.20	20.48	17.01	30.87	0.34	0.060	0.008	0.010
3	1.89	4.29	1.89	3.50	3.12	19.83	0.74	0.126	0.040	0.009
5	3.86	4.08	5.20	1.77	1.42	16.10	0.43	0.229	0.041	0.013
7	1.68	3.53	1.70	1.79	1.64	16.65	1.29	0.188	0.013	0.005
9	1.91	3.84	1.97	1.26	1.15	16.76	1.10	0.254	0.004	0.007
11	1.30	2.74	2.64	0.60	0.60	15.56	0.57	0.222	0.003	0.022
13	0.96	3.47	3.68	0.88	0.83	16.90	1.17	0.276	0.017	0.013
15	1.34	2.30	2.75	0.44	0.47	14.51	0.42	0.181	0.007	0.006
17	1.37	2.58	3.23	0.43	0.44	15.56	0.76	0.227	0.006	0.009
19	3.79	3.97	2.96	1.89	1.69	15.87	0.25	0.291	0.012	0.012
Ru108										
1	3.24	3.09	24.48	8.46	6.03	18.65	0.65	0.113	0.007	0.005
3	2.77	3.72	4.67	8.90	7.83	25.28	0.64	0.030	0.007	0.004
5	2.09	3.40	5.20	6.32	4.98	26.51	0.61	0.038	0.012	0.005
7	2.78	3.69	2.97	4.23	3.53	23.99	0.83	0.096	0.024	0.006
9	2.19	2.81	4.89	2.40	1.85	21.18	1.68	0.131	0.080	0.007
11	0.97	1.71	4.03	1.85	1.61	20.09	0.92	0.103	0.029	0.008
13	0.69	2.36	3.31	1.16	1.09	19.42	0.96	0.128	0.012	0.006
15	1.67	2.90	3.57	1.34	1.15	19.17	0.76	0.198	0.005	0.007
17	2.13	3.27	2.76	1.76	1.51	21.03	0.49	0.200	0.030	0.011

	Fe^{2+}	Mn^{2+}	S	P	SRP	NH_4^+	NO_3^-	As	Cd	Pb
19	2.64	3.60	3.87	1.63	1.53	19.76	0.52	0.264	0.019	0.006
Ru109										
1	2.07	2.51	5.10	4.15	3.63	23.23	0.23	0.081	0.020	0.006
5	1.32	1.76	4.03	1.78	1.63	20.28	0.94	0.140	0.016	0.005
7	4.17	2.06	3.74	1.39	1.32	19.81	0.57	0.135	0.017	0.359
9	0.65	1.82	4.77	0.83	0.76	19.61	0.35	0.178	0.006	0.009
11	0.71	1.81	4.00	0.69	0.65	18.81	2.18	0.155	0.006	0.004
13	0.43	1.42	3.56	0.45	0.38	17.17	0.49	0.173	0.004	0.005
15	5.46	2.86	12.84	0.70	0.67	18.65	0.52	0.198	0.010	0.010
17	2.43	1.99	5.01	0.81	0.65	18.85	1.16	0.171	0.060	0.080
19	1.93	2.20	5.26	0.81	0.77	19.64	0.52	0.202	0.281	0.009
Ru110										
1	0.80	1.40	16.68	9.62	6.51	16.19	0.78	0.098	0.004	0.004
3	6.68	4.88	7.63	18.81	13.79	28.56	0.53	0.056	0.005	0.006
5	4.12	3.23	5.67	6.73	2.62	22.35	0.55	0.069	0.030	0.003
7	3.04	2.88	6.15	3.85	4.63	22.76	1.19	0.094	0.006	0.036
9	2.66	2.29	4.84	3.08	2.37	20.64	1.48	0.078	0.018	0.003
11	1.77	2.20	5.29	2.31	1.73	19.34	0.65	0.085	0.002	0.006
13	2.07	2.11	3.98	1.02	0.72	17.93	0.76	0.110	0.066	0.004
15	1.89	1.87	5.10	0.81	0.59	17.06	0.25	0.104	0.009	0.003
17	1.88	1.98	6.17	0.77	0.56	18.63	0.90	0.099	0.005	0.004
19	2.08	2.23	5.07	0.65	0.48	17.71	0.64	0.118	0.022	0.004
Ru114	Fe^{2+}	Mn^{2+}	S	TDP	SRP	NH_4^+	NO_3^-	As	Cd	Pb	pH	Eh
0	0.11	1.04	6.3	2.91	2.09	5.82	0.29	0.63	0.003	0.002	5.93	-109
1	1.22	1.05	17.5	7.48	5.06	8.00	0.16	0.09	0.003	0.001	5.92	-29
3	0.38	0.94	8.7	2.24	1.04	5.50	0.14	0.30	0.003	0.002	5.87	-42
5	0.40	1.08	6.7	0.38	0.19	4.77	0.14	0.26	0.004	0.002	6.01	-78
7	1.41	1.64	6.4	0.18	0.10	4.43	0.22	0.16	0.001	0.003	5.98	-127
Ru115												

	Fe^{2+}	Mn^{2+}	S	TDP	SRP	NH_4^+	NO_3^-	As	Cd	Pb	pH	Eh
0	0.11	1.04	6.3	2.91	2.09	5.82	0.29	0.63	0.003	0.002	5.93	-109
1	0.67	0.87	8.2	4.59	2.16	6.26	0.16	0.09	0.005	0.002	5.74	-39
3	0.40	0.66	5.7	2.30	0.88	6.02	0.12	0.17	0.005	0.002	5.94	-118
5	0.11	1.04	6.3	2.91	2.09	5.82	0.29	0.63	0.003	0.002	5.93	-109
7	0.34	1.31	6.3	0.53	0.31	5.14	0.32	0.67	0.008	0.002	6.04	-68
9	0.81	1.35	7.2	0.28	0.19	4.79	0.25	0.73	0.005	0.004	6.05	-112
11	1.55	1.58	7.0	0.26	0.19	4.73	0.52	0.62	0.005	0.004	6.19	-105
13	0.75	1.96	6.4	0.17	0.12	4.57	2.82	0.98	0.014	0.002	6.09	-106
15	1.33	1.49		0.33	0.25	3.60	0.24	1.80	0.008	0.003	6.09	-113
Ru116												
1	1.54	1.69	8.4	0.72	0.43	29.24	0.12	0.36	0.004	0.002	6.07	-92
3	10.60	3.62	6.0	3.11	2.07	30.82	0.17	0.30	0.002	0.004	5.96	-96
5	10.54	3.14	4.9	1.49	0.99	30.85	0.15	0.47	0.002	0.002	6.10	-104
7	4.61	2.50	4.9	1.60	1.01	31.28	0.09	0.44	0.004	0.002	6.09	-111
9	10.92	3.18	3.8	2.77	2.43	32.60	0.19	0.25	0.004	0.001	6.11	-105
11	6.55	2.46	2.4	1.59	1.81	33.32	0.25	0.15	0.001	0.001	6.13	-98
13	16.75	3.70	3.4	3.59	3.39	32.39	0.23	0.19	0.006	0.002	6.14	-107
15	11.37	3.35	4.5	2.93	2.20	33.08	0.27	0.20	0.003	0.002	6.08	-105
17	3.43	2.09	5.1	0.68	0.53	32.45	0.12	0.27	0.002	0.002	6.14	-110
19	15.12	3.93	4.5	2.50	1.86	33.93	0.13	0.34	0.002	0.002	6.13	-99
21	13.33	3.76	6.0	2.59	2.09	34.22	0.14	0.28	0.004	0.001	6.15	-105
23	19.38	4.40	5.1	2.87	2.78	34.85	0.31	0.29	0.005	0.002	6.16	-104
25	8.63	3.07	4.8	0.98	0.76	33.60	0.14	0.33	0.003	0.002	6.17	-103
27	23.43	4.65	4.6	3.39	3.08	34.67	0.12	0.26	0.005	0.002	6.17	-108
29	4.86	1.56	4.5	0.97	1.94	34.69	0.25	0.08	0.000	0.001	6.16	-102
31	14.02	4.22	4.7	2.29	1.74	34.91	0.19	0.32	0.002	0.004	6.17	-109
33	4.27	1.18	3.5	0.62	1.43	34.00	0.24	0.11	0.002	0.001	6.13	-106
35	15.76	4.09	4.1	2.95	2.28	34.99	0.11	0.27	0.002	0.002	6.16	-103
37	2.47	0.87	4.5	0.34	0.92	33.69	0.12	0.11	0.002	0.001	6.23	-113

	39	17.19	3.48	5.2	2.62	1.90	34.85	0.19	0.23	0.004	0.003	6.16	-117
		Fe^{2+}	**Mn^{2+}**	**S**	**TDP**	**SRP**	**NH_4^+**	**NO_3^-**	**As**	**Cd**	**Pb**	**pH**	**Eh**
	41	0.11	1.04	6.3	2.91	2.09	5.82	0.29	0.63	0.003	0.002	5.93	-109
	43	20.58	4.73	4.4	2.42	1.76	35.78	0.19	0.54	0.007	0.002	6.14	-114
	45	8.61	2.71	5.0	0.72	0.45	33.93	0.36	0.46	0.008	0.003	6.29	-109
Ru117													
	1	10.18	2.66	15.7	5.43	4.95	24.73	0.18	0.46	0.018	0.001	6.07	-94
	3	8.33	2.61	6.1	4.29	4.02	26.15	0.17	0.21	0.002	0.002	6.06	-92
	5	8.83	3.22	3.7	5.20	4.82	28.71	0.22	0.16	0.006	0.001	6.06	-94
	7	9.51	3.02	2.2	4.39	4.12	29.64	0.17	0.26	0.005	0.001	6.07	-84
	9	4.55	2.08	0.7	2.74	2.58	29.81	0.40	0.20	0.003	0.001	6.03	-71
	11	11.69	3.51	1.7	3.82	3.22	30.99	0.22	0.28	0.001	0.001	6.11	-74
	13	11.59	3.11	1.6	3.54	2.90	30.33	0.22	0.25	0.003	0.001	6.11	-75
	15	3.86	1.21	0.9	1.03	1.81	30.61	0.16	0.14	0.001	0.001	6.13	-83
	17	3.49	1.44	0.0	1.37	2.19	31.53	0.11	0.11	0.002	0.001	6.11	-86
	19	10.21	3.67	2.1	3.00	2.32	31.76	0.16	0.28	0.003	0.001	6.07	-85
	21	7.87	3.08	0.2	1.61	0.96	31.17	0.19	0.35	0.005	0.002	6.15	-84
	23	3.30	1.92	1.4	1.23	1.48	32.03	0.19	0.11	0.001	0.001	6.16	-86
	25	10.91	3.22	2.3	2.84	2.01	31.83	0.24	0.21	0.006	0.001	6.14	-89
	27	8.94	3.16	0.8	1.47	1.05	32.27	0.27	0.26	0.006	0.001	6.18	-83
	29	5.08	2.26	0.1	1.38	1.34	32.67	0.39	0.16	0.006	0.001	6.20	-81
	31	5.27	1.56	1.0	1.18	1.82	32.83	0.15	0.13	0.003	0.001	6.22	-81
	33	12.25	4.34	2.5	2.44	1.68	33.14	0.28	0.31	0.004	0.001	6.16	-82
	35	8.36	2.24	1.0	1.28	1.43	31.37	0.23	0.17	0.004	0.001	6.15	-91
	37	14.38	3.76	1.7	2.28	1.66	33.52	0.36	0.31	0.009	0.002	6.16	-91
	39	7.09	2.78	2.6	1.00	0.73	32.57	0.13	0.27	0.011	0.006	6.16	-96
Ru118													
	0	0.19	0.51	24.0	4.88	3.16	3.18	0.10	0.03	0.001	0.001	5.92	-10
	1	7.88	1.91	13.0	10.30	7.98	12.51	0.13	0.21	0.001	0.002	6.00	-65
	3	8.73	2.08	6.9	5.00	4.21	14.86	0.12	0.22	0.002	0.001	6.04	-86

	5	5.54	1.93	2.9	3.43	2.98	16.70	0.10	0.15	0.009	0.001	5.98	-80
		Fe^{2+}	**Mn^{2+}**	**S**	**TDP**	**SRP**	**NH_4^+**	**NO_3^-**	**As**	**Cd**	**Pb**	**pH**	**Eh**
	7	0.11	1.04	6.3	2.91	2.09	5.82	0.29	0.63	0.003	0.002	5.93	-109
	9	3.50	1.27	3.9	1.11	0.72	17.36	0.13	0.30	0.001	0.002	5.82	-87
	11	7.42	2.19	1.6	3.02	2.01	20.84	0.15	0.27	0.001	0.001	5.79	-108
	13	8.77	2.32	2.7	2.62	2.34	21.63	0.14	0.25	0.009	0.001	5.91	-104
	15	1.49	1.32	1.9	0.62	0.49	20.68	0.13	0.22	0.001	0.002	5.94	-82
	17	6.73	2.30	1.5	2.45	1.70	22.47	0.12	0.18	0.005	0.003	5.90	-79
	19	4.05	1.00	1.4	0.92	1.92	22.59	0.15	0.09	0.002	0.000	5.90	-89
	21	9.12	2.12	2.1	1.81	1.97	23.25	0.16	0.20	0.002	0.003	5.91	-108
	23	7.66	2.32	2.3	1.73	1.51	23.01	0.15	0.19	0.004	0.002	5.96	-113
	25	12.31	3.11	2.2	2.49	1.85	23.87	0.16	0.26	0.001	0.003	5.80	-109
	27	7.63	2.32	1.0	1.54	1.68	23.64	0.24	0.18	0.001	0.002	5.88	-103
	29	6.44	1.74	2.3	1.13	1.35	22.93	0.17	0.19	0.001	0.002	5.76	-94
	31	10.61	2.98	1.7	1.94	1.42	22.33	0.15	0.41	0.007	0.004	5.90	-85
	33	9.98	2.89	3.3	1.54	1.11	22.82	0.14	0.36	0.002	0.003	6.00	-101
	35	13.72	3.31		2.09	1.25	21.33	0.12	0.42	0.002	0.004	6.06	-108
Ru119													
	2	0.94	0.97	13.7	1.82	1.35	12.85	0.23	0.11	0.001	0.002	5.87	-114
	5	2.68	1.07	6.5	1.78	1.59	15.00	0.29	0.16	0.002	0.001	5.88	-98
	7	2.95	1.12	5.4	1.42	1.21	15.26	0.18	0.16	0.001	0.002	5.85	-95
	9	2.55	1.28	4.3	1.08	0.74	15.92	0.11	0.25	0.001	0.002	5.65	-88
	11	0.78	0.49	2.8	0.46	1.05	16.96	0.29	0.07	0.001	0.001	5.85	-85
	13	3.41	1.42	2.6	1.18	0.92	17.34	0.15	0.21	0.003	0.006	5.78	-87
	15	2.37	1.19	3.8	1.04	1.01	18.20	0.24	0.21	0.002	0.002	5.67	-78
	17	4.83	1.38	2.9	1.42	1.28	17.44	0.13	0.16	0.001	0.005	5.87	-54
	19	4.41	1.62	2.9	1.15	0.79	17.57	0.09	0.26	0.001	0.004	5.92	-86
	21	3.09	1.27	2.0	0.96	0.67	16.74	0.14	0.25	0.002	0.004	5.65	-85
	23	3.76	1.42	2.9	0.91	0.65	17.75	0.37	0.20	0.002	0.011	5.95	-96
	25	3.25	1.45	3.3	0.99	0.73	17.89	0.08	0.24	0.008	0.005	5.98	-70

27	6.63	1.77	3.7	1.66	1.18	18.29	0.10	0.35	0.002	0.003	5.83	-80
29	4.57	1.68	3.2	0.87	0.59	18.56	0.13	0.34	0.006	0.006	5.98	-93
	Fe^{2+}	**Mn^{2+}**	**S**	**TDP**	**SRP**	**NH_4^+**	**NO_3^-**	**As**	**Cd**	**Pb**	**pH**	**Eh**
31	0.11	1.04	6.3	2.91	2.09	5.82	0.29	0.63	0.003	0.002	5.93	-109
33	5.46	1.69	4.5	1.04	0.75	18.77	0.18	0.29	0.003	0.003	5.97	-95
35	8.79	2.13	2.9	1.42	1.02	19.79	0.00	0.31	0.001	0.004	6.00	-105
37	5.28	1.91	3.9	1.20	0.86	20.44	0.00	0.25	0.001	0.003	5.88	-87
39	7.16	1.95	4.1	1.46	1.05	19.59	0.00	0.24	0.001	0.004	5.99	-64
41	5.80	1.88	4.0	1.13	0.86	19.75	0.00	0.33	0.003	0.002	6.00	-76
43	4.95	1.39	4.2	0.75	0.63	17.92	0.00	0.38	0.002	0.008	6.06	-95
Ru120												
0	0.02	0.06	31.0	0.03	0.01	0.14	0.00	0.01	0.001	0.001	6.24	161
1	0.61	0.62	12.6	0.91	0.65	3.73	0.08	0.04	0.003	0.001	5.61	27
3	0.50	0.60	6.4	0.48	0.33	6.07	0.13	0.05	0.001	0.001	5.78	-25
5	0.35	0.76	6.2	0.59	0.42	6.85	0.05	0.07	0.002	0.002	5.92	-97
7	0.33	0.92	5.5	0.58	0.36	6.57	0.00	0.09	0.003	0.002	5.99	-101
9	0.47	0.89	5.6	0.51	0.36	6.73	0.04	0.10	0.002	0.003	5.96	-97
11	0.53	1.13	6.4	0.31	0.24	6.64	0.07	0.36	0.005	0.005	6.08	-115
13	1.01	1.37	5.5	0.34	0.25	6.48	0.00	0.33	0.001	0.005	6.22	-106
15	1.44	1.32	5.4	0.44	0.28	5.76	0.05	0.29	0.001	0.003	6.14	-124
17	8.73	2.34	5.3	1.03	0.81	6.38	0.00	0.48	0.004	0.005	6.25	-117
19	8.13	2.31	6.3	0.76	0.65	6.24	0.00	0.69	0.005	0.005	6.39	-124
21	5.56	2.05	5.4	0.61	0.52	5.46	0.00	0.65	0.004	0.003	6.29	-117
23	5.87	2.14	7.0	0.58	0.49	5.53	0.00	0.79	0.006	0.004	6.43	-115
25	7.56	2.32		0.63	0.54	5.73	0.00	0.82	0.004	0.004	6.57	-118
Ru121												
1	0.58	0.48	20.1	0.28	0.26	5.64	0.14	0.04	0.003	0.001	6.15	-24
3	1.26	0.82	10.6	0.77	0.56	7.98	0.12	0.06	0.006	0.001	6.25	-81
5	2.42	0.70	7.4	0.79	0.83	9.57	0.00	0.04	0.002	0.001	6.28	-93
7	0.97	1.04	4.6	0.75	0.55	10.52	0.09	0.08	0.005	0.001	6.25	-94

	9	2.32	1.08	5.8	0.93	0.68	10.56	0.09	0.08	0.003	0.002	6.18	-86
	11	2.61	1.19	5.6	0.78	0.57	11.72	0.07	0.12	0.001	0.002	6.27	-99
		Fe^{2+}	**Mn^{2+}**	**S**	**TDP**	**SRP**	**NH_4^+**	**NO_3^-**	**As**	**Cd**	**Pb**	**pH**	**Eh**
	13	0.11	1.04	6.3	2.91	2.09	5.82	0.29	0.63	0.003	0.002	5.93	-109
	15	4.01	1.46	5.7	1.00	0.68	11.42	0.13	0.14	0.001	0.002	6.32	-92
	17	3.17	1.44	6.5	0.75	0.53	11.89	0.00	0.15	0.003	0.003	6.29	-78
	19	5.72	1.84	5.1	1.24	0.92	12.67	0.00	0.20	0.004	0.002	6.29	-93
	21	6.51	2.04	4.7	1.32	0.95	12.73	0.13	0.24	0.002	0.003	6.32	-107
	23	4.80	1.81	4.7	0.85	0.57	12.27	0.14	0.18	0.004	0.003	6.35	-95
	25	4.11	1.51	5.5	0.55	0.54	12.56	0.11	0.15	0.002	0.004	6.37	-104
	27	4.30	1.19	5.2	0.76	1.11	12.94	0.13	0.10	0.001	0.002	6.35	-93
	29	6.41	2.14	5.0	0.91	0.53	11.94	0.10	0.24	0.007	0.003	6.39	-103
	31	5.74	2.08	6.2	1.05	0.79	13.03	0.16	0.18	0.002	0.003	6.31	-98
	33	7.14	2.41	6.0	1.38	1.00	13.20	0.14	0.21	0.001	0.004	6.23	-110
	35	7.71	2.49	5.7	1.48	1.08	13.43	0.11	0.25	0.004	0.004	6.25	-102
	37	7.45	2.47	5.9	1.24	0.88	13.42	0.09	0.24	0.004	0.003	6.32	-99
	39	9.39	2.72	7.4	1.28	0.96	13.71	0.00	0.24	0.003	0.004	6.35	-114
	41	7.42	2.30	7.2	0.88	0.65	13.18	0.00	0.28	0.002	0.003	6.40	-95
Ru122													
	0	0.22	0.23	8.6	0.73	0.23	2.52	0.00	0.01	0.006	0.002	6.14	-3
	1	2.36	1.26	4.0	0.62	0.57	5.73	0.35	0.03	0.002	0.000	6.28	-80
	3	1.26	0.81	2.6	0.67	0.45	7.47	0.10	0.05	0.001	0.001	6.05	-70
	5	3.03	1.05	2.6	0.82	0.55	8.84	0.11	0.06	0.001	0.002	6.25	-83
	7	1.01	1.01	2.6	0.67	0.46	10.03	0.10	0.10	0.002	0.002	6.22	-74
	9	0.84	0.64	2.0	0.50	0.65	10.67	0.00	0.05	0.001	0.001	6.09	-73
	11	3.96	1.21	1.8	1.18	1.04	11.39	0.09	0.11	0.001	0.002	6.19	-82
	13	3.88	1.34	2.4	1.05	0.84	12.10	0.07	0.16	0.002	0.002	6.26	-84
	15	3.32	1.46	2.2	1.05	0.73	12.63	0.08	0.16	0.002	0.004	6.24	-97
	17	2.88	1.38	2.5	0.73	0.52	12.87	0.07	0.20	0.002	0.002	6.24	-94
	19	5.09	1.77	2.4	1.34	0.87	13.44	0.00	0.22	0.002	0.002	6.33	-101

	21	5.75	1.85	2.3	1.43	1.02	14.41	0.00	0.21	0.004	0.003	6.35	-97
	23	7.95	2.06	2.5	1.57	1.05	14.71	0.17	0.21	0.002	0.005	6.26	-94
	25	4.94	1.73	2.7	1.07	0.74	14.60	0.10	0.19	0.004	0.004	6.37	-108
		Fe^{2+}	**Mn^{2+}**	**S**	**TDP**	**SRP**	**NH_4^+**	**NO_3^-**	**As**	**Cd**	**Pb**	**pH**	**Eh**
	27	0.11	1.04	6.3	2.91	2.09	5.82	0.29	0.63	0.003	0.002	5.93	-109
	29	5.09	1.90	2.4	0.87	0.56	15.19	0.00	0.23	0.002	0.003	6.40	-101
	31	7.81	2.10	3.1	1.45	1.02	15.79	0.10	0.24	0.004	0.003	6.37	-109
	33	10.91	2.49		2.22	1.58	16.24	0.00	0.29	0.003	0.004	6.49	-113
Ru123													
	0	0.26	0.62	35.9	0.68	0.24	2.93	0.07	0.02	0.003	0.001	6.25	-25
	1	4.88	0.98	10.7	2.67	5.05	8.36	0.05	0.03	0.000	0.000	6.34	-89
	3	8.22	1.74	7.2	1.75	1.24	11.11	0.00	0.14	0.001	0.003	6.35	-122
	5	4.34	1.42	6.2	1.52	1.44	14.07	0.00	0.10	0.001	0.001	6.39	-115
	7	4.94	2.05	6.2	2.03	1.42	15.89	0.00	0.16	0.005	0.001	6.43	-111
	9	5.39	2.16	5.3	2.43	1.71	17.03	0.11	0.15	0.002	0.001	6.38	-101
	11	5.75	1.97	5.3	1.99	1.65	18.76	0.08	0.21	0.002	0.001	6.40	-108
	13	6.41	2.28	5.0	2.27	1.66	19.78	0.08	0.22	0.001	0.002	6.34	-110
	15	3.23	1.02	5.3	0.93	1.58	20.04	0.00	0.13	0.000	0.001	6.40	-113
	17	6.68	2.14	4.3	1.69	1.19	20.18	0.11	0.24	0.001	0.002	6.39	-98
	19	6.72	2.18	6.3	1.33	0.88	20.48	0.11	0.20	0.002	0.002	6.42	-106
	21	9.12	2.67	4.4	1.97	1.57	20.89	0.00	0.29	0.004	0.002	6.50	-87
	23	12.26	2.97	6.0	2.90	2.30	21.43	0.00	0.34	0.008	0.002	6.43	-82
	25	12.44	2.95	5.9	2.66	2.10	21.34	0.06	0.32	0.004	0.002	6.42	-91
	27	13.77	3.14	6.7	2.79	2.38	20.80	0.00	0.24	0.002	0.003	6.43	-104
	29	17.63	3.39	5.9	2.73	2.60	21.27	0.08	0.33	0.005	0.008	6.41	-106
	31	8.05	2.22	6.5	1.46	1.06	19.36	0.00	0.24	0.002	0.004	6.38	-89
	33	3.26	1.27		0.50	0.45	16.91	0.08	0.26	0.009	0.005	6.48	-79
Ru124													
	0	0.86	0.43	16.6	0.11	0.22	1.86	0.00	0.02	0.001	0.001	6.32	1
	1	0.67	0.83	16.4	0.12	0.16	2.85	0.00	0.03	0.002	0.001	6.15	8

	3	2.84	1.05	13.3	0.28	0.30	6.16	0.00	0.07	0.007	0.001	6.33	-17
	5	5.83	1.18	3.7	1.35	1.99	12.02	0.00	0.07	0.001	0.000	6.37	-72
	7	7.20	2.12	2.6	2.81	2.84	17.70	0.00	0.10	0.006	0.001	6.42	-85
		Fe^{2+}	**Mn^{2+}**	**S**	**TDP**	**SRP**	**NH_4^+**	**NO_3^-**	**As**	**Cd**	**Pb**	**pH**	**Eh**
	9	0.11	1.04	6.3	2.91	2.09	5.82	0.29	0.63	0.003	0.002	5.93	-109
	11	6.40	2.06	1.3	2.79	3.13	22.24	0.00	0.12	0.002	0.001	6.30	-105
	13	11.17	3.16	2.4	3.06	3.02	23.29	0.00	0.27	0.005	0.002	6.46	-102
	15	7.92	2.41	0.3	2.14	2.13	24.08	0.00	0.22	0.001	0.002	6.42	-87
	17	8.91	2.90	1.2	2.83	2.64	24.25	0.22	0.23	0.002	0.003	6.48	-83
	19	12.22	3.31	1.6	2.80	2.40	24.42	0.00	0.33	0.003	0.002	6.48	-82
	21	10.82	3.35	3.2	2.96	2.38	25.43	0.00	0.28	0.001	0.001	6.50	-69
	23	15.40	3.71	3.4	3.26	2.92	24.84	0.12	0.30	0.002	0.002	6.40	-86
	25	17.78	4.12	5.3	3.98	3.71	26.03	0.00	0.32	0.007	0.002	6.38	-86
	27	20.65	4.43	3.7	3.66	3.37	26.08	0.11	0.45	0.003	0.003	6.40	-96
	29	7.57	2.64	4.2	1.56	1.20	20.92	0.00	0.27	0.009	0.003	6.42	-100
	31	22.38	4.39	3.7	3.80	3.45	25.79	0.00	0.38	0.006	0.006	6.36	-88
	33	14.67	3.62		2.39	1.80	25.70	0.00	0.39	0.006	0.005	6.39	-95
Ru125													
	0	0.03	0.13	20.2	0.03	0.19	0.85	0.15	0.00	0.002	0.000	6.35	-38
	1	8.23	2.27	10.5	1.57	1.12	6.36	0.00	0.10	0.003	0.001	6.30	-64
	3	9.47	2.04	7.4	2.24	1.67	9.19	0.00	0.09	0.004	0.001	6.45	-93
	5	6.09	2.05	6.7	1.91	1.52	10.88	0.00	0.07	0.002	0.001	6.22	-108
	7	4.88	1.89	6.4	1.61	1.30	11.25	0.00	0.13	0.001	0.002	6.31	-108
	9	5.67	2.14	5.9	1.75	1.32	10.92	0.00	0.16	0.002	0.001	6.27	-102
	11	2.82	1.28	4.7	0.93	1.25	11.03	0.08	0.09	0.001	0.001	6.25	-100
	13	6.86	2.06	6.0	1.74	0.89	8.42	0.00	0.21	0.008	0.004	6.07	-43
	15	10.09	2.70	6.3	2.10	1.61	10.28	0.10	0.27	0.002	0.003	6.19	-67
	17	6.49	2.07	6.8	1.30	0.99	9.08	0.00	0.15	0.005	0.002	6.21	-30
	19	7.79	2.30	5.4	1.40	1.16	9.67	0.00	0.22	0.002	0.029	6.08	-49
	21	11.14	2.84	4.8	2.35	1.75	9.32	0.00	0.20	0.003	0.003	6.21	-77

	23	7.64	2.23	6.1	1.17	1.01	8.87	0.10	0.28	0.005	0.003	6.03	-74
	25	10.55	2.67	7.0	1.51	1.25	8.89	0.17	0.35	0.005	0.003	6.03	-72
	27	14.29	3.25	6.2	1.74	1.44	9.44	0.39	0.40	0.005	0.003	6.29	-92
	29	11.29	2.90		1.52	1.32	9.15	0.00	0.39	0.004	0.003	6.15	-91
		Fe^{2+}	**Mn^{2+}**	**S**	**TDP**	**SRP**	**NH_4^+**	**NO_3^-**	**As**	**Cd**	**Pb**	**pH**	**Eh**
	31	0.11	1.04	6.3	2.91	2.09	5.82	0.29	0.63	0.003	0.002	5.93	-109
	33	15.78	3.54		1.93	1.54	9.34	0.13	0.56	0.015	0.005	6.19	-105
	35	15.68	3.42		2.01	1.84	8.95	0.00	0.55	0.011	0.005	6.30	-126
Ru126													
	1	5.40	1.42	9.4	1.41	1.74	16.10	0.00	0.09	0.003	0.001	6.10	-104
	3	1.14	0.61	4.3	0.59	1.73	18.32	0.00	0.03	0.000	0.000	6.08	-111
	5	6.40	2.22	3.3	2.42	2.36	20.80	0.00	0.10	0.001	0.001	6.07	-98
	7	7.23	2.42	3.1	2.47	2.06	21.95	0.17	0.12	0.002	0.002	6.12	-107
	9	6.79	2.38	2.2	2.77	2.51	23.29	0.00	0.14	0.003	0.001	5.96	-99
	11	8.57	2.78	2.6	2.88	2.32	23.37	0.12	0.19	0.003	0.001	6.04	-79
	13	7.74	2.81	1.7	3.03	2.35	25.21	0.00	0.16	0.002	0.001	6.00	-96
	15	4.27	1.28	0.5	1.54	2.57	25.79	0.10	0.09	0.001	0.001	5.83	-80
	17	5.58	1.86	0.8	2.07	2.43	25.98	0.00	0.14	0.002	0.001	6.00	-57
	19	7.02	2.23	1.9	2.38	2.36	26.89	0.00	0.15	0.003	0.001	6.08	-83
	21	8.65	2.98	0.5	3.06	2.00	25.69	0.00	0.18	0.004	0.002	5.97	-86
	23	11.70	3.18	0.8	3.22	2.61	27.53	0.00	0.25	0.004	0.001	5.90	-93
	25	9.78	2.77	2.1	2.61	2.27	28.22	0.09	0.27	0.008	0.003	6.20	-83
	27	8.39	2.06	2.4	2.23	2.20	25.04	0.00	0.15	0.001	0.001	6.09	-69
	29	14.68	3.73	2.2	3.19	3.01	28.66	0.00	0.25	0.002	0.001	6.09	-78
	31	17.08	3.80	2.1	3.18	2.55	26.95	0.00	0.27	0.004	0.002	6.07	-81
	33	17.43	3.64	3.4	3.08	2.37	28.77	0.00	0.28	0.002	0.006	6.17	-99
	35	11.78	3.09	0.7	2.95	2.16	28.06	0.00	0.19	0.004	0.004	6.10	-83
	37	12.68	2.53	4.0	2.96	2.91	28.74	0.00	0.19	0.001	0.003	6.15	-82
	39	26.15	4.42	1.1	4.78	4.39	29.72	0.00	0.32	0.008	0.005	6.21	-93
	41	20.45	3.95	1.7	2.73	2.11	29.36	0.00	0.50	0.002	0.003	6.22	-94

43	22.48	4.01	2.1	3.37	2.68	27.47	0.00	0.45	0.008	0.003	6.26	-76
Ru127												
0	0.06	0.16	32.3	0.00	0.13	0.23	0.00	0.01	0.003	0.006	6.11	-30
1	7.97	2.15	9.5	3.73	2.32	9.04	0.00	0.06	0.004	0.001	6.20	-127
	Fe^{2+}	**Mn^{2+}**	**S**	**TDP**	**SRP**	**NH_4^+**	**NO_3^-**	**As**	**Cd**	**Pb**	**pH**	**Eh**
3	0.11	1.04	6.3	2.91	2.09	5.82	0.29	0.63	0.003	0.002	5.93	-109
5	7.77	2.39	5.9	3.39	2.04	15.85	0.00	0.07	0.004	0.001	6.06	-105
7	7.99	2.69	6.1	3.31	1.98	17.77	0.00	0.12	0.006	0.001	6.13	-120
9	6.09	2.08	5.2	2.00	1.60	18.74	0.06	0.13	0.003	0.002	6.17	-114
11	5.98	2.51	5.1	1.89	1.21	19.36	0.00	0.17	0.005	0.002	6.11	-99
13	6.37	2.56	6.9	2.14	1.34	19.55	0.04	0.21	0.002	0.002	6.06	-101
15	9.35	3.04	4.1	2.47	1.52	20.41	0.08	0.23	0.010	0.003	6.20	-80
17	10.31	2.86	6.4	2.82	1.78	20.17	0.00	0.24	0.005	0.002	6.09	-79
19	3.50	0.92	6.3	0.87	1.74	20.32	0.00	0.08	0.001	0.001	6.12	-74
21	14.87	2.90	5.2	3.29	1.90	19.12	0.05	0.22	0.001	0.005	6.14	-77
23	9.03	2.95		1.54	0.93	20.26	0.00	0.23	0.007	0.003	6.02	-78
25	6.65	2.28		1.13	0.72	20.32	0.00	0.20	0.003	0.003	5.98	-99
27	11.17	2.55		1.85	0.91	18.10	0.06	0.33	0.012	0.004	5.96	-94
Sample ID (cm)	**Fe^{2+}**	**Mn^{2+}**	**S**	**P**	**SRP**	**NH_4^+**	**NO_3^-**	**As**	**Cd**	**Pb**	**pH**	**Eh**
Ru129												
1	4.55	1.03	8.9	1.03	0.96	3.96	0.06	0.03	0.004	0.003	5.98	-75
3	7.95	1.40	5.6	1.82	2.05	10.00	0.14	0.02	0.007	0.007	6.02	-105
5	5.69	1.39	0.0	0.88	0.98	12.28	0.00	0.09	0.006	0.005	5.92	
7	8.43	1.94	5.7	1.91	2.12	22.01	0.08	0.04	0.007	0.006	5.90	-109
9	4.90	1.75	4.0	1.03	1.14	29.20	0.06	0.07	0.009	0.012	5.99	-86
11	9.10	2.17	1.3	2.04	2.14	33.18	0.04	0.05	0.013	0.007	5.95	-73
13	10.29	2.43	1.1	2.74	2.68	40.57	0.14	0.09	0.009	0.003	5.98	-73
15	16.97	3.54	13.1	3.43	3.77	46.57	0.14	0.10	0.010	0.005	6.00	-79
17	7.71	2.34	2.9	1.98	1.58	40.32	0.11	0.10	0.011	0.007	5.78	-49

19	14.17	3.26	0.0	2.97	2.87	48.61	0.16	0.14	0.011	0.007	5.99	-23
Ru130												
1	0.71	1.11	14.1	0.05	0.21	3.58	0.04	0.02	0.006	0.002		
3	16.06	2.88	2.5	3.23	3.57	19.11	0.22	0.02	0.007	0.003		
5	10.43	2.04	1.9	2.41	2.80	23.12	0.02	0.00	0.003	0.004		
	Fe^{2+}	**Mn^{2+}**	**S**	**TDP**	**SRP**	**NH_4^+**	**NO_3^-**	**As**	**Cd**	**Pb**	**pH**	**Eh**
7	0.11	1.04	6.3	2.91	2.09	5.82	0.29	0.63	0.003	0.002	5.93	-109
9	14.11	3.71	2.8	3.27	4.13	40.05	0.22	0.01	0.003	0.004		
11	18.32	5.37	1.4	4.65	5.19	47.20	0.25	0.01	0.004	0.002		
13	9.21	3.25	0.2	2.12	1.63	32.24	0.12	0.04	0.005	0.002		
15	17.57	6.14	0.7	4.36	4.94	59.24	0.23	0.03	0.003	0.005		
17	18.06	6.22	0.4	5.87	5.28	60.64	0.27	0.06	0.007	0.007		
19	17.96	7.07	1.0	4.92	3.78	66.20	0.23	0.06	0.006	0.000		
Ru131												
1	5.13	1.84	0.0	0.95	0.87	13.39	0.10	0.15	0.027	0.017	6.02	
3	6.00	1.66	0.0	1.30	1.16	7.73	0.13	0.08	0.011	0.002	6.08	-39
5	4.21	1.29	0.9	1.49	1.05	7.44	0.09	0.06	0.008	0.008	6.05	-39
7	5.67	1.94	0.0	2.11	1.49	10.42	0.03	0.09	0.013	0.006	6.05	-52
9	6.52	2.23	0.0	2.28	1.87	13.57	0.12	0.13	0.013	0.007	6.06	-54
11	5.03	1.78	0.3	1.69	1.72	15.31	0.19	0.13	0.011	0.003	5.99	-36
13	9.45	2.91	8.2	3.29	2.26	16.65	0.04	0.27	0.006	0.003	6.11	-60
15	3.92	2.24	2.0	1.53	1.25	17.86	0.11	0.17	0.005	0.004	6.00	-55
17	7.29	2.74	3.2	2.64	1.72	17.12	0.06	0.19	0.023	0.015	6.01	-56
19	5.09	1.76	0.0	1.92	1.55	15.16	0.00	0.15	0.006	0.002	6.06	-61
Ru132												
1	2.51	1.17		0.36				0.08	0.009	0.004		
3	1.40	0.81		0.40				0.05	0.002	0.002		
5	2.65	1.41		0.73				0.08	0.008	0.007		
7	1.50	1.31		0.43				0.13	0.011	0.004		
9	2.77	1.91		0.77				0.21	0.013	0.008		

11	3.35	2.31		1.29				0.15	0.018	0.015		
13	3.87	2.40		0.92				0.15	0.021	0.012		
15	6.81	2.83		1.44				0.20	0.018	0.007		
17	8.64	3.20		1.63				0.27	0.016	0.009		
19	9.20	3.55		1.50				0.27	0.026	0.008		
Ru133	**Fe^{2+}**	**Mn^{2+}**	**S**	**P**	**SRP**	**NH_4^+**	**NO_3^-**	**As**	**Cd**	**Pb**	**pH**	**Eh**
1	9.44	2.17		0.64				0.25	0.015	0.009	6.80	
3	3.48	1.28		0.76				0.06	0.015	0.002	6.14	0
5	2.55	1.25		0.71				0.09	0.006	0.003	6.16	-39
7	3.78	1.66		1.21				0.11	0.008	0.003	6.12	-41
9	5.20	1.92		1.75				0.13	0.018	0.006	6.11	-29
11	4.37	1.80		1.37				0.13	0.024	0.009	6.04	-38
13	3.80	1.82		1.33				0.15	0.065	0.015	6.05	-37
15	6.04	2.38		2.37				0.25	0.007	0.003	6.07	-36
17	5.94	2.52		1.60				0.27	0.008	0.005	6.11	-47
19	5.15	2.27		1.23				0.26	0.024	0.010	6.08	-45
Ru134												
1	0.25	0.60		0.04				0.04	0.015	0.003		
3	1.32	0.73		0.35				0.10	0.019	0.013		
5	4.71	1.49		1.90				0.09	0.007	0.003		
7	2.69	0.89		0.92				0.08	0.013	0.007		
9	6.29	1.90		2.44				0.12	0.012	0.004		
11	4.61	1.70		1.61				0.12	0.006	0.004		
13	5.37	1.87		1.64				0.16	0.008	0.004		
15	7.41	2.26		2.29				0.18	0.005	0.008		
17	6.66	2.02		1.77				0.15	0.023	0.011		
19	7.29	2.30		1.93				0.13	0.013	0.010		
Ru135												
1	3.22	1.22		0.19				0.14	0.002	0.004	6.15	56
3	1.13	0.59		0.32				0.04	0.023	0.009	6.21	-31

	5	0.79	0.50		0.27				0.05	0.005	0.002	6.14	-24
	7	1.01	0.59		0.82				0.04	0.005	0.004	6.08	-25
	9	1.25	0.71		0.89				0.05	0.015	0.006	6.05	-20
	11	1.24	0.83		0.86				0.07	0.008	0.005	6.06	-23
	13	1.08	0.81		0.57				0.08	0.015	0.009	6.05	-16
		Fe^{2+}	**Mn^{2+}**	**S**	**P**	**SRP**	**NH_4^+**	**NO_3^-**	**As**	**Cd**	**Pb**	**pH**	**Eh**
	15	2.39	1.12		1.03				0.11	0.034	0.012	6.05	-12
	17	1.73	1.10		0.70				0.15	0.018	0.015	6.06	-21
	19	2.81	1.45		0.97				0.13	0.025	0.011	6.03	-22
Ru136													
	1	2.11	0.86		0.18				0.09	0.006	0.002		
	3	1.86	0.61		0.53				0.05	0.011	0.003		
	5	4.00	1.26		2.19				0.07	0.029	0.011		
	7	1.73	0.89		1.03				0.04	0.008	0.001		
	9	2.57	1.45		1.74				0.07	0.004	0.002		
	11	1.69	0.79		1.04				0.03	0.006	0.002		
	13	4.00	1.93		2.15				0.14	0.007	0.011		
	15	2.67	1.56		1.25				0.14	0.016	0.008		
	17	3.15	1.80		1.56				0.17	0.008	0.003		
	19	4.45	2.23		1.96				0.20	0.003	0.003		
Ru137													
	1	1.39	0.70		0.10				0.06	0.011	0.004	5.96	46
	3	2.59	0.95		0.97				0.11	0.028	0.011	6.04	14
	5	3.67	1.21		1.31				0.12	0.016	0.009	6.12	-20
	7	1.71	0.74		1.01				0.06	0.012	0.005	6.09	-12
	9	1.95	1.09		1.17				0.10	0.008	0.007	6.04	-9
	11	3.18	1.63		2.36				0.12	0.004	0.004	5.97	-7
	13	2.10	1.25		0.99				0.15	0.024	0.007	6.03	3
	15	1.37	1.00		1.12				0.13	0.006	0.007	6.04	-35
	17	2.94	1.19		1.88				0.13	0.017	0.008	6.05	1

19	3.05	1.59		1.64				0.19	0.029	0.015	6.06	-13
Ru138												
1	0.23	0.47		0.04				0.02	0.004	0.002		
3	0.28	0.72		0.04				0.02	0.005	0.002		
5	1.03	0.98		0.11				0.11	0.009	0.011		
	Fe^{2+}	**Mn^{2+}**	**S**	**P**	**SRP**	**NH_4^+**	**NO_3^-**	**As**	**Cd**	**Pb**	**pH**	**Eh**
7	5.65	2.52		0.87				0.46	0.010	0.009		
9	17.61	4.18		4.59				0.34	0.017	0.017		
11	20.70	4.46		5.18				0.32	0.007	0.014		
Ru139												
1	1.70	0.93		0.09				0.06	0.007	0.002	5.84	-24
3	0.97	0.60		0.27				0.03	0.009	0.003	5.86	-129
5	0.72	0.70		0.52				0.04	0.005	0.003	5.96	-143
7	1.01	0.92		0.47				0.08	0.008	0.002	5.99	-148
9	1.26	1.13		0.71				0.10	0.008	0.004	5.96	-136
11	2.05	1.31		0.78				0.12	0.008	0.004	6.00	-128
13	1.81	1.29		0.58				0.22	0.008	0.004	6.12	-121
15	2.24	1.34		0.54				0.18	0.010	0.004	5.99	-134
17	2.73	1.54		0.61				0.16	0.028	0.008	6.01	-116
19	1.90	1.37		0.60				0.13	0.012	0.006	5.99	-109
Ru140												
1	4.48	1.49	7.1	0.32	0.44	2.80	0.11	0.03	0.005	0.002	5.96	-165
3	0.97	0.56	0.0	0.11	0.23	3.07	0.03	0.04	0.014	0.002	6.01	-159
5	0.90	0.85	5.3	0.20	0.37	4.49	0.01	0.09	0.010	0.004	6.07	-155
7	2.26	1.38	1.7	0.62	0.53	4.99	0.07	0.13	0.005	0.004	6.04	-145
9	1.85	1.40	8.7	0.59	0.62	5.72	0.09	0.14	0.009	0.004	6.07	-156
11	1.72	1.40	4.8	0.40	0.51	6.16	0.02	0.16	0.014	0.005	6.10	-137
13	2.46	1.70	12.0	0.45	0.47	6.13	0.06	0.17	0.012	0.006	6.03	-128
15	2.00	1.75	13.3	0.49	0.48	6.01	0.06	0.15	0.005	0.006	5.99	-111
17	2.25	1.78	4.3	0.63	0.57	6.03	0.09	0.15	0.012	0.006	6.04	-128

19	2.37	1.75	4.5	0.60	0.59	6.56	0.05	0.16	0.013	0.006	6.06	-124
Ru141												
1	1.80	1.15	2.8	1.08	0.97	6.67	0.08	0.02	0.004	0.002	5.85	-131
3	3.46	1.50	0.9	2.04	1.57	6.59	0.06	0.01	0.008	0.002	6.01	-166
5	0.75	0.55	0.6	0.35	0.66	5.94	0.02	0.02	0.004	0.001	6.05	-155
	Fe^{2+}	**Mn^{2+}**	**S**	**P**	**SRP**	**NH_4^+**	**NO_3^-**	**As**	**Cd**	**Pb**	**pH**	**Eh**
7	1.55	1.06	0.6	0.88	0.86	7.02	0.03	0.06	0.005	0.003	6.01	-131
9	1.25	0.91	1.0	0.70	0.66	6.30	0.02	0.07	0.004	0.002	6.07	-114
11	1.98	1.38	1.3	0.99	0.86	8.87	0.04	0.13	0.005	0.003	6.05	-103
13	1.36	0.86	0.6	0.62	0.65	8.70	0.03	0.10	0.005	0.002	6.07	-75
15	4.50	1.87	1.0	2.19	1.55	11.52	0.09	0.17	0.007	0.003	6.01	-130
17	1.32	0.79	0.9	0.58	0.96	12.14	0.05	0.08	0.002	0.001	6.27	-137
19	4.35	1.81	1.3	1.38	0.98	12.60	0.07	0.26	0.008	0.003	6.06	-134
Ru142												
1	5.79	1.74	13.3	1.72	1.69	9.35	0.13	0.02	0.006	0.002	6.00	-146
3	3.59	1.56	3.2	1.56	0.99	7.23	0.07	0.05	0.006	0.002	6.13	-147
5	3.89	1.53	1.3	1.86	1.34	8.94	0.10	0.06	0.004	0.003	6.06	-138
7	3.95	1.85	2.3	1.86	1.20	11.32	0.09	0.10	0.005	0.002	6.04	-125
9	5.32	2.08	4.3	2.69	1.64	11.85	0.06	0.12	0.006	0.002	6.11	-124
11	2.67	1.83	9.6	1.82	1.18	14.09	0.08	0.12	0.008	0.003	6.04	-114
13	3.88	1.89	4.0	1.27	0.79	14.78	0.03	0.20	0.007	0.002	6.02	-110
15	4.60	1.89	5.1	1.93	1.63	16.02	0.04	0.11	0.005	0.002	6.04	-115
17	5.11	2.34	2.4	1.92	1.25	16.85	0.09	0.18	0.006	0.003	6.04	-111
19	5.88	2.23	3.6	2.22	1.26	14.01	0.08	0.20	0.014	0.003	6.06	-114
Ru143												
1	1.05	1.00	20.5	0.08	0.00	4.00	0.07	0.04	0.007	0.002	6.19	-73
3	3.82	1.49	2.9	0.77	0.41	7.61	0.13	0.06	0.007	0.001	6.20	-116
5	6.00	1.80	3.1	1.30	1.12	11.03	0.14	0.10	0.004	0.001	6.19	-139
7	7.39	2.35	1.4	2.90	1.94	12.59	0.11	0.08	0.009	0.001	6.15	-125
9	5.72	2.25	1.2	2.95	2.57	16.91	0.14	0.07	0.010	0.001	6.14	-109

11	7.54	3.14	0.6	3.14	1.82	17.64	0.08	0.16	0.009	0.002	6.13	-129
13	7.69	2.93	1.1	3.73	2.52	20.55	0.10	0.10	0.002	0.003	6.10	-108
15	7.26	2.71	1.2	3.48	2.23	19.37	0.06	0.13	0.013	0.002	6.12	-120
17	6.38	2.57	0.9	2.04	1.35	19.79	0.11	0.20	0.014	0.003	6.10	-111
19	4.50	1.75	1.0	1.48	0.60	16.99	0.08	0.15	0.006	0.002	6.15	-114
	Fe^{2+}	**Mn^{2+}**	**S**	**P**	**SRP**	**NH_4^+**	**NO_3^-**	**As**	**Cd**	**Pb**	**pH**	**Eh**
Ru144												
1	0.90	0.92	0.0	0.13	0.00	3.45	0.16	0.03	0.003	0.001	6.14	-21
3	4.86	1.34	0.0	0.86	0.57	8.03	0.20	0.05	0.010	0.002	6.11	-123
5	7.82	2.14	0.0	1.69	1.33	11.21	0.18	0.12	0.007	0.002	6.13	-105
7	4.99	1.91	0.0	2.18	1.59	13.43	0.23	0.06	0.015	0.002	6.04	-113
9	4.75	1.89	0.0	1.89	1.57	18.21	0.27	0.07	0.009	0.002	6.05	-116
11	5.96	2.19	0.0	2.11	1.66	19.57	0.23	0.12	0.004	0.002	6.11	-110
13	5.89	2.02	0.0	1.89	1.69	21.08	0.22	0.12	0.013	0.002	6.07	-93
15	2.95	1.72	0.0	0.76	0.74	23.05	0.24	0.20	0.005	0.001	6.11	-100
17	6.89	2.60	0.0	2.44	1.73	23.74	0.18	0.15	0.008	0.004	6.07	-105
19	5.14	2.23	0.0	1.40	1.02	22.71	0.17	0.19			6.07	-86
Ru145												
1	0.36	0.52	15.5	0.03	0.00	6.33	0.14	0.08	0.016	0.004	5.99	-14
3	3.37	1.22	4.2	1.05	1.05	12.61	0.24	0.12	0.011	0.005	6.09	-92
5	4.87	1.43	2.0	1.67	1.84	14.38	0.22	0.11	0.004	0.002	6.06	-94
7	6.83	2.03	0.9	2.08	1.67	15.12	0.20	0.14	0.006	0.003	6.08	-106
9	7.48	2.24	1.4	2.42	1.94	17.04	0.28	0.16	0.008	0.003	6.07	-90
11	3.51	1.33	1.1	1.07	0.98	15.66	0.28	0.09	0.006	0.002	6.04	-100
13	7.57	2.74	0.2	1.83	1.03	18.51	0.14	0.21	0.009	0.004	6.09	-101
15	10.10	3.39	0.0	2.40	1.71	23.40	0.27	0.50	0.016	0.004	6.08	-104
17	6.94	2.86	0.3	1.64	1.04	23.78	0.29	0.35	0.013	0.004	6.12	-70
19	7.78	2.87	0.3	2.30	1.50	22.55	0.20	0.24	0.006	0.003	6.10	-107
Ru146												
3	3.63	0.93	10.7	0.79	0.47	6.10	0.13	0.06	0.003	0.004	6.20	-93

	5	6.58	1.91	5.0	2.30	1.63	12.92	0.21	0.07	0.008	0.002	5.90	-83
	7	3.39	1.21	6.1	1.07	0.71	12.10	0.21	0.06	0.009	0.002	6.02	-62
	9	5.00	1.99	14.9	1.24	0.89	17.68	0.17	0.15	0.010	0.003	6.05	-89
	11	8.22	2.51	11.4	2.25	1.47	18.84	0.21	0.15	0.005	0.002	6.08	-98
	13	4.44	1.38	3.8	1.25	0.82	12.68	0.19	0.08	0.004	0.002	6.05	-76
		Fe^{2+}	**Mn^{2+}**	**S**	**P**	**SRP**	**NH_4^+**	**NO_3^-**	**As**	**Cd**	**Pb**	**pH**	**Eh**
	15	7.78	2.35	2.7	1.42	0.84	17.78	0.22	0.14	0.012	0.006	6.12	-78
	17	7.45	2.60	4.1	1.27	0.85	22.82	0.23	0.17	0.024	0.009	6.08	-103
	19	8.03	2.89	14.2	1.43	0.87	23.62	0.20	0.20	0.017	0.005	6.16	-93
Ru147													
	1	11.11	2.81		4.53				0.02	0.011	0.001	5.89	-118
	3	4.13	1.24		0.67				0.05	0.005	0.001	6.09	-142
	5	12.64	3.33		3.83				0.10	0.013	0.002	6.17	-132
	7	5.71	1.94		1.76				0.06	0.007	0.002	6.12	-116
	9	6.25	1.69		1.61				0.06	0.003	0.001	6.12	-117
	11	7.56	2.43		2.36				0.06	0.002	0.002	6.14	-108
	13	6.77	2.42		1.57				0.09	0.005	0.002	6.13	-106
	15	14.65	4.10		3.67				0.12	0.006	0.001	6.11	-109
	17	17.76	5.16		4.48				0.16	0.019	0.007	6.10	-101
	19	8.45	3.00		1.78				0.14	0.011	0.002	6.15	-99
Ru148													
	1	1.90	2.78		0.13				0.05	0.023	0.005		
	3	3.77	2.53		0.33				0.13	0.073	0.013		
	5	2.57	1.88		0.37				0.27	0.015	0.006		
	7	2.33	1.50		0.37				0.19	0.015	0.009		
	9	2.85	1.60		0.34				0.16	0.023	0.037		
Ru149													
	1	0.90	0.68		0.04				0.06	0.003	0.006		
	3	4.37	1.20		0.44				0.15	0.029	0.006		
	5	3.65	1.12		0.99				0.04	0.033	0.008		

	7	3.03	1.24		1.17				0.05	0.023	0.006		
	9	0.81	0.79		0.36				0.06	0.020	0.006		
	11	1.98	1.12		0.88				0.08	0.007	0.002		
	13	2.46	1.42		0.81				0.16	0.006	0.009		
	15	2.12	0.91		0.55				0.17	0.004	0.007		
		Fe^{2+}	**Mn^{2+}**	**S**	**P**	**SRP**	**NH_4^+**	**NO_3^-**	**As**	**Cd**	**Pb**	**pH**	**Eh**
	17	1.97	0.94		0.64				0.12	0.007	0.001		
	19	3.24	1.27		1.27				0.15	0.007	0.007		
Ru150													
	1	4.87	1.74		0.70				0.02	0.015	0.002	5.60	-64
	3	2.15	1.24		0.65				0.01	0.005	0.002	6.16	-117
	5	0.43	0.77		0.08				0.18	0.018	0.009	6.31	-119
	7	1.26	1.16		0.40				0.21	0.004	0.003	6.36	-84
	9	0.79	1.04		0.28				0.19	0.027	0.016	6.31	-69
	11	1.14	1.06		0.26				0.20	0.006	0.008	6.25	-84
	13	0.64	0.67		0.19				0.14	0.022	0.008	6.25	-78
	15	1.25	0.86		0.30				0.13	0.006	0.003	6.25	-90
	17	0.96	1.07		0.20				0.27	0.024	0.007	6.26	-76
	19	1.63	1.12		0.32				0.23	0.018	0.014	6.30	-82
Ru151													
	1	1.73	0.98		0.47				0.02	0.003	0.008		
	3	4.86	1.31		1.48				0.03	0.002	0.001		
	5	1.78	0.81		0.69				0.04	0.002	0.002		
	7	1.79	0.89		0.62				0.04	0.002	0.005		
	9	1.29	0.87		0.54				0.06	0.002	0.005		
	11	1.30	1.05		0.50				0.10	0.002	0.003		
	13	4.24	1.59		1.31				0.13	0.001	0.004		
	15	2.84	1.29		0.69				0.15	0.001	0.003		
	17	2.68	1.73		1.18				0.14	0.003	0.006		
	19	5.31	2.18		1.72				0.13	0.001	0.003		

Ru152												
1	3.15	1.51		1.11				0.10	0.011	0.030		
3	1.94	1.36		0.55				0.08	0.004	0.006		
5	3.76	1.66		0.89				0.15	0.005	0.006		
7	3.43	1.82		0.94				0.17	0.001	0.004		
	Fe^{2+}	**Mn^{2+}**	**S**	**P**	**SRP**	**NH_4^+**	**NO_3^-**	**As**	**Cd**	**Pb**	**pH**	**Eh**
9	2.92	1.49		0.94				0.13	0.003	0.005		
11	5.35	1.97		1.73				0.16	0.001	0.003		
13	4.23	1.90		1.15				0.14	0.003	0.011		
15	7.30	2.46		1.78				0.14	0.003	0.006		
17	4.50	2.02		1.34				0.19	0.001	0.004		
19	9.78	2.85		3.09				0.29	0.002	0.006		
Ru153												
1	6.73	2.14		2.04				0.14	0.001	0.004		
3	14.22	4.54		2.17				0.31	0.002	0.008		
5	9.36	3.74		4.03				0.08	0.003	0.009		
7	6.07	2.41		2.22				0.07	0.002	0.003		
9	4.82	2.40		1.84				0.07	0.001	0.001		
11	6.19	2.80		1.88				0.12	0.001	0.003		
13	11.96	4.35		4.32				0.13	0.001	0.003		
15	4.87	2.17		1.29				0.13	0.001	0.003		
17	9.92	3.80		3.17				0.18	0.001	0.004		
19	6.69	3.38		1.66				0.19	0.002	0.002		
Ru154												
1	4.73	2.01		1.64				0.10	0.003	0.007		
3	10.81	3.75		3.57				0.24	0.001	0.004		
5	9.73	3.49		3.65				0.15	0.001	0.006		
7	5.77	1.79		1.99				0.09	0.001	0.001		
9	12.33	3.80		4.06				0.20	0.001	0.005		
11	8.61	2.60		3.00				0.18	0.001	0.001		

13	6.37	2.65		1.61				0.19	0.003	0.005		
15	6.34	2.60		1.68				0.15	0.001	0.005		
17	8.67	3.31		2.09				0.25	0.004	0.005		
19	12.01	3.85		3.45				0.22	0.004	0.003		
Ru155	**Fe^{2+}**	**Mn^{2+}**	**S**	**P**	**SRP**	**NH_4^+**	**NO_3^-**	**As**	**Cd**	**Pb**	**pH**	**Eh**
1	1.98	0.95		0.12				0.06	0.001	0.002		
3	10.35	2.82		3.02				0.16	0.003	0.004		
5	12.54	3.21		2.56				0.20	0.003	0.011		
7	11.29	3.08		1.75				0.25	0.005	0.009		
Ru156												
1	0.51	0.53		0.06				0.02	0.002	0.002		
3	1.70	0.87		0.29				0.07	0.001	0.006		
5	4.43	1.38		1.23				0.07	0.003	0.005		
7	4.93	1.72		1.30				0.17	0.003	0.007		
9	5.75	1.90		1.28				0.18	0.002	0.004		
11	6.49	1.81		1.30				0.13	0.003	0.006		
13	12.31	3.04		1.86				0.20	0.005	0.014		
15	3.59	1.42		0.58				0.11	0.002	0.009		
17	9.46	2.63		1.65				0.16	0.007	0.005		
19	6.03	2.38		1.25				0.13	0.002	0.005		
Ru157												
1	3.59	1.42		1.35				0.09	0.001	0.003		
3	6.95	2.72		3.80				0.06	0.003	0.006		
5	6.93	2.58		3.80				0.05	0.003	0.003		
7	4.20	2.19		2.18				0.08	0.002	0.004		
9	4.62	1.86		1.76				0.14	0.002	0.003		
11	5.72	2.15		3.28				0.08	0.004	0.006		
13	7.52	2.92		3.53				0.17	0.003	0.008		
15	4.71	1.99		3.10				0.10	0.001	0.002		

17	7.45	2.56		4.24				0.13	0.002	0.002		
19	5.61	2.83		3.76				0.17	0.006	0.006		
Ru158												
1	1.76	1.44		0.54				0.10	0.002	0.009		
3	6.57	2.60		2.71				0.21	0.001	0.007		
	Fe^{2+}	**Mn^{2+}**	**S**	**P**	**SRP**	**NH_4^+**	**NO_3^-**	**As**	**Cd**	**Pb**	**pH**	**Eh**
5	5.72	2.73		2.39				0.19	0.002	0.006		
7	6.04	2.48		2.45				0.14	0.003	0.006		
9	7.53	2.86		2.89				0.20	0.002	0.004		
11	6.33	2.49		2.41				0.19	0.002	0.002		
13	2.43	1.39		0.42				0.14	0.001	0.003		
15	7.38	2.81		2.98				0.13	0.002	0.006		
17	11.32	4.56		3.68				0.26	0.004	0.009		
19	8.50	2.67		3.01				0.16	0.001	0.001		
Ru159												
1	0.30	0.60		0.03				0.04	0.002	0.004		
3	1.82	1.07		0.30				0.06	0.003	0.006		
5	1.91	1.39		0.54				0.01	0.002	0.008		
7	0.82	0.75		0.27				0.04	0.002	0.006		
9	1.11	0.92		0.38				0.06	0.004	0.005		
11	2.86	1.41		0.94				0.11	0.003	0.007		
13	3.43	1.36		1.03				0.09	0.005	0.008		
15	1.44	0.76		0.43				0.07	0.002	0.005		
17	4.54	1.50		0.88				0.11	0.004	0.013		
19	3.76	1.19		0.65				0.09	0.005	0.005		
Ru160												
1	2.86	0.68		0.82				0.02	0.001	0.003		
3	4.83	1.20		1.72				0.06	0.002	0.004		
5	4.16	1.26		1.54				0.05	0.004	0.006		
7	4.03	1.34		1.56				0.06	0.002	0.002		

	9	3.14	1.09		1.28				0.06	0.001	0.003		
	11	4.46	1.47		1.52				0.07	0.003	0.008		
	13	4.14	1.39		1.35				0.08	0.002	0.002		
	15	6.12	1.86		1.71				0.12	0.003	0.006		
	17	5.87	1.90		1.83				0.13	0.007	0.004		
		Fe^{2+}	**Mn^{2+}**	**S**	**P**	**SRP**	**NH_4^+**	**NO_3^-**	**As**	**Cd**	**Pb**	**pH**	**Eh**
	19	5.35	1.74		1.45				0.12	0.001	0.002		
Ru161													
	1	7.23	2.46		2.59				0.14	0.002	0.006		
	3	6.64	2.34		2.15				0.16	0.001	0.004		
	5	10.55	3.01		3.36				0.19	0.003	0.004		
	7	8.90	2.81		2.97				0.16	0.002	0.003		
	9	12.72	3.90		3.88				0.18	0.005	0.005		
	11	13.28	3.83		4.08				0.15	0.003	0.004		
	13	14.05	4.16		3.93				0.17	0.001	0.006		
	15	7.68	2.19		2.24				0.13	0.001	0.001		
	17	17.12	5.00		4.42				0.27	0.005	0.010		
	19	16.52	4.53		4.19				0.22	0.006	0.003		
Ru162													
	1	11.31	3.90		3.31				0.29	0.003	0.006		
	3	10.91	3.72		3.56				0.24	0.003	0.004		
	5	8.78	2.86		2.93				0.16	0.001	0.001		
	7	10.74	4.16		3.28				0.22	0.006	0.007		
	9	9.89	3.38		2.83				0.18	0.001	0.003		
	11	13.33	4.67		4.14				0.24	0.003	0.005		
	13	17.00	5.04		3.89				0.29	0.004	0.002		
	15	16.04	4.78		4.06				0.28	0.001	0.005		
	17	10.92	3.41		2.86				0.14	0.002	0.002		
	19	14.91	4.18		3.20				0.21	0.022	0.009		
Ru163													

	1	5.99	2.16		2.24				0.13	0.003	0.006		
	3	7.66	2.76		3.70				0.19	0.004	0.005		
	5	4.99	1.76		2.41				0.11	0.003	0.005		
	7	6.40	2.20		3.30				0.15	0.002	0.004		
	9	6.38	2.16		2.69				0.20	0.003	0.006		
		Fe^{2+}	**Mn^{2+}**	**S**	**P**	**SRP**	**NH_4^+**	**NO_3^-**	**As**	**Cd**	**Pb**	**pH**	**Eh**
	11	9.17	3.04		4.23				0.21	0.005	0.007		
	13	7.47	2.61		2.93				0.19	0.004	0.006		
	15	5.86	2.06		2.68				0.13	0.002	0.003		
	17	9.21	2.86		3.79				0.18	0.002	0.005		
	19	8.39	2.70		2.80				0.23	0.003	0.004		
Ru164													
	1	6.79	2.56		1.54				0.21		0.001	6.26	-79
	3	9.59	3.71		2.29				0.36		0.002	6.48	-87
	5	10.42	4.09		3.11				0.29		0.001	6.37	-93
	7	12.38	4.39		3.57				0.25		0.002	6.36	-102
	9	6.99	2.73		1.79				0.20		0.001	6.47	-79
	11	12.35	4.71		3.25				0.26		0.001	6.37	-92
	13	9.81	3.53		2.49				0.23		0.001	6.41	-89
	15	12.89	4.56		3.10				0.29		0.002	6.55	-92
	17	11.97	4.49		2.62				0.28		0.002	6.27	-66
	19	13.01	4.43		2.69				0.31		0.003	6.31	-81

Peeper raw concentrations

Sample ID (cm)	Fe^{2+}	Mn^{2+}	S	TDP	NH_4^+	NO_3^-	As	Cd	Pb	pH	Eh
P1											
26	4.01	2.63		1.60	15.97	0.16	0.017	0.002	0.053	6.99	-9
24	1.86	1.56		0.67	10.80	0.17	0.005	0.000	0.020	6.98	-9
22	1.51	1.20		0.70	8.25	0.16	0.003	0.000	0.019	7.03	-9
20	1.36	1.03		0.71	7.92	0.15	0.002	0.001	0.029	7.02	-9
18	2.11	1.16		1.18	7.64	0.13	0.003	0.000	0.016	6.94	-7
16	2.01	1.09		1.09	6.97	0.07	0.002	0.000	0.020	6.96	-7
14	1.50	0.85		0.79	5.87	0.11	0.002	0.000	0.027	6.99	-7
12	0.97	0.62		0.47	4.30	0.10	0.003	0.001	0.032	6.85	-8
10	0.69	0.44		0.26	3.17	0.09	0.003	0.000	0.027	6.95	-7
8	0.31	0.28		0.10	1.90	0.05	0.002	0.000	0.020	6.89	-8
6	0.12	0.14		0.01	1.09	0.01	0.001	0.000	0.020	6.81	-9
4	0.08	0.09		0.00	0.72	0.10	0.001	0.001	0.034	6.79	-9
2	0.10	0.07		0.01	0.53	0.08	0.003	0.002	0.038	6.67	-9
0	0.08	0.05		0.00	0.24	0.00	0.002	0.006	0.036	6.83	-10
-2	0.04	0.10		0.00	0.18	0.08	0.002	0.008	0.032	6.85	-10
-4	0.00	0.03		0.00	0.19	0.04	0.001	0.008	0.027	6.62	-10
-6	0.00	0.06		0.00	0.19	0.08	0.001	0.007	0.025	6.48	-12
-8	0.07	0.21		0.00	0.28	0.06	0.003	0.008	0.033	6.49	-12
-10	0.08	0.24		0.01	0.24	0.06	0.003	0.008	0.034	6.33	-13
-12	0.09	0.25		0.01	0.14	0.07	0.004	0.008	0.032	6.28	-13

-14	0.10	0.25		0.03	0.26	0.07	0.004	0.008	0.034	6.27	-14
-16	0.05	0.14		0.05	0.05	0.06	0.003	0.007	0.034	6.36	-15
-18	0.20	0.43		0.03	0.19	0.05	0.007	0.007	0.034	6.26	-17
-20	0.16	0.36		0.02	0.24	0.07	0.005	0.007	0.032	6.34	-14
-22	0.04	0.11		0.00	0.23	0.01	0.002	0.006	0.035	6.38	-13
P2	**Fe^{2+}**	**Mn^{2+}**	**S**	**TDP**	**NH_4^+**	**NO_3^-**	**As**	**Cd**	**Pb**	**pH**	**Eh**
-16	0.02	0.32		0.05			0.003	0.000	0.007	6.81	35
-14	0.01	0.51		0.10			0.004	0.000	0.008	6.94	36
-12	0.01	0.60		0.15			0.004	0.000	0.007	7.01	38
-10	0.01	0.60		0.18			0.005	0.000	0.005	7.13	44
-8	0.02	0.66		0.26			0.006	0.000	0.004	7.21	49
-6	missing sample										
-4	0.02	0.42		0.29			0.006	0.000	0.002	7.22	53
-2	0.21	0.70		0.33			0.005	0.000	0.001	7.20	82
0	1.87	2.27		0.79			0.006	0.000	0.003	7.02	65
2	3.61	2.25		1.91			0.007	0.000	0.003	6.60	3
4	10.51	3.81		4.32			0.010	0.000	0.004	6.44	-8
6	10.12	3.30		4.67			0.006	0.000	0.002	6.34	-8
8	9.44	2.99		4.26			0.005	0.000	0.002	6.37	-25
10	11.95	3.68		5.19			0.006	0.000	0.002	6.41	-31
12	12.23	3.59		5.32			0.006	0.000	0.002	6.48	-38
14	13.31	3.83		5.53			0.016	0.000	0.006	6.39	-25
16	missing sample										
18	missing sample										
20	13.72	4.05		6.08			0.016	0.000	0.003	6.67	-12
22	15.13	4.61		6.51			0.014	0.000	0.002	6.42	-8
24	13.77	3.97		5.77			0.013	0.000	0.002	6.37	-26
26	15.90	4.83		6.36			0.012	0.000	0.002	6.37	-10
28	missing sample										
30	16.46	4.89		6.44			0.027	0.000	0.005	6.36	-5

32	15.47	4.63		6.21			0.014	0.000	0.002	6.39	-16
P3											
-28	0.02	0.09		0.02			0.004	0.001	0.009	6.39	109
-26	0.00	0.03		0.00			0.003	0.001	0.012	6.54	117
-24	0.10	0.03		0.00			0.003	0.001	0.014	6.58	104
	Fe^{2+}	**Mn^{2+}**	**S**	**TDP**	**NH_4^+**	**NO_3^-**	**As**	**Cd**	**Pb**	**pH**	**Eh**
-22	0.00	0.03		0.00			0.003	0.001	0.010	6.61	107
-20	-0.01	0.03		0.00			0.003	0.001	0.008	6.62	128
-18	0.03	0.06		0.02			0.003	0.001	0.010	6.59	118
-16	0.00	0.07		0.01			0.003	0.001	0.008	6.59	133
-14	0.00	0.13		0.01			0.003	0.001	0.009	6.58	122
-12	0.04	0.30		0.08			0.004	0.001	0.013	6.83	128
-10	0.02	0.57		0.18			0.004	0.001	0.012	7.02	117
-8	0.01	0.82		0.31			0.005	0.001	0.010	6.63	133
-6	0.03	0.92		0.43			0.006	0.000	0.011	7.16	138
-4	0.07	0.73		0.47			0.006	0.000	0.008	7.08	139
-2	0.51	0.40		0.59			0.006	0.000	0.010	7.03	137
0	0.86	0.24		0.88			0.007	0.000	0.006	6.95	136
2	10.55	1.05		4.80			0.027	0.000	0.016	6.93	142
4	missing sample										
6	missing sample										
8	missing sample										
10	missing sample										
12	missing sample										
14	15.02	3.86		6.15			0.033	0.000	0.014	6.51	139
16	10.39	3.05		4.74			0.018	0.000	0.006	6.54	42
18	17.31	5.09		7.79			0.032	0.001	0.018	6.60	20
P4											
-42	0.14	0.10	14.69	0.11			0.061	0.001	0.014	6.47	86
-40	0.04	0.05	14.12	0.03			0.048	0.001	0.021	6.55	98

-38	0.04	0.06	13.30	0.03			0.042	0.001	0.015	6.55	111
-36	0.07	0.05	12.61	0.03			0.056	0.001	0.019	6.53	120
-34	0.03	0.04	9.97	0.02			0.050	0.000	0.016	6.55	121
-32	0.02	0.06	11.76	0.02			0.050	0.001	0.014	6.57	138
-30	0.02	0.06	8.59	0.03			0.048	0.001	0.013	6.57	138
-28	0.02	0.05	17.49	0.02			0.047	0.001	0.013	6.61	136
	Fe^{2+}	**Mn^{2+}**	**S**	**TDP**	**NH_4^+**	**NO_3^-**	**As**	**Cd**	**Pb**	**pH**	**Eh**
-26	0.01	0.04	4.84	0.02			0.044	0.001	0.011	6.59	152
-24	0.05	0.10	9.54	0.03			0.051	0.001	0.017	6.51	167
-22	0.05	0.04	8.10	0.03			0.033	0.000	0.010	6.27	169
-20	0.02	0.06	5.96	0.03			0.042	0.001	0.013	6.48	168
-18	0.01	0.08	13.41	0.02			0.039	0.001	0.013	6.43	174
-16	missing sample										
-14	0.00	0.06	7.07	0.01			0.023	0.001	0.010	6.39	172
-12	0.02	0.12	10.74	0.06			0.045	0.001	0.014	6.39	190
-10	0.09	0.14	6.95	0.10			0.053	0.001	0.009	6.45	188
-8	0.06	0.38	5.97	0.06			0.038	0.000	0.015	5.88	178
-6	0.08	0.50	3.44	0.08			0.029	0.000	0.008	5.59	194
-4	0.18	0.48	7.30	0.12			0.023	0.000	0.004	5.41	205
-2	0.73	0.67	9.71	0.37			0.033	0.000	0.003	5.51	214
0	2.43	0.98	14.08	1.13			0.053	0.000	0.002	5.92	206
2	2.73	1.03	6.29	1.54			0.031	0.000	0.003	6.02	143
4	4.13	1.46	0.00	2.41			0.040	0.000	0.004	6.14	126
6	5.07	2.06	1.22	2.78			0.045	0.000	0.006	6.23	96

Concentration profiles obtained from sediment cores

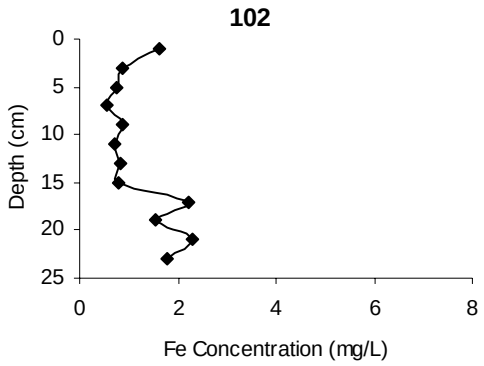

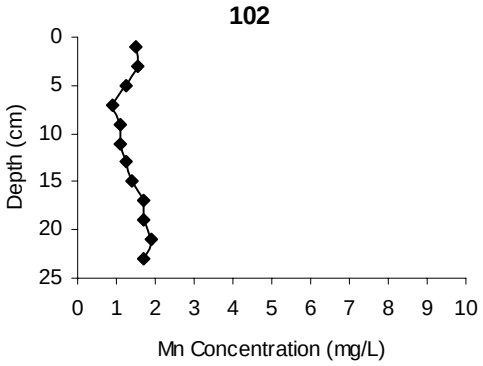

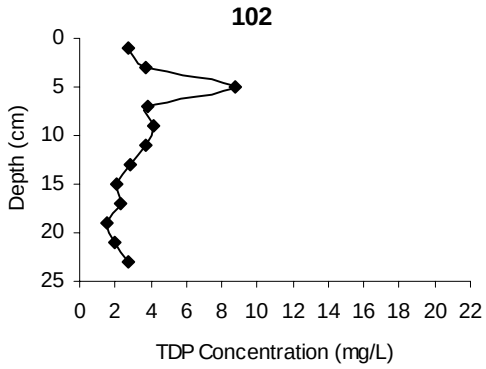

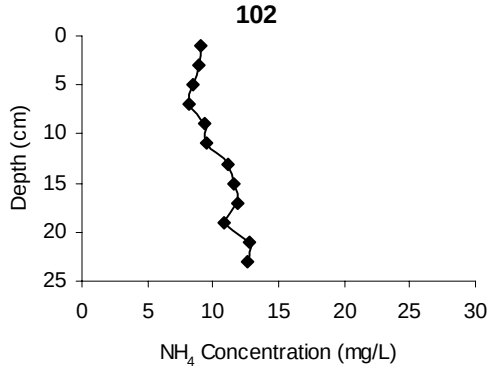

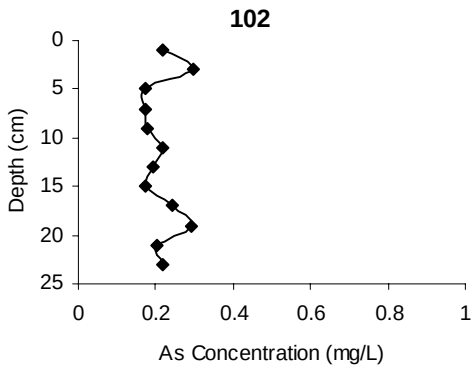

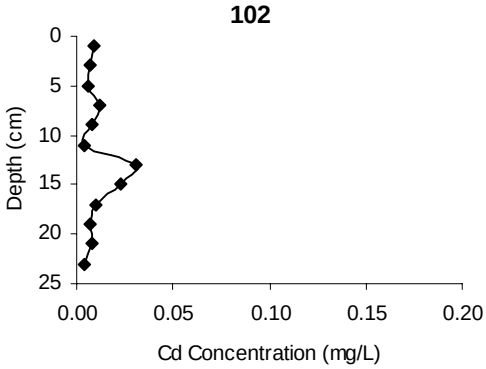

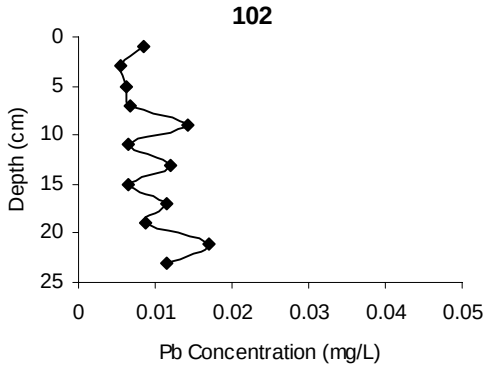

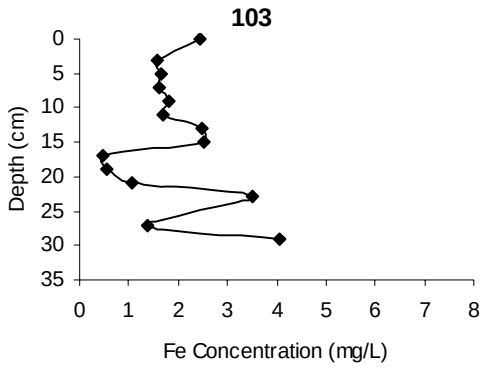
103
Depth (cm)
0 5 10 15 20 25 30 35
0 1 2 3 4 5 6 7 8
Fe Concentration (mg/L)

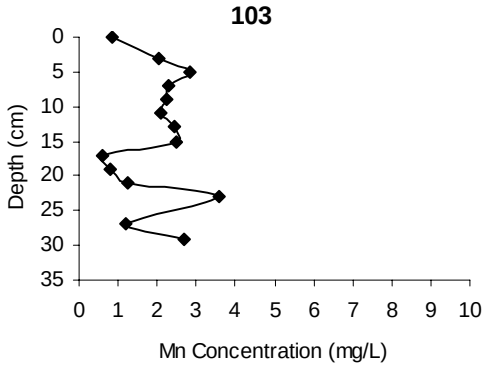
103
Depth (cm)
0 5 10 15 20 25 30 35
0 1 2 3 4 5 6 7 8 9 10
Mn Concentration (mg/L)

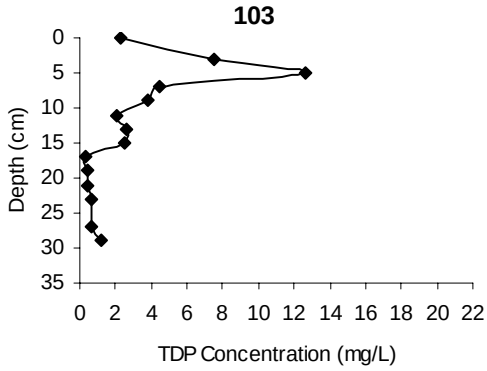
103
Depth (cm)
0 5 10 15 20 25 30 35
0 2 4 6 8 10 12 14 16 18 20 22
TDP Concentration (mg/L)

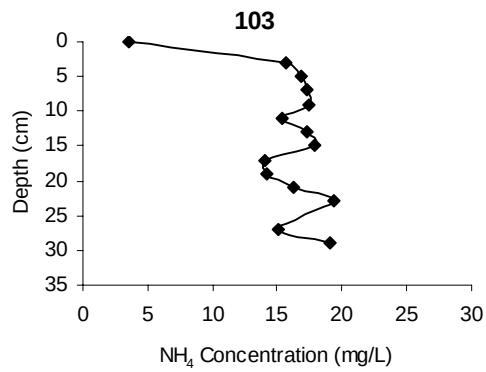
103
Depth (cm)
0 5 10 15 20 25 30 35
0 5 10 15 20 25 30
NH4 Concentration (mg/L)

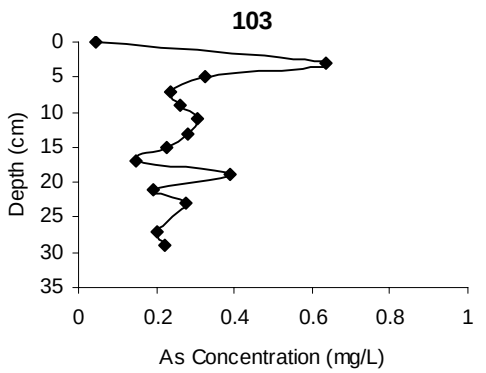
103
Depth (cm)
0 5 10 15 20 25 30 35
0 0.2 0.4 0.6 0.8 1
As Concentration (mg/L)

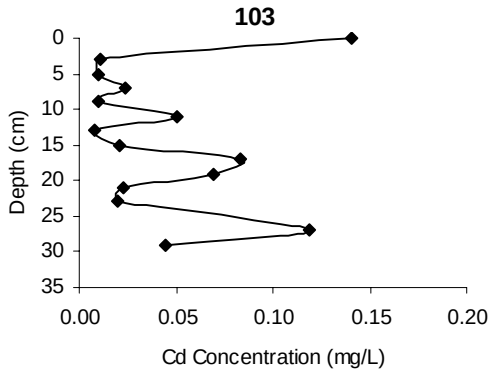
103
Depth (cm)
0 5 10 15 20 25 30 35
0.00 0.05 0.10 0.15 0.20
Cd Concentration (mg/L)

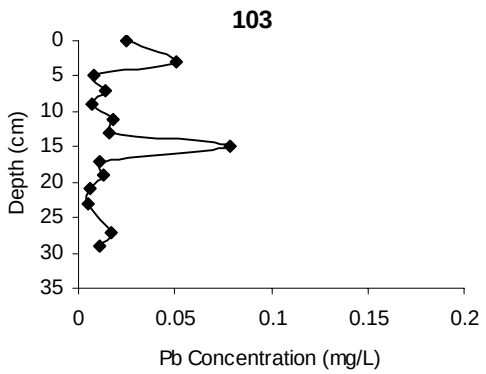
103
Depth (cm)
0 5 10 15 20 25 30 35
0 0.05 0.1 0.15 0.2
Pb Concentration (mg/L)

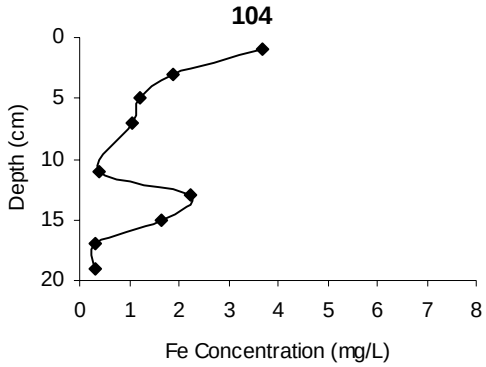
104
Depth (cm)
0
5
10
15
20
0 1 2 3 4 5 6 7 8
Fe Concentration (mg/L)

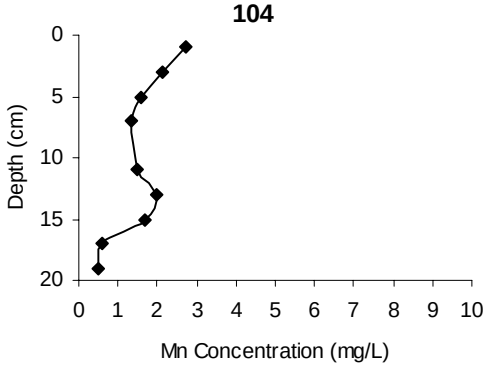
104
Depth (cm)
0
5
10
15
20
0 1 2 3 4 5 6 7 8 9 10
Mn Concentration (mg/L)

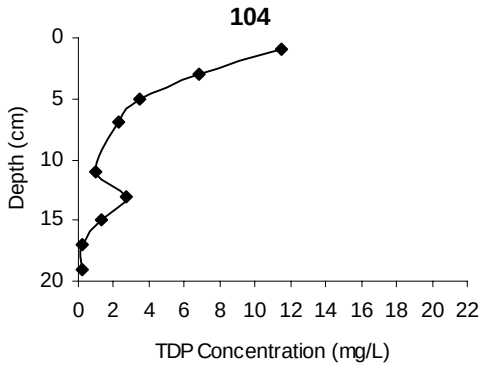
104
Depth (cm)
0
5
10
15
20
0 2 4 6 8 10 12 14 16 18 20 22
TDP Concentration (mg/L)

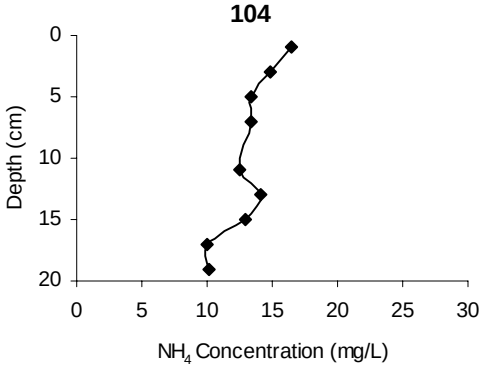
104
Depth (cm)
0
5
10
15
20
0 5 10 15 20 25 30
NH4 Concentration (mg/L)

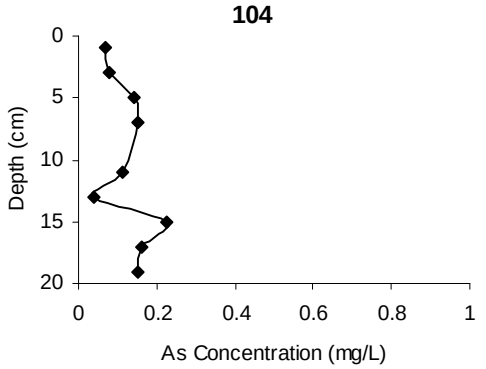
104
Depth (cm)
0
5
10
15
20
0 0.2 0.4 0.6 0.8 1
As Concentration (mg/L)

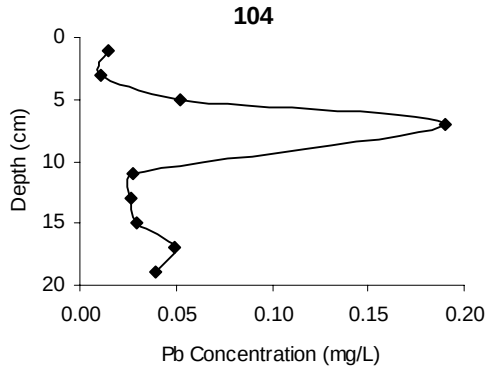
104
Depth (cm)
0
5
10
15
20
0.00 0.05 0.10 0.15 0.20
Pb Concentration (mg/L)

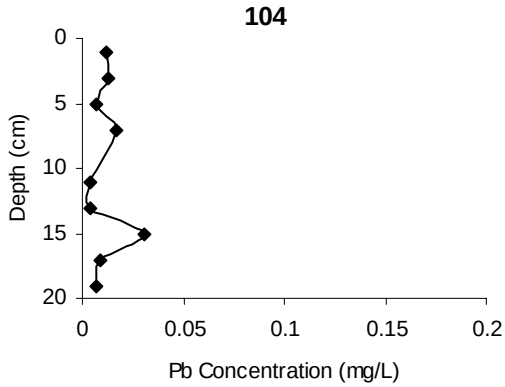
104
Depth (cm)
0
5
10
15
20
0 0.05 0.1 0.15 0.2
Pb Concentration (mg/L)

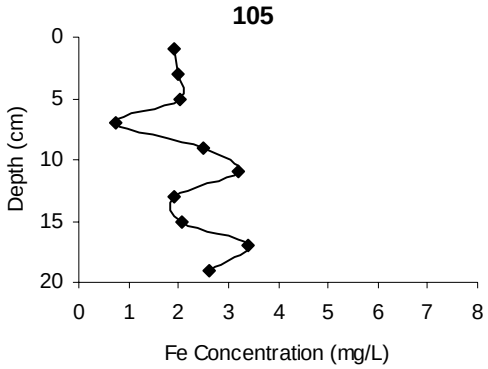
105
Depth (cm)
0
5
10
15
20
0 1 2 3 4 5 6 7 8
Fe Concentration (mg/L)

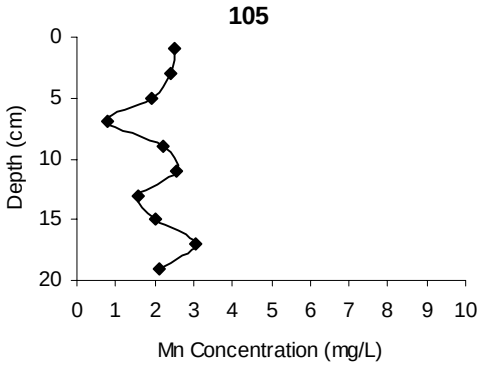
105
Depth (cm)
0
5
10
15
20
0 1 2 3 4 5 6 7 8 9 10
Mn Concentration (mg/L)

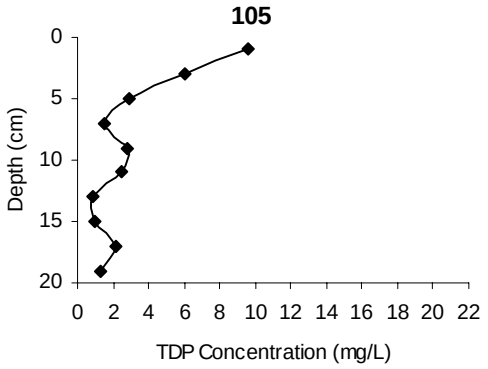
105
Depth (cm)
0
5
10
15
20
0 2 4 6 8 10 12 14 16 18 20 22
TDP Concentration (mg/L)

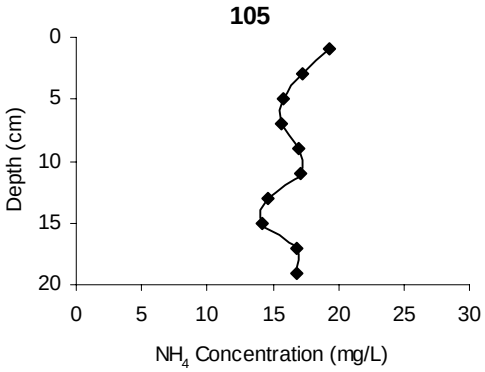
105
Depth (cm)
0
5
10
15
20
0 5 10 15 20 25 30
NH4 Concentration (mg/L)

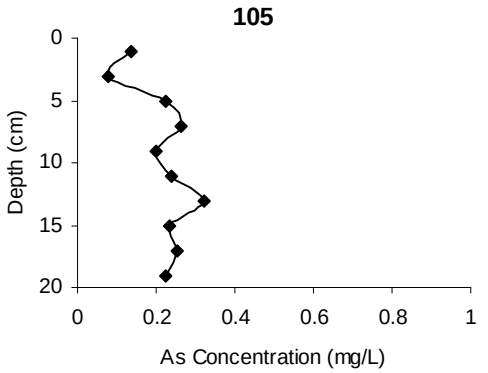
105
Depth (cm)
0
5
10
15
20
0 0.2 0.4 0.6 0.8 1
As Concentration (mg/L)

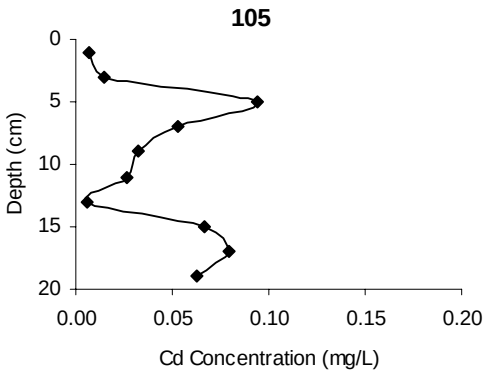
105
Depth (cm)
0
5
10
15
20
0.00 0.05 0.10 0.15 0.20
Cd Concentration (mg/L)

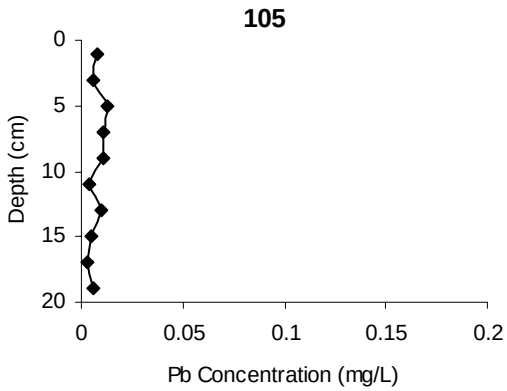
105
Depth (cm)
0
5
10
15
20
0 0.05 0.1 0.15 0.2
Pb Concentration (mg/L)

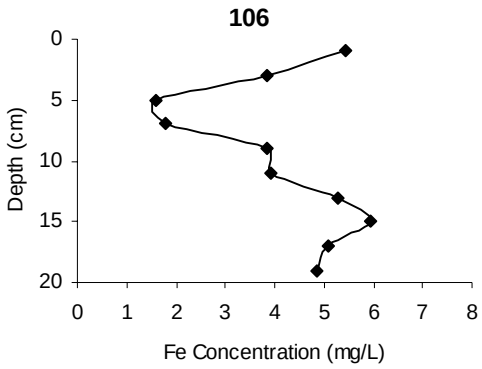
106
Depth (cm)
0
5
10
15
20
0 1 2 3 4 5 6 7 8
Fe Concentration (mg/L)

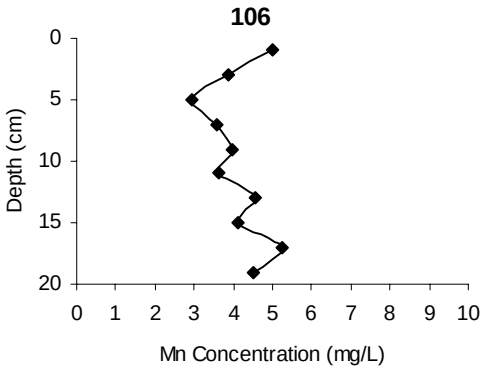
106
Depth (cm)
0
5
10
15
20
0 1 2 3 4 5 6 7 8 9 10
Mn Concentration (mg/L)

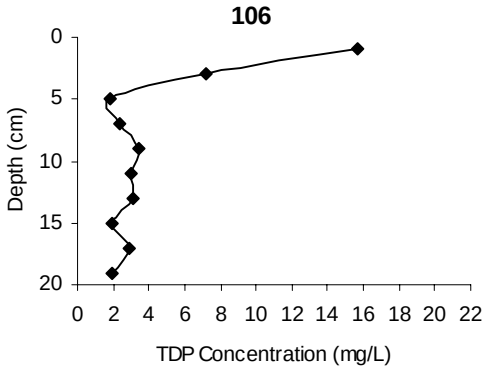
106
Depth (cm)
0
5
10
15
20
0 2 4 6 8 10 12 14 16 18 20 22
TDP Concentration (mg/L)

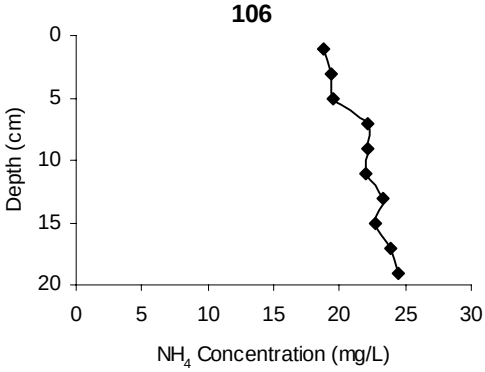
106
Depth (cm)
0
5
10
15
20
0 5 10 15 20 25 30
NH4 Concentration (mg/L)

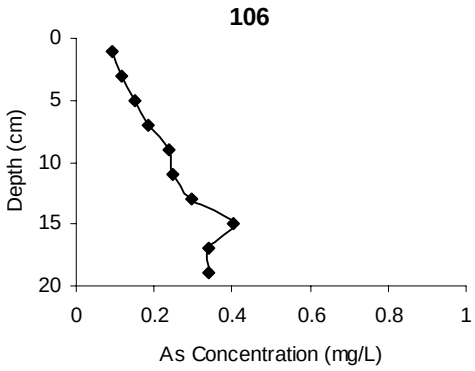
106
Depth (cm)
0
5
10
15
20
0 0.2 0.4 0.6 0.8 1
As Concentration (mg/L)

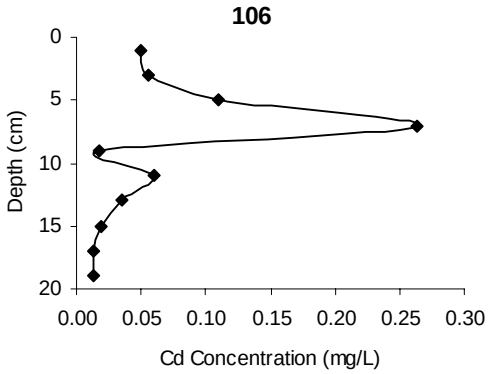
106
Depth (cm)
0
5
10
15
20
0.00 0.05 0.10 0.15 0.20 0.25 0.30
Cd Concentration (mg/L)

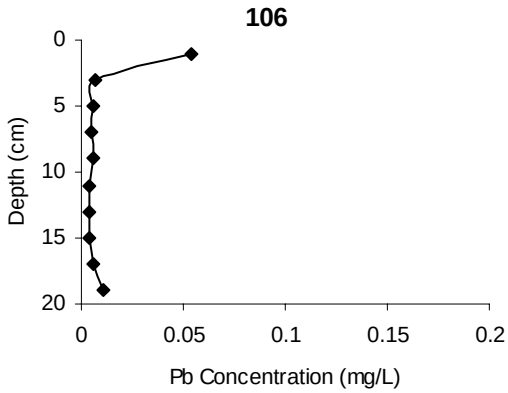
106
Depth (cm)
0
5
10
15
20
0 0.05 0.1 0.15 0.2
Pb Concentration (mg/L)

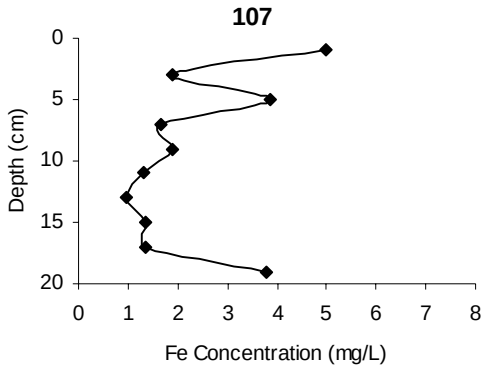
107
Depth (cm)
0
5
10
15
20
0 1 2 3 4 5 6 7 8
Fe Concentration (mg/L)

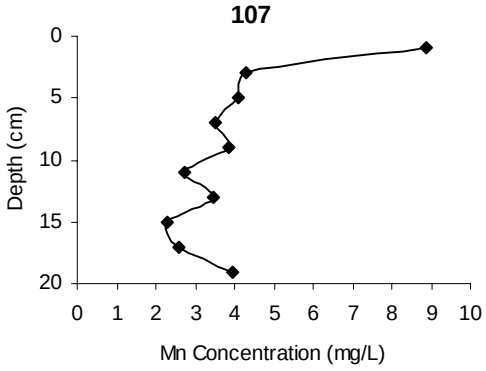
107
Depth (cm)
0
5
10
15
20
0 1 2 3 4 5 6 7 8 9 10
Mn Concentration (mg/L)

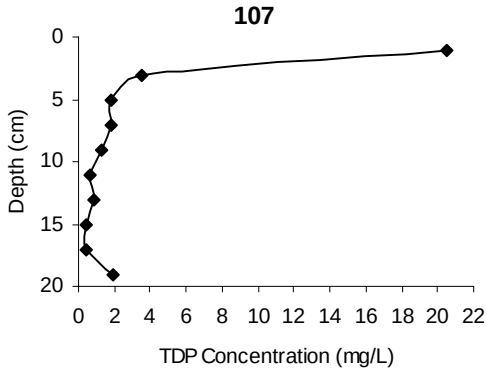
107
Depth (cm)
0
5
10
15
20
0 2 4 6 8 10 12 14 16 18 20 22
TDP Concentration (mg/L)

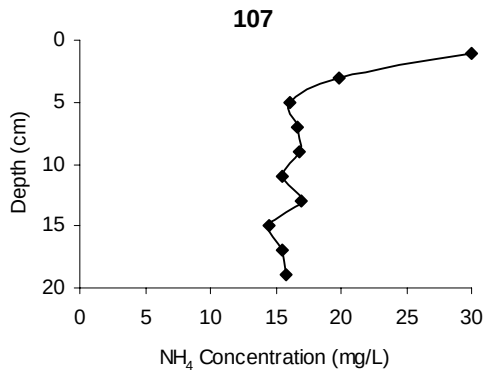
107
Depth (cm)
0
5
10
15
20
0 5 10 15 20 25 30
NH4 Concentration (mg/L)

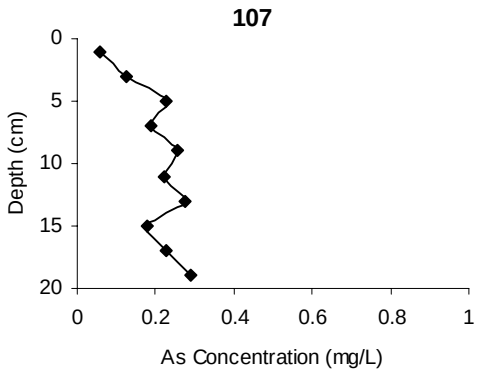
107
Depth (cm)
0
5
10
15
20
0 0.2 0.4 0.6 0.8 1
As Concentration (mg/L)

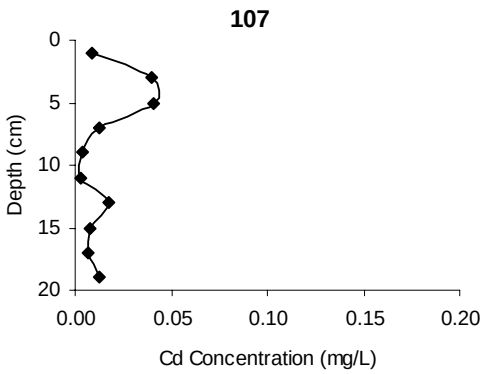
107
Depth (cm)
0
5
10
15
20
0.00 0.05 0.10 0.15 0.20
Cd Concentration (mg/L)

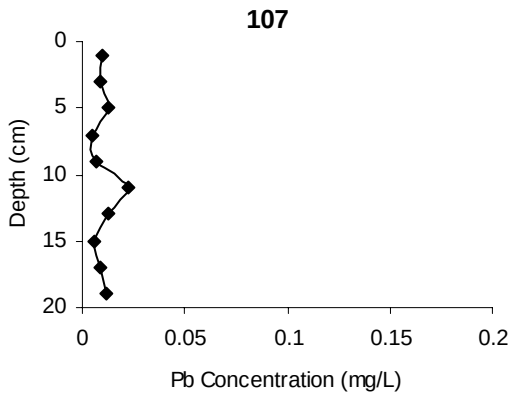
107
Depth (cm)
0
5
10
15
20
0 0.05 0.1 0.15 0.2
Pb Concentration (mg/L)

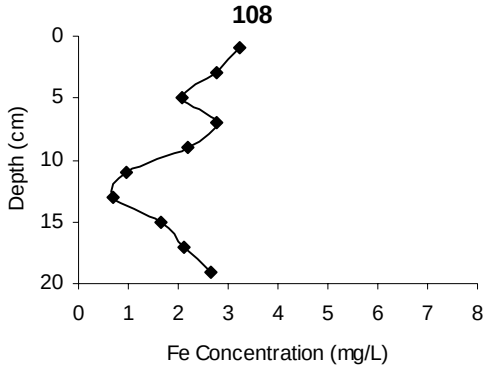
108
Depth (cm)
0
5
10
15
20
0 1 2 3 4 5 6 7 8
Fe Concentration (mg/L)

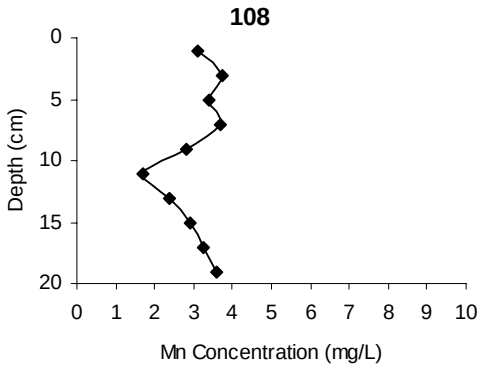
108
Depth (cm)
0
5
10
15
20
0 1 2 3 4 5 6 7 8 9 10
Mn Concentration (mg/L)

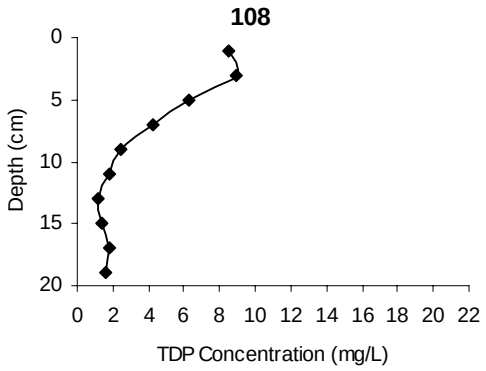
108
Depth (cm)
0
5
10
15
20
0 2 4 6 8 10 12 14 16 18 20 22
TDP Concentration (mg/L)

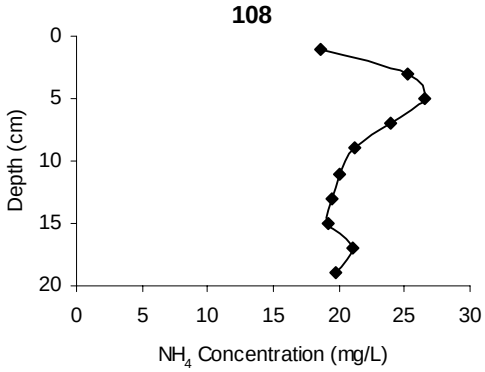
108
Depth (cm)
0
5
10
15
20
0 5 10 15 20 25 30
NH4 Concentration (mg/L)

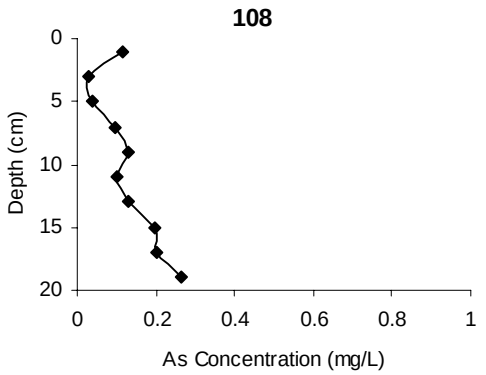
108
Depth (cm)
0
5
10
15
20
0 0.2 0.4 0.6 0.8 1
As Concentration (mg/L)

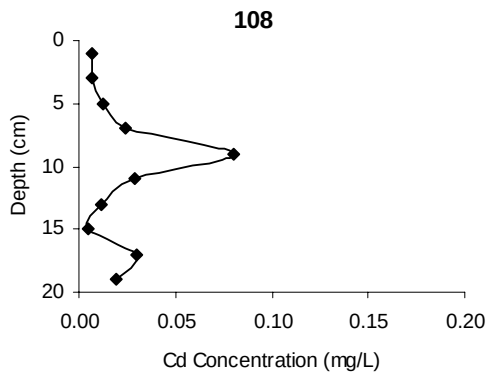
108
Depth (cm)
0
5
10
15
20
0.00 0.05 0.10 0.15 0.20
Cd Concentration (mg/L)

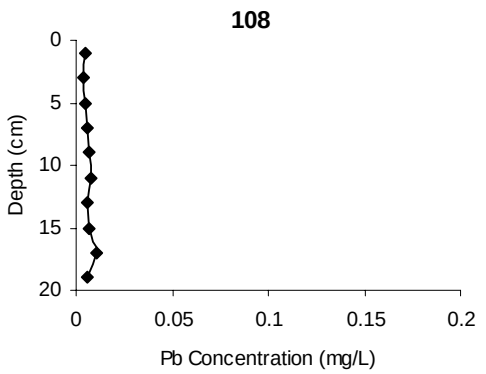
108
Depth (cm)
0
5
10
15
20
0 0.05 0.1 0.15 0.2
Pb Concentration (mg/L)

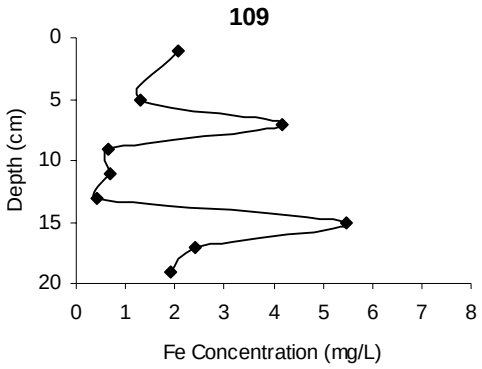
109
Depth (cm)
0
5
10
15
20
0 1 2 3 4 5 6 7 8
Fe Concentration (mg/L)

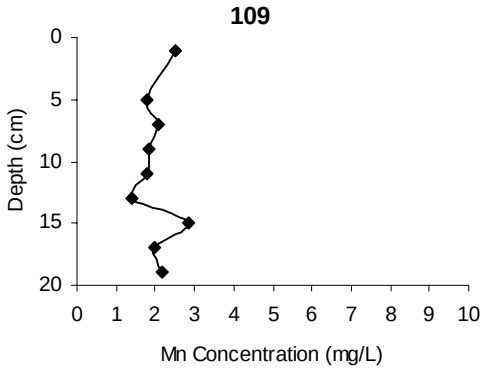
109
Depth (cm)
0
5
10
15
20
0 1 2 3 4 5 6 7 8 9 10
Mn Concentration (mg/L)

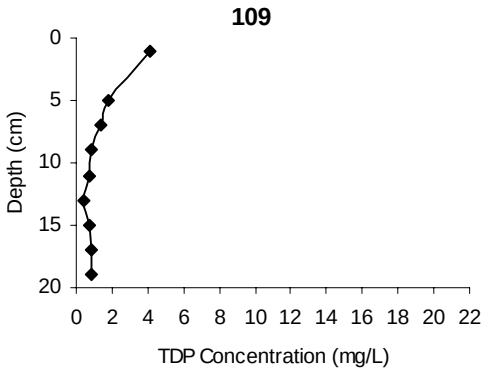
109
Depth (cm)
0
5
10
15
20
0 2 4 6 8 10 12 14 16 18 20 22
TDP Concentration (mg/L)

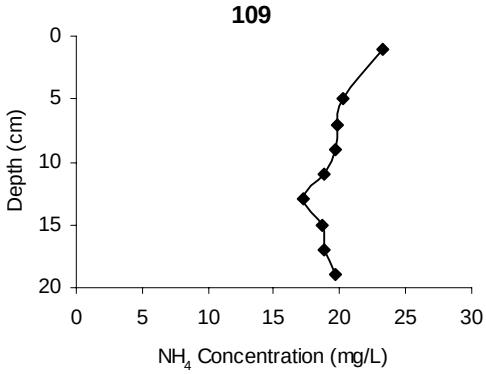
109
Depth (cm)
0
5
10
15
20
0 5 10 15 20 25 30
NH4 Concentration (mg/L)

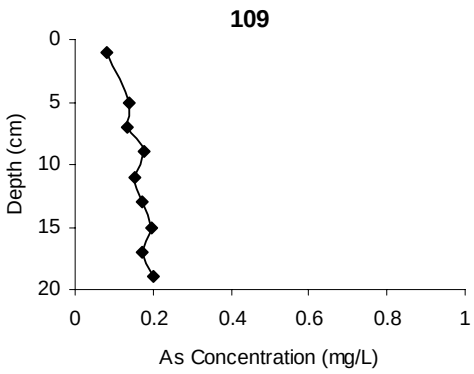
109
Depth (cm)
0
5
10
15
20
0 0.2 0.4 0.6 0.8 1
As Concentration (mg/L)

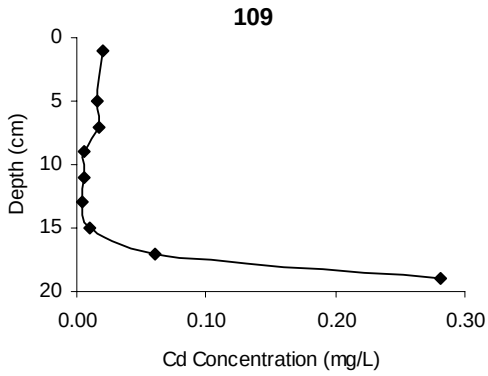
109
Depth (cm)
0
5
10
15
20
0.00 0.10 0.20 0.30
Cd Concentration (mg/L)

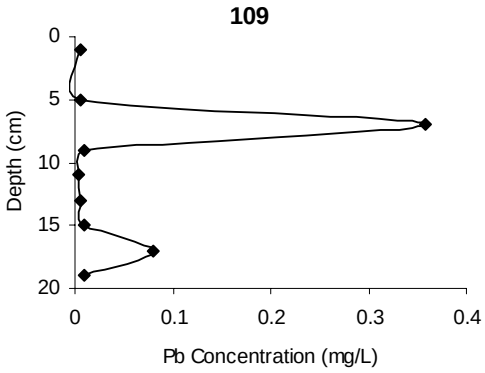
109
Depth (cm)
0
5
10
15
20
0 0.1 0.2 0.3 0.4
Pb Concentration (mg/L)

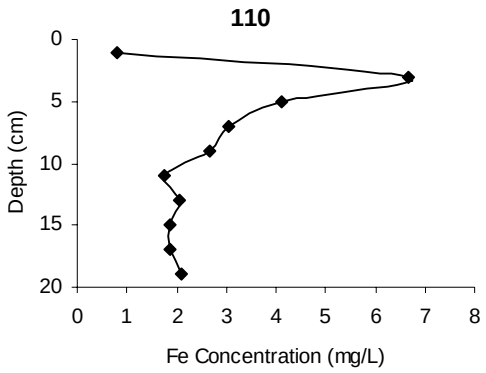
110
Depth (cm)
0
5
10
15
20
0 1 2 3 4 5 6 7 8
Fe Concentration (mg/L)

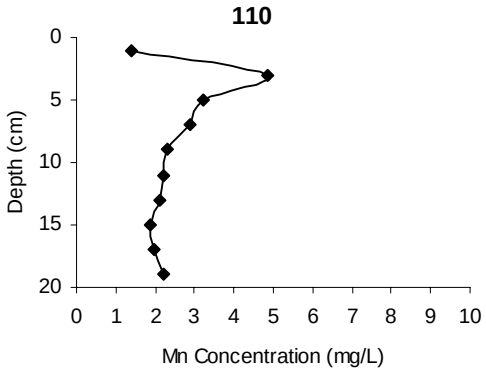
110
Depth (cm)
0
5
10
15
20
0 1 2 3 4 5 6 7 8 9 10
Mn Concentration (mg/L)

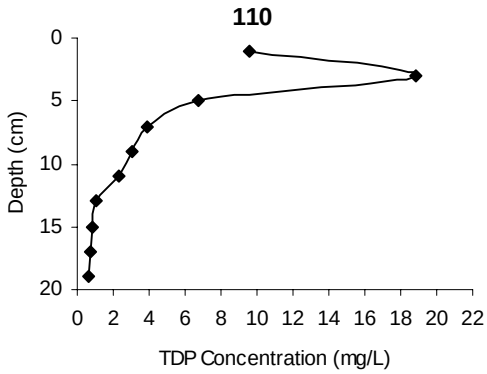
110
Depth (cm)
0
5
10
15
20
0 2 4 6 8 10 12 14 16 18 20 22
TDP Concentration (mg/L)

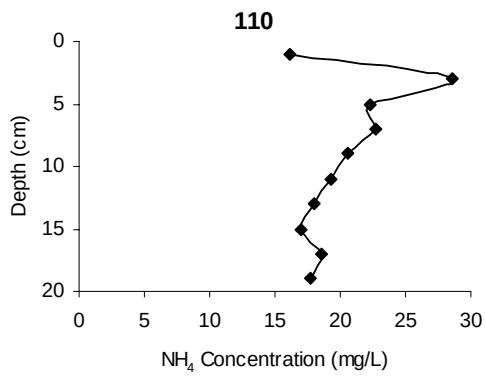
110
Depth (cm)
0
5
10
15
20
0 5 10 15 20 25 30
NH4 Concentration (mg/L)

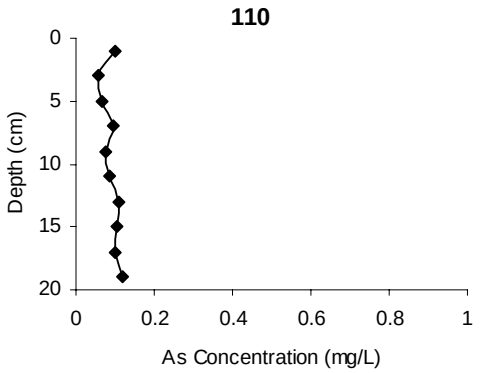
110
Depth (cm)
0
5
10
15
20
0 0.2 0.4 0.6 0.8 1
As Concentration (mg/L)

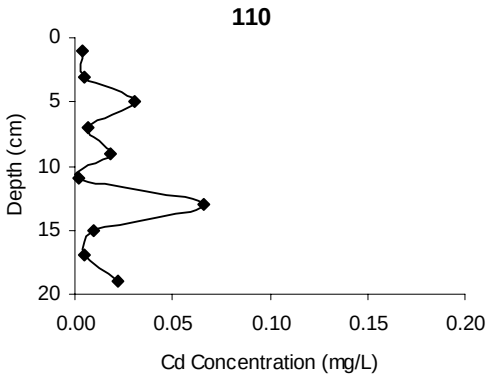
110
Depth (cm)
0
5
10
15
20
0.00 0.05 0.10 0.15 0.20
Cd Concentration (mg/L)

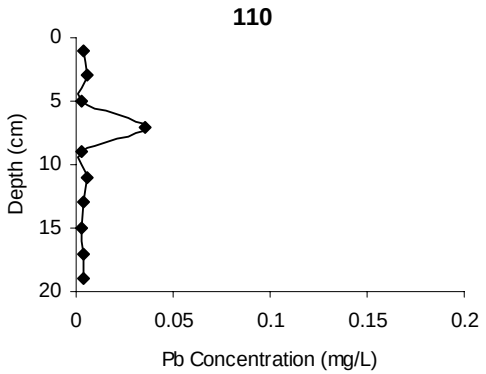
110
Depth (cm)
0
5
10
15
20
0 0.05 0.1 0.15 0.2
Pb Concentration (mg/L)

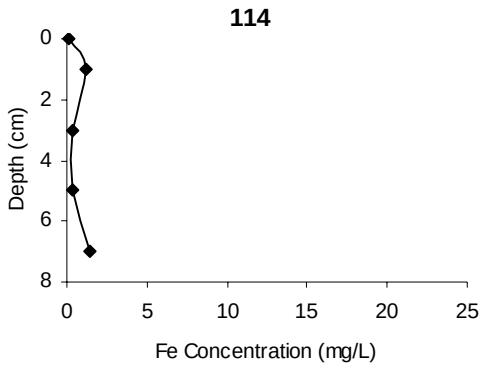
114
Depth (cm)
0
2
4
6
8
0
5
10
15
20
25
Fe Concentration (mg/L)

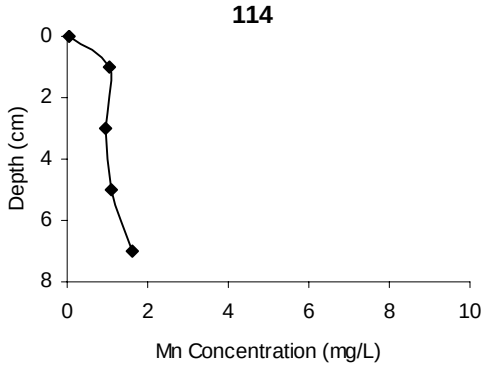
114
Depth (cm)
0
2
4
6
8
0
2
4
6
8
10
Mn Concentration (mg/L)

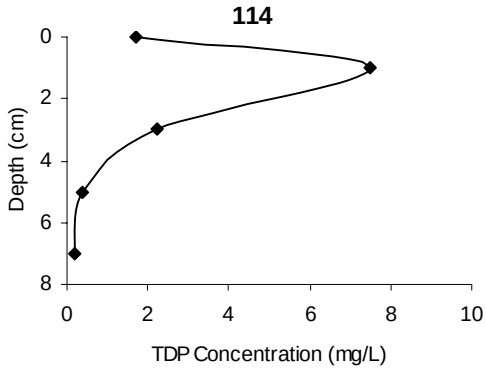
114
Depth (cm)
0
2
4
6
8
0
2
4
6
8
10
TDP Concentration (mg/L)

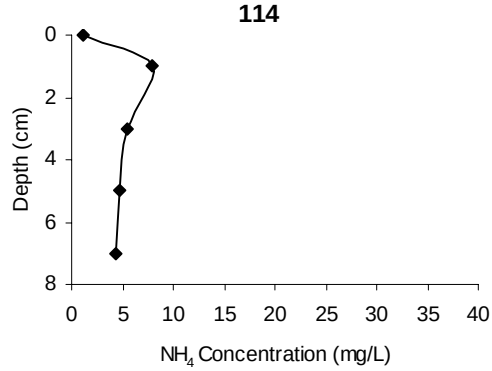
114
Depth (cm)
0
2
4
6
8
0
5
10
15
20
25
30
35
40
NH4 Concentration (mg/L)

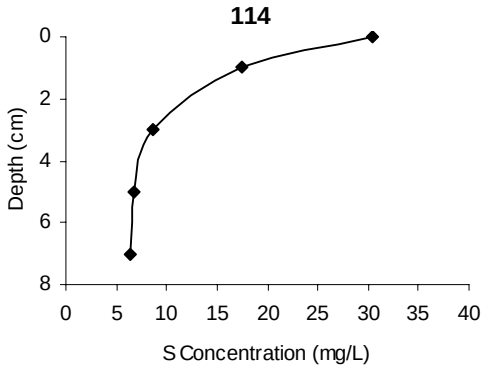
114
Depth (cm)
0
2
4
6
8
0
5
10
15
20
25
30
35
40
S Concentration (mg/L)

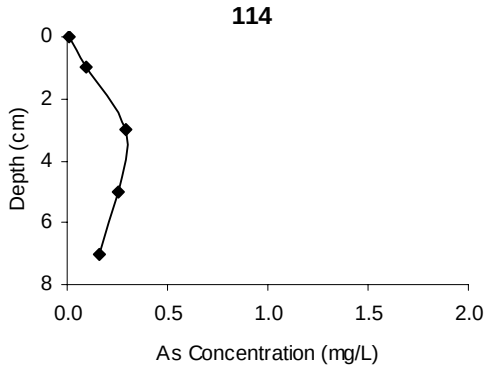
114
Depth (cm)
0
2
4
6
8
0.0
0.5
1.0
1.5
2.0
As Concentration (mg/L)

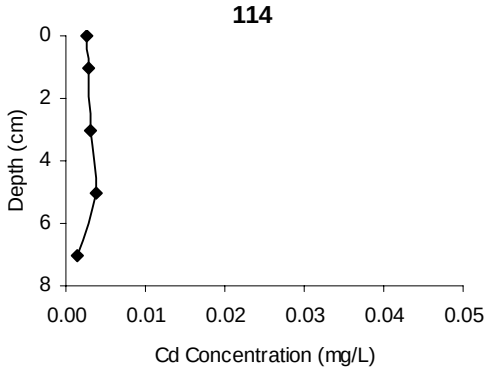
114
Depth (cm)
0
2
4
6
8
0.00
0.01
0.02
0.03
0.04
0.05
Cd Concentration (mg/L)

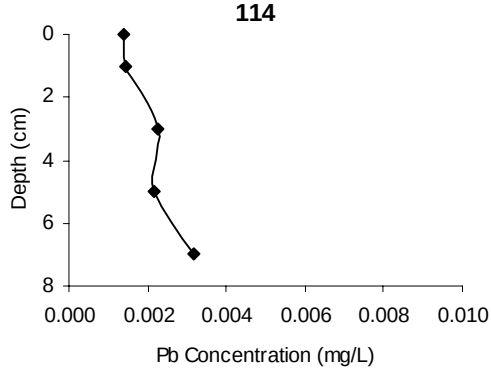
114
Depth (cm)
0
2
4
6
8
0.000
0.002
0.004
0.006
0.008
0.010
Pb Concentration (mg/L)

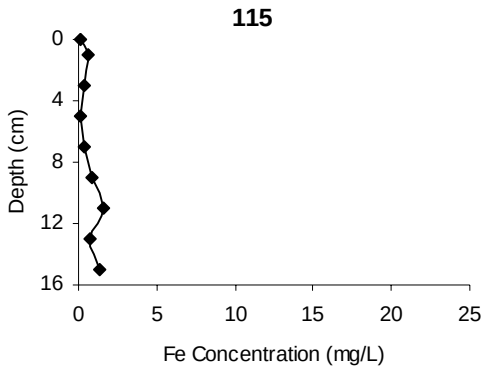
115
Depth (cm)
0
4
8
12
16
0
5
10
15
20
25
Fe Concentration (mg/L)

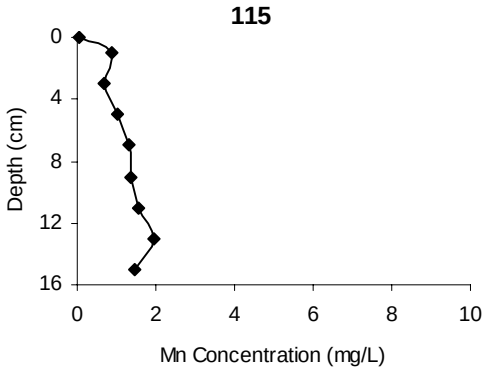
115
Depth (cm)
0
4
8
12
16
0
2
4
6
8
10
Mn Concentration (mg/L)

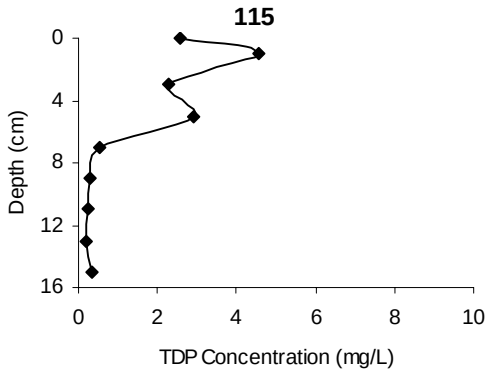
115
Depth (cm)
0
4
8
12
16
0
2
4
6
8
10
TDP Concentration (mg/L)

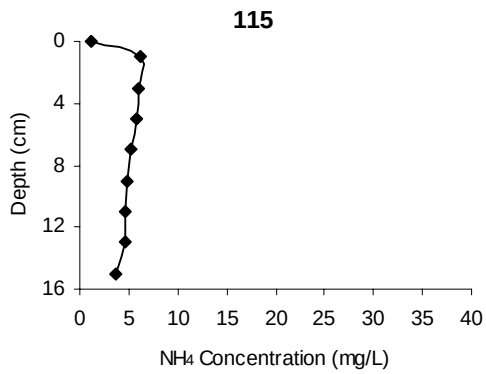
115
Depth (cm)
0
4
8
12
16
0
5
10
15
20
25
30
35
40
NH4 Concentration (mg/L)

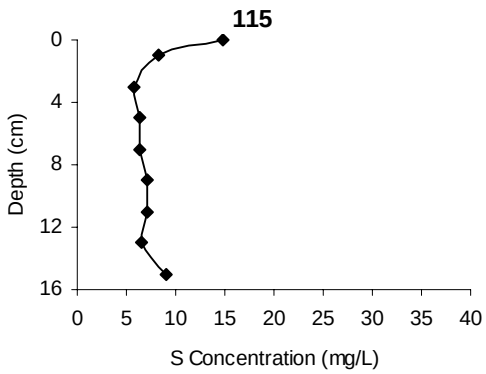
115
Depth (cm)
0
4
8
12
16
0
5
10
15
20
25
30
35
40
S Concentration (mg/L)

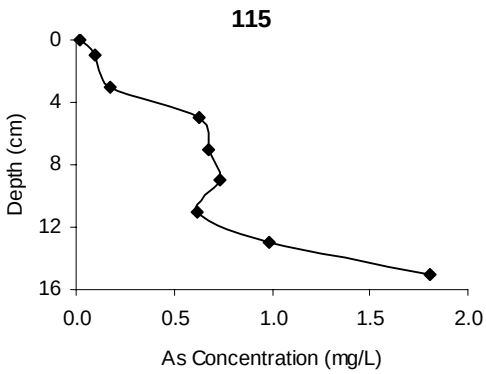
115
Depth (cm)
0
4
8
12
16
0.0
0.5
1.0
1.5
2.0
As Concentration (mg/L)

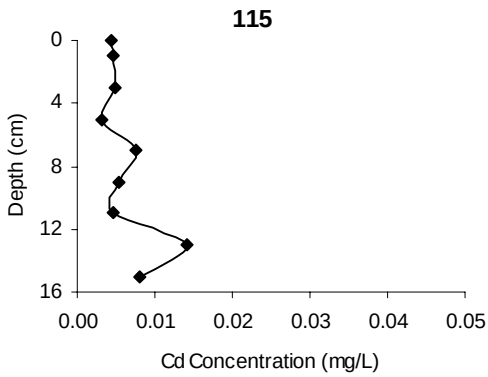
115
Depth (cm)
0
4
8
12
16
0.00
0.01
0.02
0.03
0.04
0.05
Cd Concentration (mg/L)

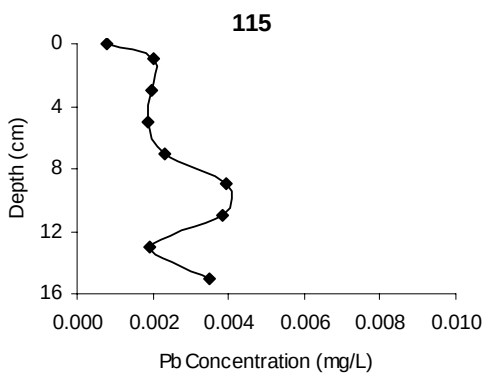
115
Depth (cm)
0
4
8
12
16
0.000
0.002
0.004
0.006
0.008
0.010
Pb Concentration (mg/L)

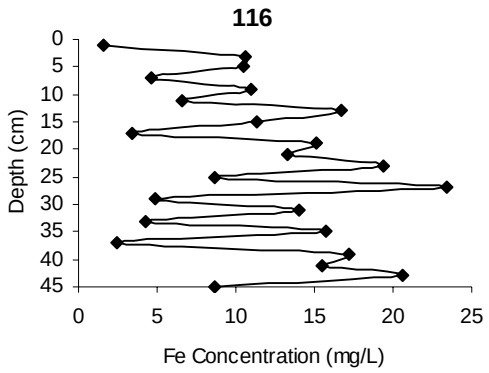
116
Depth (cm)
Fe Concentration (mg/L)

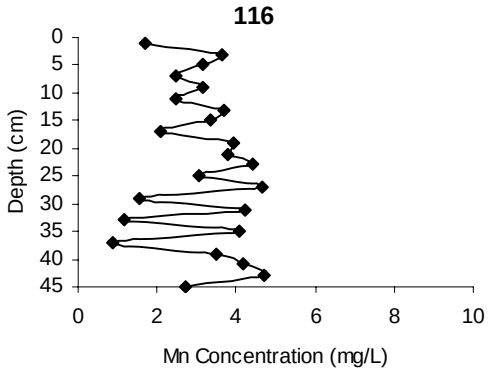
116
Depth (cm)
Mn Concentration (mg/L)

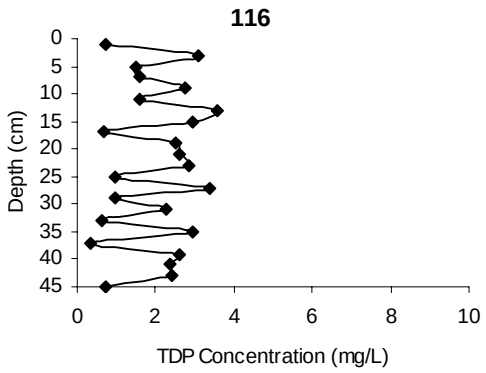
116
Depth (cm)
TDP Concentration (mg/L)

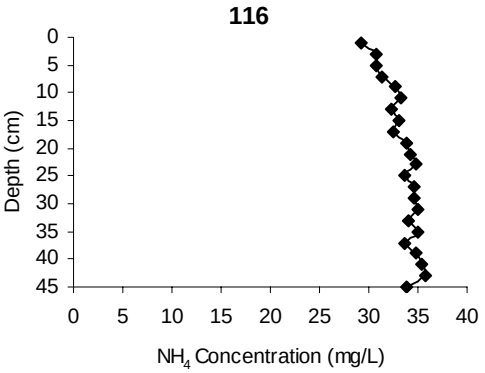
116
Depth (cm)
NH4 Concentration (mg/L)

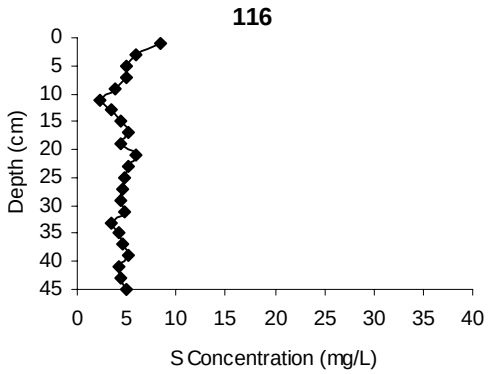
116
Depth (cm)
S Concentration (mg/L)

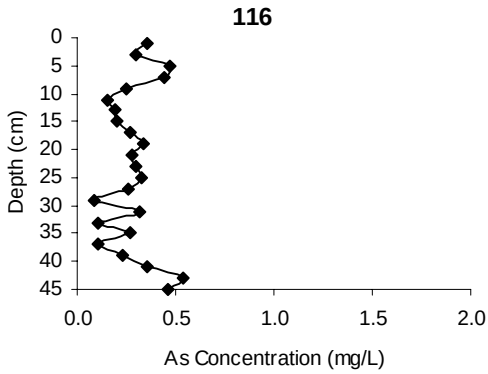
116
Depth (cm)
As Concentration (mg/L)

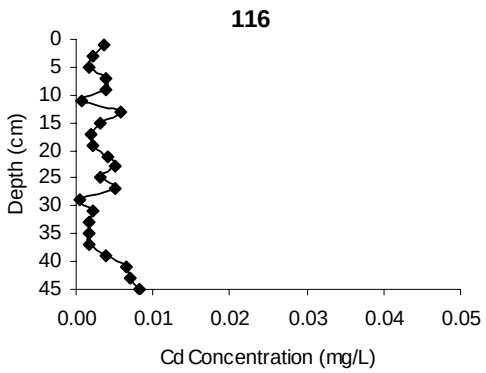
116
Depth (cm)
Cd Concentration (mg/L)

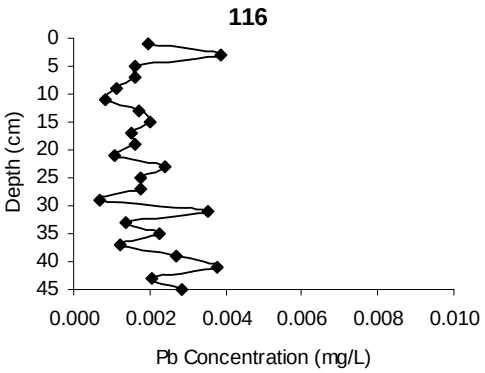
116
Depth (cm)
Pb Concentration (mg/L)

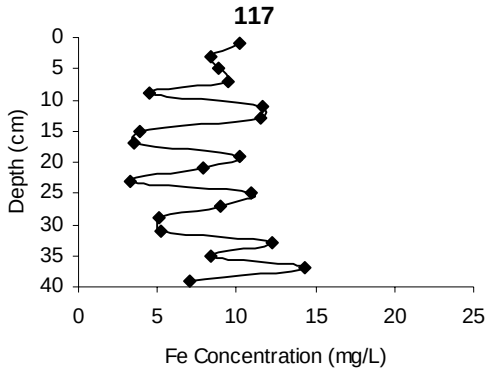
117
Depth (cm)
Fe Concentration (mg/L)

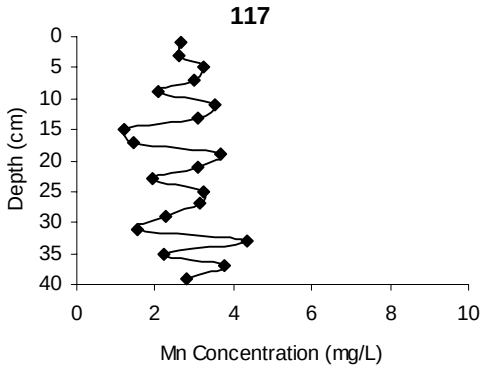
117
Depth (cm)
Mn Concentration (mg/L)

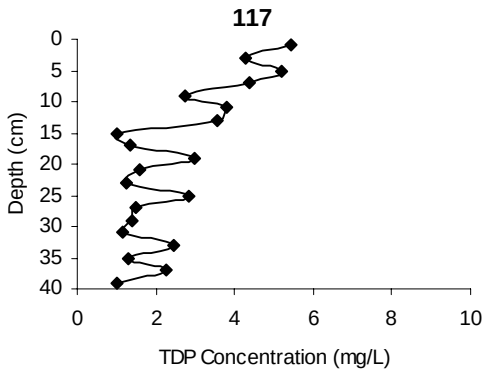
117
Depth (cm)
TDP Concentration (mg/L)

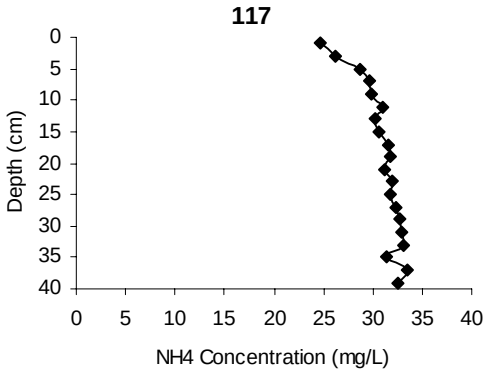
117
Depth (cm)
NH4 Concentration (mg/L)

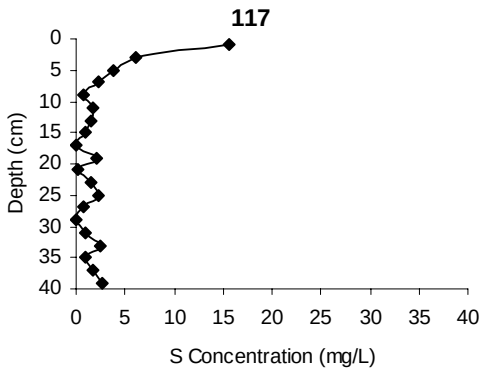
117
Depth (cm)
S Concentration (mg/L)

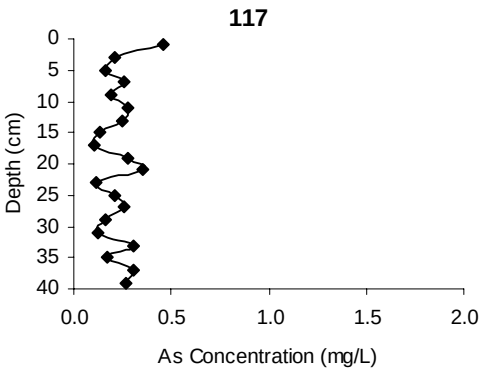
117
Depth (cm)
As Concentration (mg/L)

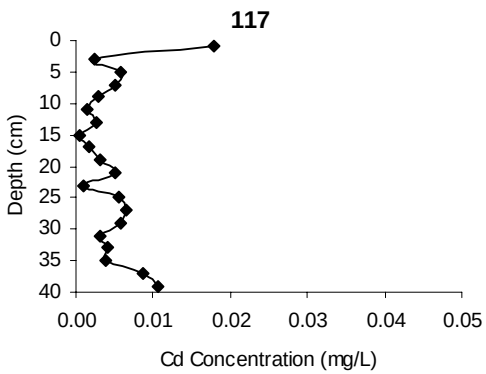
117
Depth (cm)
Cd Concentration (mg/L)

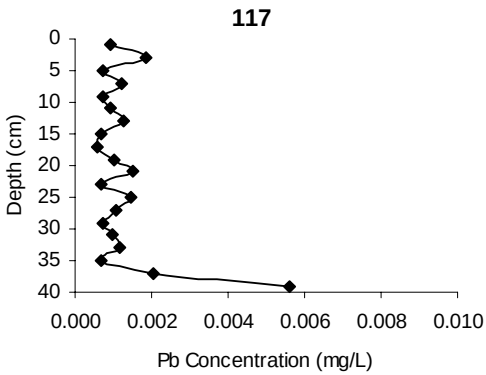
117
Depth (cm)
Pb Concentration (mg/L)

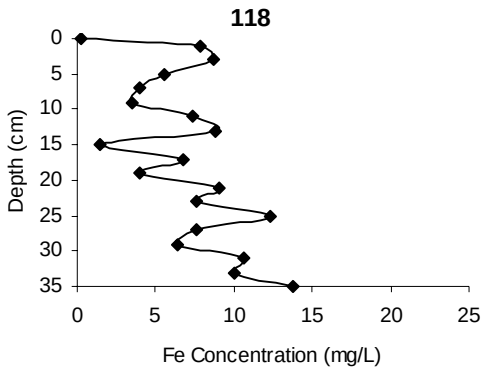
118
Depth (cm)
0
5
10
15
20
25
30
35
0
5
10
15
20
25
Fe Concentration (mg/L)

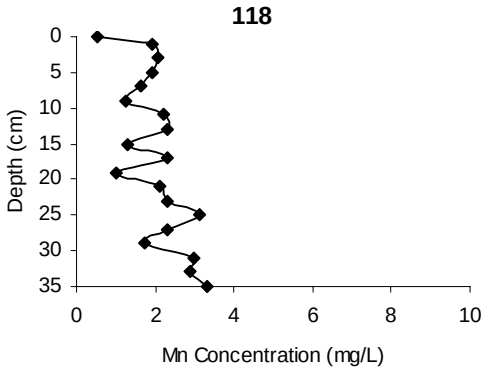
118
Depth (cm)
0
5
10
15
20
25
30
35
0
2
4
6
8
10
Mn Concentration (mg/L)

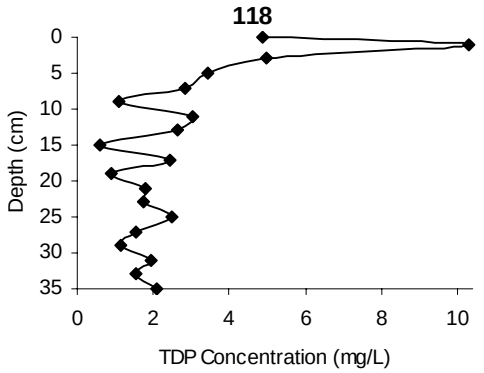
118
Depth (cm)
0
5
10
15
20
25
30
35
0
2
4
6
8
10
TDP Concentration (mg/L)

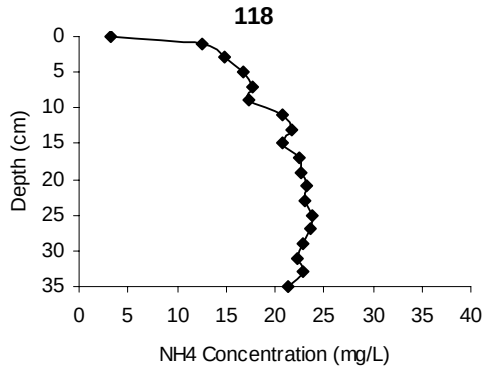
118
Depth (cm)
0
5
10
15
20
25
30
35
0
5
10
15
20
25
30
35
40
NH4 Concentration (mg/L)

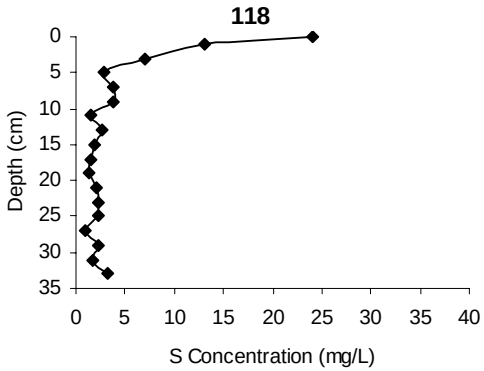
118
Depth (cm)
0
5
10
15
20
25
30
35
0
5
10
15
20
25
30
35
40
S Concentration (mg/L)

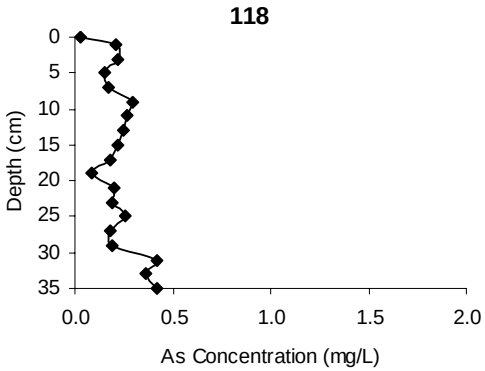
118
Depth (cm)
0
5
10
15
20
25
30
35
0.0
0.5
1.0
1.5
2.0
As Concentration (mg/L)

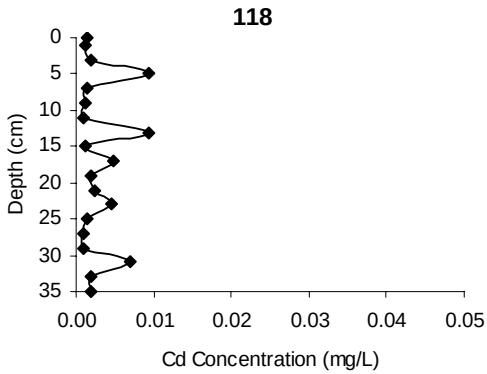
118
Depth (cm)
0
5
10
15
20
25
30
35
0.00
0.01
0.02
0.03
0.04
0.05
Cd Concentration (mg/L)

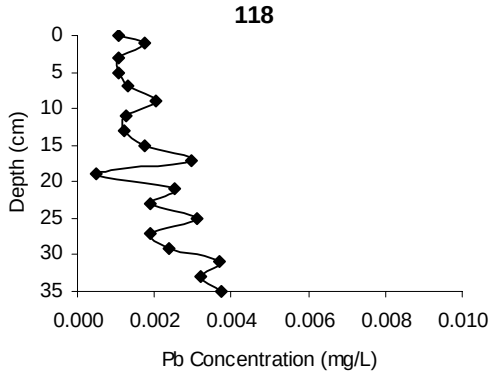
118
Depth (cm)
0
5
10
15
20
25
30
35
0.000
0.002
0.004
0.006
0.008
0.010
Pb Concentration (mg/L)

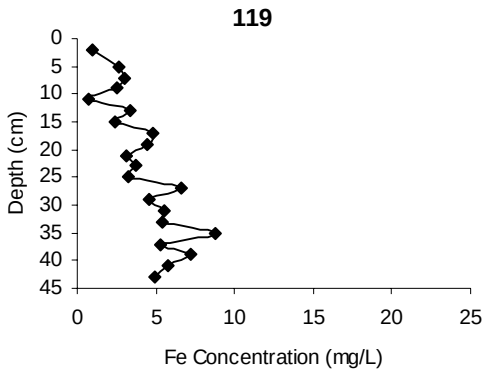
119
Depth (cm)
0 5 10 15 20 25 30 35 40 45
0 5 10 15 20 25
Fe Concentration (mg/L)

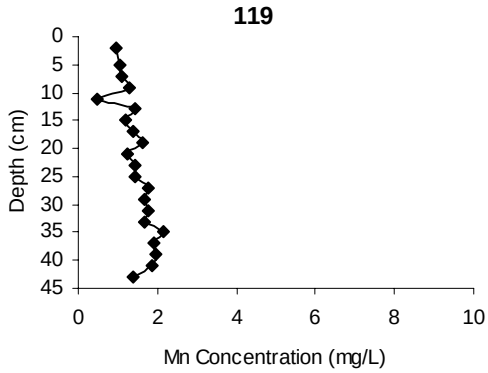
119
Depth (cm)
0 5 10 15 20 25 30 35 40 45
0 2 4 6 8 10
Mn Concentration (mg/L)

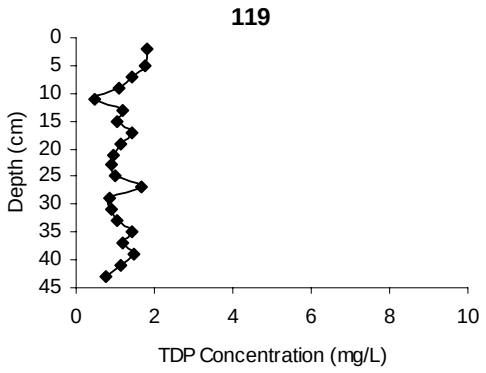
119
Depth (cm)
0 5 10 15 20 25 30 35 40 45
0 2 4 6 8 10
TDP Concentration (mg/L)

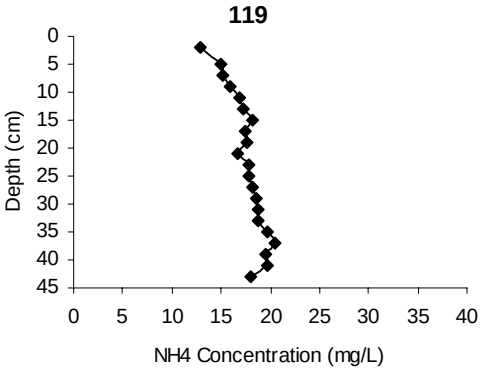
119
Depth (cm)
0 5 10 15 20 25 30 35 40 45
0 5 10 15 20 25 30 35 40
NH4 Concentration (mg/L)

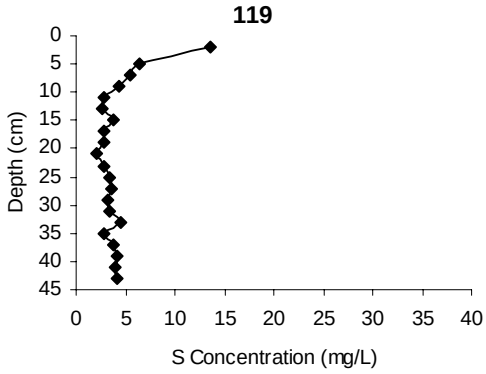
119
Depth (cm)
0 5 10 15 20 25 30 35 40 45
0 5 10 15 20 25 30 35 40
S Concentration (mg/L)

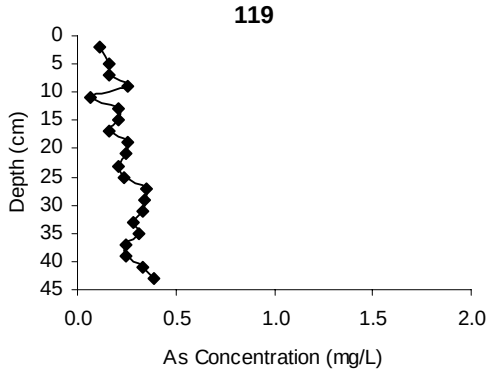
119
Depth (cm)
0 5 10 15 20 25 30 35 40 45
0.0 0.5 1.0 1.5 2.0
As Concentration (mg/L)

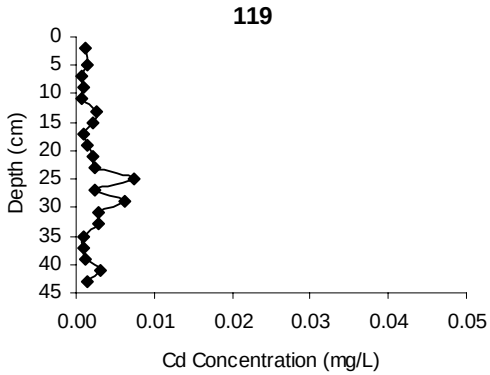
119
Depth (cm)
0 5 10 15 20 25 30 35 40 45
0.00 0.01 0.02 0.03 0.04 0.05
Cd Concentration (mg/L)

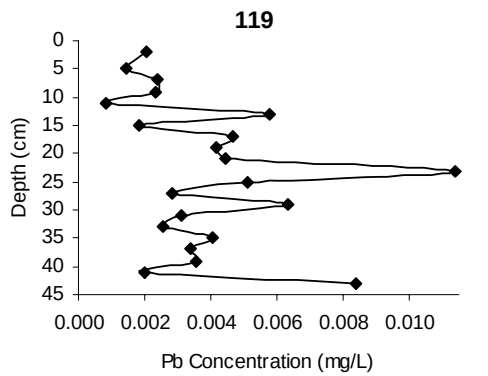
119
Depth (cm)
0 5 10 15 20 25 30 35 40 45
0.000 0.002 0.004 0.006 0.008 0.010
Pb Concentration (mg/L)

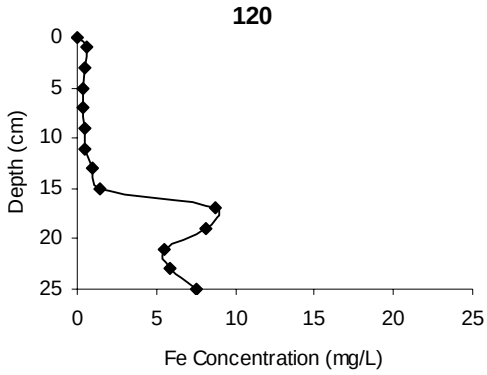
120
Depth (cm)
0
5
10
15
20
25
0
5
10
15
20
25
Fe Concentration (mg/L)

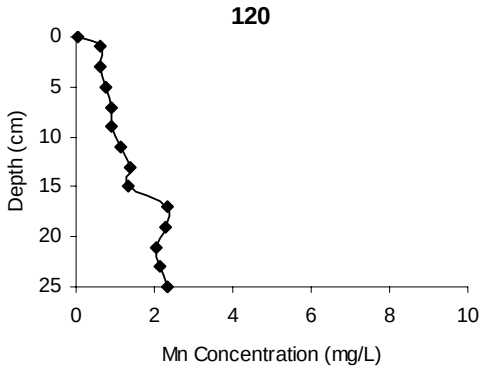
120
Depth (cm)
0
5
10
15
20
25
0
2
4
6
8
10
Mn Concentration (mg/L)

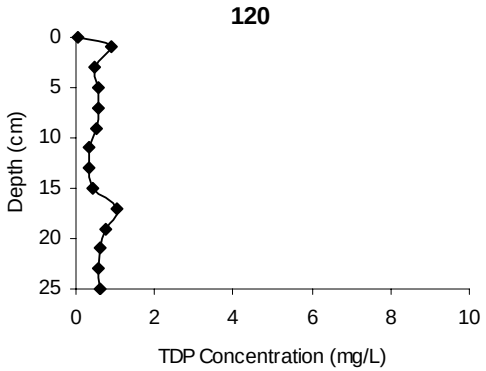
120
Depth (cm)
0
5
10
15
20
25
0
2
4
6
8
10
TDP Concentration (mg/L)

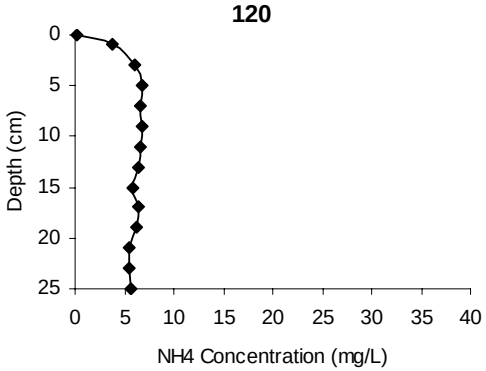
120
Depth (cm)
0
5
10
15
20
25
0
5
10
15
20
25
30
35
40
NH4 Concentration (mg/L)

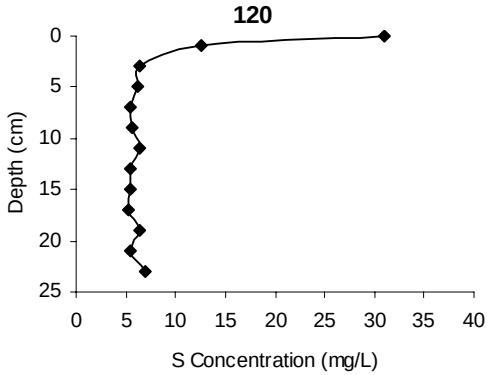
120
Depth (cm)
0
5
10
15
20
25
0
5
10
15
20
25
30
35
40
S Concentration (mg/L)

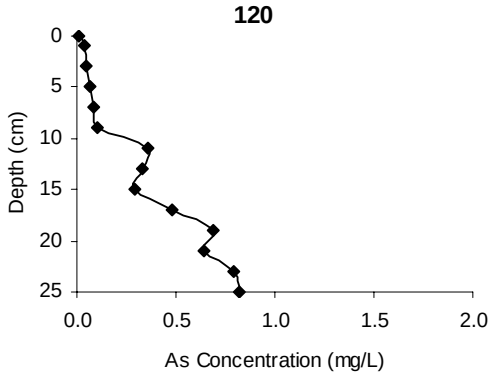
120
Depth (cm)
0
5
10
15
20
25
0.0
0.5
1.0
1.5
2.0
As Concentration (mg/L)

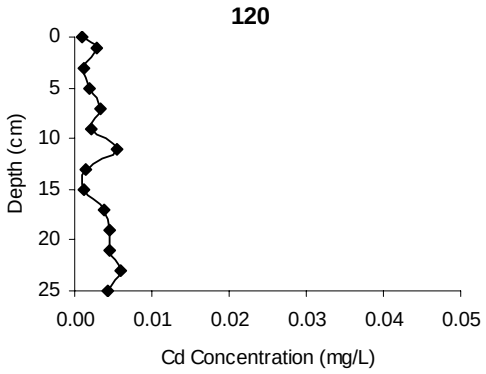
120
Depth (cm)
0
5
10
15
20
25
0.00
0.01
0.02
0.03
0.04
0.05
Cd Concentration (mg/L)

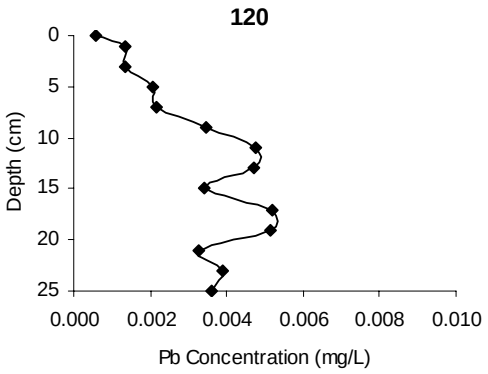
120
Depth (cm)
0
5
10
15
20
25
0.000
0.002
0.004
0.006
0.008
0.010
Pb Concentration (mg/L)

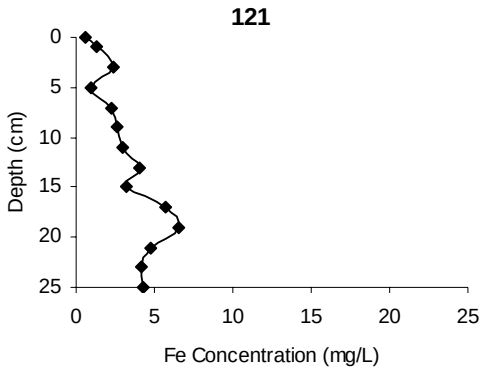
121
Depth (cm)
0
5
10
15
20
25
0
5
10
15
20
25
Fe Concentration (mg/L)

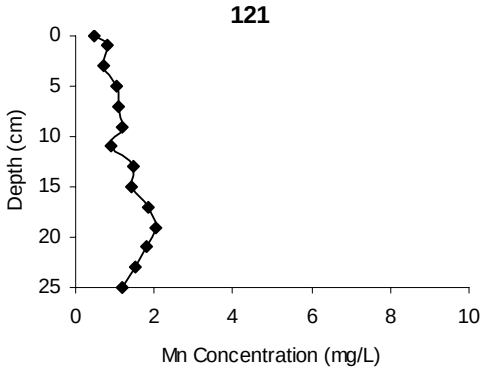
121
Depth (cm)
0
5
10
15
20
25
0
2
4
6
8
10
Mn Concentration (mg/L)

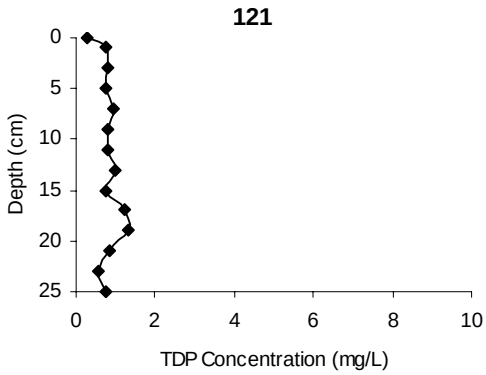
121
Depth (cm)
0
5
10
15
20
25
0
2
4
6
8
10
TDP Concentration (mg/L)

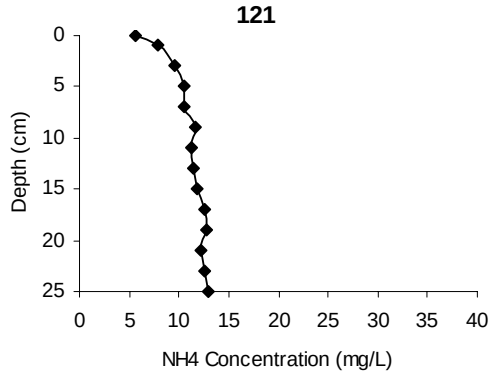
121
Depth (cm)
0
5
10
15
20
25
0
5
10
15
20
25
30
35
40
NH4 Concentration (mg/L)

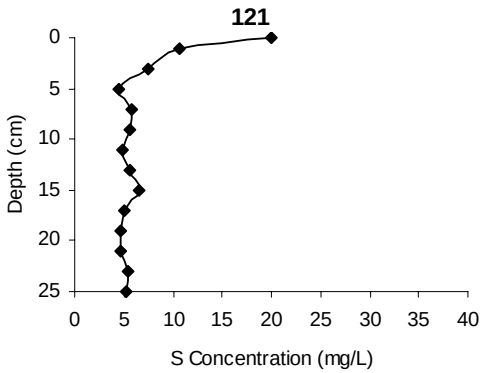
121
Depth (cm)
0
5
10
15
20
25
0
5
10
15
20
25
30
35
40
S Concentration (mg/L)

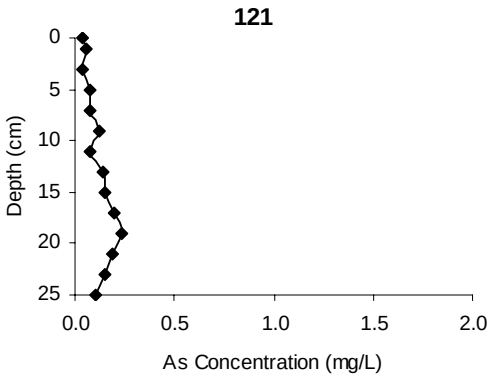
121
Depth (cm)
0
5
10
15
20
25
0.0
0.5
1.0
1.5
2.0
As Concentration (mg/L)

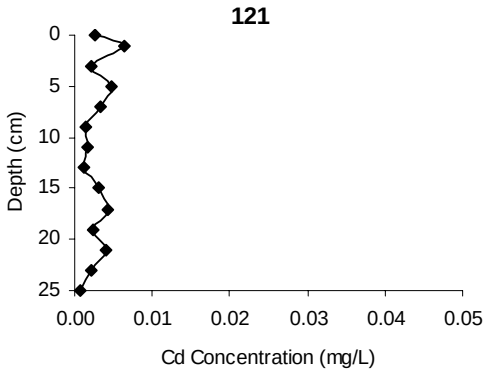
121
Depth (cm)
0
5
10
15
20
25
0.00
0.01
0.02
0.03
0.04
0.05
Cd Concentration (mg/L)

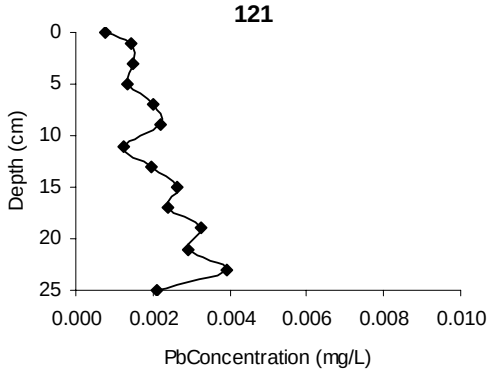
121
Depth (cm)
0
5
10
15
20
25
0.000
0.002
0.004
0.006
0.008
0.010
PbConcentration (mg/L)

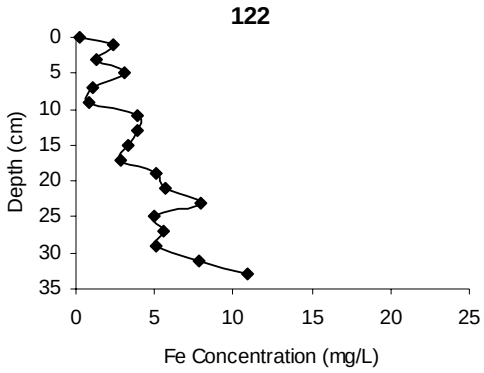
122
Depth (cm)
0
5
10
15
20
25
30
35
0
5
10
15
20
25
Fe Concentration (mg/L)

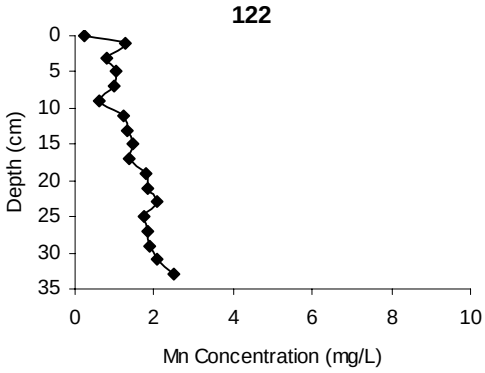
122
Depth (cm)
0
5
10
15
20
25
30
35
0
2
4
6
8
10
Mn Concentration (mg/L)

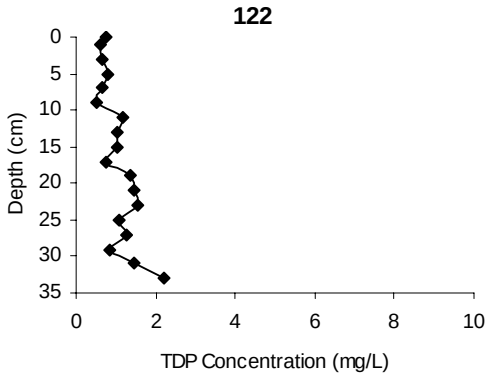
122
Depth (cm)
0
5
10
15
20
25
30
35
0
2
4
6
8
10
TDP Concentration (mg/L)

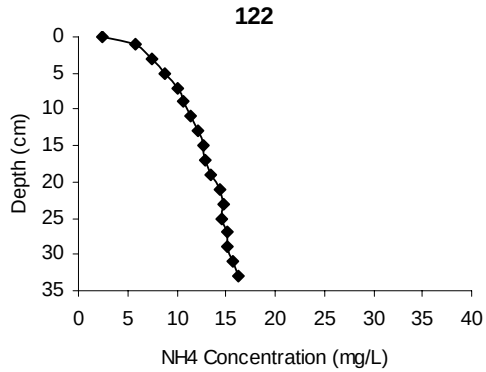
122
Depth (cm)
0
5
10
15
20
25
30
35
0
5
10
15
20
25
30
35
40
NH4 Concentration (mg/L)

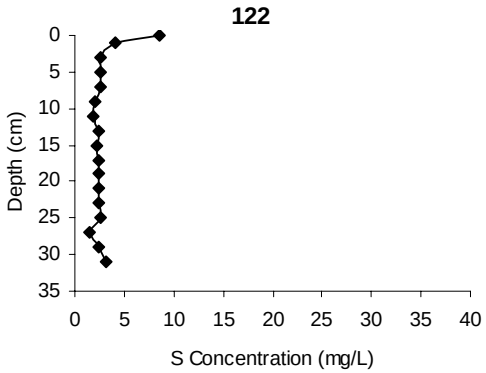
122
Depth (cm)
0
5
10
15
20
25
30
35
0
5
10
15
20
25
30
35
40
S Concentration (mg/L)

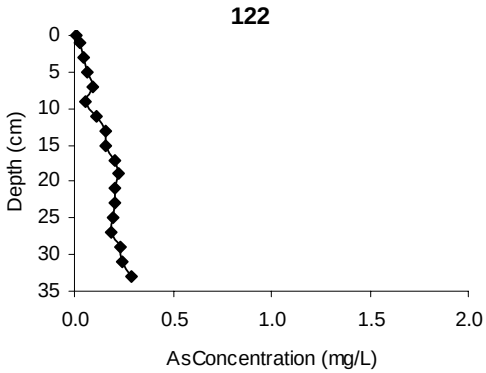
122
Depth (cm)
0
5
10
15
20
25
30
35
0.0
0.5
1.0
1.5
2.0
AsConcentration (mg/L)

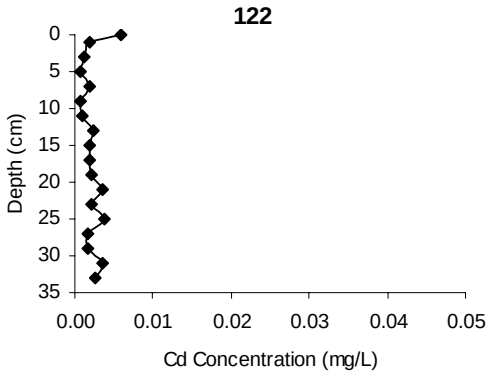
122
Depth (cm)
0
5
10
15
20
25
30
35
0.00
0.01
0.02
0.03
0.04
0.05
Cd Concentration (mg/L)

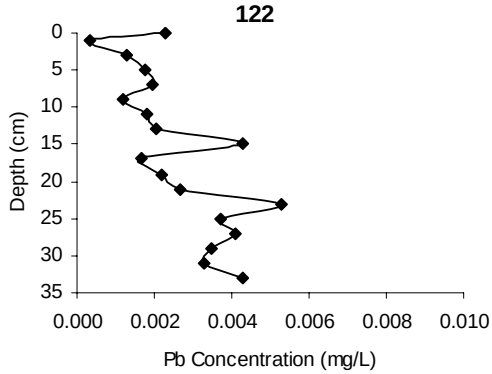
122
Depth (cm)
0
5
10
15
20
25
30
35
0.000
0.002
0.004
0.006
0.008
0.010
Pb Concentration (mg/L)

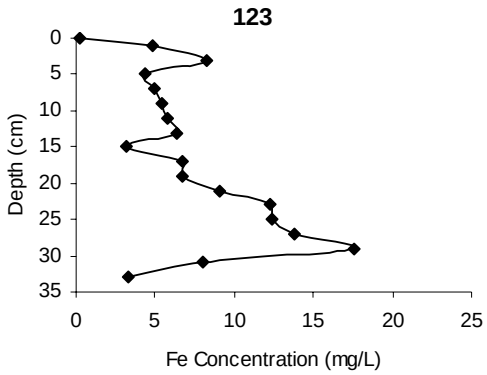
123
Depth (cm)
0
5
10
15
20
25
30
35
0
5
10
15
20
25
Fe Concentration (mg/L)

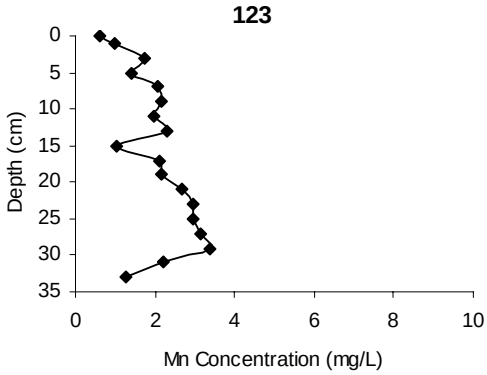
123
Depth (cm)
0
5
10
15
20
25
30
35
0
2
4
6
8
10
Mn Concentration (mg/L)

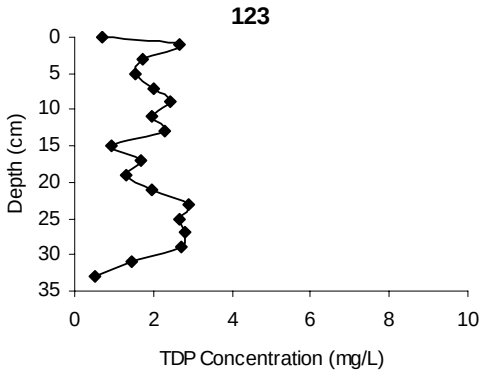
123
Depth (cm)
0
5
10
15
20
25
30
35
0
2
4
6
8
10
TDP Concentration (mg/L)

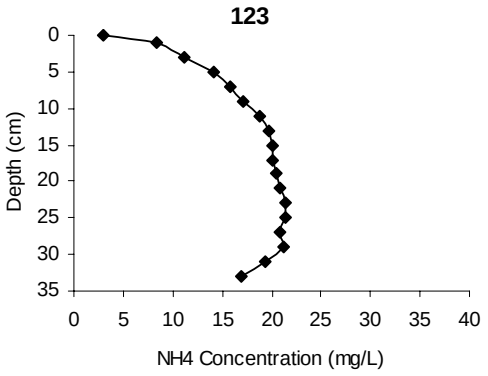
123
Depth (cm)
0
5
10
15
20
25
30
35
0
5
10
15
20
25
30
35
40
NH4 Concentration (mg/L)

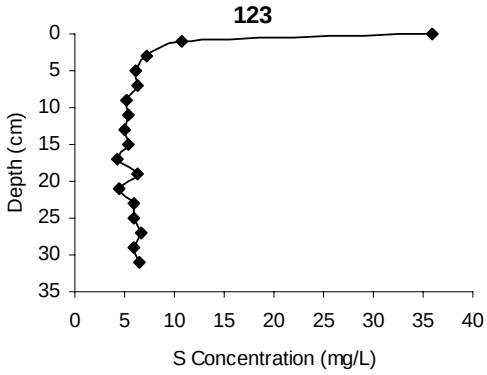
123
Depth (cm)
0
5
10
15
20
25
30
35
0
5
10
15
20
25
30
35
40
S Concentration (mg/L)

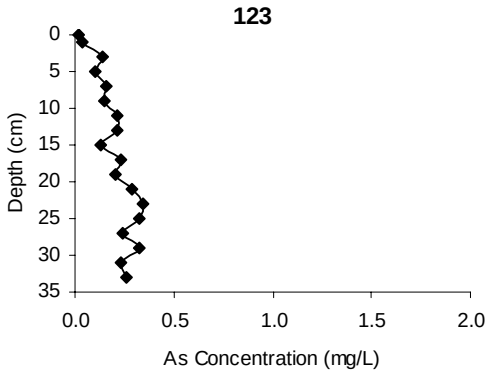
123
Depth (cm)
0
5
10
15
20
25
30
35
0.0
0.5
1.0
1.5
2.0
As Concentration (mg/L)

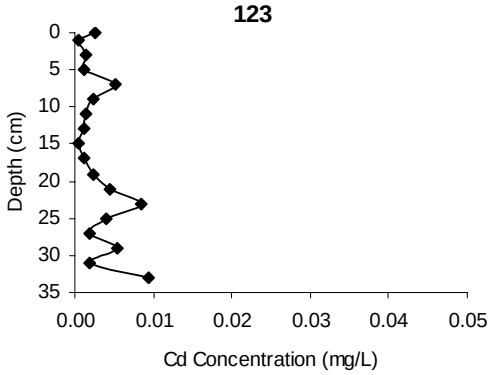
123
Depth (cm)
0
5
10
15
20
25
30
35
0.00
0.01
0.02
0.03
0.04
0.05
Cd Concentration (mg/L)

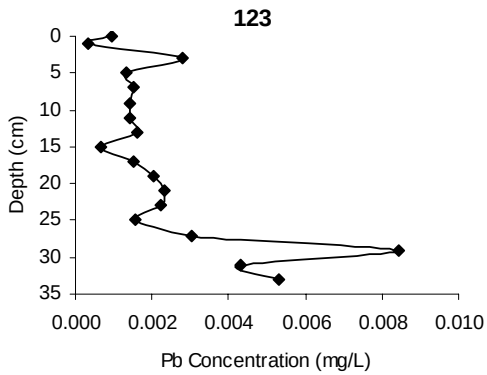
123
Depth (cm)
0
5
10
15
20
25
30
35
0.000
0.002
0.004
0.006
0.008
0.010
Pb Concentration (mg/L)

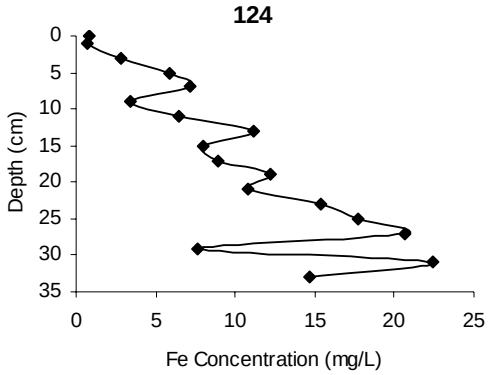
124
Depth (cm)
0
5
10
15
20
25
30
35
0
5
10
15
20
25
Fe Concentration (mg/L)

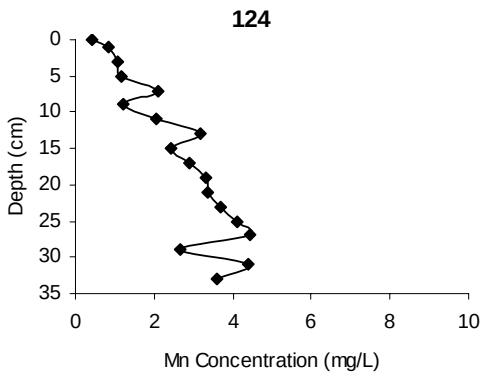
124
Depth (cm)
0
5
10
15
20
25
30
35
0
2
4
6
8
10
Mn Concentration (mg/L)

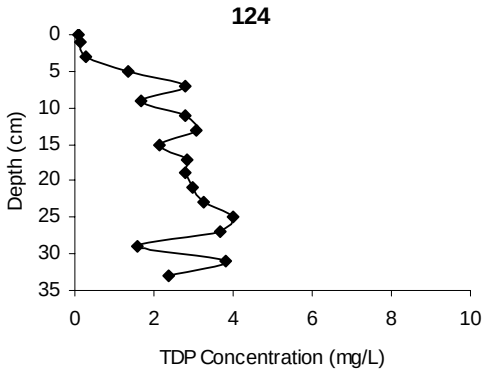
124
Depth (cm)
0
5
10
15
20
25
30
35
0
2
4
6
8
10
TDP Concentration (mg/L)

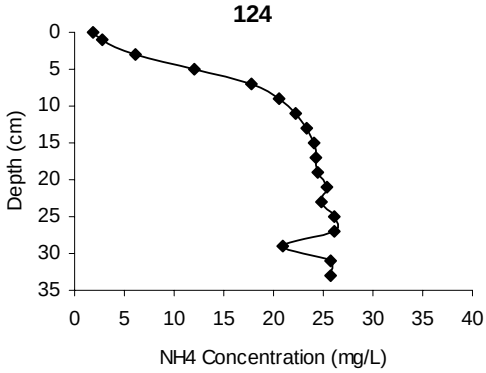
124
Depth (cm)
0
5
10
15
20
25
30
35
0
5
10
15
20
25
30
35
40
NH4 Concentration (mg/L)

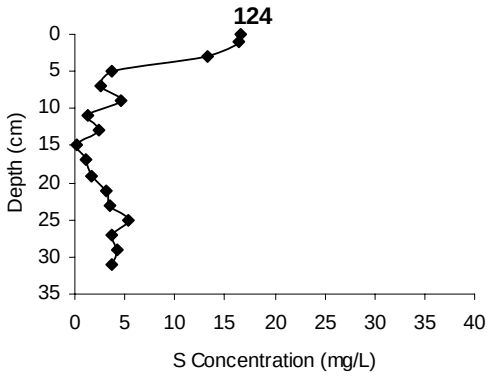
124
Depth (cm)
0
5
10
15
20
25
30
35
0
5
10
15
20
25
30
35
40
S Concentration (mg/L)

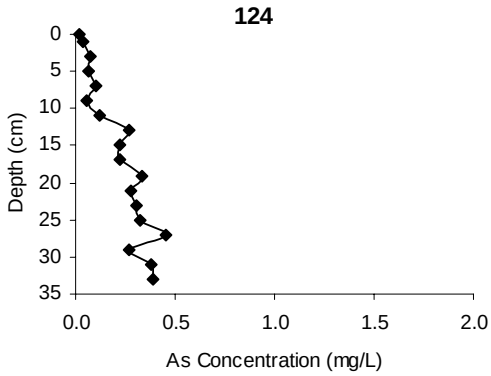
124
Depth (cm)
0
5
10
15
20
25
30
35
0.0
0.5
1.0
1.5
2.0
As Concentration (mg/L)

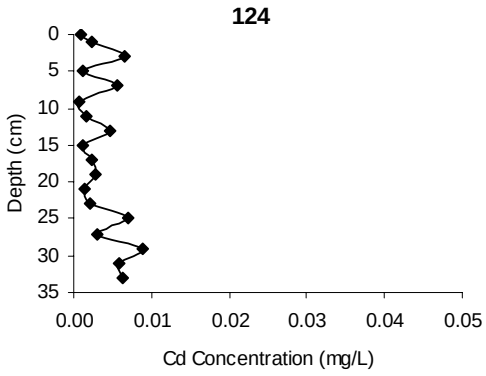
124
Depth (cm)
0
5
10
15
20
25
30
35
0.00
0.01
0.02
0.03
0.04
0.05
Cd Concentration (mg/L)

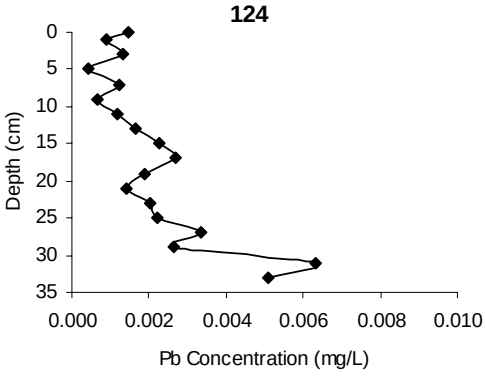
124
Depth (cm)
0
5
10
15
20
25
30
35
0.000
0.002
0.004
0.006
0.008
0.010
Pb Concentration (mg/L)

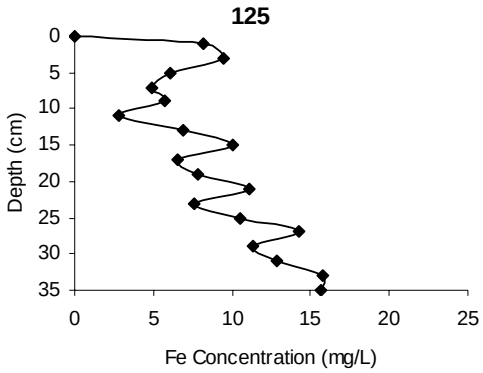
125
Depth (cm)
0
5
10
15
20
25
30
35
0
5
10
15
20
25
Fe Concentration (mg/L)

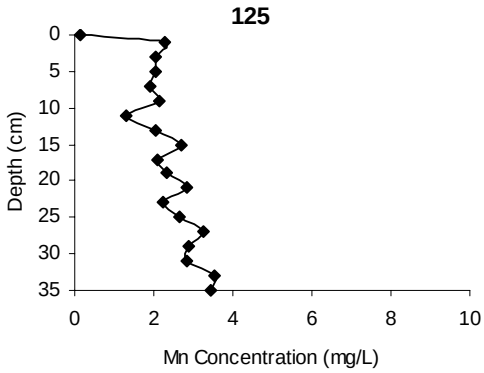
125
Depth (cm)
0
5
10
15
20
25
30
35
0
2
4
6
8
10
Mn Concentration (mg/L)

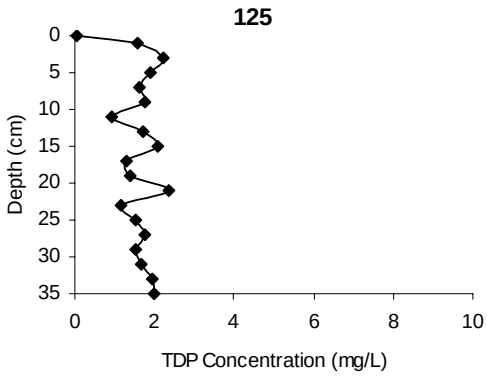
125
Depth (cm)
0
5
10
15
20
25
30
35
0
2
4
6
8
10
TDP Concentration (mg/L)

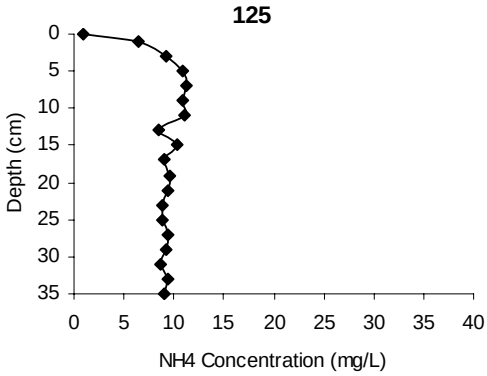
125
Depth (cm)
0
5
10
15
20
25
30
35
0
5
10
15
20
25
30
35
40
NH4 Concentration (mg/L)

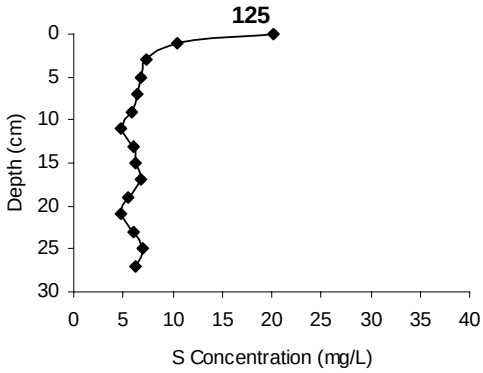
125
Depth (cm)
0
5
10
15
20
25
30
0
5
10
15
20
25
30
35
40
S Concentration (mg/L)

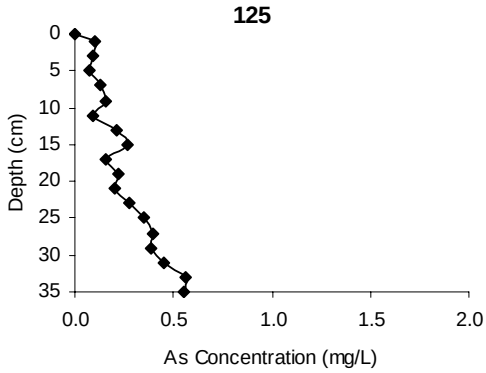
125
Depth (cm)
0
5
10
15
20
25
30
35
0.0
0.5
1.0
1.5
2.0
As Concentration (mg/L)

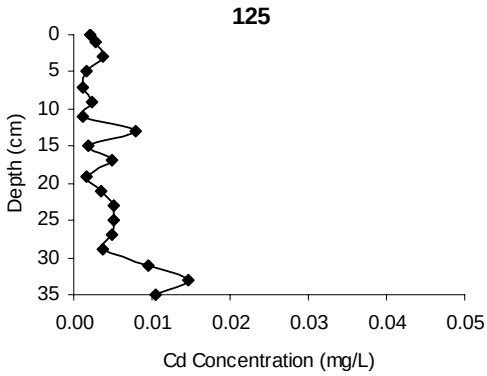
125
Depth (cm)
0
5
10
15
20
25
30
35
0.00
0.01
0.02
0.03
0.04
0.05
Cd Concentration (mg/L)

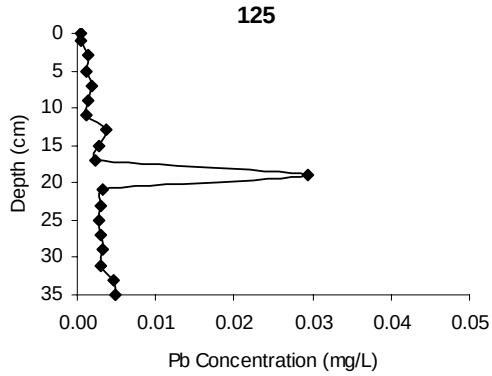
125
Depth (cm)
0
5
10
15
20
25
30
35
0.00
0.01
0.02
0.03
0.04
0.05
Pb Concentration (mg/L)

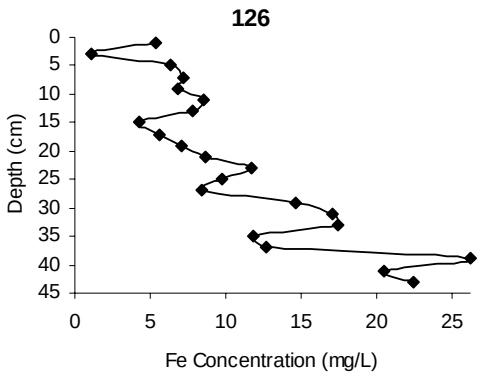
126
Depth (cm)
Fe Concentration (mg/L)

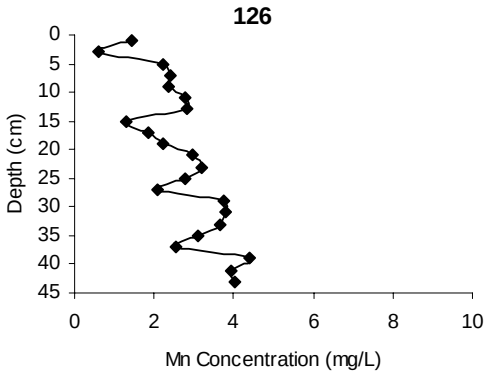
126
Depth (cm)
Mn Concentration (mg/L)

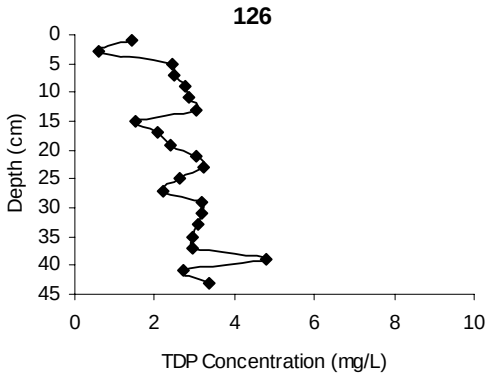
126
Depth (cm)
TDP Concentration (mg/L)

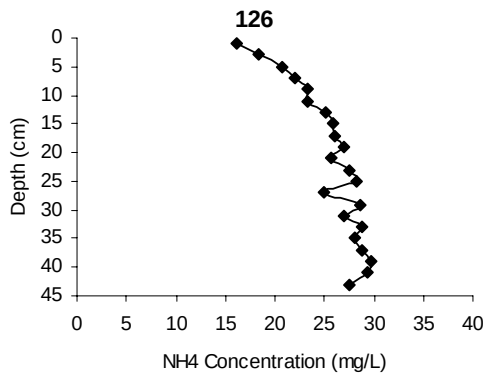
126
Depth (cm)
NH4 Concentration (mg/L)

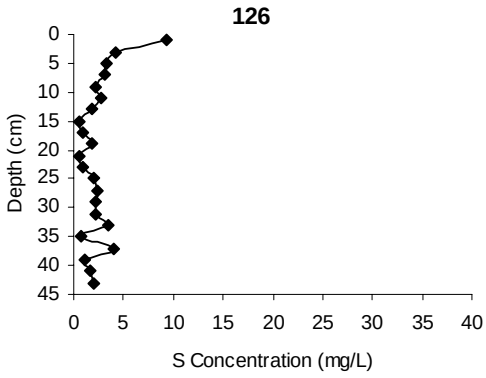
126
Depth (cm)
S Concentration (mg/L)

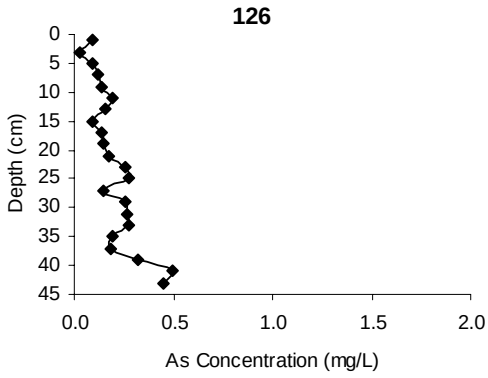
126
Depth (cm)
As Concentration (mg/L)

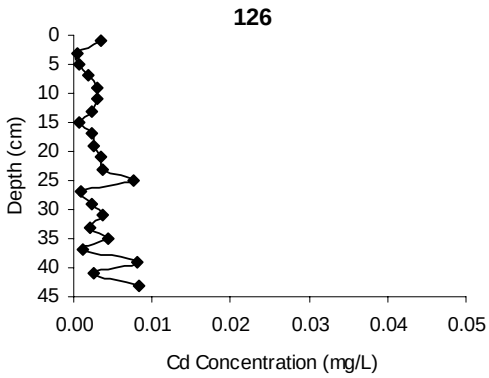
126
Depth (cm)
Cd Concentration (mg/L)

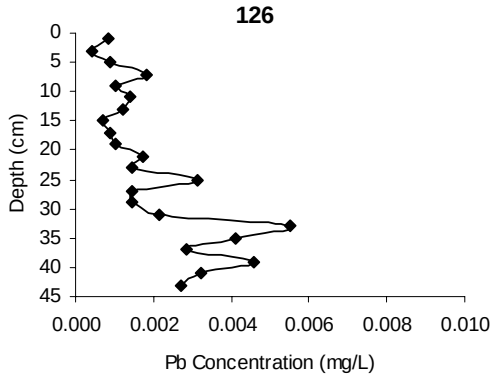
126
Depth (cm)
Pb Concentration (mg/L)

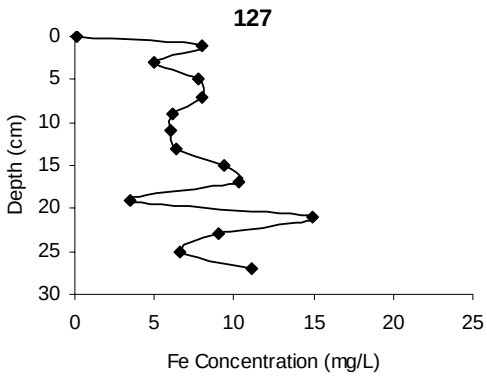
127
Depth (cm)
0
5
10
15
20
25
30
0
5
10
15
20
25
Fe Concentration (mg/L)

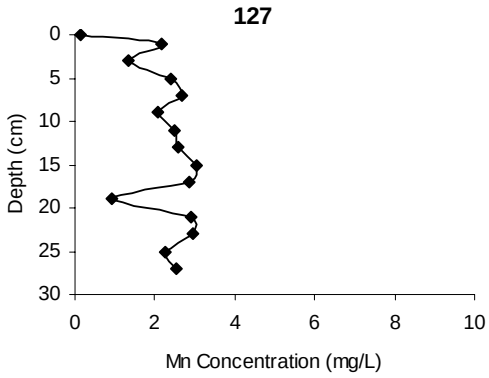
127
Depth (cm)
0
5
10
15
20
25
30
0
2
4
6
8
10
Mn Concentration (mg/L)

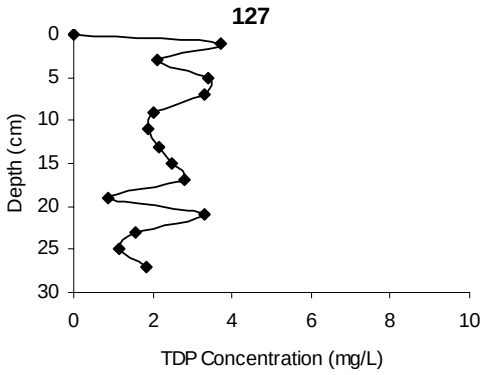
127
Depth (cm)
0
5
10
15
20
25
30
0
2
4
6
8
10
TDP Concentration (mg/L)

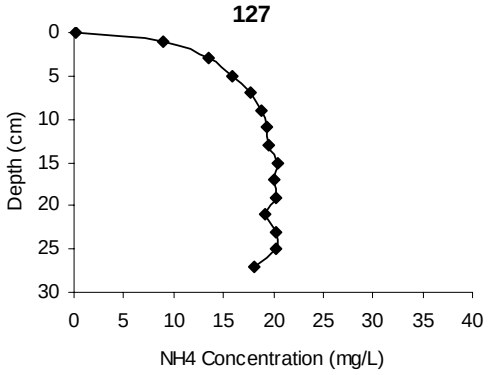
127
Depth (cm)
0
5
10
15
20
25
30
0
5
10
15
20
25
30
35
40
NH4 Concentration (mg/L)

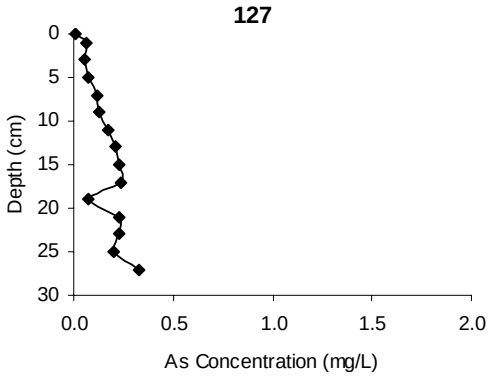
127
Depth (cm)
0
5
10
15
20
25
30
0.0
0.5
1.0
1.5
2.0
As Concentration (mg/L)

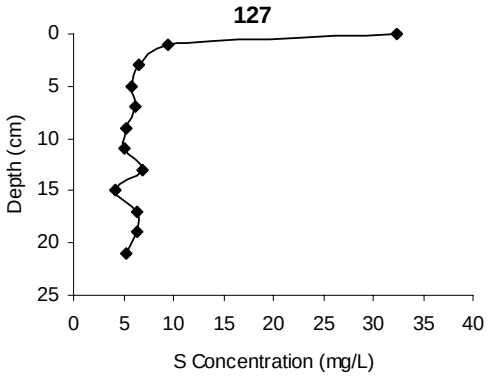
127
Depth (cm)
0
5
10
15
20
25
0
5
10
15
20
25
30
35
40
S Concentration (mg/L)

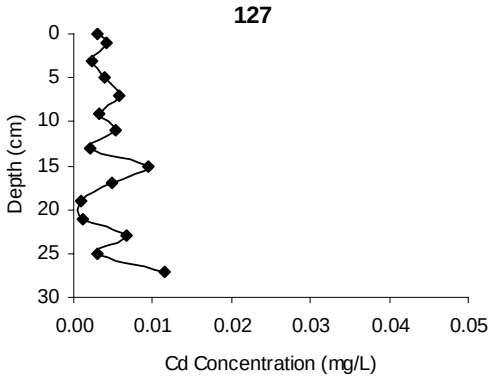
127
Depth (cm)
0
5
10
15
20
25
30
0.00
0.01
0.02
0.03
0.04
0.05
Cd Concentration (mg/L)

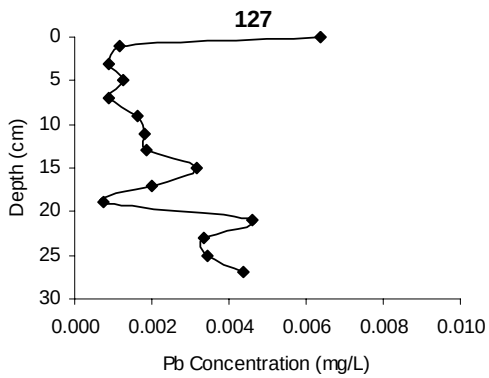
127
Depth (cm)
0
5
10
15
20
25
30
0.000
0.002
0.004
0.006
0.008
0.010
Pb Concentration (mg/L)

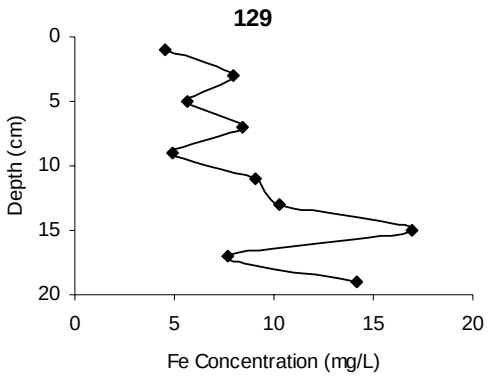
129
Depth (cm)
0
5
10
15
20
0
5
10
15
20
Fe Concentration (mg/L)

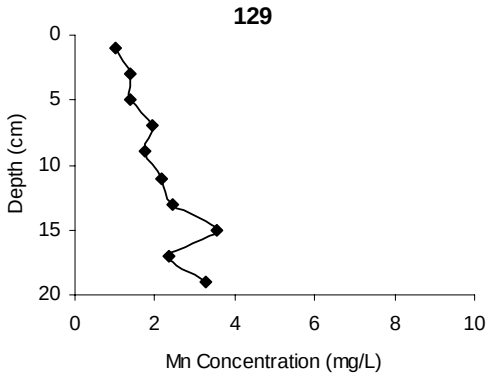
129
Depth (cm)
0
5
10
15
20
0
2
4
6
8
10
Mn Concentration (mg/L)

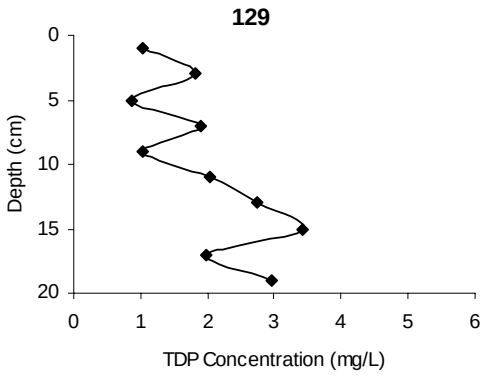
129
Depth (cm)
0
5
10
15
20
0
1
2
3
4
5
6
TDP Concentration (mg/L)

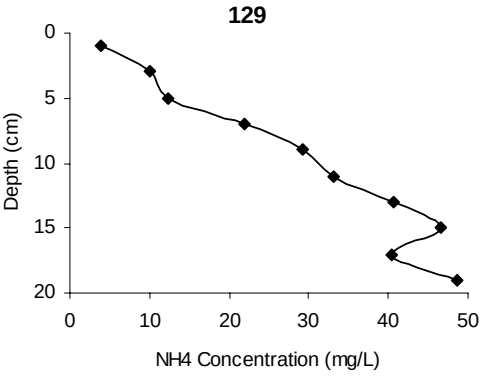
129
Depth (cm)
0
5
10
15
20
0
10
20
30
40
50
NH4 Concentration (mg/L)

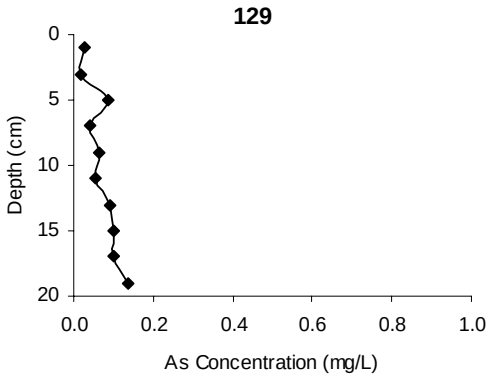
129
Depth (cm)
0
5
10
15
20
0.0
0.2
0.4
0.6
0.8
1.0
As Concentration (mg/L)

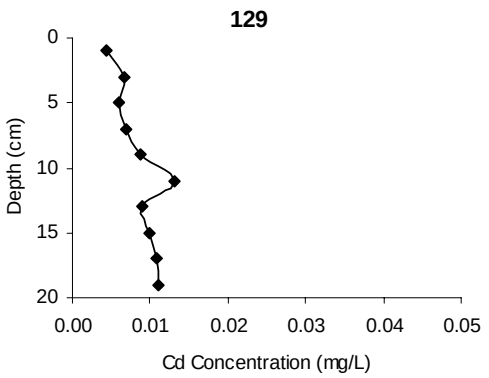
129
Depth (cm)
0
5
10
15
20
0.00
0.01
0.02
0.03
0.04
0.05
Cd Concentration (mg/L)

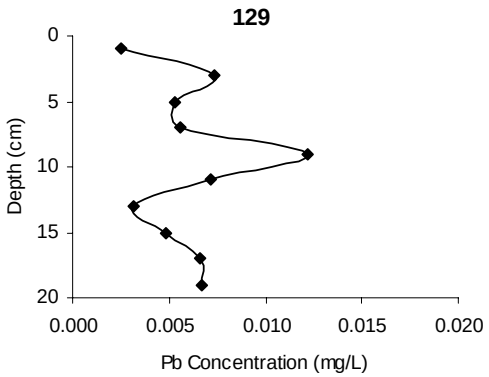
129
Depth (cm)
0
5
10
15
20
0.000
0.005
0.010
0.015
0.020
Pb Concentration (mg/L)

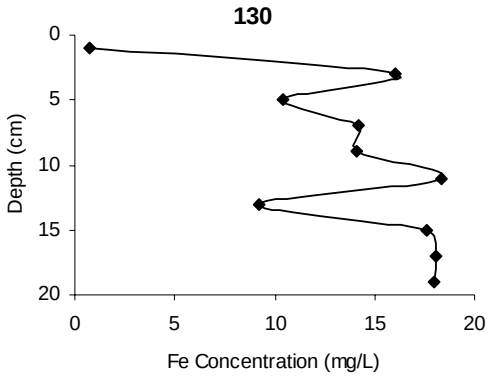
130
Depth (cm)
0
5
10
15
20
0
5
10
15
20
Fe Concentration (mg/L)

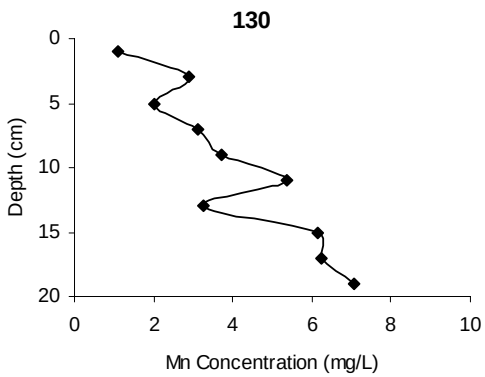
130
Depth (cm)
0
5
10
15
20
0
2
4
6
8
10
Mn Concentration (mg/L)

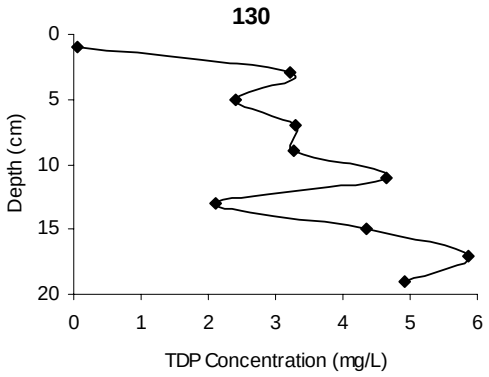
130
Depth (cm)
0
5
10
15
20
0
1
2
3
4
5
6
TDP Concentration (mg/L)

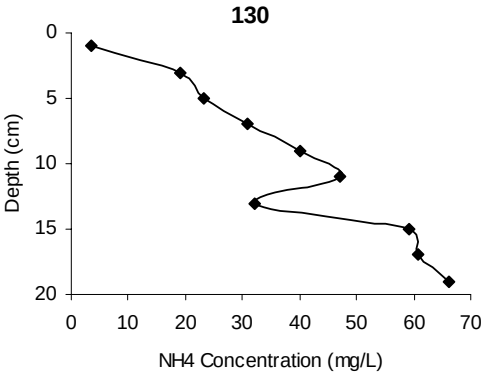
130
Depth (cm)
0
5
10
15
20
0
10
20
30
40
50
60
70
NH4 Concentration (mg/L)

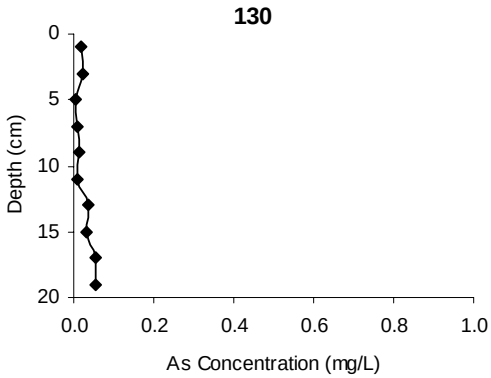
130
Depth (cm)
0
5
10
15
20
0.0
0.2
0.4
0.6
0.8
1.0
As Concentration (mg/L)

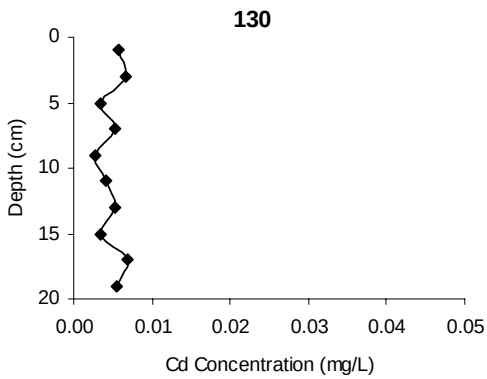
130
Depth (cm)
0
5
10
15
20
0.00
0.01
0.02
0.03
0.04
0.05
Cd Concentration (mg/L)

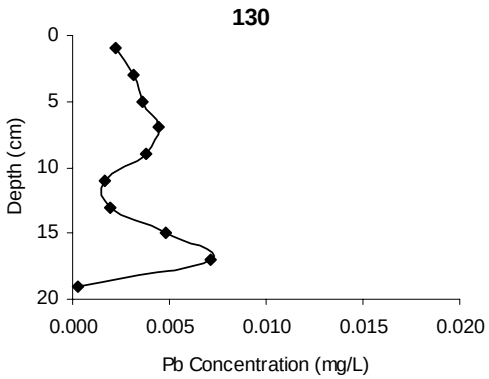
130
Depth (cm)
0
5
10
15
20
0.000
0.005
0.010
0.015
0.020
Pb Concentration (mg/L)

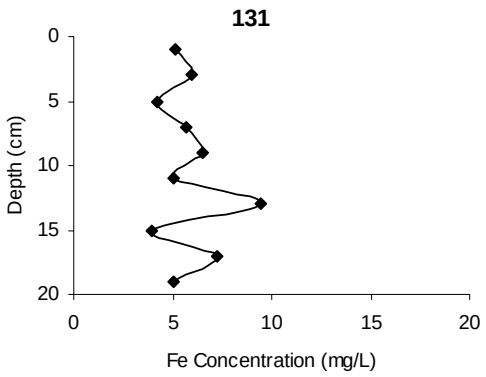
131
Depth (cm)
0
5
10
15
20
0
5
10
15
20
Fe Concentration (mg/L)

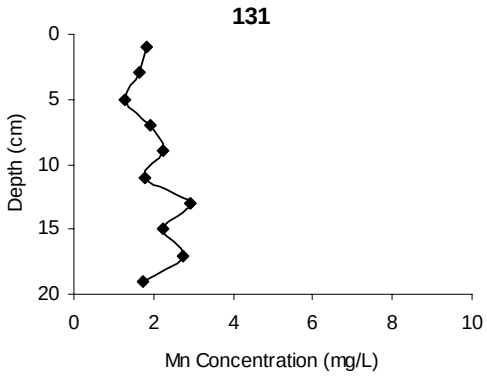
131
Depth (cm)
0
5
10
15
20
0
2
4
6
8
10
Mn Concentration (mg/L)

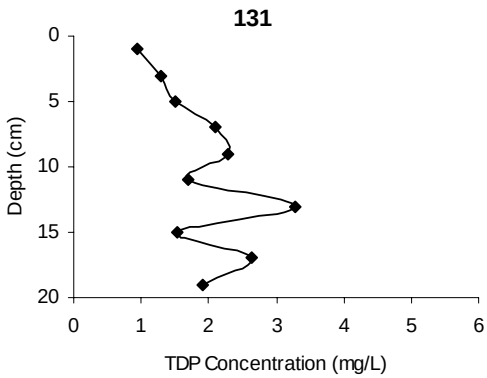
131
Depth (cm)
0
5
10
15
20
0
1
2
3
4
5
6
TDP Concentration (mg/L)

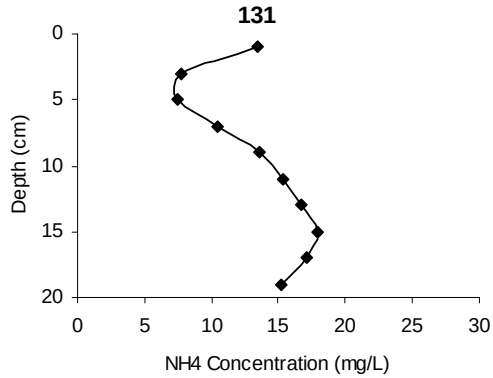
131
Depth (cm)
0
5
10
15
20
0
5
10
15
20
25
30
NH4 Concentration (mg/L)

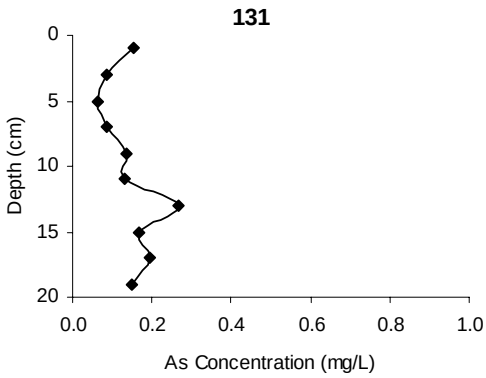
131
Depth (cm)
0
5
10
15
20
0.0
0.2
0.4
0.6
0.8
1.0
As Concentration (mg/L)

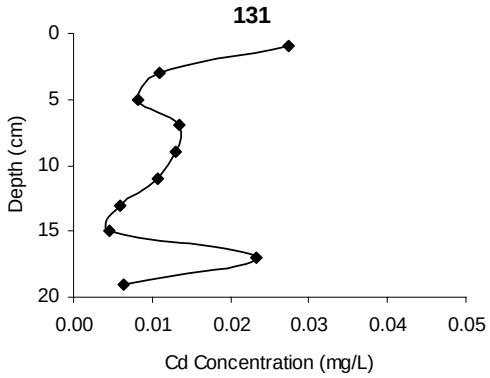
131
Depth (cm)
0
5
10
15
20
0.00
0.01
0.02
0.03
0.04
0.05
Cd Concentration (mg/L)

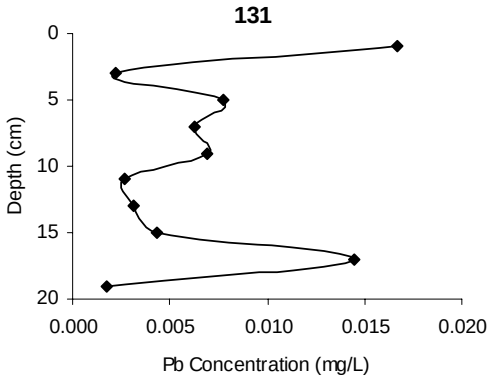
131
Depth (cm)
0
5
10
15
20
0.000
0.005
0.010
0.015
0.020
Pb Concentration (mg/L)

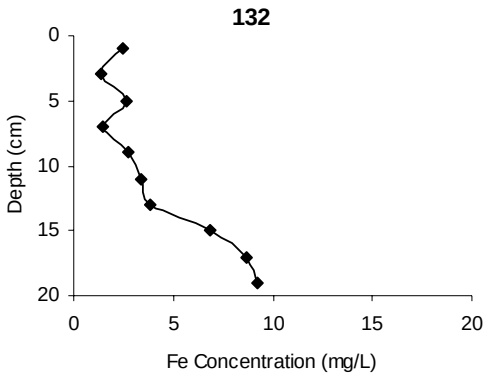
132
Depth (cm)
0
5
10
15
20
0
5
10
15
20
Fe Concentration (mg/L)

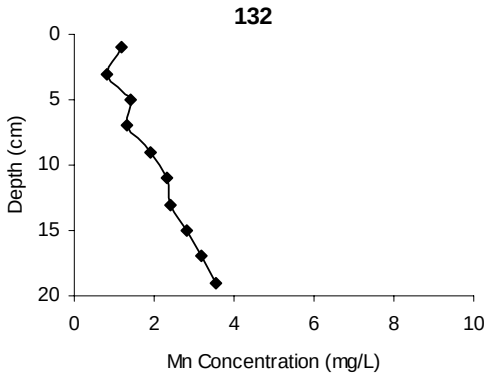
132
Depth (cm)
0
5
10
15
20
0
2
4
6
8
10
Mn Concentration (mg/L)

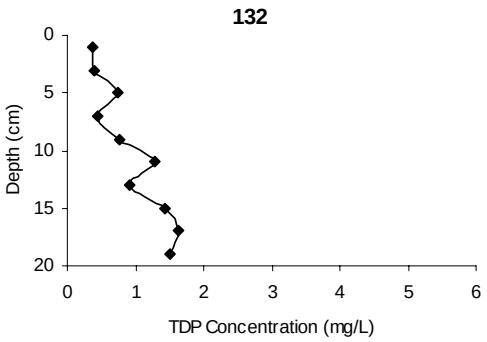
132
Depth (cm)
0
5
10
15
20
0
1
2
3
4
5
6
TDP Concentration (mg/L)

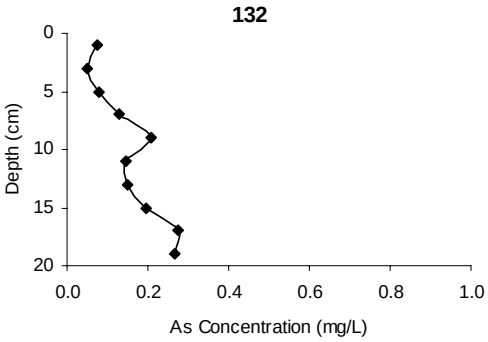
132
Depth (cm)
0
5
10
15
20
0.0
0.2
0.4
0.6
0.8
1.0
As Concentration (mg/L)

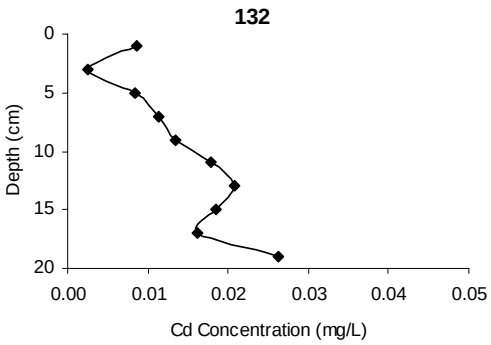
132
Depth (cm)
0
5
10
15
20
0.00
0.01
0.02
0.03
0.04
0.05
Cd Concentration (mg/L)

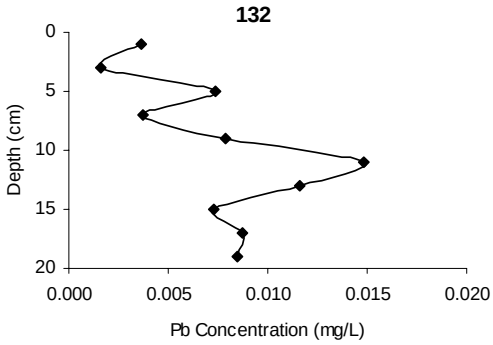
132
Depth (cm)
0
5
10
15
20
0.000
0.005
0.010
0.015
0.020
Pb Concentration (mg/L)

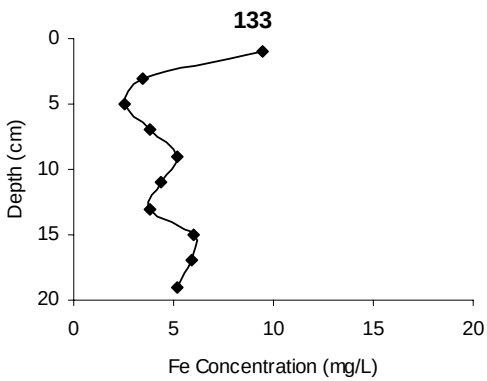
133
Depth (cm)
0
5
10
15
20
0
5
10
15
20
Fe Concentration (mg/L)

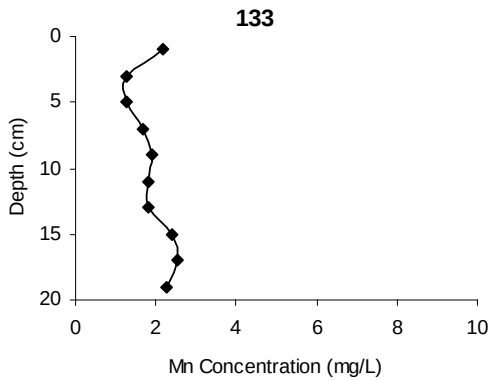
133
Depth (cm)
0
5
10
15
20
0
2
4
6
8
10
Mn Concentration (mg/L)

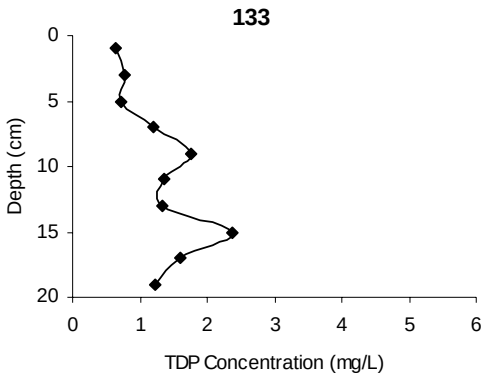
133
Depth (cm)
TDP Concentration (mg/L)

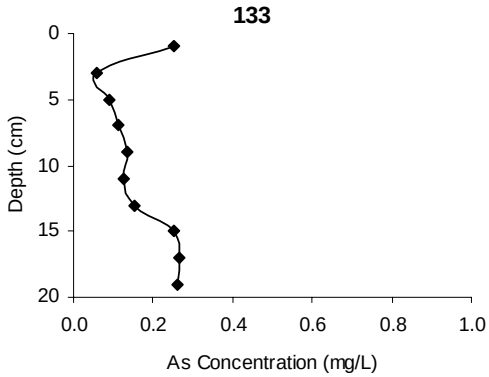
133
Depth (cm)
As Concentration (mg/L)

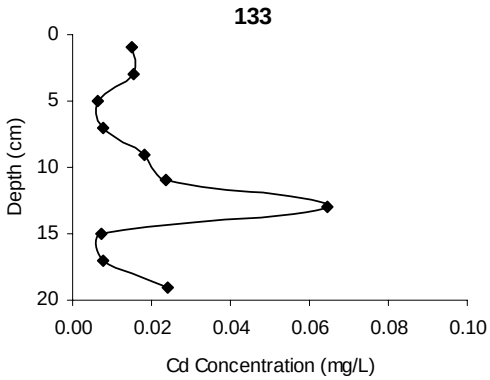
133
Depth (cm)
Cd Concentration (mg/L)

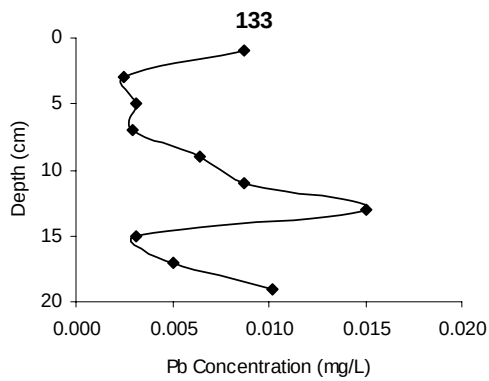
133
Depth (cm)
Pb Concentration (mg/L)

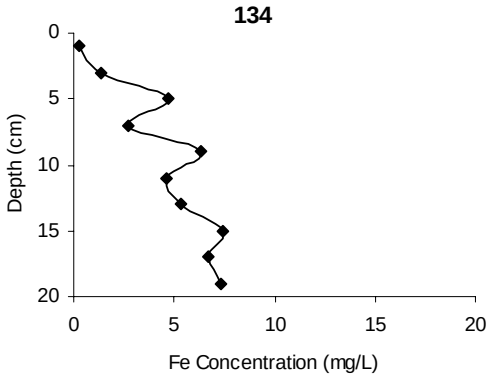
134
Depth (cm)
Fe Concentration (mg/L)

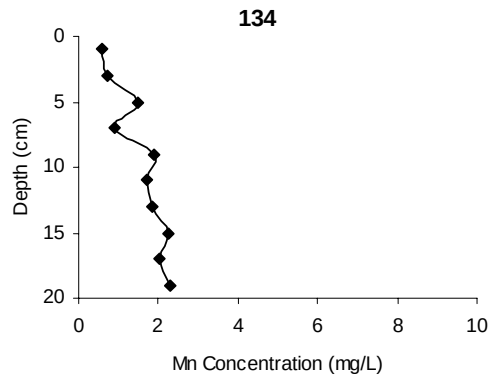
134
Depth (cm)
Mn Concentration (mg/L)

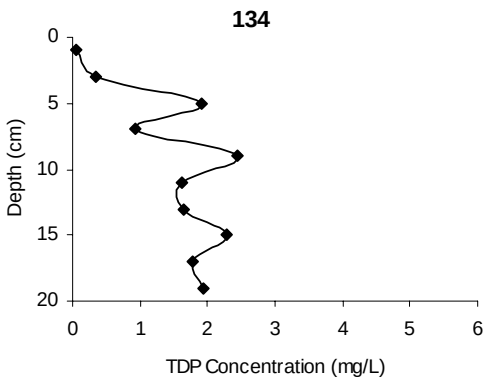
134
Depth (cm)
TDP Concentration (mg/L)

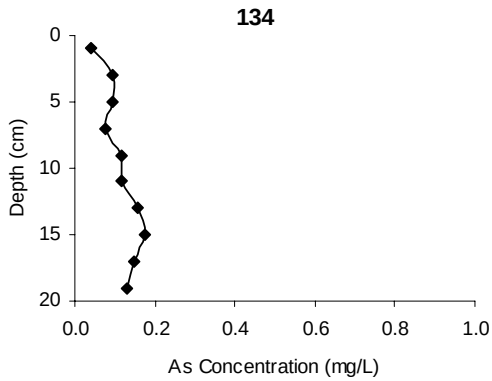
134
Depth (cm)
As Concentration (mg/L)

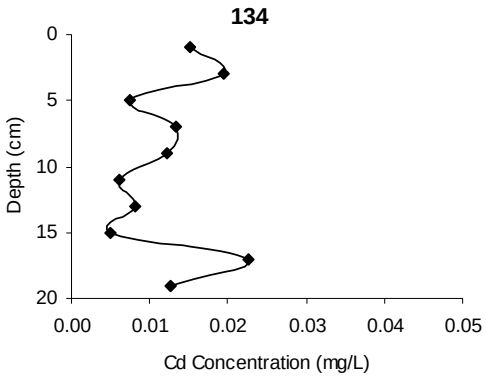
134
Depth (cm)
0
5
10
15
20
0.00
0.01
0.02
0.03
0.04
0.05
Cd Concentration (mg/L)

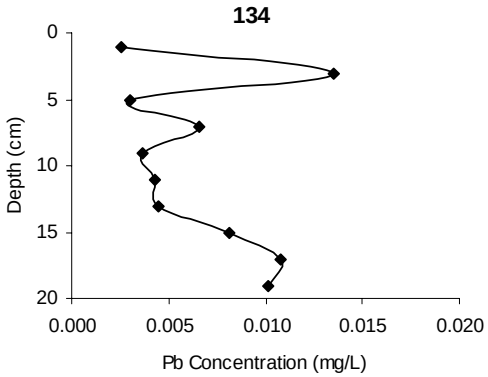
134
Depth (cm)
0
5
10
15
20
0.000
0.005
0.010
0.015
0.020
Pb Concentration (mg/L)

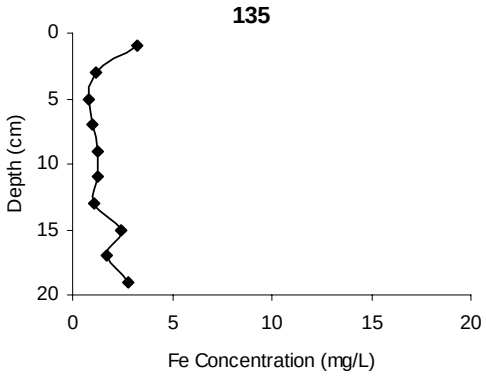
135
Depth (cm)
0
5
10
15
20
0
5
10
15
20
Fe Concentration (mg/L)

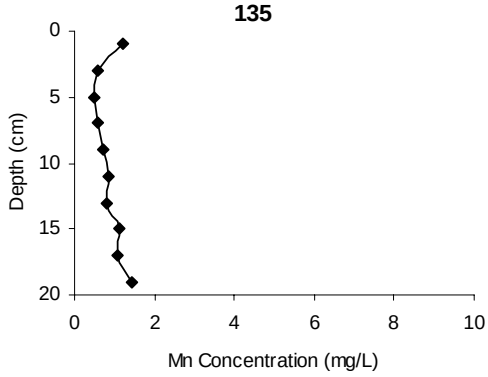
135
Depth (cm)
0
5
10
15
20
0
2
4
6
8
10
Mn Concentration (mg/L)

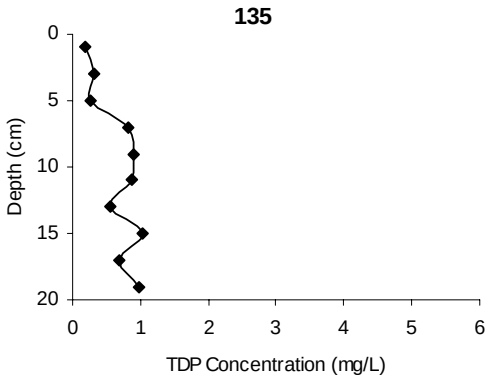
135
Depth (cm)
0
5
10
15
20
0
1
2
3
4
5
6
TDP Concentration (mg/L)

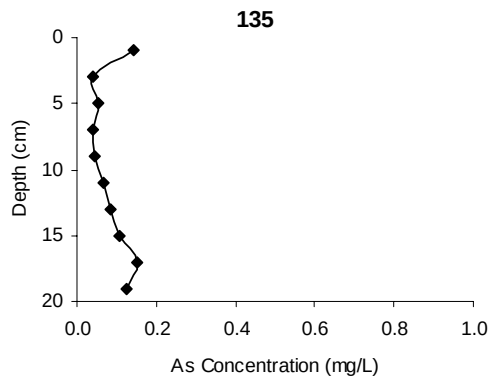
135
Depth (cm)
0
5
10
15
20
0.0
0.2
0.4
0.6
0.8
1.0
As Concentration (mg/L)

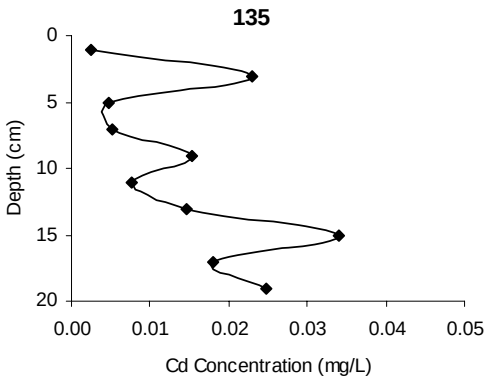
135
Depth (cm)
0
5
10
15
20
0.00
0.01
0.02
0.03
0.04
0.05
Cd Concentration (mg/L)

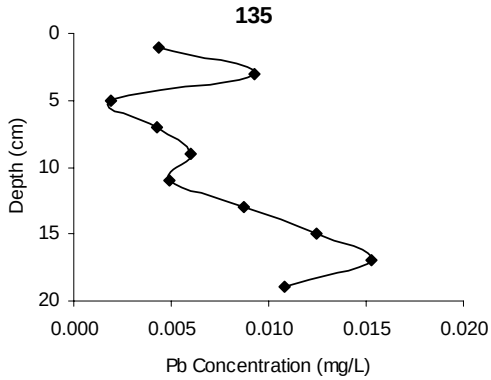
135
Depth (cm)
0
5
10
15
20
0.000
0.005
0.010
0.015
0.020
Pb Concentration (mg/L)

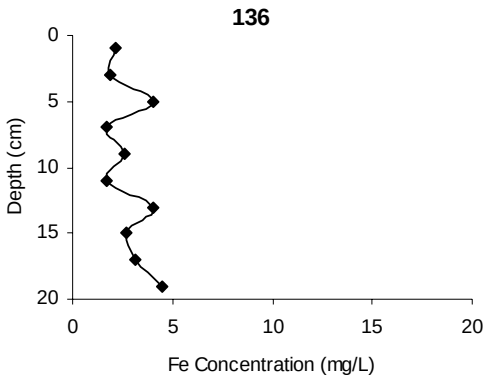
136
Depth (cm)
0
5
10
15
20
0
5
10
15
20
Fe Concentration (mg/L)

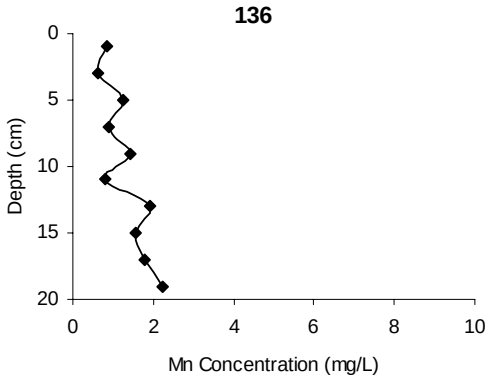
136
Depth (cm)
0
5
10
15
20
0
2
4
6
8
10
Mn Concentration (mg/L)

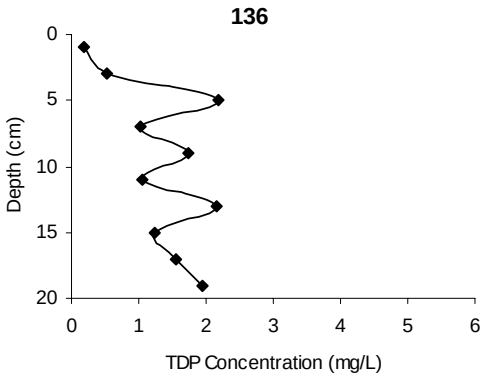
136
Depth (cm)
0
5
10
15
20
0
1
2
3
4
5
6
TDP Concentration (mg/L)

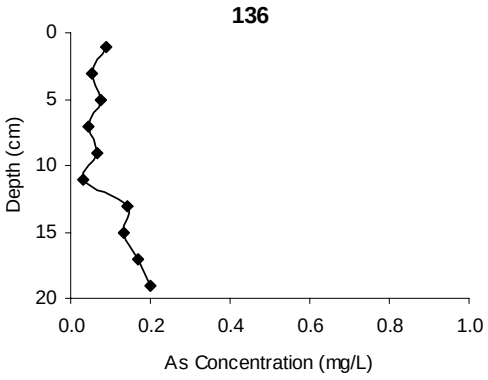
136
Depth (cm)
0
5
10
15
20
0.0
0.2
0.4
0.6
0.8
1.0
As Concentration (mg/L)

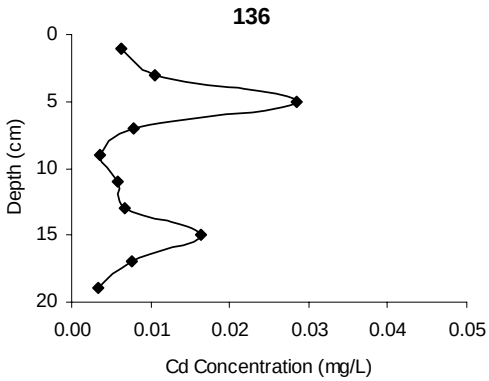
136
Depth (cm)
0
5
10
15
20
0.00
0.01
0.02
0.03
0.04
0.05
Cd Concentration (mg/L)

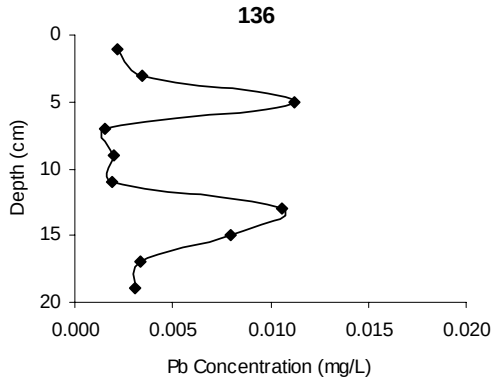
136
Depth (cm)
0
5
10
15
20
0.000
0.005
0.010
0.015
0.020
Pb Concentration (mg/L)

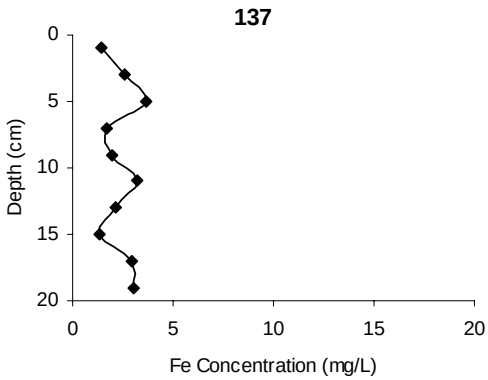
137
Depth (cm)
0
5
10
15
20
0
5
10
15
20
Fe Concentration (mg/L)

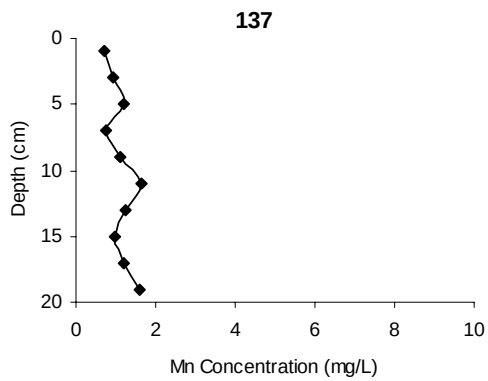
137
Depth (cm)
0
5
10
15
20
0
2
4
6
8
10
Mn Concentration (mg/L)

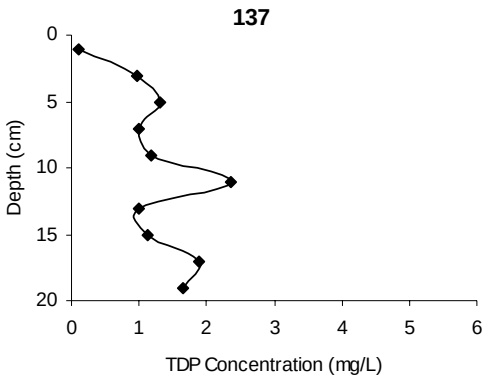
137
Depth (cm)
0
5
10
15
20
0
1
2
3
4
5
6
TDP Concentration (mg/L)

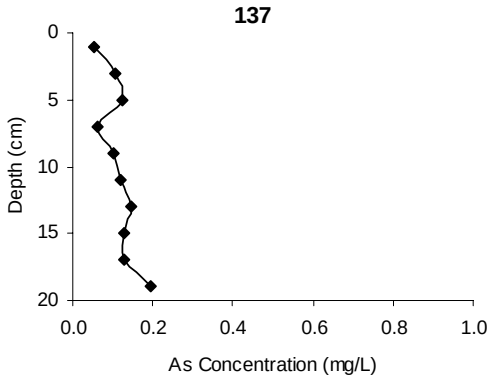
137
Depth (cm)
0
5
10
15
20
0.0
0.2
0.4
0.6
0.8
1.0
As Concentration (mg/L)

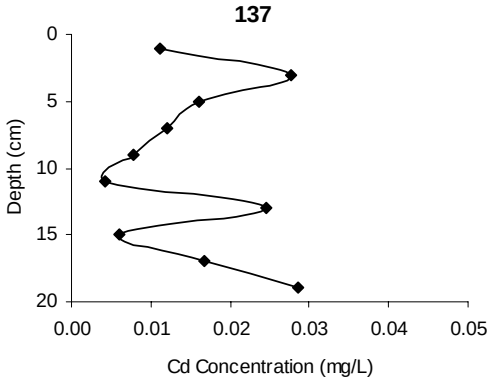
137
Depth (cm)
0
5
10
15
20
0.00
0.01
0.02
0.03
0.04
0.05
Cd Concentration (mg/L)

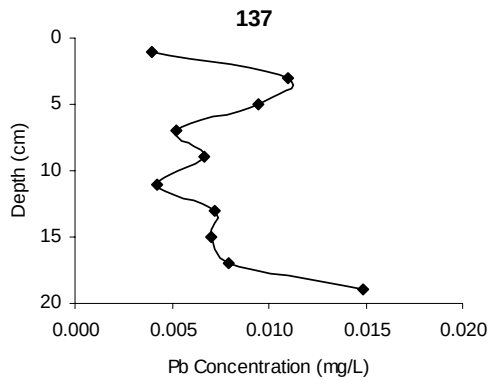
137
Depth (cm)
0
5
10
15
20
0.000
0.005
0.010
0.015
0.020
Pb Concentration (mg/L)

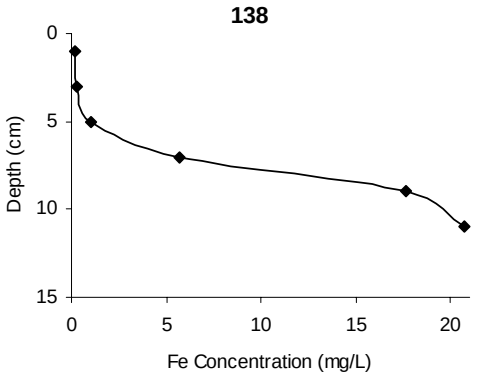
138
Depth (cm)
0
5
10
15
0
5
10
15
20
Fe Concentration (mg/L)

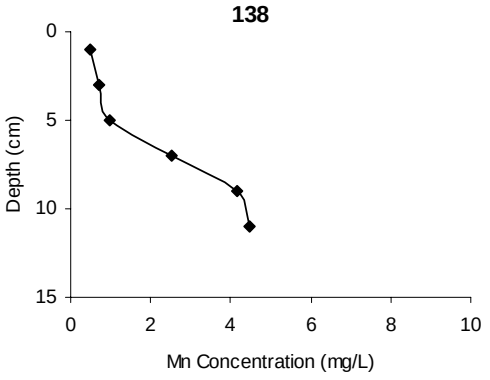
138
Depth (cm)
0
5
10
15
0
2
4
6
8
10
Mn Concentration (mg/L)

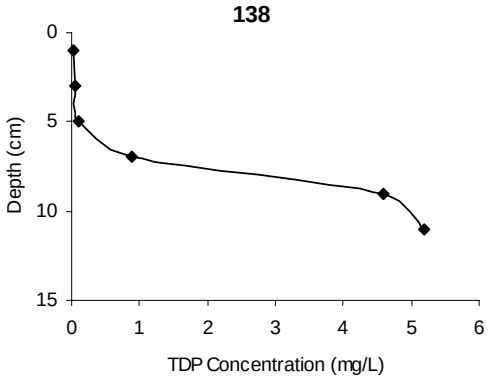
138
Depth (cm)
0
5
10
15
0
1
2
3
4
5
6
TDP Concentration (mg/L)

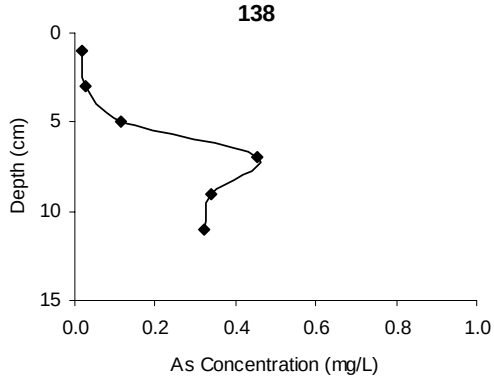
138
Depth (cm)
0
5
10
15
0.0
0.2
0.4
0.6
0.8
1.0
As Concentration (mg/L)

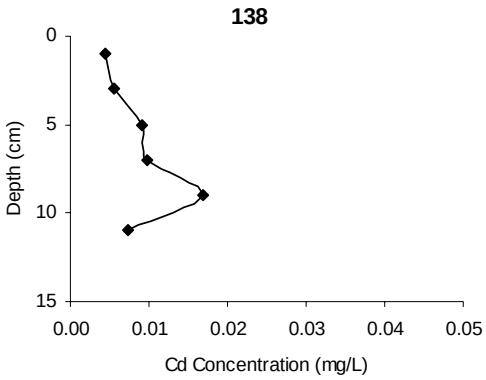
138
Depth (cm)
0
5
10
15
0.00
0.01
0.02
0.03
0.04
0.05
Cd Concentration (mg/L)

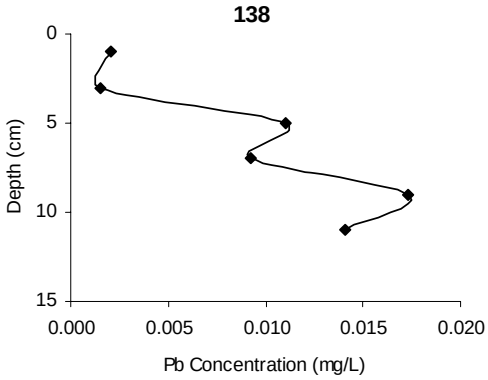
138
Depth (cm)
0
5
10
15
0.000
0.005
0.010
0.015
0.020
Pb Concentration (mg/L)

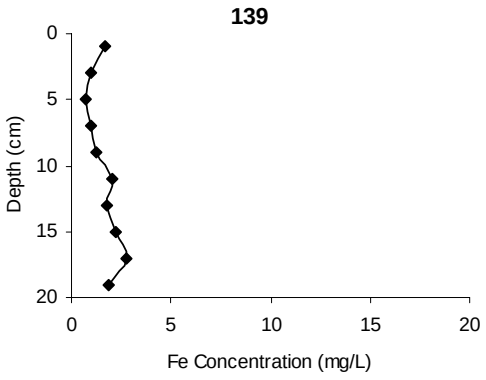
139
Depth (cm)
0
5
10
15
20
0
5
10
15
20
Fe Concentration (mg/L)

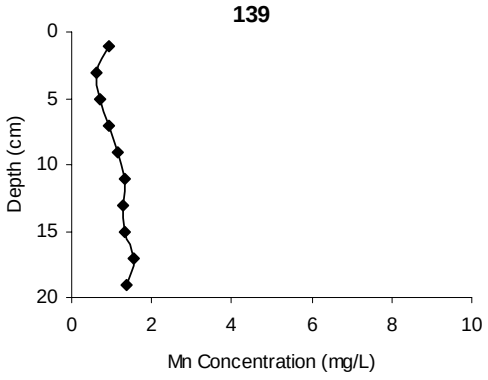
139
Depth (cm)
0
5
10
15
20
0
2
4
6
8
10
Mn Concentration (mg/L)

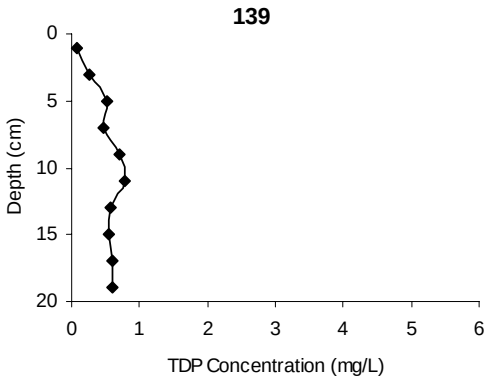
139
Depth (cm)
0
5
10
15
20
0
1
2
3
4
5
6
TDP Concentration (mg/L)

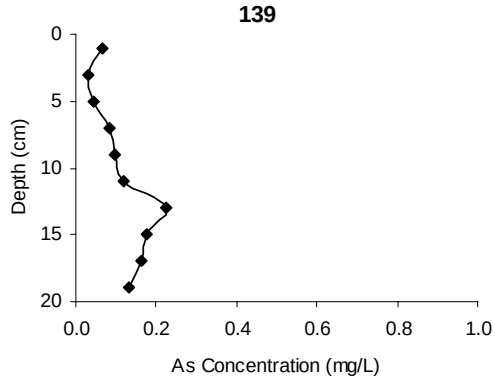
139
Depth (cm)
0
5
10
15
20
0.0
0.2
0.4
0.6
0.8
1.0
As Concentration (mg/L)

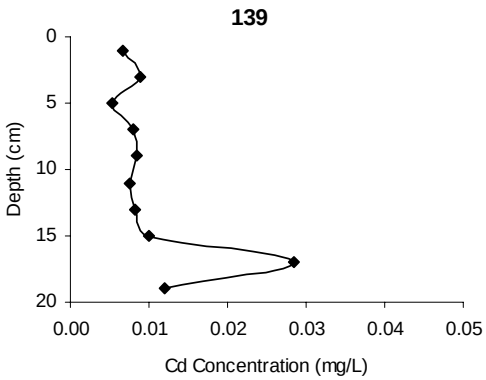
139
Depth (cm)
0
5
10
15
20
0.00
0.01
0.02
0.03
0.04
0.05
Cd Concentration (mg/L)

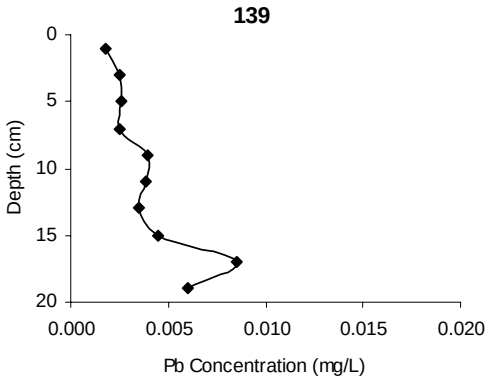
139
Depth (cm)
0
5
10
15
20
0.000
0.005
0.010
0.015
0.020
Pb Concentration (mg/L)

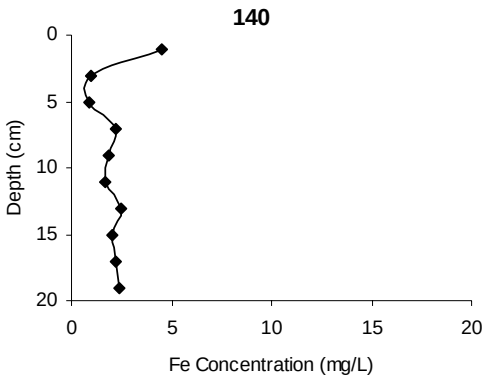
140
Depth (cm)
0
5
10
15
20
0
5
10
15
20
Fe Concentration (mg/L)

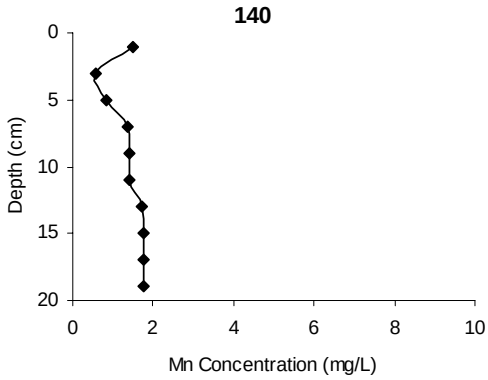
140
Depth (cm)
0
5
10
15
20
0
2
4
6
8
10
Mn Concentration (mg/L)

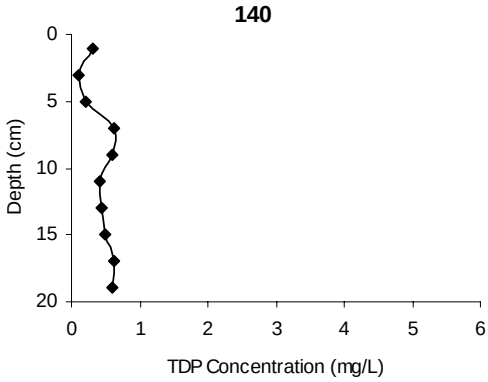
140
Depth (cm)
0
5
10
15
20
0
1
2
3
4
5
6
TDP Concentration (mg/L)

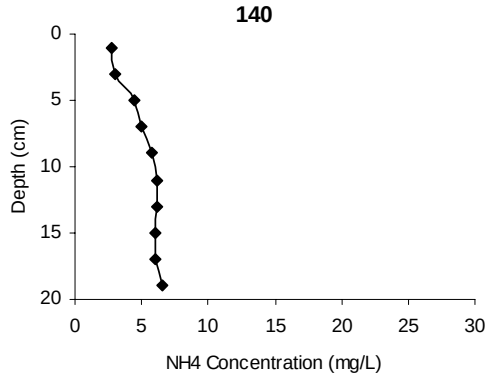
140
Depth (cm)
0
5
10
15
20
0
5
10
15
20
25
30
NH4 Concentration (mg/L)

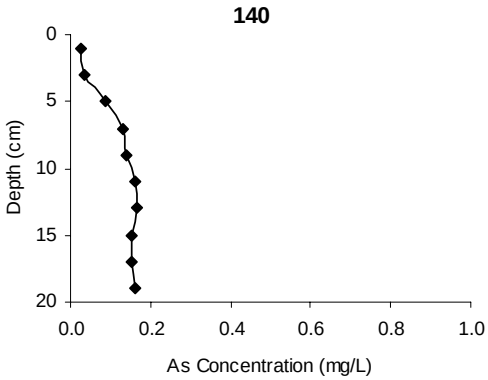
140
Depth (cm)
0
5
10
15
20
0.0
0.2
0.4
0.6
0.8
1.0
As Concentration (mg/L)

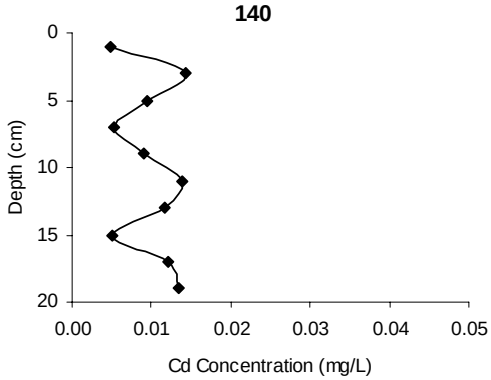
140
Depth (cm)
0
5
10
15
20
0.00
0.01
0.02
0.03
0.04
0.05
Cd Concentration (mg/L)

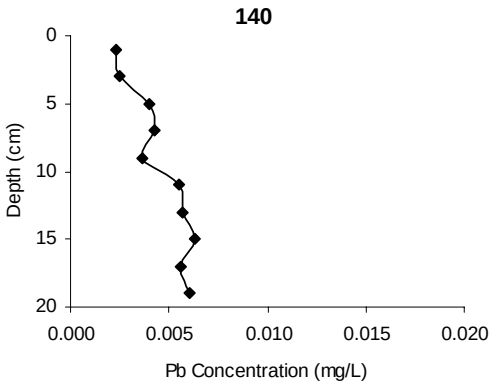
140
Depth (cm)
0
5
10
15
20
0.000
0.005
0.010
0.015
0.020
Pb Concentration (mg/L)

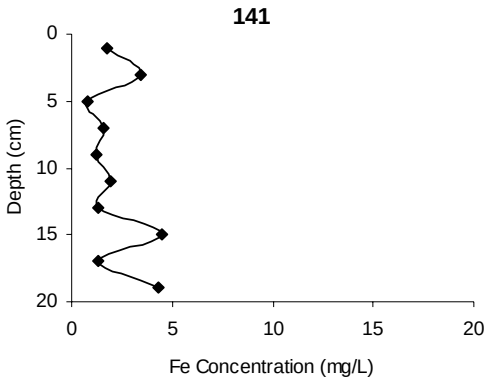
141
Depth (cm)
0
5
10
15
20
0
5
10
15
20
Fe Concentration (mg/L)

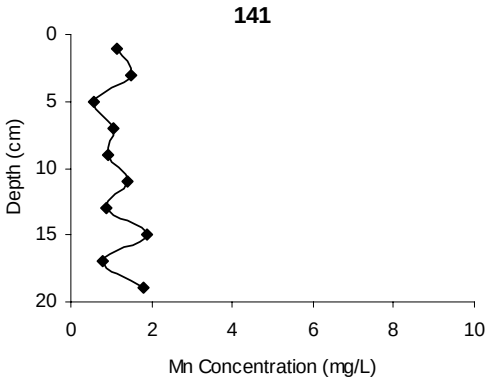
141
Depth (cm)
0
5
10
15
20
0
2
4
6
8
10
Mn Concentration (mg/L)

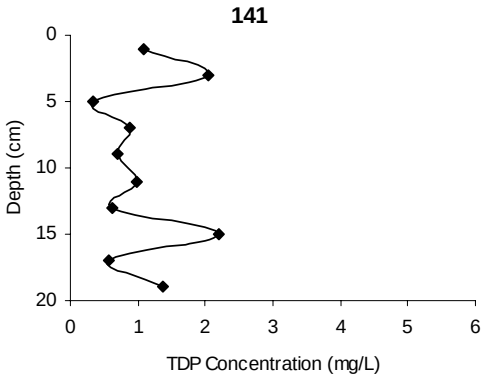
141
Depth (cm)
0
5
10
15
20
0
1
2
3
4
5
6
TDP Concentration (mg/L)

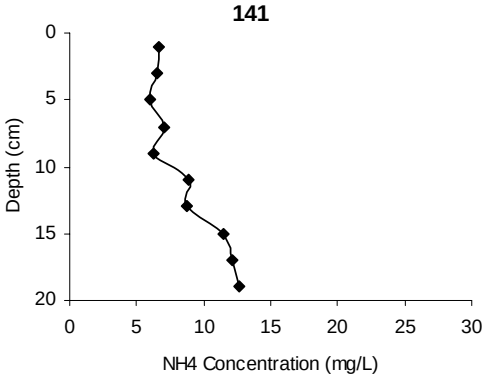
141
Depth (cm)
0
5
10
15
20
0
5
10
15
20
25
30
NH4 Concentration (mg/L)

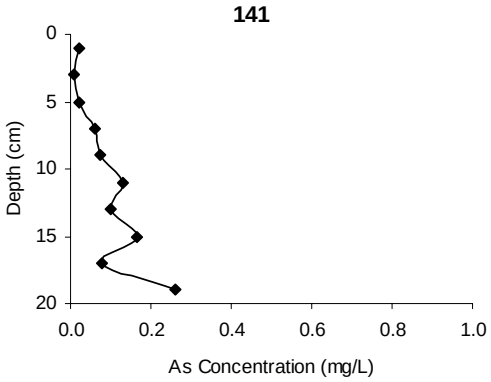
141
Depth (cm)
0
5
10
15
20
0.0
0.2
0.4
0.6
0.8
1.0
As Concentration (mg/L)

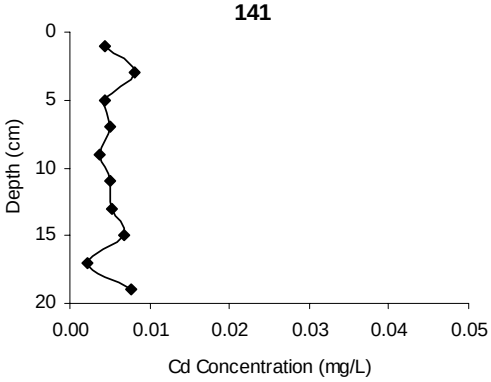
141
Depth (cm)
0
5
10
15
20
0.00
0.01
0.02
0.03
0.04
0.05
Cd Concentration (mg/L)

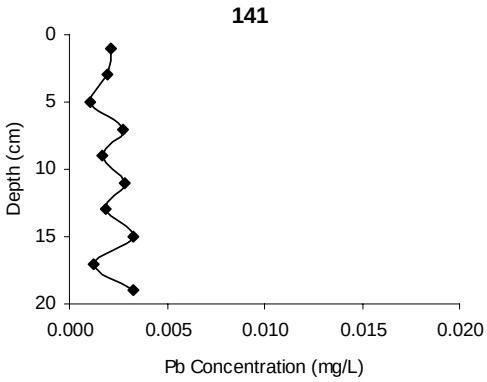
141
Depth (cm)
0
5
10
15
20
0.000
0.005
0.010
0.015
0.020
Pb Concentration (mg/L)

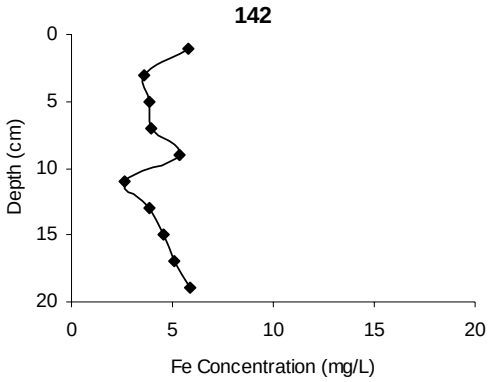
142
Depth (cm)
0
5
10
15
20
0
5
10
15
20
Fe Concentration (mg/L)

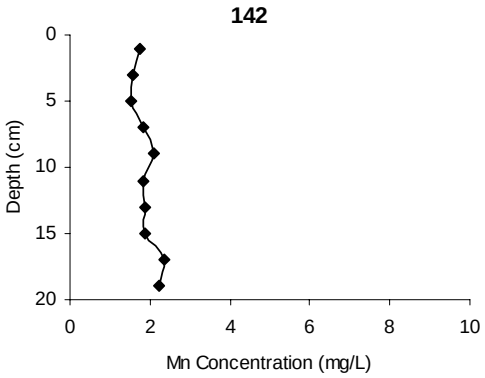
142
Depth (cm)
0
5
10
15
20
0
2
4
6
8
10
Mn Concentration (mg/L)

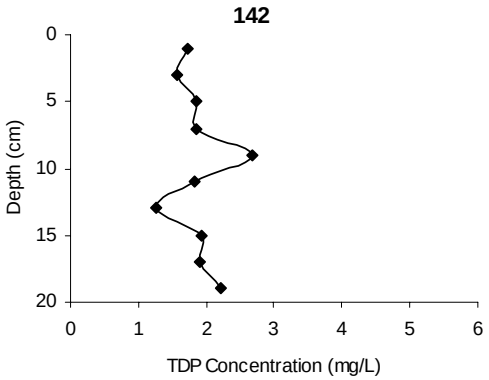
142
Depth (cm)
0
5
10
15
20
0
1
2
3
4
5
6
TDP Concentration (mg/L)

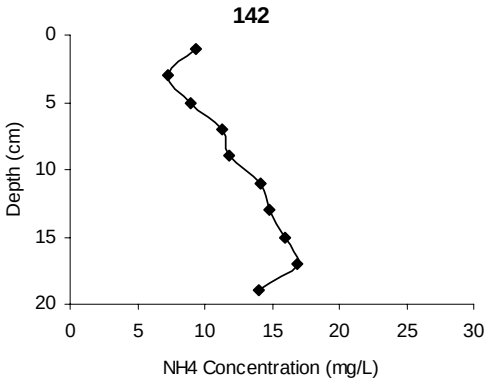
142
Depth (cm)
0
5
10
15
20
0
5
10
15
20
25
30
NH4 Concentration (mg/L)

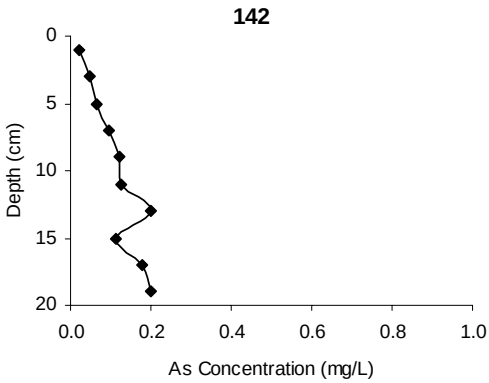
142
Depth (cm)
0
5
10
15
20
0.0
0.2
0.4
0.6
0.8
1.0
As Concentration (mg/L)

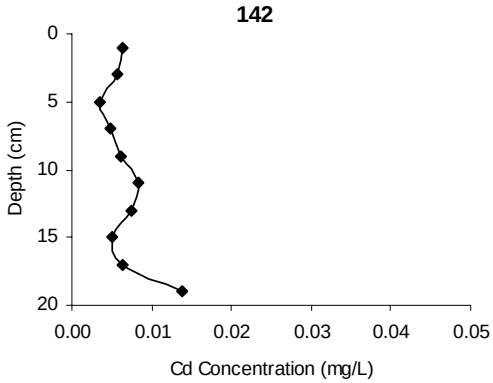
142
Depth (cm)
0
5
10
15
20
0.00
0.01
0.02
0.03
0.04
0.05
Cd Concentration (mg/L)

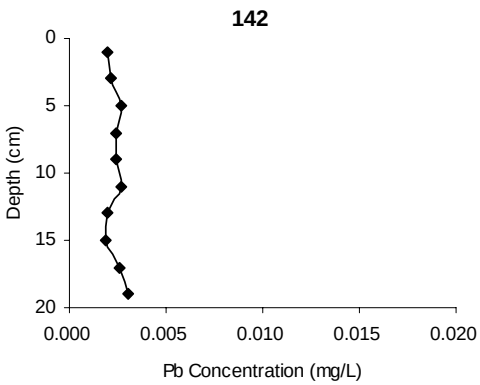
142
Depth (cm)
0
5
10
15
20
0.000
0.005
0.010
0.015
0.020
Pb Concentration (mg/L)

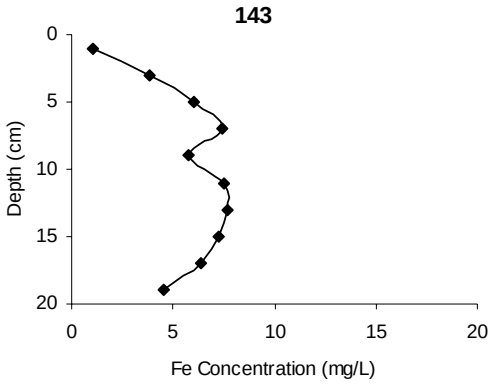
143
Depth (cm)
0
5
10
15
20
0
5
10
15
20
Fe Concentration (mg/L)

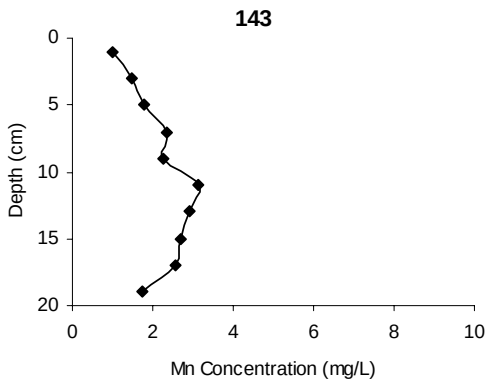
143
Depth (cm)
0
5
10
15
20
0
2
4
6
8
10
Mn Concentration (mg/L)

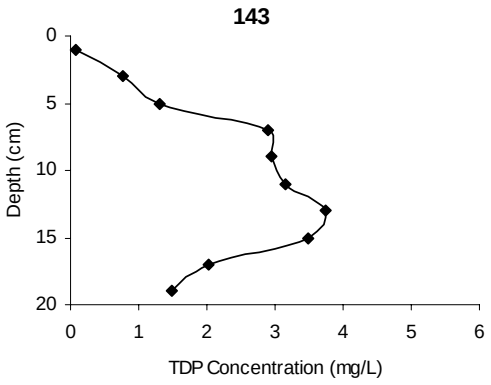
143
Depth (cm)
0
5
10
15
20
0
1
2
3
4
5
6
TDP Concentration (mg/L)

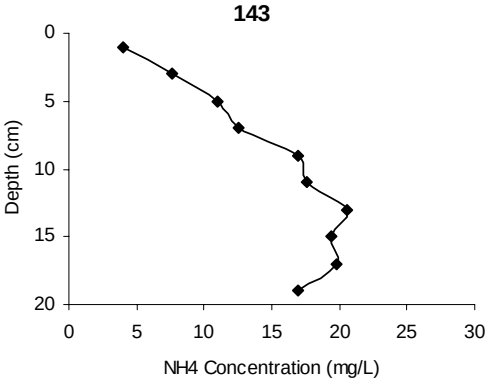
143
Depth (cm)
0
5
10
15
20
0
5
10
15
20
25
30
NH4 Concentration (mg/L)

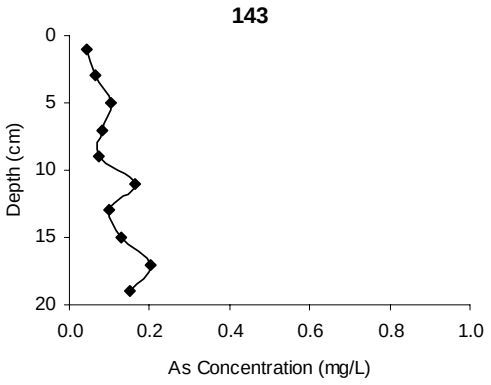
143
Depth (cm)
0
5
10
15
20
0.0
0.2
0.4
0.6
0.8
1.0
As Concentration (mg/L)

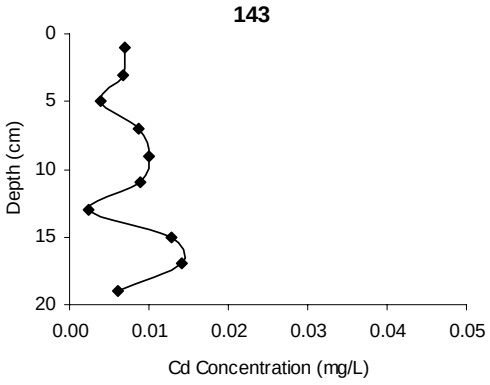
143
Depth (cm)
0
5
10
15
20
0.00
0.01
0.02
0.03
0.04
0.05
Cd Concentration (mg/L)

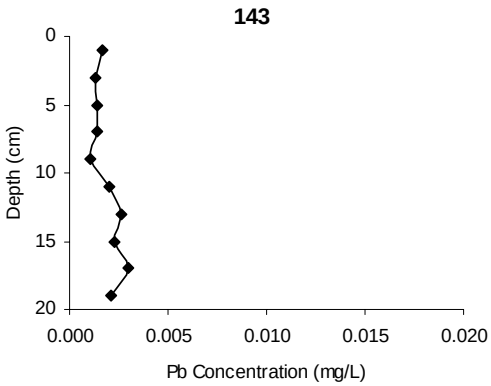
143
Depth (cm)
0
5
10
15
20
0.000
0.005
0.010
0.015
0.020
Pb Concentration (mg/L)

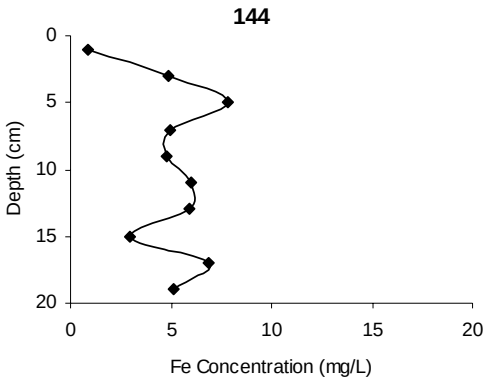
144
Depth (cm)
0
5
10
15
20
0
5
10
15
20
Fe Concentration (mg/L)

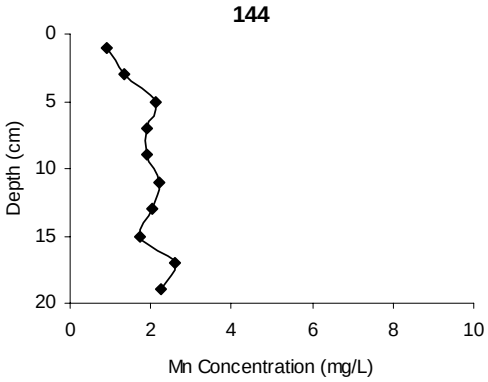
144
Depth (cm)
0
5
10
15
20
0
2
4
6
8
10
Mn Concentration (mg/L)

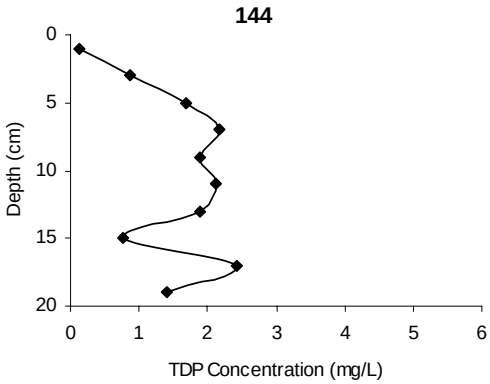
144
Depth (cm)
0
5
10
15
20
0
1
2
3
4
5
6
TDP Concentration (mg/L)

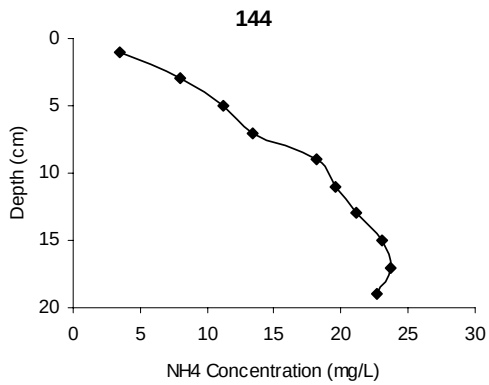
144
Depth (cm)
0
5
10
15
20
0
5
10
15
20
25
30
NH4 Concentration (mg/L)

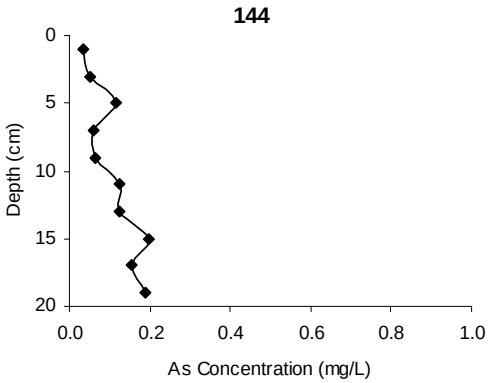
144
Depth (cm)
0
5
10
15
20
0.0
0.2
0.4
0.6
0.8
1.0
As Concentration (mg/L)

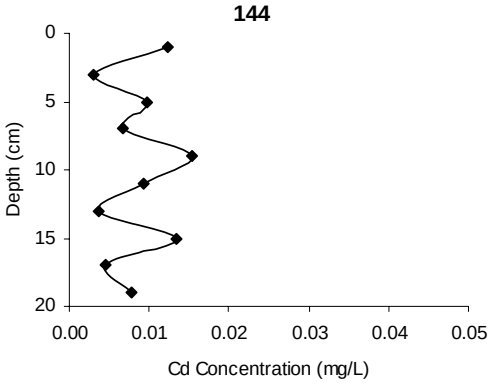
144
Depth (cm)
0
5
10
15
20
0.00
0.01
0.02
0.03
0.04
0.05
Cd Concentration (mg/L)

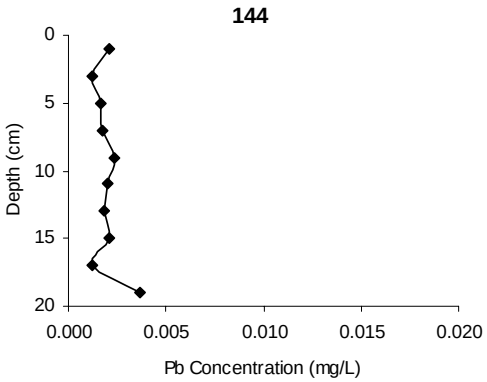
144
Depth (cm)
0
5
10
15
20
0.000
0.005
0.010
0.015
0.020
Pb Concentration (mg/L)

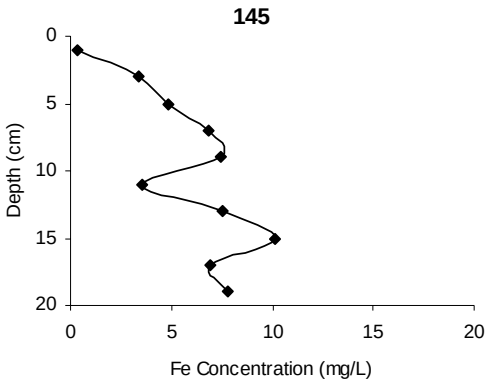
145
Depth (cm)
0
5
10
15
20
0
5
10
15
20
Fe Concentration (mg/L)

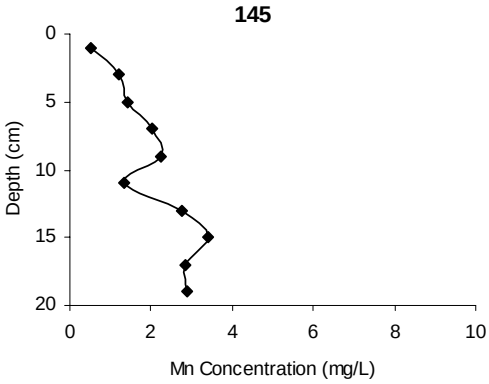
145
Depth (cm)
0
5
10
15
20
0
2
4
6
8
10
Mn Concentration (mg/L)

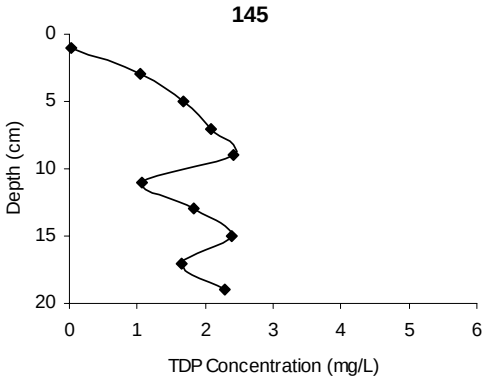
145
Depth (cm)
0
5
10
15
20
0
1
2
3
4
5
6
TDP Concentration (mg/L)

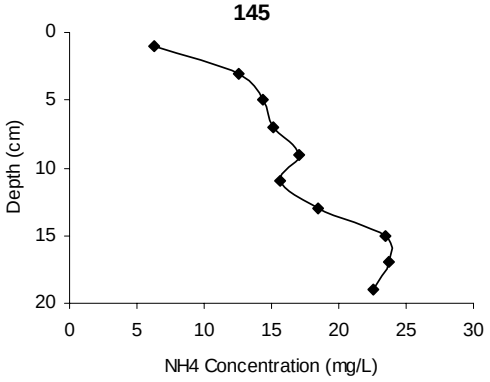
145
Depth (cm)
0
5
10
15
20
0
5
10
15
20
25
30
NH4 Concentration (mg/L)

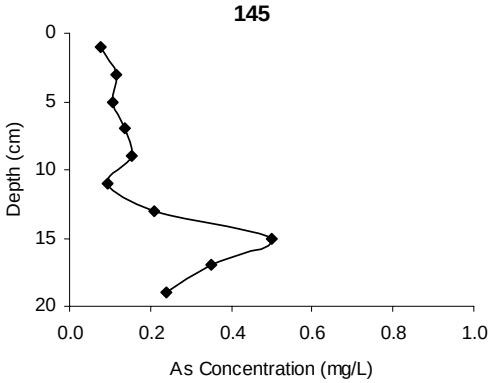
145
Depth (cm)
0
5
10
15
20
0.0
0.2
0.4
0.6
0.8
1.0
As Concentration (mg/L)

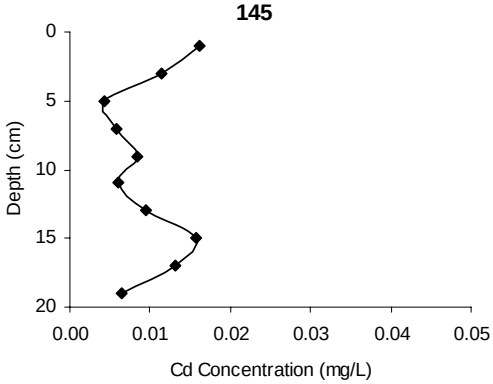
145
Depth (cm)
0
5
10
15
20
0.00
0.01
0.02
0.03
0.04
0.05
Cd Concentration (mg/L)

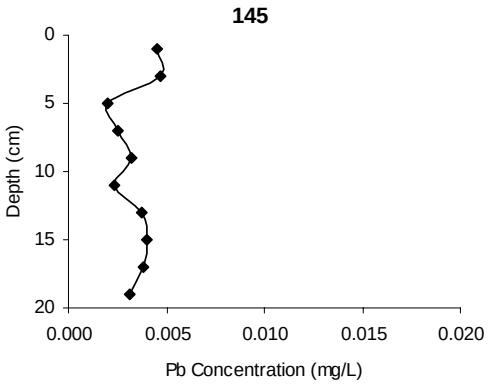
145
Depth (cm)
0
5
10
15
20
0.000
0.005
0.010
0.015
0.020
Pb Concentration (mg/L)

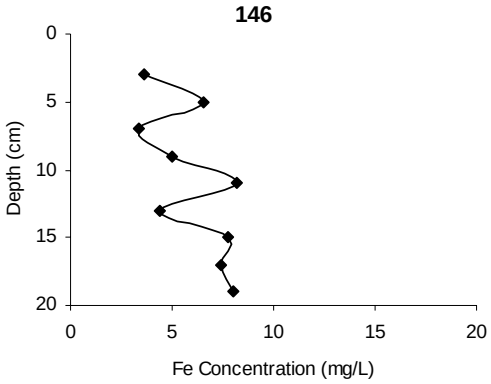
146
Depth (cm)
0
5
10
15
20
0
5
10
15
20
Fe Concentration (mg/L)

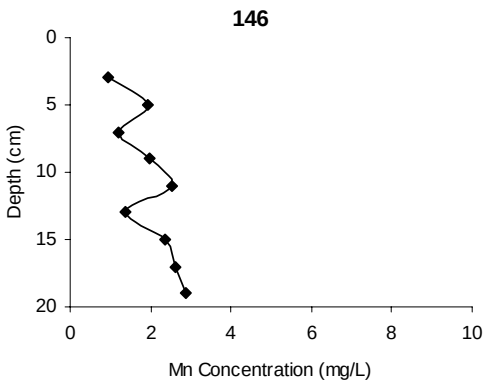
146
Depth (cm)
0
5
10
15
20
0
2
4
6
8
10
Mn Concentration (mg/L)

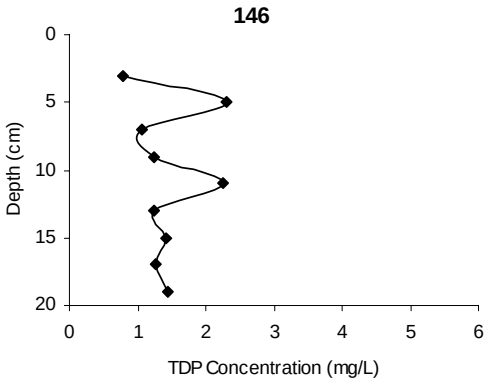
146
Depth (cm)
0
5
10
15
20
0
1
2
3
4
5
6
TDP Concentration (mg/L)

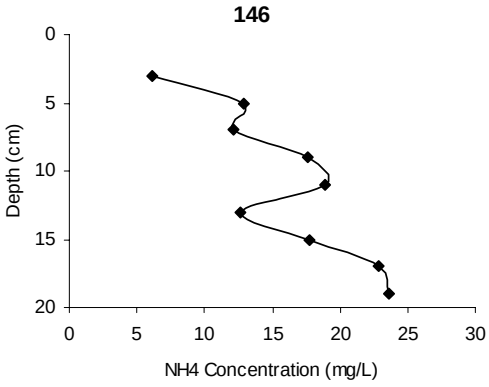
146
Depth (cm)
0
5
10
15
20
0
5
10
15
20
25
30
NH4 Concentration (mg/L)

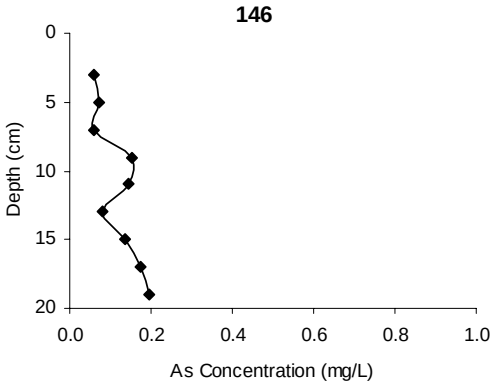
146
Depth (cm)
0
5
10
15
20
0.0
0.2
0.4
0.6
0.8
1.0
As Concentration (mg/L)

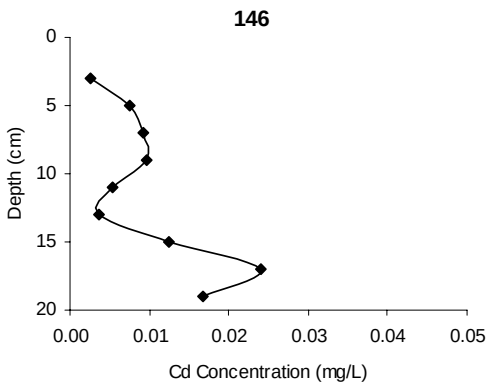
146
Depth (cm)
0
5
10
15
20
0.00
0.01
0.02
0.03
0.04
0.05
Cd Concentration (mg/L)

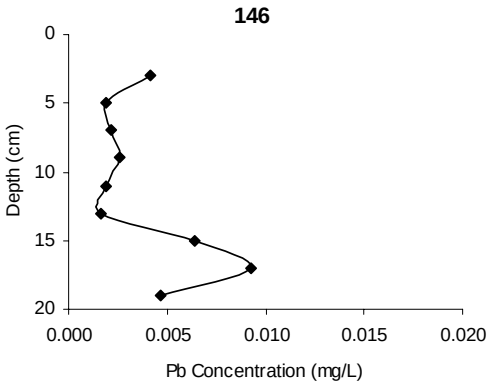
146
Depth (cm)
0
5
10
15
20
0.000
0.005
0.010
0.015
0.020
Pb Concentration (mg/L)

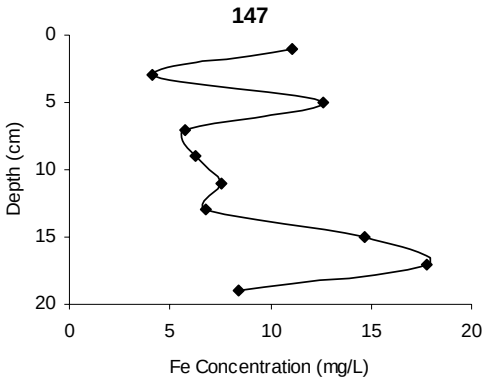
147
Depth (cm)
0
5
10
15
20
0
5
10
15
20
Fe Concentration (mg/L)

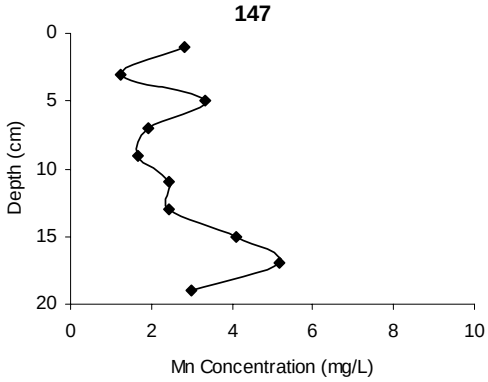
147
Depth (cm)
0
5
10
15
20
0
2
4
6
8
10
Mn Concentration (mg/L)

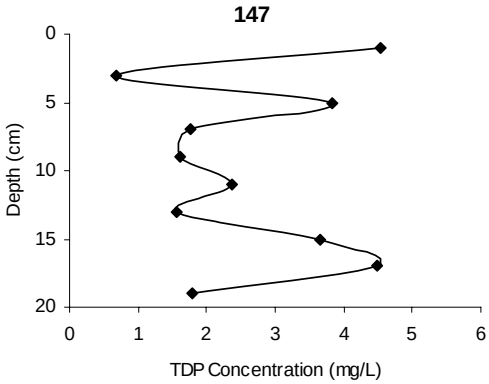
147
Depth (cm)
0
5
10
15
20
0
1
2
3
4
5
6
TDP Concentration (mg/L)

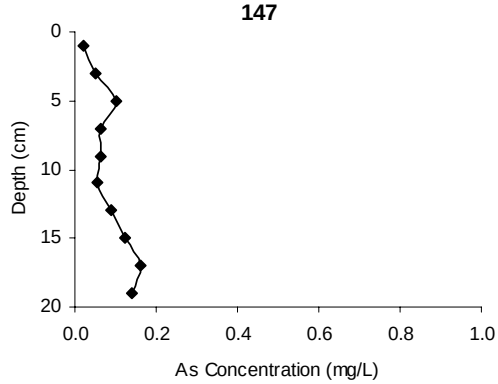
147
Depth (cm)
0
5
10
15
20
0.0
0.2
0.4
0.6
0.8
1.0
As Concentration (mg/L)

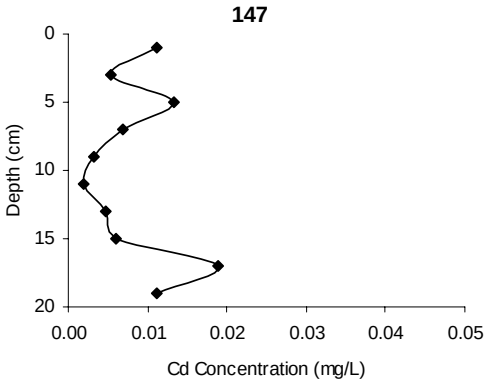
147
Depth (cm)
0
5
10
15
20
0.00
0.01
0.02
0.03
0.04
0.05
Cd Concentration (mg/L)

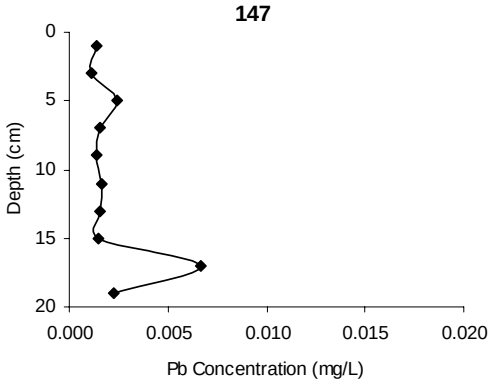
147
Depth (cm)
0
5
10
15
20
0.000
0.005
0.010
0.015
0.020
Pb Concentration (mg/L)

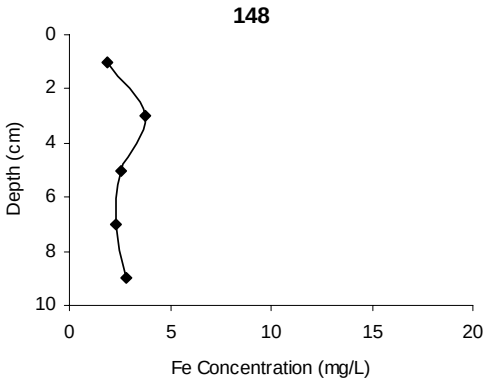
148
Depth (cm)
0
2
4
6
8
10
0
5
10
15
20
Fe Concentration (mg/L)

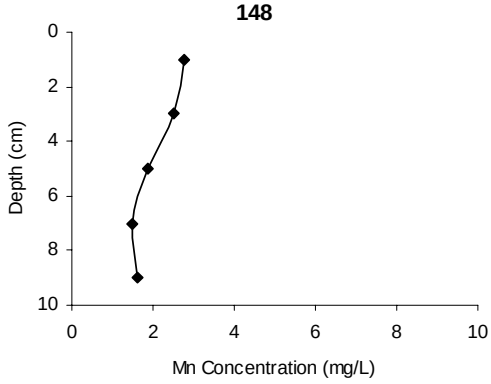
148
Depth (cm)
0
2
4
6
8
10
0
2
4
6
8
10
Mn Concentration (mg/L)

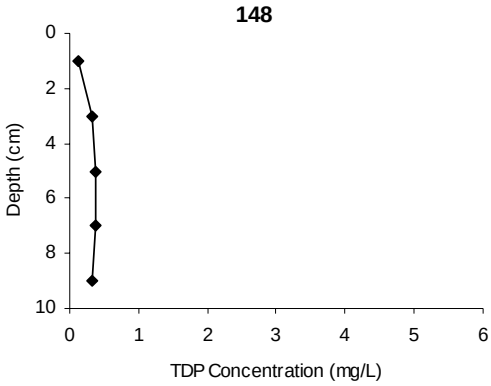
148
Depth (cm)
TDP Concentration (mg/L)

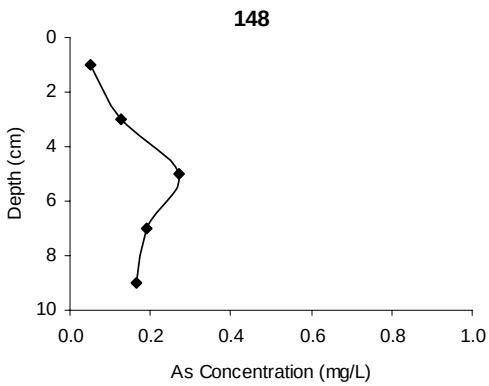
148
Depth (cm)
As Concentration (mg/L)

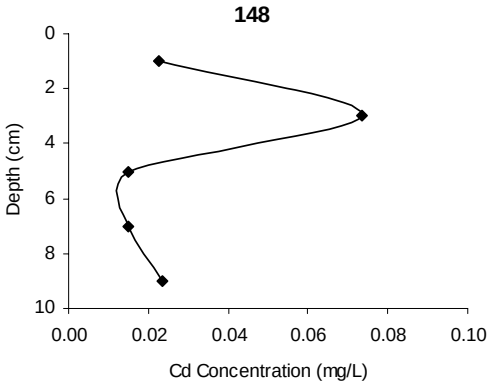
148
Depth (cm)
Cd Concentration (mg/L)

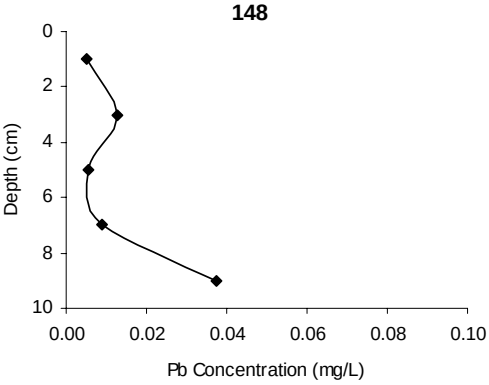
148
Depth (cm)
Pb Concentration (mg/L)

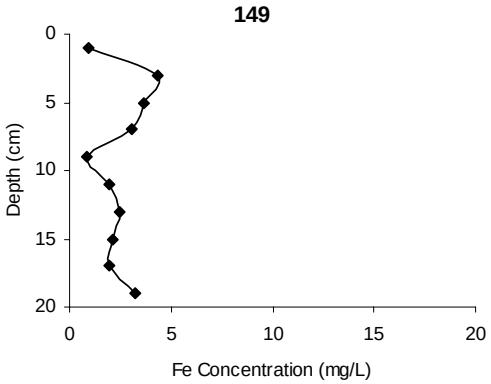
149
Depth (cm)
Fe Concentration (mg/L)

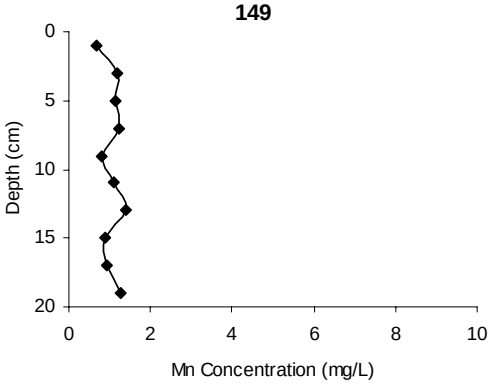
149
Depth (cm)
Mn Concentration (mg/L)

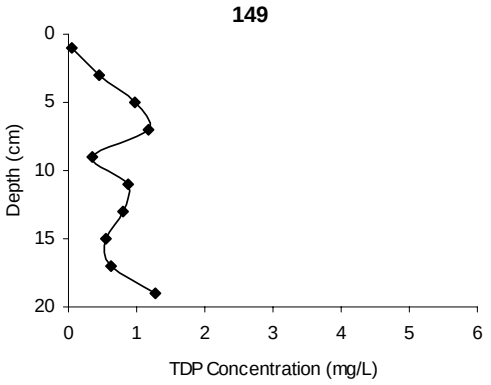
149
Depth (cm)
TDP Concentration (mg/L)

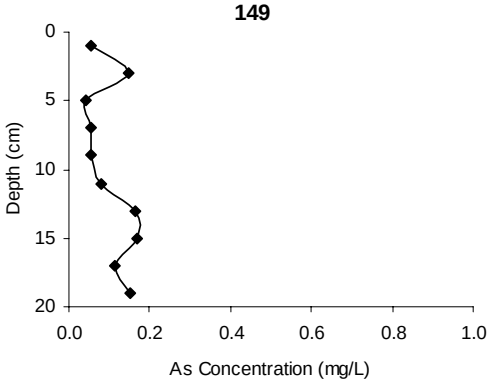
149
Depth (cm)
As Concentration (mg/L)

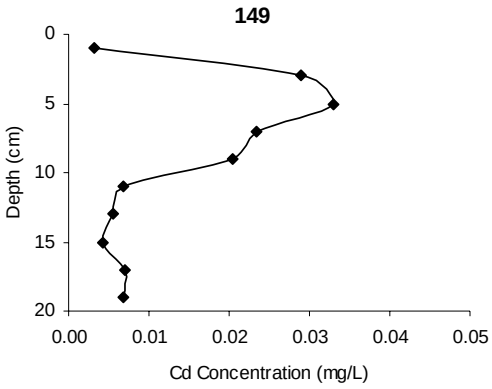
149
Depth (cm)
0
5
10
15
20
0.00
0.01
0.02
0.03
0.04
0.05
Cd Concentration (mg/L)

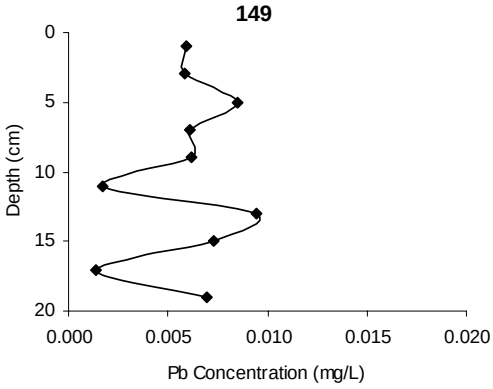
149
Depth (cm)
0
5
10
15
20
0.000
0.005
0.010
0.015
0.020
Pb Concentration (mg/L)

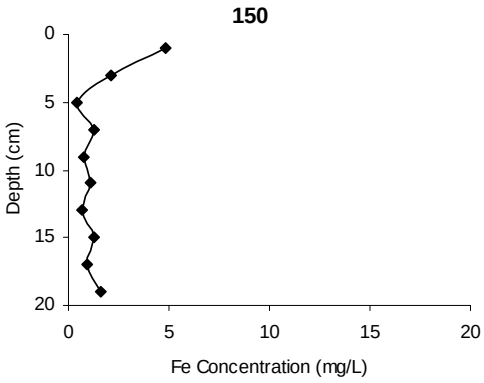
150
Depth (cm)
0
5
10
15
20
0
5
10
15
20
Fe Concentration (mg/L)

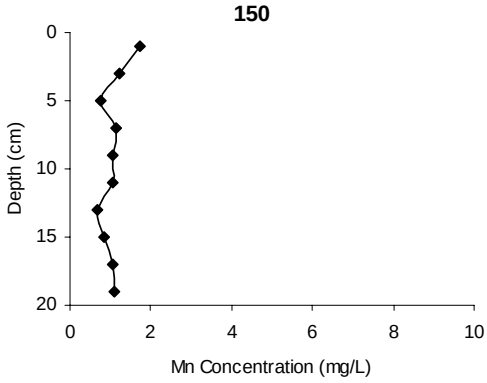
150
Depth (cm)
0
5
10
15
20
0
2
4
6
8
10
Mn Concentration (mg/L)

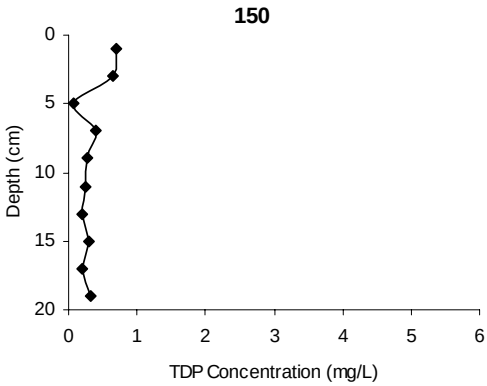
150
Depth (cm)
0
5
10
15
20
0
1
2
3
4
5
6
TDP Concentration (mg/L)

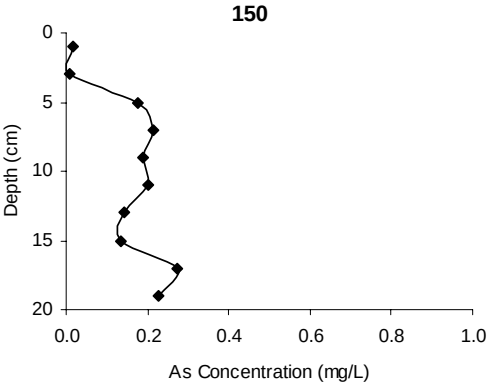
150
Depth (cm)
0
5
10
15
20
0.0
0.2
0.4
0.6
0.8
1.0
As Concentration (mg/L)

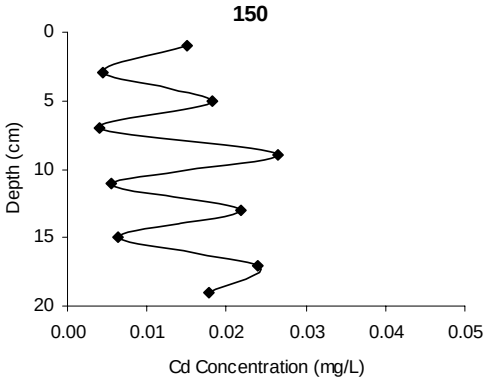
150
Depth (cm)
0
5
10
15
20
0.00
0.01
0.02
0.03
0.04
0.05
Cd Concentration (mg/L)

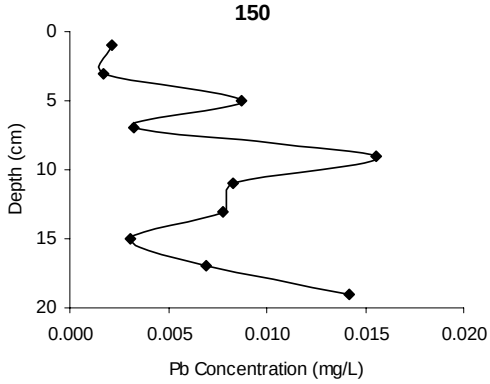
150
Depth (cm)
0
5
10
15
20
0.000
0.005
0.010
0.015
0.020
Pb Concentration (mg/L)

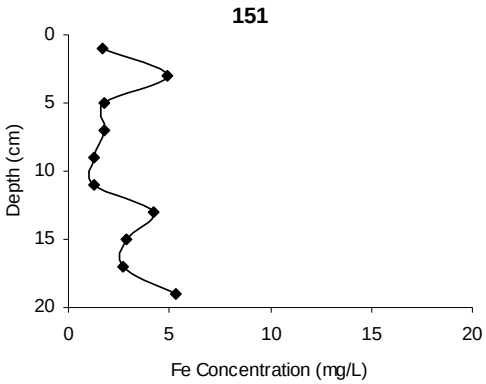
151
Depth (cm)
0
5
10
15
20
0
5
10
15
20
Fe Concentration (mg/L)

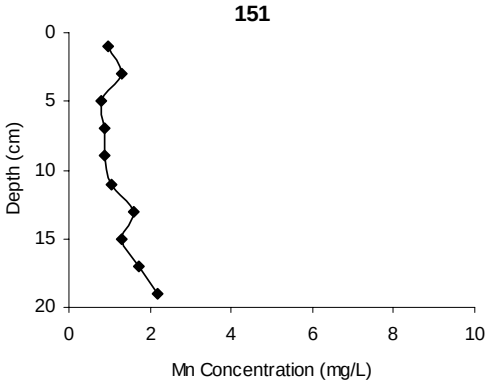
151
Depth (cm)
0
5
10
15
20
0
2
4
6
8
10
Mn Concentration (mg/L)

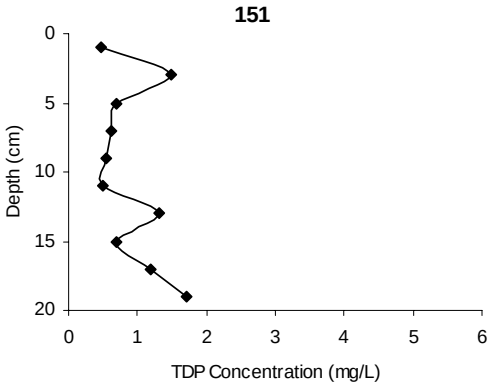
151
Depth (cm)
0
5
10
15
20
0
1
2
3
4
5
6
TDP Concentration (mg/L)

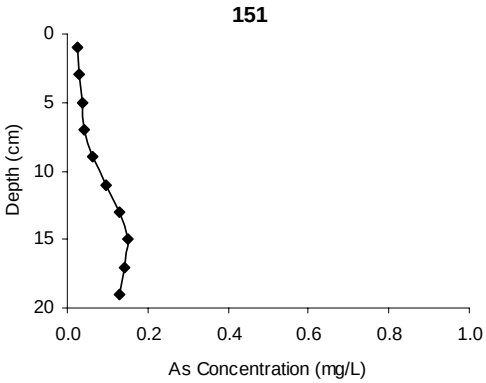
151
Depth (cm)
0
5
10
15
20
0.0
0.2
0.4
0.6
0.8
1.0
As Concentration (mg/L)

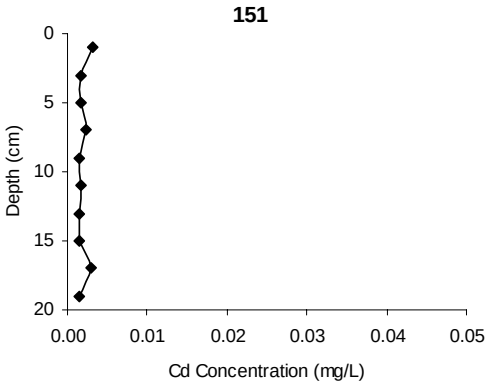
151
Depth (cm)
0
5
10
15
20
0.00
0.01
0.02
0.03
0.04
0.05
Cd Concentration (mg/L)

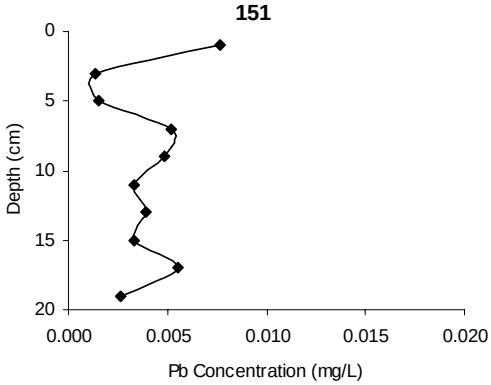
151
Depth (cm)
0
5
10
15
20
0.000
0.005
0.010
0.015
0.020
Pb Concentration (mg/L)

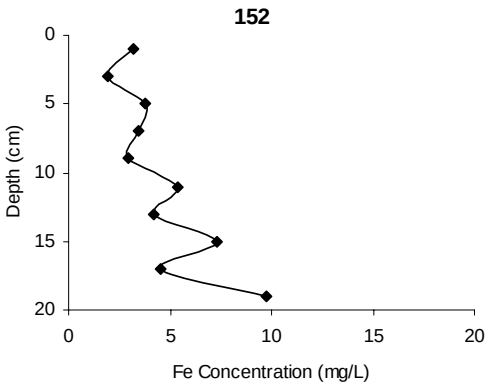
152
Depth (cm)
0
5
10
15
20
0
5
10
15
20
Fe Concentration (mg/L)

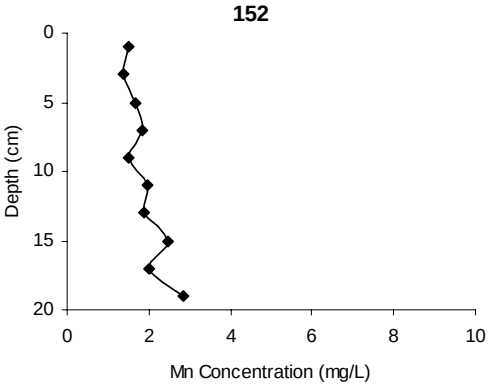
152
Depth (cm)
0
5
10
15
20
0
2
4
6
8
10
Mn Concentration (mg/L)

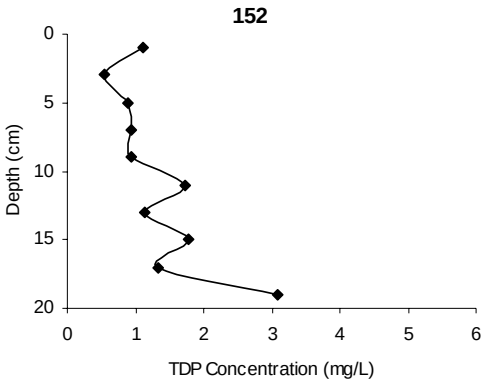
152
Depth (cm)
TDP Concentration (mg/L)

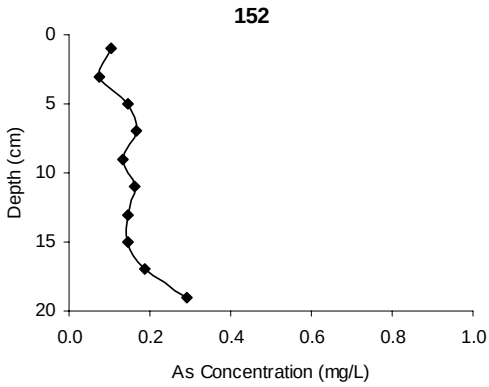
152
Depth (cm)
As Concentration (mg/L)

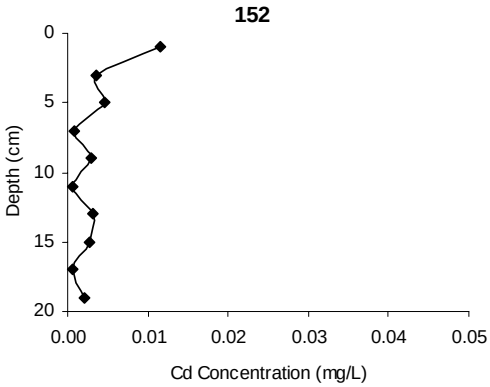
152
Depth (cm)
Cd Concentration (mg/L)

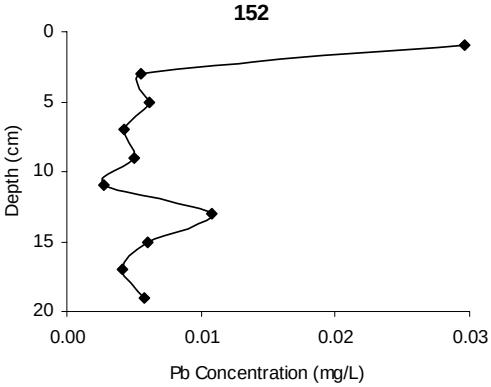
152
Depth (cm)
Pb Concentration (mg/L)

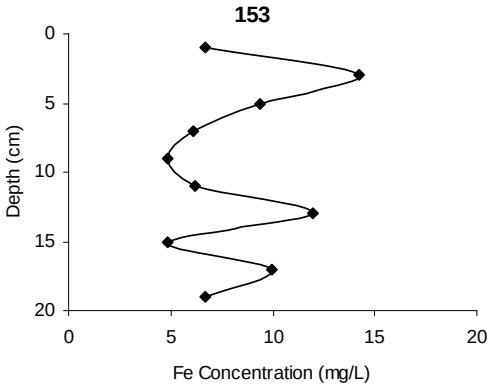
153
Depth (cm)
Fe Concentration (mg/L)

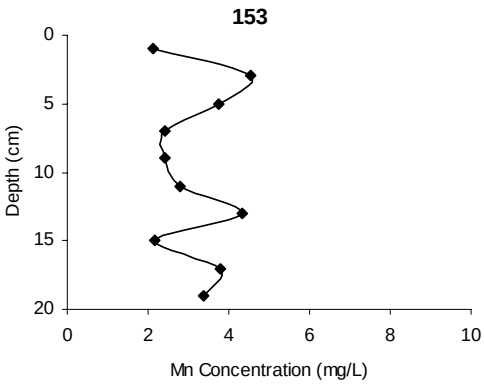
153
Depth (cm)
Mn Concentration (mg/L)

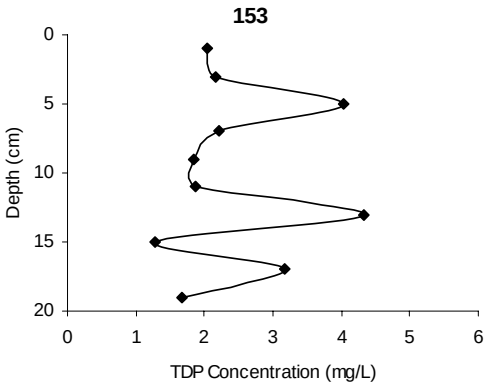
153
Depth (cm)
TDP Concentration (mg/L)

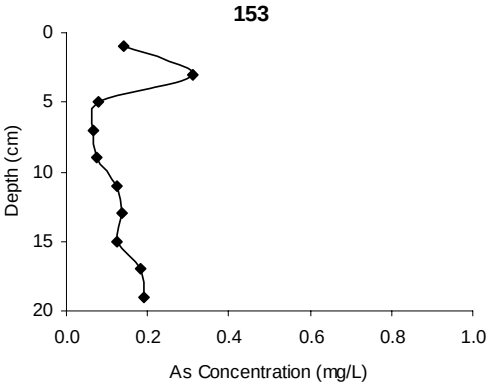
153
Depth (cm)
As Concentration (mg/L)

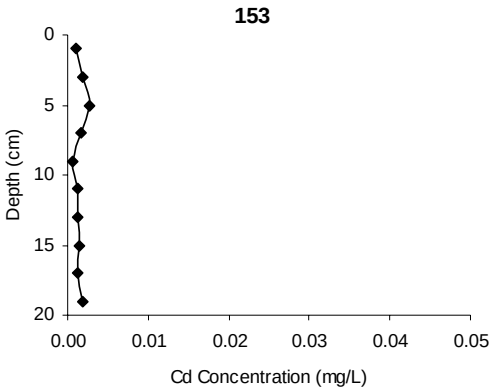
153
Depth (cm)
0
5
10
15
20
0.00
0.01
0.02
0.03
0.04
0.05
Cd Concentration (mg/L)

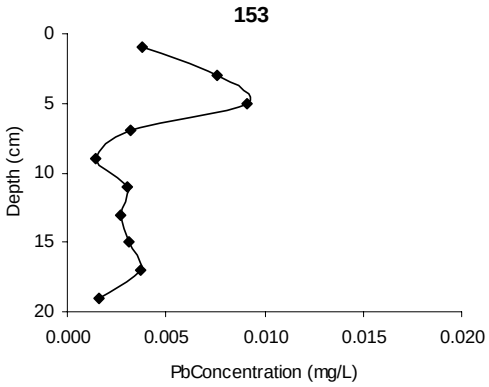
153
Depth (cm)
0
5
10
15
20
0.000
0.005
0.010
0.015
0.020
PbConcentration (mg/L)

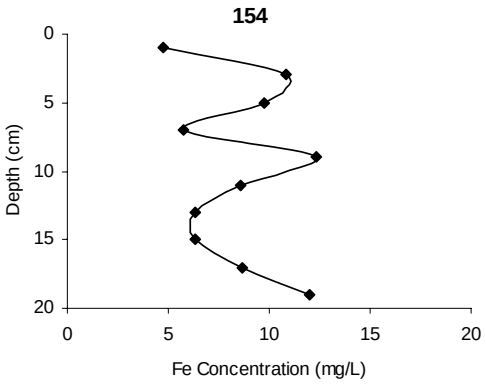
154
Depth (cm)
0
5
10
15
20
0
5
10
15
20
Fe Concentration (mg/L)

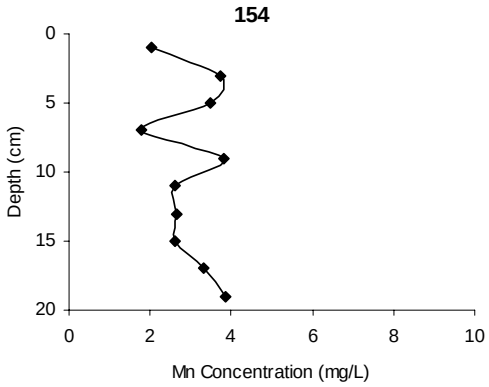
154
Depth (cm)
0
5
10
15
20
0
2
4
6
8
10
Mn Concentration (mg/L)

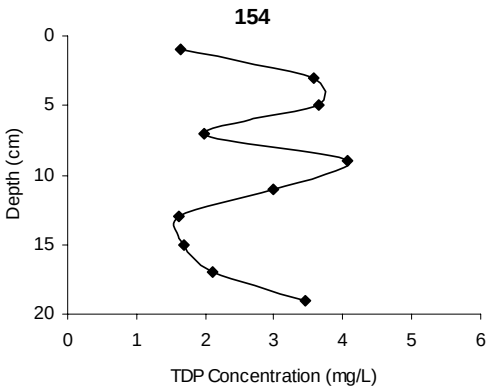
154
Depth (cm)
0
5
10
15
20
0
1
2
3
4
5
6
TDP Concentration (mg/L)

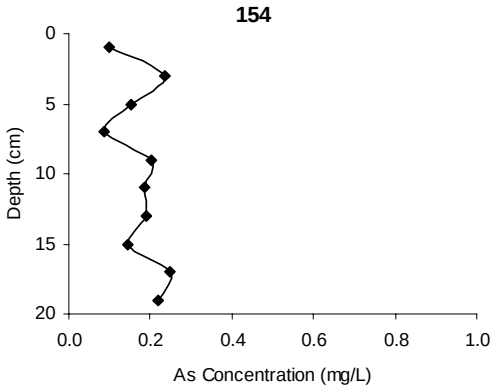
154
Depth (cm)
0
5
10
15
20
0.0
0.2
0.4
0.6
0.8
1.0
As Concentration (mg/L)

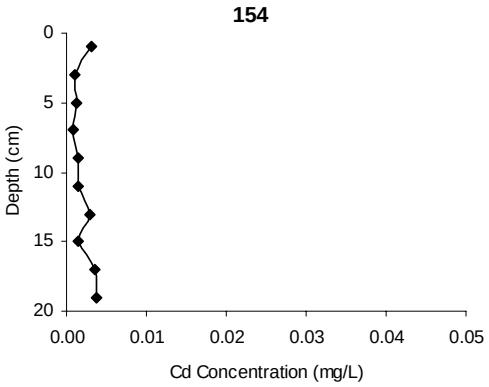
154
Depth (cm)
0
5
10
15
20
0.00
0.01
0.02
0.03
0.04
0.05
Cd Concentration (mg/L)

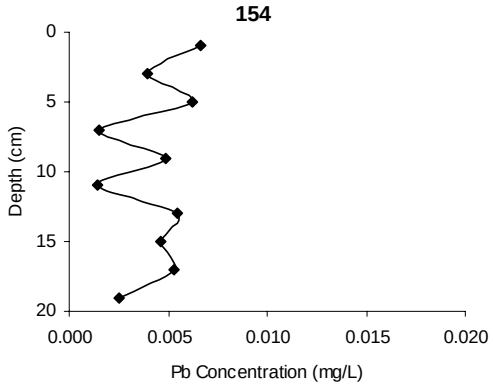
154
Depth (cm)
0
5
10
15
20
0.000
0.005
0.010
0.015
0.020
Pb Concentration (mg/L)

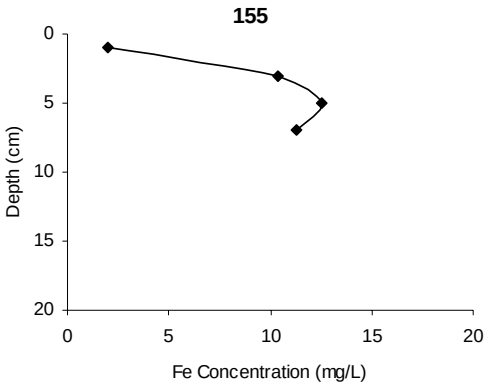
155
Depth (cm)
0
5
10
15
20
0
5
10
15
20
Fe Concentration (mg/L)

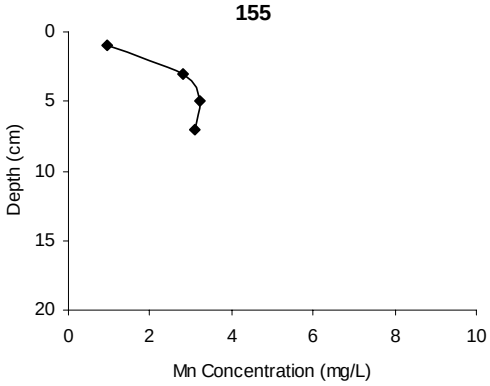
155
Depth (cm)
0
5
10
15
20
0
2
4
6
8
10
Mn Concentration (mg/L)

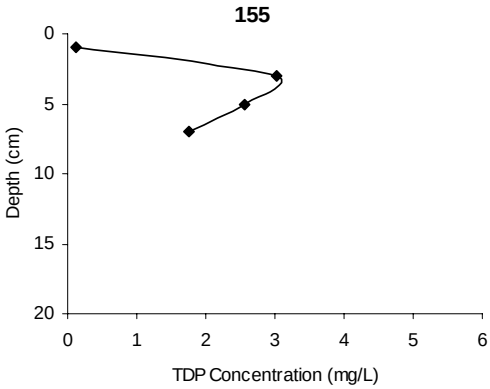
155
Depth (cm)
0
5
10
15
20
0
1
2
3
4
5
6
TDP Concentration (mg/L)

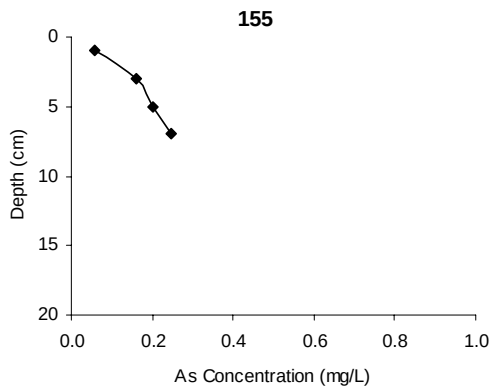
155
Depth (cm)
0
5
10
15
20
0.0
0.2
0.4
0.6
0.8
1.0
As Concentration (mg/L)

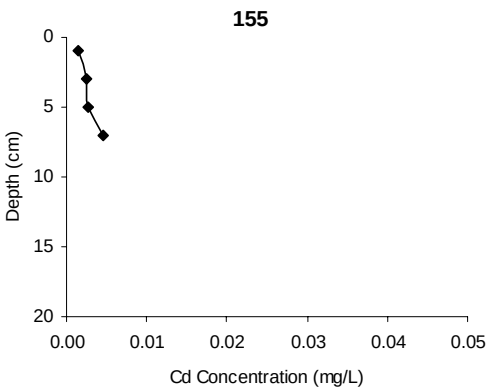
155
Depth (cm)
0
5
10
15
20
0.00
0.01
0.02
0.03
0.04
0.05
Cd Concentration (mg/L)

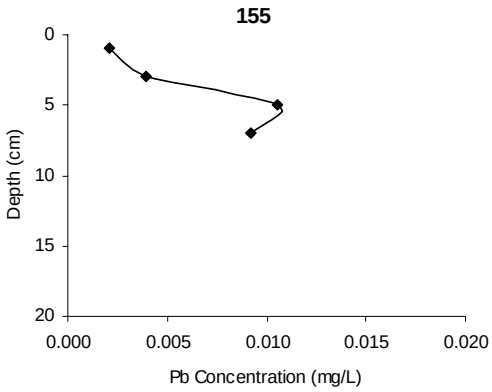
155
Depth (cm)
0
5
10
15
20
0.000
0.005
0.010
0.015
0.020
Pb Concentration (mg/L)

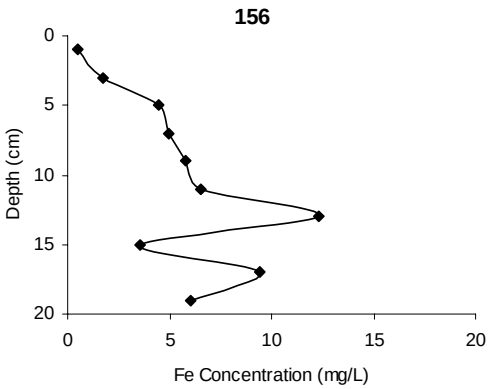
156
Depth (cm)
0
5
10
15
20
0
5
10
15
20
Fe Concentration (mg/L)

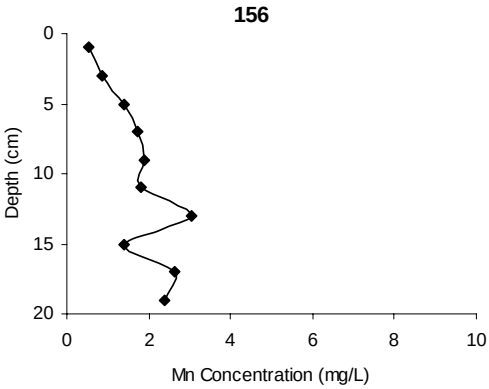
156
Depth (cm)
0
5
10
15
20
0
2
4
6
8
10
Mn Concentration (mg/L)

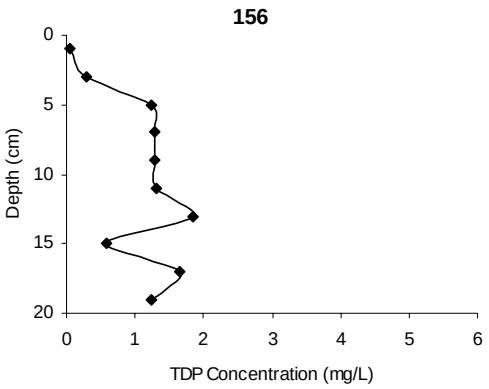
156
Depth (cm)
0
5
10
15
20
0
1
2
3
4
5
6
TDP Concentration (mg/L)

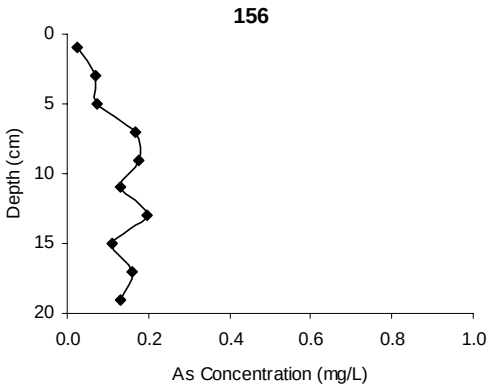
156
Depth (cm)
0
5
10
15
20
0.0
0.2
0.4
0.6
0.8
1.0
As Concentration (mg/L)

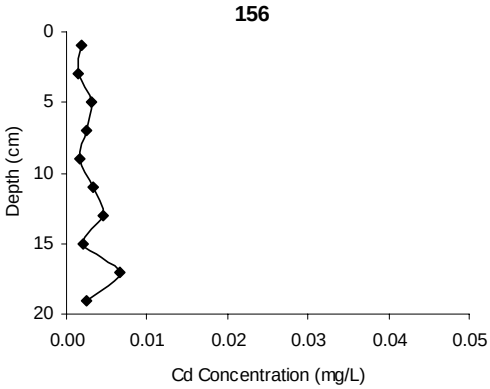
156
Depth (cm)
0
5
10
15
20
0.00
0.01
0.02
0.03
0.04
0.05
Cd Concentration (mg/L)

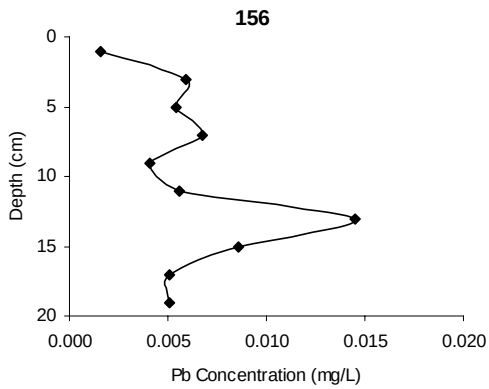
156
Depth (cm)
0
5
10
15
20
0.000
0.005
0.010
0.015
0.020
Pb Concentration (mg/L)

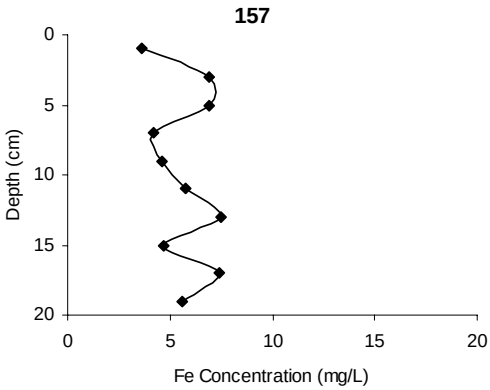
157
Depth (cm)
0
5
10
15
20
0
5
10
15
20
Fe Concentration (mg/L)

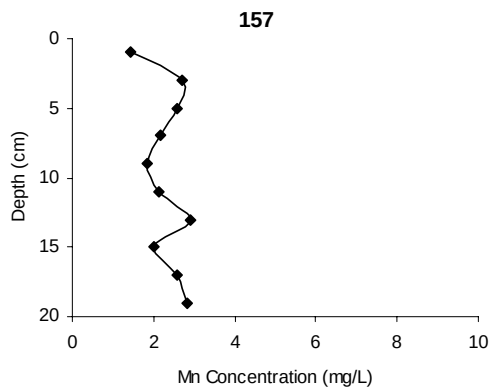
157
Depth (cm)
0
5
10
15
20
0
2
4
6
8
10
Mn Concentration (mg/L)

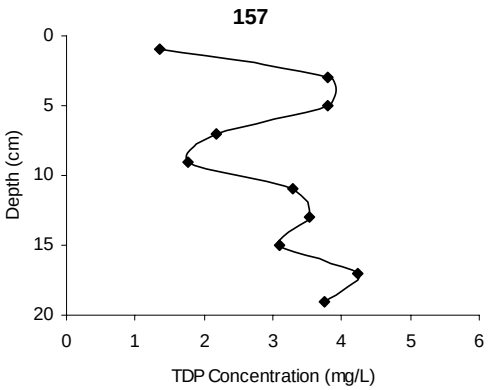
157
Depth (cm)
0
5
10
15
20
0
1
2
3
4
5
6
TDP Concentration (mg/L)

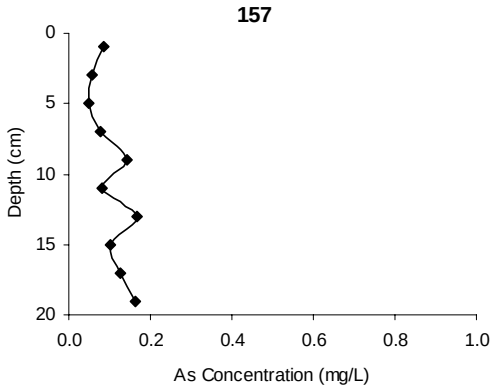
157
Depth (cm)
0
5
10
15
20
0.0
0.2
0.4
0.6
0.8
1.0
As Concentration (mg/L)

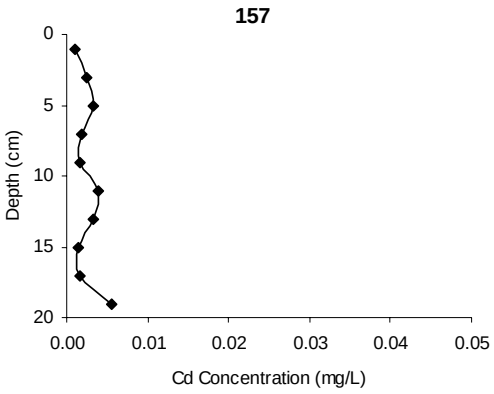
157
Depth (cm)
0
5
10
15
20
0.00
0.01
0.02
0.03
0.04
0.05
Cd Concentration (mg/L)

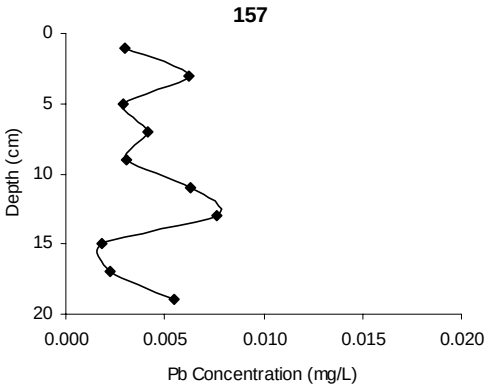
157
Depth (cm)
0
5
10
15
20
0.000
0.005
0.010
0.015
0.020
Pb Concentration (mg/L)

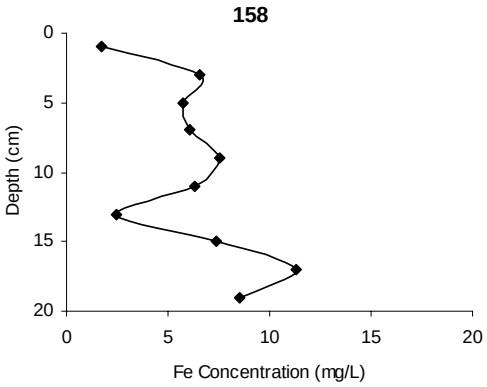
158
Depth (cm)
0
5
10
15
20
0
5
10
15
20
Fe Concentration (mg/L)

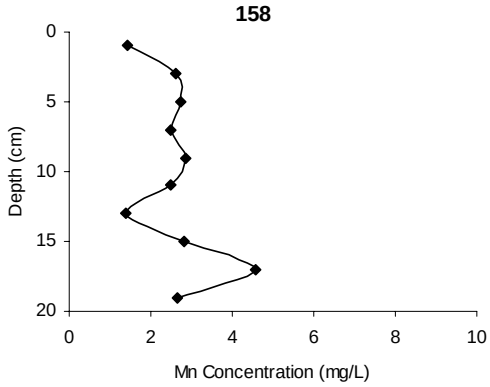
158
Depth (cm)
0
5
10
15
20
0
2
4
6
8
10
Mn Concentration (mg/L)

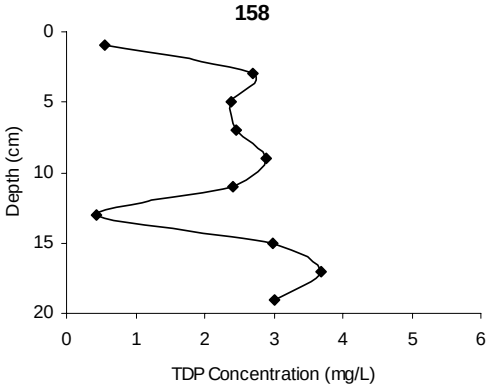
158
Depth (cm)
0
5
10
15
20
0
1
2
3
4
5
6
TDP Concentration (mg/L)

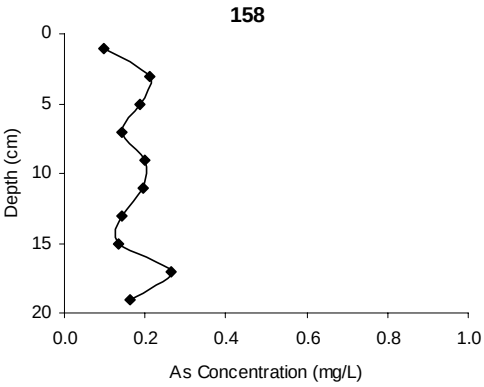
158
Depth (cm)
0
5
10
15
20
0.0
0.2
0.4
0.6
0.8
1.0
As Concentration (mg/L)

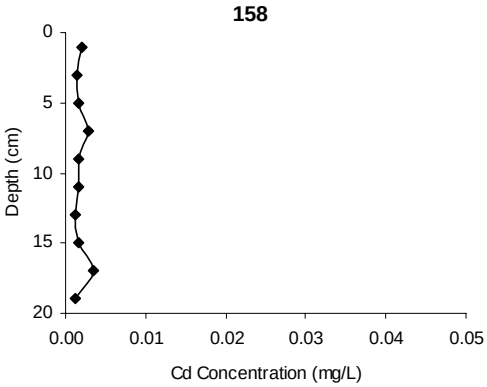
158
Depth (cm)
0
5
10
15
20
0.00
0.01
0.02
0.03
0.04
0.05
Cd Concentration (mg/L)

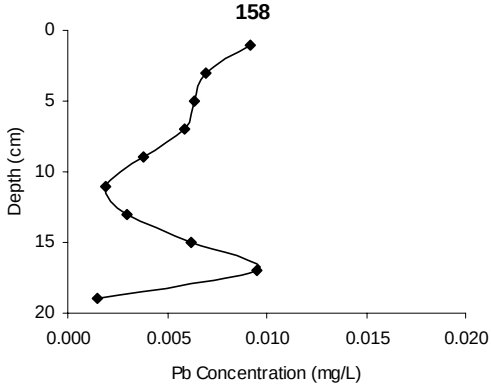
158
Depth (cm)
0
5
10
15
20
0.000
0.005
0.010
0.015
0.020
Pb Concentration (mg/L)

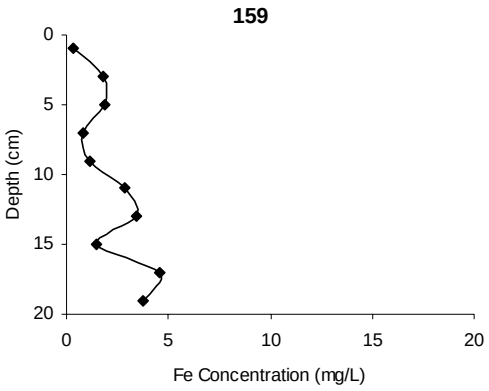
159
Depth (cm)
0
5
10
15
20
0
5
10
15
20
Fe Concentration (mg/L)

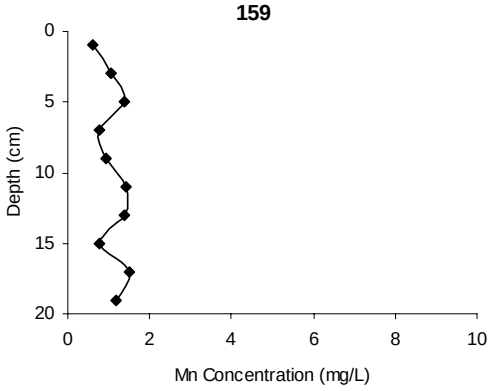
159
Depth (cm)
0
5
10
15
20
0
2
4
6
8
10
Mn Concentration (mg/L)

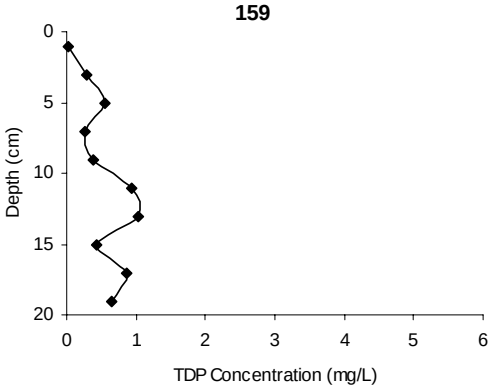
159
Depth (cm)
0
5
10
15
20
0
1
2
3
4
5
6
TDP Concentration (mg/L)

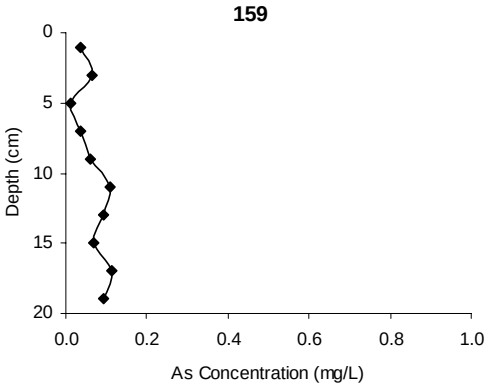
159
Depth (cm)
0
5
10
15
20
0.0
0.2
0.4
0.6
0.8
1.0
As Concentration (mg/L)

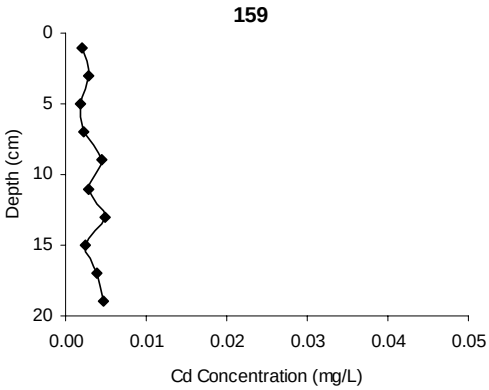
159
Depth (cm)
0
5
10
15
20
0.00
0.01
0.02
0.03
0.04
0.05
Cd Concentration (mg/L)

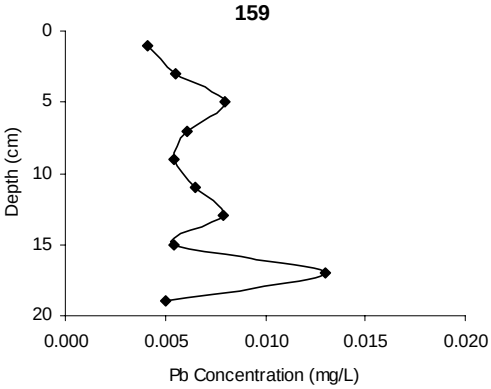
159
Depth (cm)
0
5
10
15
20
0.000
0.005
0.010
0.015
0.020
Pb Concentration (mg/L)

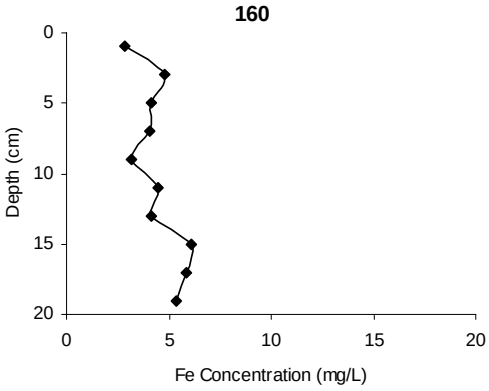
160
Depth (cm)
0
5
10
15
20
0
5
10
15
20
Fe Concentration (mg/L)

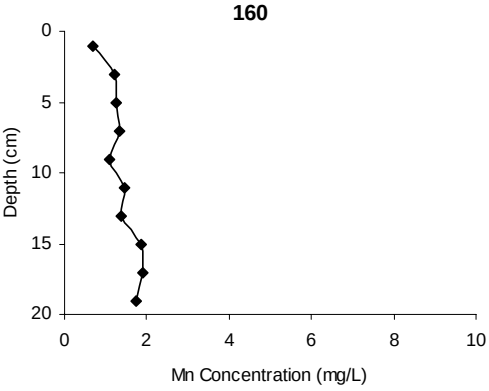
160
Depth (cm)
0
5
10
15
20
0
2
4
6
8
10
Mn Concentration (mg/L)

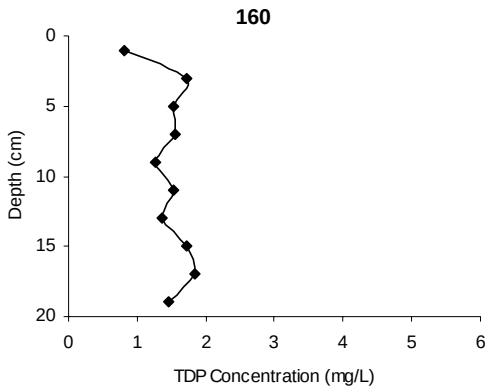
160
Depth (cm)
TDP Concentration (mg/L)

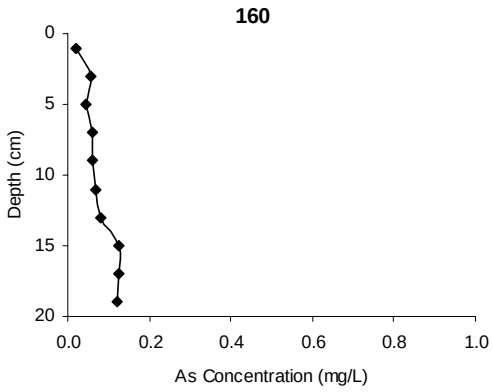
160
Depth (cm)
As Concentration (mg/L)

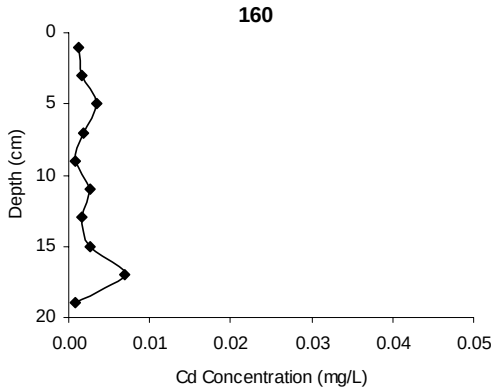
160
Depth (cm)
Cd Concentration (mg/L)

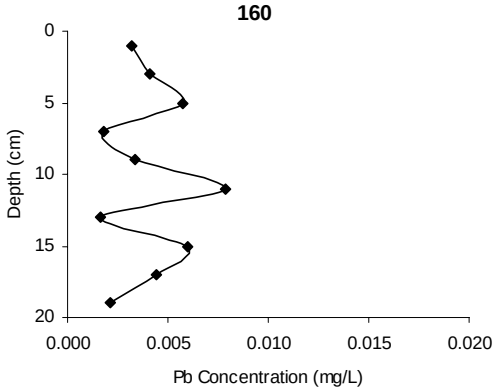
160
Depth (cm)
Pb Concentration (mg/L)

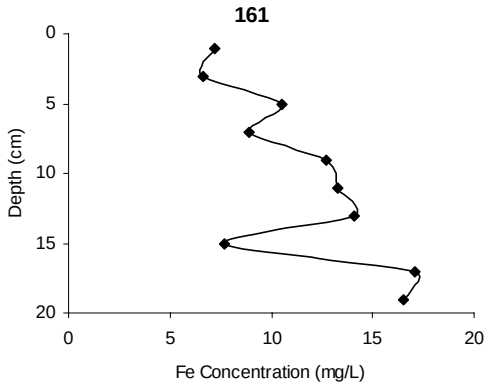
161
Depth (cm)
Fe Concentration (mg/L)

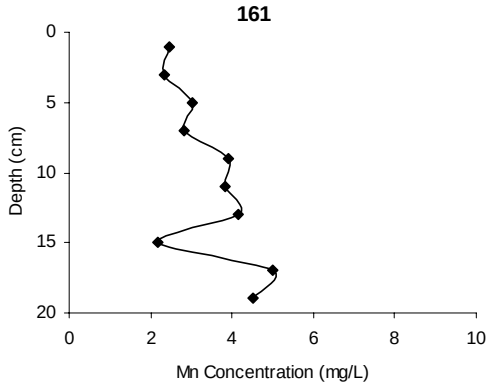
161
Depth (cm)
Mn Concentration (mg/L)

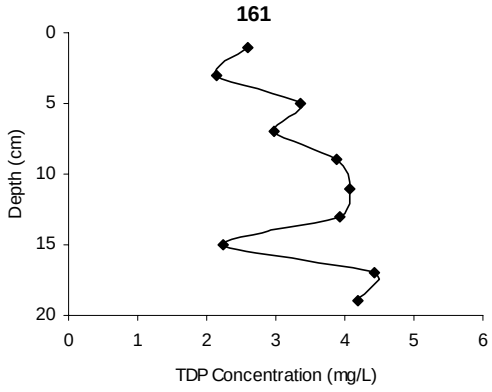
161
Depth (cm)
TDP Concentration (mg/L)

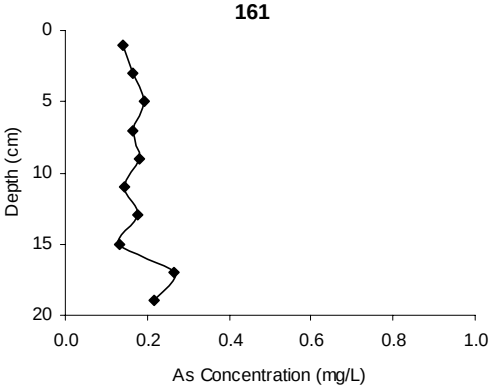
161
Depth (cm)
As Concentration (mg/L)

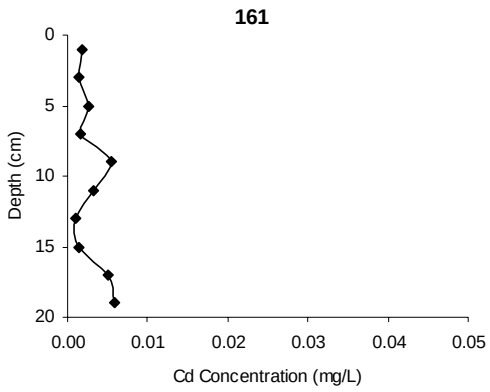
161
Depth (cm)
0
5
10
15
20
0.00
0.01
0.02
0.03
0.04
0.05
Cd Concentration (mg/L)

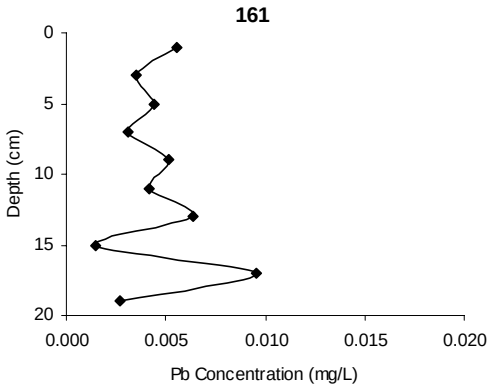
161
Depth (cm)
0
5
10
15
20
0.000
0.005
0.010
0.015
0.020
Pb Concentration (mg/L)

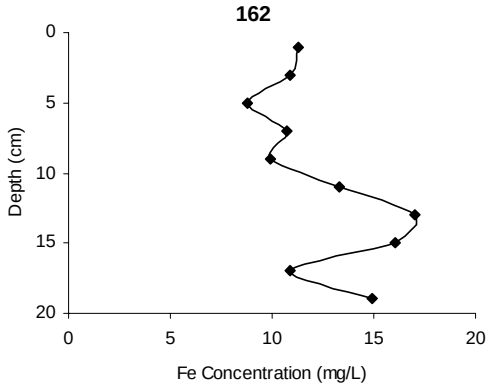
162
Depth (cm)
0
5
10
15
20
0
5
10
15
20
Fe Concentration (mg/L)

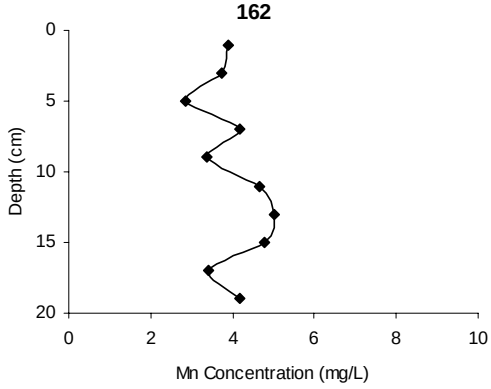
162
Depth (cm)
0
5
10
15
20
0
2
4
6
8
10
Mn Concentration (mg/L)

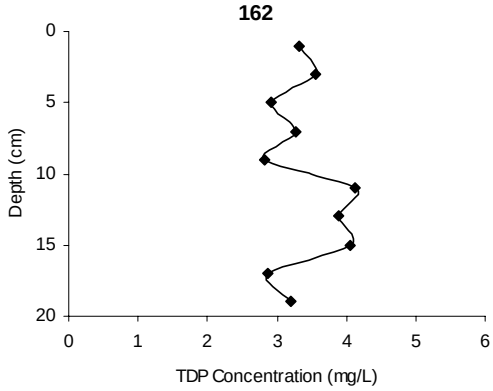
162
Depth (cm)
0
5
10
15
20
0
1
2
3
4
5
6
TDP Concentration (mg/L)

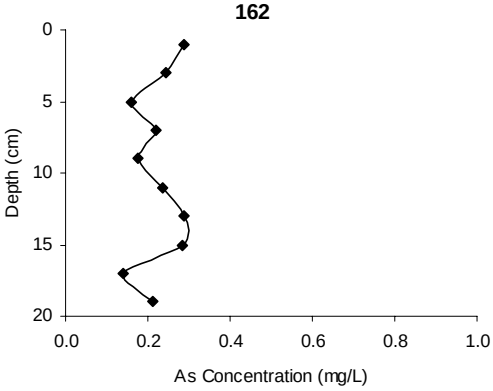
162
Depth (cm)
0
5
10
15
20
0.0
0.2
0.4
0.6
0.8
1.0
As Concentration (mg/L)

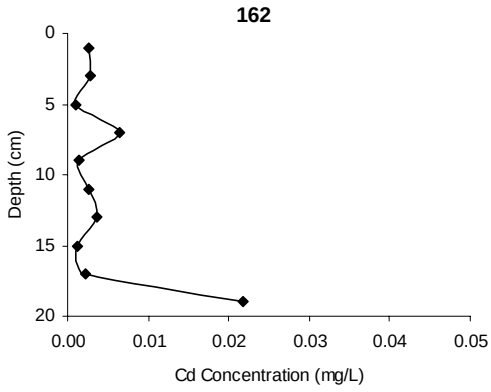
162
Depth (cm)
0
5
10
15
20
0.00
0.01
0.02
0.03
0.04
0.05
Cd Concentration (mg/L)

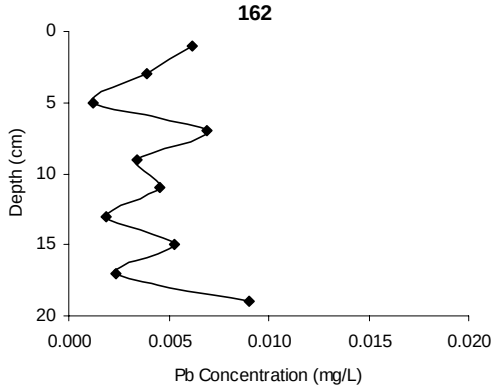
162
Depth (cm)
0
5
10
15
20
0.000
0.005
0.010
0.015
0.020
Pb Concentration (mg/L)

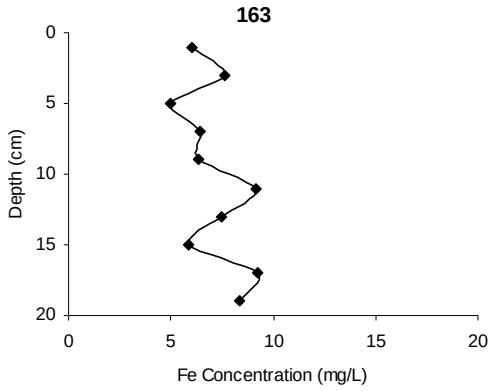
163
Depth (cm)
0
5
10
15
20
0
5
10
15
20
Fe Concentration (mg/L)

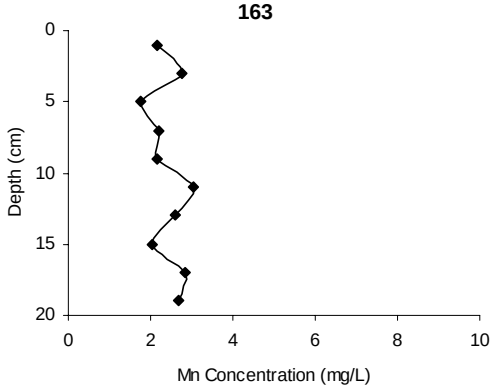
163
Depth (cm)
0
5
10
15
20
0
2
4
6
8
10
Mn Concentration (mg/L)

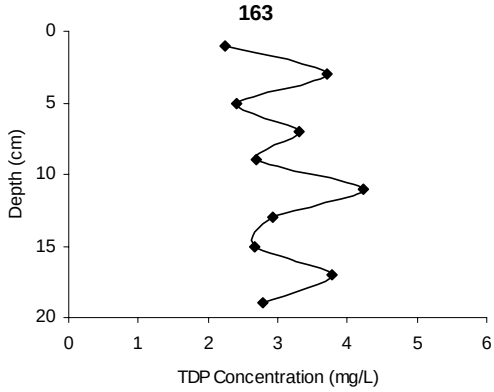
163
Depth (cm)
0
5
10
15
20
0
1
2
3
4
5
6
TDP Concentration (mg/L)

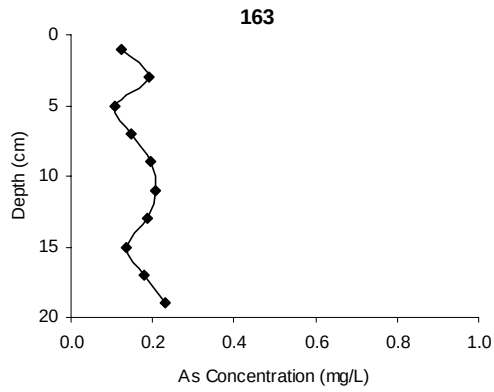
163
Depth (cm)
0
5
10
15
20
0.0
0.2
0.4
0.6
0.8
1.0
As Concentration (mg/L)

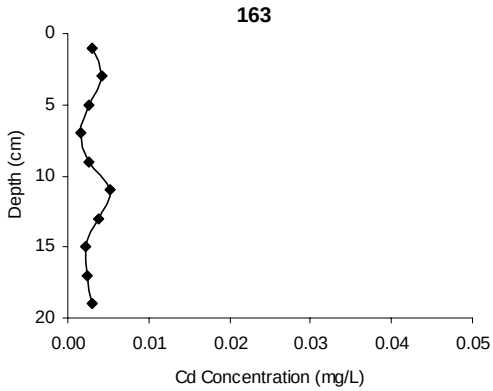
163
Depth (cm)
0
5
10
15
20
0.00
0.01
0.02
0.03
0.04
0.05
Cd Concentration (mg/L)

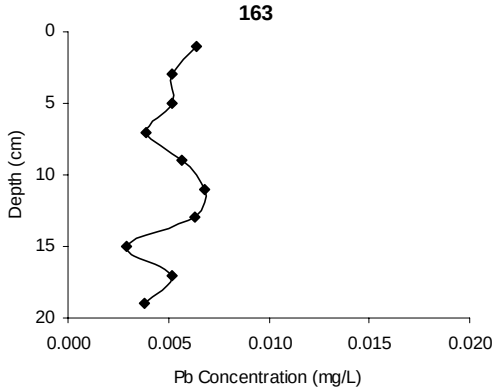
163
Depth (cm)
0
5
10
15
20
0.000
0.005
0.010
0.015
0.020
Pb Concentration (mg/L)

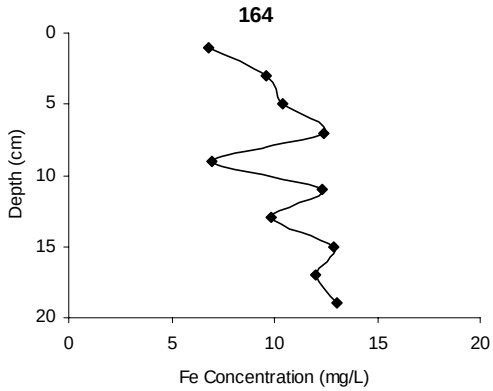
164
Depth (cm)
0
5
10
15
20
0
5
10
15
20
Fe Concentration (mg/L)

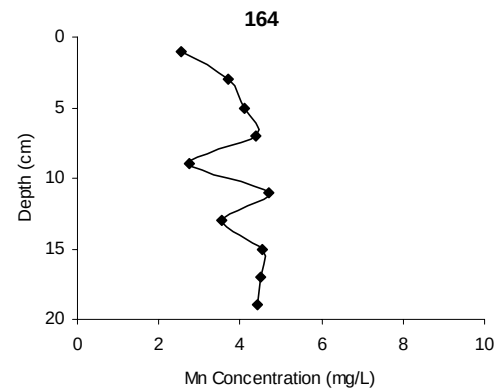
164
Depth (cm)
0
5
10
15
20
0
2
4
6
8
10
Mn Concentration (mg/L)

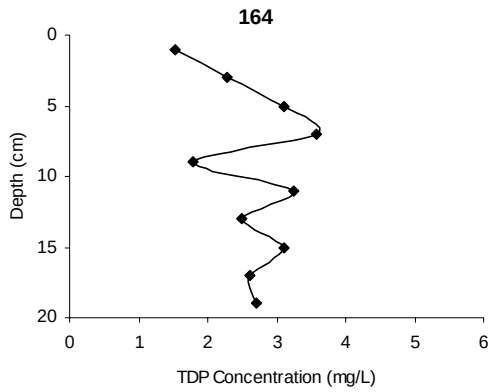
164
Depth (cm)
0
5
10
15
20
0
1
2
3
4
5
6
TDP Concentration (mg/L)

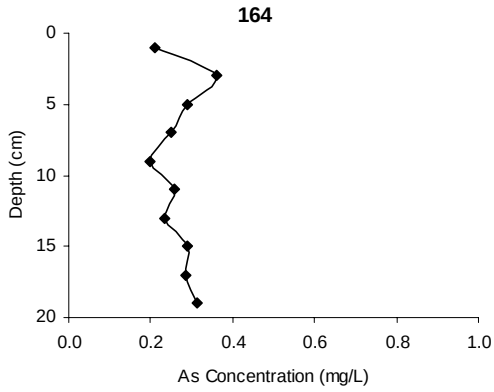
164
Depth (cm)
0
5
10
15
20
0.0
0.2
0.4
0.6
0.8
1.0
As Concentration (mg/L)

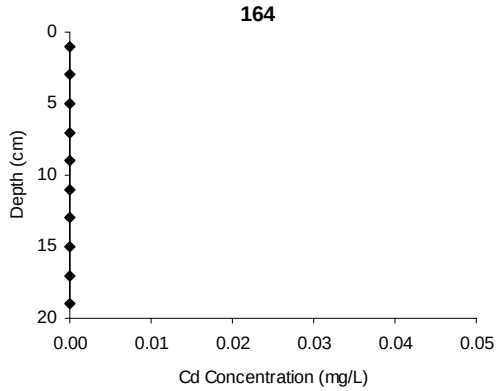
164
Depth (cm)
0
5
10
15
20
0.00
0.01
0.02
0.03
0.04
0.05
Cd Concentration (mg/L)

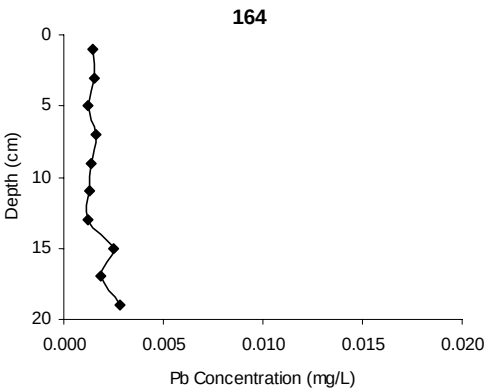
164
Depth (cm)
0
5
10
15
20
0.000
0.005
0.010
0.015
0.020
Pb Concentration (mg/L)

Appendix 3

Diffusive fluxes

		TDP	NH_4^+			TDP	NH_4^+		TDP	NH_4^+
Month	**Core ID**	mg m^{-2} d^{-1}							mg m^{-2} d^{-1}	
January	**RU102**	18.71	61.96	***September***	**RU129**	7.05	27.23	**RU152**	7.62	
	RU103	15.61	41.16		**RU130**	0.34	24.60	**RU153**	14.01	
	RU104	79.34	112.80		**RU131**	6.56	92.06	**RU154**	11.25	
	RU105	66.10	133.28		**RU132**	2.48		**RU155**	0.85	
	RU106	107.89	128.83		**RU133**	4.40		**RU156**	0.40	
	RU107	140.82	212.28		**RU134**	0.31		**RU157**	9.30	
	RU108	58.17	128.25		**RU135**	1.30		**RU158**	3.73	
	RU109	28.57	159.74		**RU136**	1.23		**RU159**	0.18	
	RU110	43.13	111.34		**RU137**	0.66		**RU160**	5.64	
May	**RU114**	51.43	55.02		**RU138**	0.24		**RU161**	17.80	
	RU115	31.53	43.02		**RU139**	0.62		**RU162**	22.79	
	RU116	4.96	201.12		**RU140**	2.21	19.29	**RU163**	15.41	
	RU117	37.36	170.07		**RU141**	7.45	45.91			
	RU118	70.84	86.06		**RU142**	11.85	64.32			
	RU119	12.53	88.40		**RU143**	0.56	27.54			
	RU120	6.22	25.65		**RU144**	0.88	23.71			
	RU121	1.91	38.77		**RU145**	0.19	43.53			
	RU122	4.27	39.44		**RU146**	5.47	41.92			
	RU123	18.36	57.52		**RU147**	31.15				
	RU124	0.80	19.60		**RU148**	0.88				
	RU125	10.81	43.76		**RU149**	0.29				
	RU126	9.68	110.73		**RU150**	4.81				
	RU127	25.64	62.15		**RU151**	3.27				

Appendix 4

Pore water saturation ion activity products

Core ID	Vivianite	Pyrite	FeS amorphous	Mackinawite	Pyrrhotite	Greigite	Calcite	Siderite	Rhodochrosite
Depth (cm)	Ru107								
1	35.31	26.21	15.53	15.53	15.53	57.26	10.27	11.11	10.86
3	35.07	27.73	16.10	16.10	16.10	59.93	10.27	10.74	10.37
5	34.73	26.54	15.35	15.35	15.35	57.24	10.27	10.43	10.39
7	35.81	27.87	16.20	16.20	16.20	60.27	10.27	10.79	10.45
9	35.95	27.69	16.08	16.08	16.08	59.85	10.27	10.74	10.42
11	37.09	27.60	16.12	16.12	16.12	59.83	10.27	10.90	10.56
13	37.16	27.44	16.11	16.11	16.11	59.65	10.27	11.03	10.46
15	37.33	27.55	16.09	16.09	16.09	59.73	10.27	10.89	10.64
17	37.32	27.40	16.01	16.01	16.01	59.42	10.27	10.88	10.59
19	34.70	27.04	15.60	15.60	15.60	58.25	10.27	10.44	10.40
Depth (cm)	Ru110								
1	35.31	26.21	15.53	15.53	15.53	57.26	10.27	11.11	10.86
3	31.96	25.97	14.95	14.95	14.95	55.86	10.27	10.19	10.31
5	33.49	26.44	15.28	15.28	15.28	57.01	10.27	10.40	10.49
7	34.37	26.50	15.38	15.38	15.38	57.26	10.27	10.53	10.54
9	34.74	26.76	15.54	15.54	15.54	57.85	10.27	10.59	10.64
11	35.52	26.86	15.68	15.68	15.68	58.23	10.27	10.77	10.66
13	36.02	27.04	15.74	15.74	15.74	58.52	10.27	10.70	10.68
15	36.35	26.87	15.67	15.67	15.67	58.21	10.27	10.74	10.73
17	36.39	26.70	15.59	15.59	15.59	57.88	10.27	10.74	10.70
19	36.41	26.83	15.63	15.63	15.63	58.09	10.27	10.70	10.65
Depth (cm)	Ru115								

0	41.78	28.56	17.11	17.11	17.11	62.79	10.98	12.65	12.95
1	39.23	28.43	16.68	16.68	16.68	61.78	11.03	11.95	11.82
3	39.69	28.55	16.85	16.85	16.85	62.25	10.83	11.97	11.74
5	41.17	29.05	17.37	17.37	17.37	63.79	10.84	12.53	11.55
7	40.79	28.35	16.78	16.78	16.78	61.92	10.73	11.95	11.34
9	40.16	27.84	16.34	16.34	16.34	60.52	10.72	11.56	11.32
11	38.82	27.30	15.93	15.93	15.93	59.15	10.58	11.14	11.11
13	40.52	27.89	16.38	16.38	16.38	60.65	10.68	11.55	11.12
15	39.23						10.68	11.30	11.24

Depth (cm)	Ru118								
0	40.08	27.67	16.57	16.57	16.57	60.81	10.85	12.31	11.88
1	34.27	26.43	15.14	15.14	15.14	56.72	10.77	10.62	11.22
3	34.61	26.85	15.33	15.33	15.33	57.52	10.73	10.53	11.14
5	35.77	27.92	15.96	15.96	15.96	59.85	10.79	10.79	11.23
7	36.70	28.02	16.08	16.08	16.08	60.19	10.88	11.02	11.40
9	37.98	28.20	16.20	16.20	16.20	60.59	10.95	11.15	11.58
11	36.26	28.71	16.29	16.29	16.29	61.29	10.98	10.86	11.37
13	35.68	27.94	15.87	15.87	15.87	59.69	10.86	10.66	11.22
15	39.13	28.96	16.77	16.77	16.77	62.50	10.83	11.40	11.44
17	36.12	28.58	16.25	16.25	16.25	61.08	10.87	10.79	11.24
19	37.64	28.88	16.51	16.51	16.51	61.90	10.87	11.01	11.60
21	35.95	28.13	15.96	15.96	15.96	60.04	10.86	10.65	11.26
23	36.02	28.02	15.94	15.94	15.94	59.91	10.81	10.67	11.17
25	35.72	28.17	15.91	15.91	15.91	60.00	10.97	10.63	11.21
27	36.45	28.90	16.39	16.39	16.39	61.67	10.89	10.75	11.25
29	37.42	28.52	16.23	16.23	16.23	60.98	11.01	10.95	11.50
31	35.73	28.26	15.99	15.99	15.99	60.25	10.87	10.59	11.13
33	35.62	27.53	15.64	15.64	15.64	58.81	10.77	10.52	11.04
35	34.70						10.71	10.32	10.92

Depth (cm)	Ru124								
0	39.80	26.54	15.68	15.68	15.68	57.90	10.45	11.26	11.54
1	40.78	27.00	15.96	15.96	15.96	58.93	10.62	11.54	11.43
3	37.43	26.20	15.25	15.25	15.25	56.70	10.44	10.73	11.15
5	34.95	26.92	15.45	15.45	15.45	57.83	10.40	10.38	11.06
7	33.84	27.03	15.46	15.46	15.46	57.95	10.35	10.24	10.75
9	35.62	27.05	15.63	15.63	15.63	58.30	10.44	10.65	11.09
11	34.48	27.92	15.93	15.93	15.93	59.77	10.47	10.41	10.89
13	33.03	26.83	15.27	15.27	15.27	57.36	10.31	10.01	10.54
15	33.95	29.00	16.42	16.42	16.42	61.85	10.35	10.20	10.70
17	33.32	27.52	15.66	15.66	15.66	58.84	10.29	10.09	10.56
19	32.91	27.09	15.38	15.38	15.38	57.84	10.29	9.95	10.50
21	32.94	26.52	15.12	15.12	15.12	56.76	10.27	9.98	10.47
23	32.80	26.50	15.03	15.03	15.03	56.55	10.37	9.93	10.53
25	32.52	26.10	14.80	14.80	14.80	55.70	10.39	9.89	10.51
27	32.32	26.30	14.87	14.87	14.87	56.04	10.37	9.80	10.45
29	34.28	26.59	15.23	15.23	15.23	57.05	10.35	10.22	10.66
31	32.34	26.34	14.87	14.87	14.87	56.08	10.41	9.81	10.50

Depth (cm)	Ru127								
0	46.74	27.51	16.73	16.73	16.73	60.97	10.66	12.60	12.19
1	34.34	26.31	15.08	15.08	15.08	56.46	10.57	10.41	10.97
3	35.41	26.81	15.43	15.43	15.43	57.68	10.56	10.61	11.16
5	35.01	27.01	15.43	15.43	15.43	57.87	10.71	10.57	11.06
7	34.72	26.82	15.34	15.34	15.34	57.50	10.64	10.48	10.94
9	35.35	27.00	15.48	15.48	15.48	57.96	10.60	10.56	11.01
11	35.67	27.15	15.56	15.56	15.56	58.27	10.66	10.63	10.99
13	35.67	26.96	15.45	15.45	15.45	57.86	10.71	10.65	11.03
15	34.49	26.96	15.37	15.37	15.37	57.70	10.57	10.34	10.82

17	34.69	26.75	15.24	15.24	15.24	57.24	10.68	10.41	10.95
19	36.99	27.17	15.69	15.69	15.69	58.55	10.65	10.85	11.42
21	33.88	26.67	15.12	15.12	15.12	56.92	10.63	10.20	10.90
23	35.66						10.75	10.54	11.01
25	36.50						10.79	10.71	11.16
27	35.47						10.81	10.51	11.13

Depth (cm)	Ru130								
1	41.96	27.37	16.13	16.13	16.13	59.63	10.75	11.64	11.43
3	34.03	27.39	15.47	15.47	15.47	58.33	10.69	10.23	10.96
5	34.97	27.88	15.80	15.80	15.80	59.49	10.72	10.45	11.14
7	34.30	28.63	16.11	16.11	16.11	60.85	10.72	10.31	10.95
9	34.27	27.41	15.50	15.50	15.50	58.41	10.71	10.31	10.87
11	33.90	28.05	15.77	15.77	15.77	59.59	10.78	10.26	10.78
13	35.00	29.85	16.82	16.82	16.82	63.49	10.66	10.44	10.88
15	33.97	28.65	16.07	16.07	16.07	60.80	10.77	10.27	10.71
17	33.64	29.12	16.30	16.30	16.30	61.72	10.76	10.25	10.70
19	33.60	28.21	15.85	15.85	15.85	59.92	10.71	10.20	10.59

Depth (cm)	Ru143								
1	40.35	26.54	15.63	15.63	15.63	57.80	10.58	11.31	11.31
3	36.67	27.64	15.91	15.91	15.91	59.46	10.57	10.73	11.13
5	35.66	27.43	15.70	15.70	15.70	58.83	10.58	10.55	11.06
7	34.86	28.09	15.99	15.99	15.99	60.06	10.62	10.50	10.98
9	35.22	28.39	16.19	16.19	16.19	60.77	10.63	10.62	11.01
11	34.84	28.87	16.37	16.37	16.37	61.62	10.64	10.51	10.87
13	34.79	28.38	16.12	16.12	16.12	60.61	10.67	10.53	10.93
15	34.84	28.33	16.11	16.11	16.11	60.55	10.65	10.53	10.95
17	35.55	28.61	16.28	16.28	16.28	61.16	10.67	10.61	10.99
19	36.09	28.63	16.36	16.36	16.36	61.35	10.62	10.71	11.11

Depth (cm)	Ru145								
1	43.45	27.64	16.42	16.42	16.42	60.48	10.78	11.97	11.80
3	37.00	27.61	15.92	15.92	15.92	59.44	10.68	10.90	11.32
5	36.24	28.17	16.12	16.12	16.12	60.40	10.71	10.77	11.29
7	35.53	28.63	16.27	16.27	16.27	61.17	10.69	10.60	11.11
9	35.32	28.27	16.07	16.07	16.07	60.42	10.70	10.57	11.08
11	37.14	28.83	16.52	16.52	16.52	61.87	10.73	10.93	11.34
13	35.47	29.91	16.89	16.89	16.89	63.69	10.68	10.55	10.97
15	34.89						10.69	10.43	10.89
17	35.55	29.48	16.70	16.70	16.70	62.88	10.65	10.55	10.92
19	35.19	29.51	16.69	16.69	16.69	62.88	10.67	10.52	10.94